

**Novel Polybenzimidazoles as Polymer Electrolytes  
for Fuel Cell**

**A thesis submitted to the  
UNIVERSITY OF PUNE**

**for the degree of  
DOCTOR OF PHILOSOPHY**

**in**

**CHEMISTRY**

**by**

**Ravindra A. Potrekar**

Polymer Science and Engineering Division  
National Chemical Laboratory  
Pune 411 008, India.

**March 2009**

## DECLARATION

I hereby declare that all the experiments embodied in this thesis entitled “**Novel Polybenzimidazoles as Polymer Electrolytes for Fuel Cell**”, submitted for the degree of Doctor of Philosophy in Chemistry, to the University of Pune has been carried out by me at the Polymer Science and Engineering Division, National Chemical Laboratory, Pune-411 008, India, under the guidance of Dr. S. P. Vernekar. The work is original and has not been submitted in part or full by me, for any degree or diploma to this or to any other University.

March, 2009

Pune



**Ravindra A. Potrekar**

Senior Research Fellow  
Polymer Science and Engineering Division  
National Chemical Laboratory  
Pune-411 008, India.



राष्ट्रीय रासायनिक प्रयोगशाला  
(वैज्ञानिक तथा औद्योगिक अनुसंधान परिषद)  
डॉ. होमी भाभा मार्ग पुणे - 411 008. भारत  
**NATIONAL CHEMICAL LABORATORY**



(Council of Scientific & Industrial Research)  
Dr. Homi Bhabha Road, Pune - 411 008. India.

**Certificate of the Guide**

Certified that the work incorporated in this thesis entitled: **“Novel Polybenzimidazoles as Polymer Electrolytes for Fuel Cell”** submitted by **Mr. Ravindra A. Potrekar** was carried out by the candidate under my supervision/ guidance. Such material as has been obtained from other sources has been duly acknowledged in the thesis.

March, 2009

Pune

**Dr. S. P. Vernekar**

(Research Guide)

**Dr. R. A. Kulkarni**

(Research Co-Guide)

**Communication  
Channels**

NCL Level DID : 2590  
NCL Board No. : +91-20-25902000  
EPABX : +91-20-25893300  
+91-20-25893400

**FAX**

Director's Office : +91-20-25902601  
COA's Office : +91-20-25902660  
COS&P's Office : +91-20-25902664

**WEBSITE**

[www.ncl-india.org](http://www.ncl-india.org)



*Dedicated  
to*

*Sri Sri Ravishankar*

*&*

*My Family*



## **Acknowledgement**

*I would first like to thank my research supervisor, Dr. S. P. Vernekar, Emeritus Scientist, Polymer Science and Engineering Division, National Chemical Laboratory, Pune, India, for his valuable guidance and support over the past years. It has been my life-time opportunity to pursue my career under his leadership and vision. I am highly impressed by his knowledge and approach to solve problems. I especially enjoyed his style of mentoring students from which I have benefited tremendously in my personal and professional growth. My everlasting gratitude goes to him.*

*I also would like to thank my research co-supervisor Dr. R. A. Kulkarni for his helpful suggestions for preparing this thesis. His comments and insightful observations have substantially improved the quality of my work.*

*I wish to express my deep felt gratitude to Dr. M. G. Kulkarni, Head, Polymer Science and Engineering Division, National Chemical Laboratory, Pune, India, for providing the possible infrastructural facilities from time to time.*

*I would like to thank the Council of Scientific and Industrial Research, New Delhi for the award of fellowship and Director, NCL for providing facilities which enabled me to carry out my research in such a prestigious research laboratory.*

*The advice and help rendered by Dr. K. Vijayamohan for the successful completion of this work especially for the fuel cell characterization is gratefully acknowledged.*

*I owe special thanks to Dr. C. V. Avadhani, Dr. P. P. Wadgoankar, Mr. A. S. Patil, Dr. B. B. Idage, Dr. R. P. Singh, Mr. K. G. Raut and Dr. U. K. Kharul who extended their help and support whenever it was required.*

*I sincerely acknowledge, Dr.(Mrs.) A. N. Bote, Dr. (Mrs.) S.B. Idage, Dr. S. Shreekumar, Dr. C. V. Rode, Dr. R. S. Khisti, Mr. S. K. Menon, Dr. N. N. Chavan, Mr. A. A. Gunari, Dr. S. S. Mahajan, Dr. S. D. Patil, Dr. M. B. Sabne, Dr. S.D. Patil, Dr. (Mrs.) Garnaik, Mrs. D. A. Dhoble, Dr. B. D. Sarwade, Dr. A. S. Jadhav Dr. B. M. Shinde, Dr. T. P. Mohandas, Dr. P. G. Sukhla, Mr. Harshwardhan Pol, Dr. I. S. Mulla, Dr. C. Ramesh, Mr. Kiran Pandhare and Mr. K. D. Deshpande for their valuable help and cooperation during my research stay in NCL. I am grateful to Mr. Mahesh Rote, Mr. Siddheshwar, Mr. Zine, Mr. More, Mr. Shelar, Mr. Singh and Mr. Jori for their cooperation. I thank the members of central NMR facility, micro analysis, CMC, SMIS, glass blowing, stores, workshop and administrative section for their help.*

*I am also thankful to Dr. N. N. Karde, Dr. Uday Joshi, Dr. S. G. Shirodkar, Dr. S. P. Pachling, Dr. J. S. Jadhav, Dr. Gore (N.S.B. College, Nanded) for sharing their knowledge and support whenever it was required.*

*I would like to express my deep felt gratitude to my colleagues and friends Sandeep Kothawade, Mahesh Kulkarni, Panjab, Girish, Kannan, Aniruddha, Renuka, Madhavi, Jayprakash (JP), and Mahesh Kadgaonkar for their helpful hand and sympathetic ear.*

*I also wish to thank my friends Wasif, Rakesh, Hamid, Mahesh Sonar, Ravi Sonawane, Mallikarjuna, Vivek, Sharad, Shivkumar, Asmita, Nilakshi, Yogita Poorvi, Parimal, Rajeshwari, Kedar, Sony, Arun, Vijay, Pandurang, Arvind, Prakash, Sushil, Pratheep, Yogesh, Santosh, Harshada, Anjana, Mukesh, Depan, Sunil, Rahul Shingate, Dnyaneshwar, Shreekuttan, Jadab, Niranjana, Bhaskar, Bhalchandra, Mahima, Mukta, Vishal, Husian, Pinak, Bhure, Ausutosh, Satish Patil, Pandu, Sundar, Shivaji and Neha Prabhu for their support and co-operation.*

*I am grateful to God and my guru H. H. Sri Sri Ravishankar who gave me a very caring and loving family. My special gratitude goes to my brother (Dada), who instilled in me a desire to learn, strong work ethics and the value of common sense. I do not have any word to thank my mother and father and other family members Upendra, Vahini, Omkar, Rushi, Mayuri, Aboli, sisters, brother-in-law, father-in-law, and mother-in-law and Paratkar Mama & Mami for their immense love, support and patience beyond limits.*

*Finally I would like to thank my wife, Sonali, whose love, patience and encouragement eased the way to this achievement.*

**Ravindra A. Potrekar**

---

**CONTENTS**

<b>Description</b>	<b>Page No.</b>
❖ Abstract	i
❖ Glossary	iii
❖ List of Tables	v
❖ List of Schemes	vi
❖ List of Figures	vii

---

<b>Chapter 1</b>	<b>Introduction and literature review</b>	
------------------	---	--

---

1.1	Introduction	1
1.1.1	General background of fuel cells and polymer electrolytes for fuel cells	1
1.1.2	Types of fuel cells	2
1.1.3	Polymer electrolyte membrane fuel cells (PEMFCs)	3
1.1.4	Types of polymer electrolyte membranes	4
1.1.4.1	Fluorinated polymers	4
1.1.4.2	Non-fluorinated polymers	5
1.2	Polytriazoles	7
1.2.1	Synthetic methods for the preparation of polytriazoles	7
1.2.1.1	One-step polycondensation	8
1.2.1.2	Two-step polycondensation	8
1.2.2	Polymers containing triazole groups	9
1.2.3	Applications of polytriazoles to PEM fuel cells	11
1.3	Polyoxadiazoles	14
1.3.1	Synthetic methods for the preparation of polyoxadiazoles	14
1.3.1.1	One-step polycondensation	15
1.3.1.2	Two-step polycondensation	16
1.3.2	Structure-property relationship of aromatic polyoxadiazoles	17
1.3.3	Application of polyoxadiazoles to PEM fuel cells	21
1.4	Polybenzimidazoles	23
1.4.1	Synthetic methods for the preparation of aromatic PBI	24
1.4.1.1	Interfacial polycondensation of tetraamines and diacid chlorides	24

1.4.1.2	Polycondensation of tetraamines and dialdehyde	25
1.4.1.3	Polycondensation of dinitro dichlorobenzene with diamine	26
1.4.1.4	Two stage solid/melt polycondensation of tetraamines and dicarboxylic acid esters	27
1.4.1.5	Solution polycondensation of tetraamines and dicarboxylic acid in PPA	28
1.4.2	Structural modification of PBI	28
1.4.3	Applications of PBI	31
1.4.4	Phosphoric acid doped PBI membranes for PEMFCs	32
1.4.4.1	Methods for preparation of acid doped PBI membranes	33
1.4.4.2	Proton conductivity of acid doped PBI	34
1.4.5	Polybenzimidazoles in H <sub>2</sub> /O <sub>2</sub> fuel cells	38
1.4.6	Modification of PBI	40
1.4.6.1	Sulfonated PBI	40
1.4.6.1 (a)	Post sulfonation of PBI	40
1.4.6.1 (b)	Chemically grafting of PBI	41
1.4.6.1 (c)	Direct polymerization of sulfonated monomer units	43
1.4.6.2	Blends of PBI with other polymers	44
1.5	Summary	46
1.6	Scope and objective of the present work	46
	References	48

## Chapter 2 Synthesis and characterization of monomers

2.1	Introduction	56
2.2	Experimental	58
2.2.1	Materials	58
2.2.2	Analytical methods	58
2.2.3	Synthesis of new substituted aromatic diacids	58
2.2.3.1	Synthesis of 3, 3'-(4-phenyl-4H-1,2,4-triazole-3,5-diyl) dibenzoic acid (PTDBA)	58
2.2.3.2	Synthesis of 5-(4,5-diphenyl-4H-1,2,4-triazol-3-yl)isophthalic acid (DTIA)	61



	2.2.3.3	Synthesis of 3,3'-(1,3,4-oxadiazole-2,5-diyl)dibenzoic acid (ODBA)	64
	2.2.3.4	Synthesis of 5-(5-phenyl-1,3,4-oxadiazol-2-yl) isophthalic acid (POIA)	66
2.3		Results and Discussion	68
	2.3.1	Synthesis and characterization of 3, 3'-(4-phenyl-4H-1,2,4-triazole-3,5-diyl) dibenzoic acid (PTDBA)	68
	2.3.2	Synthesis and characterization of 5-(4,5-diphenyl-4H-1,2,4-triazol-3-yl)isophthalic acid (DTIA)	73
	2.3.3	Synthesis and characterization of 3,3'-(1,3,4-oxadiazole-2,5-diyl)dibenzoic acid (ODBA)	79
	2.3.4	Synthesis and characterization of 5-(5-phenyl-1,3,4-oxadiazol-2-yl) isophthalic acid (POIA)	82
2.4		Conclusions	87
		References	87

---

**Synthesis and characterization of polybenzimidazoles and copolybenzimidazoles containing triazole groups and their application as polymer electrolyte membranes for Fuel Cells**

**Chapter 3**

---

3.1		Introduction	89
3.2		Experimental	90
	3.2.1	Materials	90
	3.2.2	Analytical methods	91
	3.2.3	Synthesis of polybenzimidazoles	94
	3.2.3.1	Synthesis of PBI having NPT group in main chain and side chain	94
3.3		Results and Discussion	97
	3.3.1	Synthesis and structural characterization of polybenzimidazoles	97
	3.3.2	Properties of polybenzimidazoles	101
	3.3.2.1	Polymer solubility	101
	3.3.2.2	Thermal Properties	103
	3.3.2.2.1	Thermogravimetric analyses (TGA)	103
	3.3.2.2.2	Glass transition temperature ( $T_g$ )	106
	3.3.2.3	Crystallinity	108
	3.3.2.4	Mechanical properties	110
	3.3.2.5	Water uptake	113

	3.3.2.6	Oxidative stability	113
	3.3.2.7	Phosphoric acid doping study	116
	3.3.2.8	Proton conductivity measurements	121
	3.3.2.9	Membrane electrode assembly fabrication	124
	3.3.2.10	Polarization Study	125
3.4		Conclusions	127
		References	127

**Chapter 4      Synthesis and characterization of polybenzimidazoles and  
copolybenzimidazoles containing oxadiazole groups and their  
application as polymer electrolyte membranes for Fuel Cells**

4.1		Introduction	130
4.2		Experimental	132
	4.2.1	Materials	132
	4.2.2	Analytical methods	132
	4.2.3	Synthesis of polybenzimidazoles	135
	4.2.3.1	Synthesis of PBI having oxadiazole group in main chain and side chain	135
4.3		Results and Discussion	138
	4.3.1	Synthesis and structural characterization of polybenzimidazoles	138
	4.3.2	Properties of polybenzimidazoles	141
	4.3.2.1	Polymer solubility	141
	4.3.2.2	Thermal properties	143
		4.3.2.2.1 Thermogravimetric analyses (TGA)	143
		4.3.2.2.2 Glass transition temperature ( $T_g$ )	146
	4.3.2.3	Crystallinity	149
	4.3.2.4	Mechanical properties	152
	4.3.2.5	Water uptake	155
	4.3.2.6	Oxidative stability	155
	4.3.2.7	Phosphoric acid doping study	158
	4.3.2.8	Proton conductivity measurements	163
	4.3.2.9	Membrane electrode assembly fabrication	165
	4.3.2.10	Polarization study	165
4.4		One-pot synthesis of poly (benzimidazole-oxadiazole) copolymers and their use	167

---

	as proton conducting membranes	
4.4.1	Introduction	167
4.4.2	Experimental	167
4.4.2.1	Reagents and solvents	167
4.4.2.2	Measurements	168
4.4.2.3	Polymer synthesis	168
4.4.3	Results and Discussion	169
4.4.3.1	Polymer synthesis	169
4.4.3.2	FTIR spectroscopy	170
4.4.3.3	Polymer solubility and inherent viscosities	171
4.4.3.4	Thermal properties	172
4.4.3.5	Crystallinity	173
4.4.3.6	Mechanical properties	174
4.4.3.7	Water uptake	175
4.4.3.8	Oxidative stability	175
4.4.3.9	Phosphoric acid doping study	176
4.4.3.10	Proton conductivity measurements	178
4.4.3.11	Membrane electrode assembly fabrication	180
4.4.3.12	Polarization study	181
4.5	Conclusions	182
	References	183

---

## **Chapter 5      Summary and Conclusions**

---

5.1	Summary of the work	185
5.2	Conclusions	186
5.3	Future work	187
	List of publications	189
	Synopsis	191

## **Abstract**

Polymer electrolyte membrane fuel cells (PEMFCs) have attracted significant attention due to their high energy efficiency and as environmentally benign source of energy alternative to current power sources, for portable, stationary and automotive applications. Polymer electrolyte membrane (PEM), a key component of fuel cell, is normally an ion containing polymer bearing sulfonic acid functionality. The currently preferred electrolyte material for PEMFCs, perfluorosulfonic acid polymers such as Nafion<sup>®</sup> (DuPont), has many disadvantages such as, high cost, difficult water management, high fuel crossover, low operational temperature, sensitivity to impurities (e.g. carbon monoxide) etc., which have prompted researchers to look for alternative less expensive polymer membrane for proton transport operating at higher than 120 °C. Polybenzimidazoles (PBI) are important class of high-performance polymers, which exhibit excellent thermal and hydrolytic stability, high mechanical strength, good chemical resistance, low gas and methanol permeability and good proton conductivity at high temperature on doping with phosphoric acid. However, PBI has low proton conductivity compared to Nafion<sup>®</sup> at less than 80 °C, poor oxidative stability at operational conditions and susceptibility to lose unbound phosphoric acid by leaching with water and methanol.

Poly-1,2,4-triazoles (PT) and poly-1,2,4-oxadiazoles (POD) are another class of thermally stable high performance heterocyclic polymers known for their high thermal stability and good chemical resistance. PT and POD on complexing with strong acids, transport protons similar to imidazoles and have adequate electrochemical stability for use in fuel cells as polymer electrolyte. But the main hurdle for application of these polymers is its processability due to their high softening point and poor solubility in organic solvents. So, little attention has been paid towards the application of polymers containing triazole and oxadiazole groups as polymer electrolyte for fuel cells. The present work is a step towards this to design and prepare polymers containing triazole and oxadiazole groups and study their properties as polymer electrolytes for fuel cells. This work presents synthesis and characterization of novel polybenzimidazoles containing 1,2,4 triazole and 1,2,4-oxadiazole moiety in the main as well as side chain and their application as polymer electrolytes for fuel cells.

**Chapter 1**, presents a detailed review of literature on the polymer electrolyte membrane fuel cells in general, with emphasis on synthesis and characterization of

polytriazole, polyoxadiazole and polybenzimidazole and their use as a polymer electrolyte membrane for fuel cell applications. This chapter also includes the scope and objective of the thesis.

**Chapter 2**, presents the synthesis and characterization of four designed aromatic diacids having triazole and oxadiazole groups, viz. (i) 3,3'-(4-phenyl-4H-1,2,4-triazole-3,5-diyl) dibenzoic acid (PTDBA), (ii) 5-(4,5-diphenyl-4H-1,2,4-triazol-3-yl)isophthalic acid (DTIA) (iii) 5-(5-phenyl-1,3,4-oxadiazol-2-yl) isophthalic acid (POIA) and (iv) 3,3'-(1,3,4-oxadiazole-2,5-diyl)dibenzoic acid (ODBA). These aromatic diacids are characterized using routine analytical methods like NMR, IR and elemental analysis.

**Chapter 3**, presents a detailed study on the synthesis of polybenzimidazoles and copolybenzimidazoles having N-Phenyl 1,2,4-triazole (NPT) moiety in the main chain and side chain from two aromatic diacids, PTDBA and DTIA, respectively and characterization of these polymers by solubility tests, inherent viscosity measurement, IR spectroscopy, X-ray diffraction, differential scanning calorimetry, thermogravimetry and measurement of tensile properties. It also describes measurements of physico-chemical properties such as water and phosphoric acid uptake, oxidative stability, and proton conductivity of membranes to explore applications for polymer electrolyte membrane fuel cells. Incorporation of NPT groups in polybenzimidazoles improved solubility, oxidative stability and acid uptake compared to commercial PBI membranes. These polymers are amorphous in nature and showed high thermal and good mechanical properties.

**Chapter 4**, presents a detailed study on the synthesis and characterization of polybenzimidazoles and copolybenzimidazoles having 1,2,4-oxadiazole moiety in the main as well as side chain from two aromatic diacids, ODBA and POIA, respectively. This chapter also comprises (a) synthesis and characterization of copolymers containing varying extents of benzimidazole and 1,2,4-oxadiazole groups by polycondensation of tetraamine, dicarboxylic acid and dihydrazide of dicarboxylic acid in polyphosphoric acid and (b) comparison of properties like crystallinity, solubility, glass transition temperature, thermal stability and mechanical properties with those prepared by condensing ODBA and isophthalic acid with 3,3',4,4'-tetra-amino biphenyl. It also consists of a detailed study on physico-chemical properties such as water and phosphoric acid uptake, oxidative stability, and proton conductivity of membranes of these polymers to explore the possible applications as electrolyte membrane for fuel cells.

**Chapter 5**, presents the summary and conclusions.

## Glossary

<b>AA</b>	Adipic acid
<b>AB-PBI</b>	Poly(2,5-benzimidazole
<b>AFC</b>	Alkaline Fuel Cells
<b>BASPAPS</b>	Bis-3-amino-4-[3-(triethylammoniumsulfonato)phenylamino]phenyl sulfone
<b>BDBH</b>	N'-benzoyl-3,5-dimethylbenzohydrazide
<b>BiSA</b>	1H-benzimidazole-2-sulphonic Acid
<b>CDA</b>	Carboxylic Diacids
<b>DMAc</b>	N,N-dimethyl acetamide
<b>CO</b>	Carbon Monoxide
<b>DMF</b>	N,N-dimethyl formamide
<b>DCTz</b>	4,5-Dicyano-1H-[1,2,3]-triazole
<b>DMSO</b>	Dimethyl sulphoxide
<b>DSC</b>	Differential Scanning Calorimetry
<b>EGDE</b>	Ethylene Glycol Diglycidyl Ether
<b>DPDT</b>	3-(3,5-dimethylphenyl)-4,5-diphenyl-4H-1,2,4-triazole
<b>DPPO</b>	2-(3,5-Dimethyl Phenyl)-5-Phenyl-1,3,4-Oxadiazole
<b>DTIA</b>	5-(4,5-diphenyl-4H-1,2,4-triazol-3-yl)isophthalic acid
<b>DTO</b>	2,5-di-tolyl-1,3,4-oxadiazole
<b>FTIR</b>	Fourier Transform Infra Red
<b>HMPA</b>	Hexamethylphosphoramide
<b>IEC</b>	Ion-Exchange Capacity
<b>IDT</b>	Initial Decomposition Temperature
<b>IPA</b>	Isophthalic Acid
<b>MBH</b>	3-methyl-N'-(3-methylbenzoyl) benzohydrazide
<b>MCF</b>	Molton Carbonate Fuel Cell
<b>MEA</b>	Membrane Electrode Assembly
<b>MDSPPPO</b>	Bis(3-methyldimethoxysilyl)polypropylene Oxide
<b>MSA</b>	Methane Sulfonic Acid
<b>NMR</b>	Nuclear Magnetic Resonance
<b>NPT</b>	N-Phenyl 1,2,4-triazole
<b>ODBA</b>	3'-(1,3,4-oxadiazole-2,5-diyl)dibenzoic acid
<b>OLEDs</b>	Organic Light-Emitting Diodes
<b>PAFC</b>	Phosphoric Acid Fuel cell
<b>PAN</b>	Polyacrylonitrile
<b>PBI</b>	Polybenzimidazoles
<b>PDCA</b>	Pyridine 2,6-dicarboxylic acid
<b>PDT</b>	4-phenyl-3,5-dim-tolyl-4H-1,2,4-triazole
<b>PEGMEA</b>	Poly(ethylene glycol)methyl ether acrylate
<b>PEEK</b>	Polyetheretherketones
<b>PEEKK</b>	Polyetheretherketonesketone
<b>PEMFCs</b>	Proton Exchange Membrane Fuel Cells
<b>PEM</b>	Polymer Electrolyte Membrane
<b>PES</b>	Polyethersulfone
<b>PI</b>	Polyimide
<b>PPA</b>	Polyphosphoric Acid
<b>PPBP</b>	Poly(4-phenoxybenzoyl-1,4-phenylene
<b>PP</b>	Poly(p-phenylenes

---

<b>PPMA</b>	Phosphorus pentoxide/methanesulfonic acid
<b>PSF</b>	Polysulfone
<b>POD</b>	Polyoxadiazole
<b>POIA</b>	5-(5-phenyl-1,3,4-oxadiazol-2-yl) isophthalic acid
<b>PPO</b>	Polyphenylene oxide
<b>PT</b>	Polytriazoles
<b>PTDBA</b>	3'-(4-phenyl-4H-1,2,4-triazole-3,5-diyl) dibenzoic acid
<b>SA</b>	Sebacic Acid
<b>SD</b>	Degree of Sulfonation
<b>SOFC</b>	Solid Oxide Fuel Cell
<b>TAB</b>	3,3',4,4,'-tetra-amino biphenyl
<b>TEOS</b>	Tetraethoxysilane
<b>TFA</b>	Trifluoroacetic acid
<b>TGA</b>	Thermo Gravimetric Analysis
<b>TPA</b>	Terephthaldehyde
<b>T<sub>5</sub></b>	Decomposition temperature at 5% weight loss
<b>T<sub>10</sub></b>	Decomposition temperature at 10% weight loss
<b>WAXS</b>	Wide angle X-ray Diffraction Spectroscopy
<b><math>\eta_{inh}</math></b>	Inherent viscosity

## List of Tables

Table No.	Description	Page No.
1.1	Types of fuel cells	2
1.2	Structurally modified polytriazoles	10
1.3	Structurally modified polyoxadiazoles	17
1.4	Chemical structures of selected examples of PBI derivatives	34
3.1	Inherent viscosity (IV), yield, film appearance and film nature of Polybenzimidazoles having NPT groups in main chain	95
3.2	Inherent viscosity, yield, film appearance and film nature of Polybenzimidazoles having NPT groups in side chain	95
3.3	Solubility behavior of Polybenzimidazoles having NPT groups in main chain (PTDBA-based polymers)	102
3.4	Solubility behavior of Polybenzimidazoles having NPT groups in side chain (DTIA-based polymers)	102
3.5	Thermal properties of polybenzimidazoles having NPT groups in main chain (PTDBA-based polymers)	104
3.6	Thermal properties of polybenzimidazoles having NPT groups in side chain (DTIA -based polymers)	105
3.7	Mechanical properties PTDBA-based PBIs	111
3.8	Mechanical properties DTIA-based PBIs	112
3.9	Proton conductivity of PTDBA-based polymers	122
3.10	Proton conductivity of DTIA based polymers	124
4.1	Inherent viscosity (IV), yield, film appearance and film nature of PBI containing oxadiazole groups in main chain and its copolymers (ODBA-based polymers)	136
4.2	Inherent viscosity (I.V.) yield, film appearance and film nature of PBI containing oxadiazole groups in side chain and its copolymers (POIA-based polymers)	137
4.3	Solubility behavior of polybenzimidazoles having oxadiazole groups in main chain	142
4.4	Solubility behavior of polybenzimidazoles having oxadiazole groups in side chain	142
4.5	Thermal properties of polybenzimidazoles having oxadiazole groups in main chain (ODBA-based polymers)	144
4.6	Thermal properties of polybenzimidazole having oxadiazole group in side chain (POIA-based polymers)	145
4.7	Mechanical properties ODBA-based PBIs	152
4.8	Mechanical properties POIA-based PBIs	154
4.9	Proton conductivity of ODBA based polymers	163
4.10	Proton conductivity of POIA based polymers	165
4.11	Inherent viscosity, yield, film appearance and film nature	169



4.12	Solubility behavior of (benzimidazole-co-oxadiazole) copolymers	172
4.13	Thermal properties of (benzimidazole-co-oxadiazole) copolymers	173
4.14	Mechanical properties of PBI and its copolymers with varying oxadiazole contents	174
4.15	Oxidative stability and water uptake of PBI and its copolymers with varying oxadiazole contents	176
4.16	Proton conductivity of benzimidazole-co-oxadiazole copolymers	178
4.17	Comparative data of OMPBI and CPBI polymers	180

## List of Schemes

Scheme No.	Description	Page No.
1.1	Synthesis of polytriazoles from bistetrazole and N,N'-diphenylisophthalimidoyl chloride	7
1.2	Synthesis of polytriazoles by one step-polycondensation	8
1.3	Synthesis of polytriazoles by two-step polycondensation	8
1.4	Synthesis of polyoxadiazoles by C. J. Abshire and C.S. Marvel method	14
1.5	Synthesis of POD from hydradine sulfate by one-step polycondensation method	15
1.6	Synthesis of POD from dihydrazide by two-step polycondensation method	16
1.7	Synthesis of PBI by interfacial polycondensation	24
1.8	PBI synthesis from tetraamines and dialdehydes	25
1.9	PBI Synthesis from tetraamines and isophthalaldehyde bis bisulfite adduct	25
1.10	Synthesis of PBI starting from bis-3-amino-4-[3-(triethylammoniumsulfonato)phenylamino]phenyl sulfone(BASPAPS)	26
1.11	Proposed mechanism of PBI synthesis by solid stage polymerization	27
1.12	Synthesis of PBI by Solution polycondensation of tetraamines and dicarboxylic acid in PPA	28
1.13	Synthetic route to sulfonated PBI by chemically grafting of 1,3-propane sultone and 4-bromobenzyl sulfonic acid respectively	42
2.1	Synthesis of 3,3'-(4-phenyl-4H-1,2,4-triazole-3,5-diyl) dibenzoic acid (PTDBA)	61
2.2	Synthesis of 5-(4,5-diphenyl-4H-1,2,4-triazol-3-yl)isophthalic acid (DTIA)	62
2.3	Synthesis of 3,3'-(1,3,4-oxadiazole-2,5-diyl)dibenzoic acid (ODBA)	64
2.4	Synthesis of 5-(5-phenyl-1,3,4-oxadiazol-2-yl) isophthalic acid (POIA)	66
3.1	Synthesis of polybenzimidazoles from PTDBA	96
3.2	Synthesis of polybenzimidazoles from DTIA	97
4.1	Synthesis of polybenzimidazoles from ODBA	136
4.2	Synthesis of polybenzimidazoles from POIA	137

4.3	Synthesis of (A) polybenzimidazole (PBI), (B) polyoxadiazole (POD) and (C) copolymers (CPBI)	170
-----	--	-----

## List of Figures

Figure No.	Description	Page No.
1.1	Schematic diagram of PEMFC	3
1.2	Chemical structure of Nafion	4
1.3	proton-conducting mechanism in SPOD–SPT/BiSA membranes	13
1.4	Structure of PBI (Poly 2,2'-(m-phenylene)-5,5' bibenzimidazole)	23
1.5	Schematic presentation of proton conduction in acid-doped PBI membranes	35
1.6	Structure of AB-PBI	37
1.7	Dicarboxylic acids having triazole group	47
1.8	Dicarboxylic acids having oxadiazole group	48
2.1	FTIR spectrum of 3-methyl-N'-(3-methylbenzoyl)benzohydrazide (MBH) in KBr	68
2.2	<sup>1</sup> H NMR spectrum of 3-methyl-N'-(3-methylbenzoyl)benzohydrazide (MBH) in DMSO-d <sub>6</sub>	69
2.3	<sup>13</sup> C NMR spectrum of 3-methyl-N'-(3-methylbenzoyl)benzohydrazide (MBH) in DMSO-d <sub>6</sub>	69
2.4	FTIR spectrum of 4-phenyl-3, 5-di-m-tolyl-4H-1, 2, 4-triazole (PDT) in KBr	70
2.5	<sup>1</sup> H NMR spectrum of 4-phenyl-3, 5-di-m-tolyl-4H-1, 2, 4-triazole in CDCl <sub>3</sub>	71
2.6	<sup>13</sup> C NMR spectrum of 4-phenyl-3, 5-di-m-tolyl-4H-1, 2, 4-triazole (PDT) in CDCl <sub>3</sub>	71
2.7	FTIR spectrum of 3, 3'-(4-phenyl-4H-1,2,4-triazole-3,5-diyl) dibenzoic acid (PTDBA) in KBr	72
2.8	<sup>1</sup> H and <sup>13</sup> C NMR spectra of 3, 3'-(4-phenyl-4H-1,2,4-triazole-3,5-diyl) dibenzoic acid (PTDBA) in DMSO-d <sub>6</sub>	73
2.9	FTIR spectrum of N'-benzoyl-3,5-dimethylbenzohydrazide (BDBH) in KBr	74
2.10	<sup>1</sup> H NMR spectrum of N'-benzoyl-3,5-dimethylbenzohydrazide (BDBH) in DMSO-d <sub>6</sub>	75
2.11	<sup>13</sup> C NMR spectrum of N'-benzoyl-3,5-dimethylbenzohydrazide (BDBH) in DMSO-d <sub>6</sub>	75
2.12	FTIR spectrum of 3-(3,5-dimethylphenyl)-4,5-diphenyl-4H-1,2,4-triazole (DPDT) in KBr	76
2.13	<sup>1</sup> H NMR spectrum of 3-(3,5-dimethylphenyl)-4,5-diphenyl-4H-1,2,4-triazole (DPDT) in CDCl <sub>3</sub>	76
2.14	<sup>13</sup> C NMR spectrum of 3-(3,5-dimethylphenyl)-4,5-diphenyl-4H-1,2,4-triazole (DPDT) in CDCl <sub>3</sub>	77
2.15	FTIR spectrum of 5-(4,5-diphenyl-4H-1,2,4-triazol-3-yl)isophthalic acid	78

	(DTIA) in KBr	
2.16	<sup>1</sup> H NMR spectrum of 5-(4,5-diphenyl-4H-1,2,4-triazol-3-yl)isophthalic acid (DTIA) in DMSO-d <sub>6</sub>	78
2.17	<sup>13</sup> C NMR spectrum of 5-(4,5-diphenyl-4H-1,2,4-triazol-3-yl)isophthalic acid (DTIA) in DMSO-d <sub>6</sub>	79
2.18	FTIR spectrum of 2,5- <i>dim</i> -tolyl-1,3,4-oxadiazole (DTO) in KBr	80
2.19	<sup>1</sup> H NMR spectrum of 2,5- <i>dim</i> -tolyl-1,3,4-oxadiazole (DTO) in CDCl <sub>3</sub>	80
2.20	FTIR spectrum of 3,3'-(1,3,4-oxadiazole-2,5-diyl)dibenzoic acid (ODBA) in KBr	81
2.21	<sup>1</sup> H NMR spectrum of 3,3'-(1,3,4-oxadiazole-2,5-diyl)dibenzoic acid (ODBA) in DMSO-d <sub>6</sub>	81
2.22	<sup>13</sup> C NMR spectrum of 3,3'-(1,3,4-oxadiazole-2,5-diyl)dibenzoic acid (ODBA) in DMSO-d <sub>6</sub>	82
2.23	FTIR spectrum of 2-(3,5-Dimethyl Phenyl)-5-Phenyl-1,3,4-Oxadiazole (DPPO) in KBr	83
2.24	<sup>1</sup> H NMR spectrum of 2-(3,5-Dimethyl Phenyl)-5-Phenyl-1,3,4-Oxadiazole (DPPO) in CDCl <sub>3</sub>	84
2.25	<sup>13</sup> C NMR spectrum of 2-(3,5-Dimethyl Phenyl)-5-Phenyl-1,3,4-Oxadiazole (DPPO) in CDCl <sub>3</sub>	84
2.26	FTIR spectrum of 5-(5-phenyl-1,3,4-oxadiazol-2-yl) isophthalic acid (POIA) in KBr	85
2.27	<sup>1</sup> H NMR spectrum of 5-(5-phenyl-1,3,4-oxadiazol-2-yl) isophthalic acid (POIA) in DMDO-d <sub>6</sub>	85
2.28	<sup>13</sup> C NMR spectrum of 5-(5-phenyl-1,3,4-oxadiazol-2-yl) isophthalic acid (POIA) in DMDO-d <sub>6</sub>	86
3.1	FTIR spectra of NPT group containing PBI in main chain (TM-100) and PBI (film)	99
3.2	FTIR spectra of NPT group containing PBI in side chain (TS-100) and PBI (film)	99
3.3	FTIR spectra of polymer films of copolymers of PTDBA and IPA	100
3.4	<sup>1</sup> H-NMR spectrum of homo polymer (TM-100) in DMSO-d <sub>6</sub>	100
3.5	<sup>1</sup> H-NMR spectrum of homo polymer (TS-100) in DMSO- d <sub>6</sub>	101
3.6	Thermograms and derivatives of thermograms of polybenzimidazoles from PTDBA in N <sub>2</sub> atmosphere (purging rate 20 mL/min) recorded at a heating rate 10 °C/min	103
3.7	Thermograms of other polybenzimidazoles from PTDBA in nitrogen	104
3.8	Thermograms and derivatives of thermograms of polybenzimidazoles from DTIA in N <sub>2</sub> atmosphere (purging rate 20 mL/min) recorded at a heating rate 10 °C/min	106
3.9	Thermograms of other polybenzimidazoles from DTIA in nitrogen	106
3.10	DSC Thermograms of homo polymer and copolymers based on PTDBA in N <sub>2</sub> , (heating rate 20 °C min <sup>-1</sup> )	107
3.11	DSC Thermograms of homo polymer and copolymers based on DTIA in N <sub>2</sub> , (heating rate 20 °C min <sup>-1</sup> )	108

3.12	WAXD diffractograms of PBIs from PTDBA	109
3.13	WAXD diffractograms of other coPBIs from PTDBA	109
3.14	WAXD diffractograms of PBIs from DTIA	110
3.15	Mechanical properties PTDBA-based PBIs	111
3.16	Tensile stress versus strain graph of PBIs from PTDBA	112
3.17	Oxidative stability of PBI and coPBI of IPA containing NPT groups in main chain. Membrane degradation in terms of %wt. loss of a membrane measured at different time intervals. Membranes were dipped in 3% H <sub>2</sub> O <sub>2</sub> containing 4 ppm Fe <sup>2+</sup> (Fenton solution) at 70 °C in an oven, taken out after 24 h and measured their wt loss after drying. The procedure is repeated with fresh Fenton solutions	114
3.18	Oxidative stability of PBI and coPBI of other diacids containing NPT groups in main chain	115
3.19	Oxidative stability of PBI and coPBI of IPA containing NPT groups in side chain	115
3.20	Oxidative stability of PBI and coPBI of other diacids containing NPT groups in side chain	116
3.21	Doping level of phosphoric acid (wt%) in PTDBA based polymers as a function of the concentration of H <sub>3</sub> PO <sub>4</sub>	117
3.22	Doping level of phosphoric acid (wt%) in PTDBA based polymers as a function of the concentration H <sub>3</sub> PO <sub>4</sub>	118
3.23	Doping levels of PTDBA based polymers at different time intervals. Concentration of H <sub>3</sub> PO <sub>4</sub> for TM-100, TM-90, TM-70, TM-50 (10 M) , for TM-10 and TM-30 (12M) and for PBI (14M)	118
3.24	Doping levels of PTDBA based polymers at different time intervals. Concentration of H <sub>3</sub> PO <sub>4</sub> for TM-100, (10 M), for TM-T and TM-P (12M) and for TM-S and TM-A (8M)	119
3.25	Doping level of phosphoric acid (wt%) in DTIA based polymers and PBI polymers as a function of acid concentration	120
3.26	Doping level of phosphoric acid (wt%) in DTIA based polymers as a function of acid concentration	120
3.27	Acid doping levels DTIA based polymers at different time intervals. Concentration of H <sub>3</sub> PO <sub>4</sub> for TS-100, TS-90, TS-70 and TS-50 (10 M) , for TS-10 and TS-30 (12M) and for PBI (14M).	121
3.28	Acid doping levels at different time intervals. Concentration of H <sub>3</sub> PO <sub>4</sub> for TS-100, (10 M) , for TS-T and TS-P (12M) and for TS-S and TS-A (8M)	121
3.29	Polarization curves obtained with TM-100 membrane fuel cell at different temperatures with dry H <sub>2</sub> and O <sub>2</sub> (flow rate 0.2 slpm). The cell was conditioned for 30 min at open-circuit potential and at 0.2 V for 15 min before measurements. Key: (■□) 100, (●○) 125 and (▲Δ) 150 °C	125
3.30	Polarization curves obtained with TS-100 membrane fuel cell at different temperatures with dry H <sub>2</sub> and O <sub>2</sub> (flow rate 0.2 slpm). The cell was conditioned for 30 min at open-circuit potential and at 0.2 V for 15 min before measurements. Key: (■□) 100, (●○) 125 and (▲Δ) 150 °C	126
3.31	Polarization curves obtained with PBI membrane fuel cell at different temperatures with dry H <sub>2</sub> and O <sub>2</sub> (flow rate 0.2 slpm). The cell was	126

	conditioned for 30 min at open-circuit potential and at 0.2 V for 15 min before measurements. Key: (■□) 100, (●○) 125 and (▲△) 150 °C	
4.1	FTIR spectra of oxadiazole groups containing PBI in main chain (OMPBI) and PBI (film)	139
4.2	FTIR spectra of oxadiazole groups containing PBI in side chain (OSPBI) and PBI (film)	139
4.3	FTIR spectra of polymer films of copolymers of ODBA and IPA Dotted line shows increase in the peak intensity of 1070 cm <sup>-1</sup> (-C-O-C stretching in oxadiazole ring) with increase in the oxadiazole groups in PBI	140
4.4	<sup>1</sup> H NMR spectrum of OMPBI in TFA (D <sub>2</sub> O lock)	140
4.5	<sup>1</sup> H NMR spectrum of OSPBI in TFA (D <sub>2</sub> O lock)	141
4.6	Thermogram and derivatives of thermograms of polybenzimidazoles from ODBA in N <sub>2</sub> atmosphere (purging rate 20 mL/min) recorded at a heating rate 10 °C/min	144
4.7	Thermograms of other polybenzimidazoles from ODBA in nitrogen	145
4.8	Thermograms and derivatives of thermograms of polybenzimidazoles from POIA in N <sub>2</sub> atmosphere (purging rate 20 mL/min) recorded at a heating rate 10 °C/min	146
4.9	Thermograms of other polybenzimidazoles from POIA in nitrogen	146
4.10	DSC Thermograms of homo polymer and copolymers based on ODBA in N <sub>2</sub> , (heating rate 20 °C min <sup>-1</sup> )	147
4.11	DSC Thermograms of other copolymers based on ODBA in N <sub>2</sub> , (heating rate 20 °C min <sup>-1</sup> )	147
4.12	DSC Thermograms of homo polymer and copolymers based on POIA in N <sub>2</sub> , (heating rate 20 °C min <sup>-1</sup> )	148
4.13	DSC Thermograms of other copolymers based on POIA in N <sub>2</sub> , (heating rate 20 °C min <sup>-1</sup> )	149
4.14	WAXS diffractograms of PBIs from ODBA	150
4.15	WAXS diffractograms of other coPBIs from ODBA	150
4.16	WAXS diffractograms of PBIs from POIA (OSPBI)s	151
4.17	WAXS diffractograms of other coPBIs from POIA (OSPBI)s	151
4.18	Mechanical properties ODBA-based PBIs	153
4.19	Mechanical properties POIA-based PBIs	154
4.20	Oxidative stability of PBI and coPBI of IPA containing oxadiazole groups in main chain.	156
4.21	Oxidative stability of PBI and coPBI of other diacids containing oxadiazole groups in main chain.	156
4.22	Oxidative stability of PBI and coPBI of IPA containing oxadiazole groups in side chain	157
4.23	Oxidative stability of PBI and coPBI of other diacids containing oxadiazole groups in side chain	157
4.24	Doping level of phosphoric acid (wt%) in ODBA based polymers as a function of the concentration of H <sub>3</sub> PO <sub>4</sub>	158
4.25	Doping level of phosphoric acid (wt%) in ODBA based polymers as a	159

	function of the concentration of H <sub>3</sub> PO <sub>4</sub>	
4.26	Acid doping levels of ODBA based polymers at different time intervals. Concentration of H <sub>3</sub> PO <sub>4</sub> for OMPBI, OMPBI-1, OMPBI-2, OMPBI-3 (12 M) , for OMPBI-4 and OMPBI-5 and PBI (14M)	159
4.27	Acid doping levels of ODBA based polymers at different time intervals. Concentration of H <sub>3</sub> PO <sub>4</sub> for OMPBI-6(14M) and for OMPBI-7, OMPBI-8 and OMPBI-9 (10M)	160
4.28	Doping level of phosphoric acid (wt%) in polymers as a function of the concentration of POIA based polymers and PBI	161
4.29	Doping level of phosphoric acid (wt%) in of POIA based other polymers as a function of the acid concentration	161
4.30	Acid doping levels POIA based polymers and PBI at different time intervals. Concentration of H <sub>3</sub> PO <sub>4</sub> for OSPBI, OSPBI-1, OSPBI-2, OSPBI-3 and OSPBI-4 (12 M) , for OSPBI-5 and PBI (14M)	162
4.31	Acid doping levels POIA based polymers and PBI at different time intervals. Concentration of H <sub>3</sub> PO <sub>4</sub> for OSPBI-6(12M) and for OSPBI-7,and OSPBI-8 (10M)	162
4.32	Polarization curves obtained with OMPBI membrane fuel cell at different temperatures with dry H <sub>2</sub> and O <sub>2</sub> (flow rate 0.2 slpm). The cell was conditioned for 30 min at open-circuit potential and at 0.2 V for 15 min before measurements. Key: (■□) 100, (●○) 125 and (▲Δ) 150 °C	166
4.33	Polarization curves obtained with TSPBI membrane fuel cell at different temperatures with dry H <sub>2</sub> and O <sub>2</sub> (flow rate 0.2 slpm). The cell was conditioned for 30 min at open-circuit potential and at 0.2 V for 15 min before measurements. Key: (■□) 100, (●○) 125 and (▲Δ) 150 °C	166
4.34	FTIR spectrum of (benzimidazole-co-oxadiazole) copolymers (KBr pellets)	171
4.35	Thermograms and derivatives of thermograms of (benzimidazole-co-oxadiazole) copolymers in N <sub>2</sub> atmosphere (purging rate 20 mL/min) recorded at a heating rate 10 °C/min	173
4.36	WAXS diffractograms of PBI and its copolymers with varying oxadiazole contents	174
4.37	Tensile stress versus strain measurements of PBI and its copolymers with varying oxadiazole contents	175
4.38	Doping level of phosphoric acid (wt%) in (benzimidazole-co-oxadiazole) copolymers, as a function of the concentration of H <sub>3</sub> PO <sub>4</sub>	177
4.39	Acid doping levels of (benzimidazole-co-oxadiazole) copolymers at different time intervals	177
4.40	Conductivity of phosphoric acid doped PBI and benzimidazole-co-oxadiazole) copolymers	179
4.41	Polarization curves obtained with CPBI membrane fuel cell at different temperatures with dry H <sub>2</sub> and O <sub>2</sub> (flow rate 0.2 slpm). The cell was conditioned for 30 min at open-circuit potential and at 0.2 V for 15 min before measurements. Key: (■□)100, (●○) 125 and (▲Δ) 150 °C	181

# Chapter

1

**Introduction and literature review**

## 1.1 Introduction

The global energy demands, especially, in terms of transportation and day to day use of diverse equipment is steadily increasing due to increasing population of world. The energy demands are being met by fossil fuel as a traditional energy source. The burning of fossil fuel generally emits harmful gases such as carbon monoxide (CO), carbon dioxide, oxides of nitrogen and sulphur (NO<sub>x</sub> and SO<sub>x</sub>), which pose a serious challenge to environment and human life. Moreover, fossil fuel is limited and extinguishing gradually. So, it is a need of today to find out a concrete pollution free energy source alternative to fossil fuel. In this respect, hydrogen as the energy source is considered to be the most promising. Among the various devices, fuel cells with hydrogen as fuel have received wide attention of researchers due to their high power density and potential applications in vehicular transportation, electric utility, and other applications requiring clean, quiet, pollution free and portable power. Presently significant research work is being expended to develop cost effective fuel cells for various applications.

### 1.1.1 General background of fuel cells and polymer electrolytes for fuel cells

A fuel cell is an electrochemical device that converts chemical energy into electrical energy directly. Typically hydrogen and oxygen/air are used to generate electricity. There are various electrochemical similarities between batteries and fuel cells and they serve many of the same applications. In batteries chemical energy is stored internally and need to be recharged, whereas in fuel cells, fuel is stored externally to its core components. Fuel cells are not electrically recharged, but after use the tank is refilled with fuel, like internal combustion engine. Compared to batteries, fuel cells provide high specific energy density, high efficiency for longer operations and ability to satisfy the power requirements in space vehicles.

The basic principle of fuel cell was first demonstrated by Sir William Grove<sup>1</sup> in 1839 and later Phosphoric Acid Fuel cell (PAFC) and Proton Exchange Membrane Fuel Cells (PEMFCs) were developed by Mond and Langer<sup>2</sup> in 1889. In 1896, Jacques<sup>3</sup> built a 1.5 kW pilot scale Alkaline Fuel Cell (AFC) power plants and demonstrated its viability. The development and impending of Molton Carbonate Fuel Cell (MCFC) was provided by Bauer and Ehrenberg<sup>4</sup> followed by Davytan & coworkers<sup>5</sup> and Broers and Ketelaar<sup>6</sup> in 1940s. In 1952 Bacon developed the first practical 5 kW AFC for Britain's National Research Development Corporation.<sup>7</sup> The 1kW operating system of Polymer Electrolyte Membrane Fuel Cell was first developed by General Electric for NASA and used as



primary power source for Gemini spacecraft during the mid-1960s.<sup>8,9</sup> Since 1960 during the last 15 years, research in to fuel cells has grown exponentially with nearly 310 journal articles published in 2007.<sup>10</sup>

### 1.1.2 Types of fuel cells

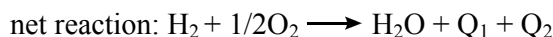
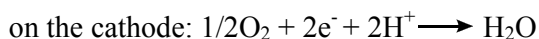
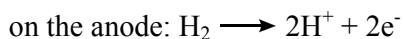
Fuel cells are basically classified in five categories on the basis of electrolyte used. Each fuel cell has its own advantages and disadvantages and they have different applications depending on fuel, electrolyte and operating temperature. The major characteristics are listed in Table 1.1.

**Table 1.1** Types of fuel cells<sup>11</sup>

Types of Fuel Cell	Electrolyte	Operating Temp.	Efficiency	Electric Power	Possible Applications	Electrochemical Reaction
Proton Exchange Membrane (PEMFC)	Ion Exchange Membrane	60-130 °C	40-60%	Up to 250 kW	Vehicles, Stationary	Anode: $H_2 \rightarrow 2H^+ + 2e^-$ Cathod: $1/2 O_2 + 2H^+ + 2e^- \rightarrow H_2O$ Cell: $H_2 + 1/2 O_2 \rightarrow H_2O$
Alkaline (AFC)	Potassium Hydroxide	60-90 °C	45-60%	Up to 20 kW	Submarines, Spacecraft	Anode: $H_2 + 2OH^- \rightarrow 2H_2O + 2e^-$ Cathod: $1/2 O_2 + H_2O + 2e^- \rightarrow 2OH^-$ Cell: $H_2 + 1/2 O_2 \rightarrow H_2O$
Phosphoric Acid (PAFC)	Immobilized Liquid Phosphoric Acid	200 °C	35-40%	> 50 kW	Power Stations	Anode: $H_2 \rightarrow 2H^+ + 2e^-$ Cathod: $1/2 O_2 + 2H^+ + 2e^- \rightarrow H_2O$ Cell: $H_2 + 1/2 O_2 \rightarrow H_2O$
Molten Carbonate (MCFC)	Liquid solution of lithium, sodium and/or $K_2CO_3$	650 °C	45-60%	> 1 MW	Power Stations	Anode: $H_2 + CO_3^{2-} \rightarrow H_2O + CO_2 + 2e^-$ Cathod: $1/2 O_2 + CO_2 + 2e^- \rightarrow CO_3^{2-}$ Cell: $H_2 + 1/2 O_2 + CO_2 \rightarrow H_2O + CO_2$ ( $CO_2$ is consumed at cathod and produced at anode)
Solid Oxide (SOFC)	Ceramic	1000 °C	50-65%	> 200 kW	Power Stations	Anode: $H_2 + O^{2-} \rightarrow H_2O + 2e^-$ Cathod: $1/2 O_2 + 2e^- \rightarrow O^{2-}$ Cell: $H_2 + 1/2 O_2 \rightarrow H_2O$

### 1.1.3 Polymer electrolyte membrane fuel cells (PEMFCs)

PEMFCs are the most promising candidates for applications such as automobiles, stationary power and power for small electronics such as laptops computers, cell phones etc.<sup>12</sup> A typical fuel cell is made up of three active components (i) an anode (ii) a cathode and (iii) a polymer electrolyte membrane sandwiched between them. Anode and cathode are carbon supported platinum, deposited on the both sides of proton conducting polymer membrane (electrolyte) and the assembly is called as Membrane Electrode Assembly (MEA). The hydrogen is supplied through anode side, where protons and electrons are generated by the dissociation of hydrogen by platinum catalyst. Protons formed at the anode are transported to the cathode through the polymer electrolyte membrane, while electrons are transported from the anode to the cathode by an external circuit through graphite plates. At the cathode side, oxygen is supplied and the protons react with oxygen and electrons to produce water and heat. The basic design of a mono PEMFC cell is shown schematically in Figure 1.1. The chemical equations of the reactions are shown below.



where,  $Q_1$  is the electrical energy and  $Q_2$  is the heat energy.

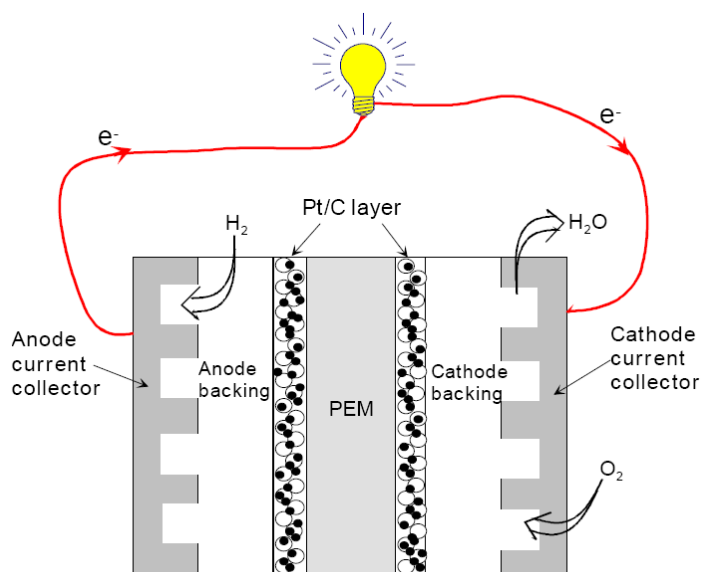


**Figure 1.1** Schematic diagram of PEMFC<sup>13</sup>

Polymer electrolyte membrane is the heart of PEMFC and following are the fundamental prerequisites for a polymeric material to be used as a polymer electrolyte membrane:

- Good mechanical strength (free standing membrane or no dimensional change and strong for MEA preparation)
- High proton conductivity (>0.01 S/cm)
- Low fuel (H<sub>2</sub>, or methanol) and gas (O<sub>2</sub>) crossover
- Good thermal stability
- Good stability in oxidative and reductive environment(sustain to free radicals (HO· and HOO·))
- Long life comparable to Nafion<sup>®</sup> at high temperature at working conditions without loss of efficiency
- Low water drag coefficient
- Low cost

#### 1.1.4 Types of polymer electrolyte membranes

Nafion<sup>®</sup> is the most successful and largely studied membrane in PEMFC technology. Presently, it is the state-of-the-art-material for synthesis of new membranes for PEMFC applications. Broadly polymer electrolyte membranes are classified in to two main categories; sulfonated polymers and non-sulfonated polymers and sulfonated polymers in turn are subdivided into two group's fluorinated and non-fluorinated polymers.

##### 1.1.4.1 Fluorinated polymers

Nafion<sup>®</sup>, among the fluorinated polymers, the most studied and widely used polymer electrolyte membrane for fuel cell applications (Figure 1.2).

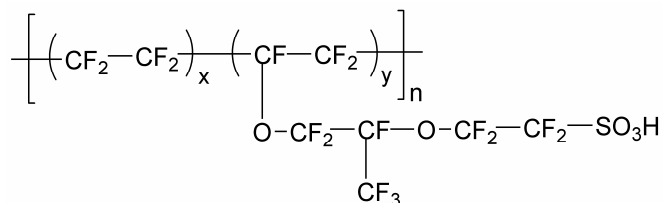


**Figure 1.2** Chemical structure of Nafion<sup>®</sup>

The Nafion<sup>®</sup> membranes are composed of carbon-fluorine backbone with sulfonic acid group in the side chain. The Teflon-like backbone gives the excellent long-term stability in both oxidative and reductive environments. The membrane performs very well below 80 °C under fully hydrated conditions. The proton conductivity is very high (>0.05 S/cm) at room temperature and 100% relative humidity (RH), although the

contents of sulfonic acid group is low (ion-exchange capacity (IEC) is 0.9). The tested lifetime of these membranes is > 60000 h under fuel cell conditions. Although, Nafion<sup>®</sup> offers high proton conductivity, long life time, excellent long-term stability in both oxidative and reductive environments, it has some serious drawbacks. The permeability of both hydrogen and oxygen through the Nafion<sup>®</sup> membrane is high of the order of  $10^{-11}$  to  $10^{-10}$  mol.cm<sup>-1</sup>.S<sup>-1</sup>.atm<sup>-1</sup>. It requires water for proton transport, which limits operational temperature up to 80 °C wherein the dynamics of electrochemical reaction is rather low. Another critical issue is poisoning of platinum catalyst due to absorption of carbon monoxide (CO) present in fuel. This poisoning effect is temperature-dependant, i.e. CO adsorption is less pronounced with increasing temperature. Thus, at 80 °C presence of 10-20 ppm of CO in fuel can poison catalyst, whereas this limit is 1000 ppm at 130 °C, and 30000 ppm at 200 °C. Nafion<sup>®</sup> has high electro-osmotic drag which renders anode dry and flooding at cathode with water during operation, which necessitates proper water management. PEM capable of transporting protons at high temperature without water will not require critical water management.<sup>14</sup> The cost of Nafion<sup>®</sup> membrane is high (Approx. US\$ 600/m<sup>2</sup>),<sup>15</sup> which is another major disadvantage. Some of these shortcomings of Nafion<sup>®</sup> membrane have made researchers to look for alternate cost effective PEM capable of functioning at high temperature (>130 °C) for long period. Subsequently, other fluorinated polymers were prepared such as, Flemion-T,<sup>®</sup> Flemion-S,<sup>®</sup> Flemion-R,<sup>®</sup> Aciplex-S,<sup>®</sup> Dow<sup>®</sup> and Hyflon<sup>®</sup> for high proton conductivity that is generally achieved at high hydration levels. These polymers also have the same drawbacks like Nafion.<sup>®</sup>

#### 1.1.4.2 Non-fluorinated polymers

Development of sulfonated polymer membranes as alternative to Nafion<sup>®</sup> has been another active area in the field. A great number of polymer materials have been prepared and functionalized as membrane electrolytes for PEMFC. These developments are principally motivated to lower the material cost for low-temperature operation, as recently reviewed.<sup>16-22</sup> Most of the sulfonated polymers were developed by post-sulfonation of preformed polymers or copolymerization produced from sulfonated monomers.<sup>23</sup> Besides these, sulfonic acid groups may be introduced through activated functional groups.<sup>23</sup> For developing polymer electrolytes for fuel cells, the most widely investigated systems include various sulfonated polymers such as, polyimide (PI)<sup>24,25</sup> polyetheretherketones (PEEK)<sup>20,26-29</sup> or polyetheretherketonesketone (PEEKK),<sup>30</sup> polyethersulfone (PES)<sup>31-36</sup> Poly(4-phenoxybenzoyl-1,4-phenylene) (PPBP),<sup>20,29,37</sup>

poly(p-phenylenes) (PP)<sup>38</sup> and polyphenylene oxide (PPO).<sup>39</sup> High conductivity is achieved at high degrees of sulfonation, but unfortunately, high sulfonation results in higher swelling leading to poor mechanical properties. Moreover, the proton conductivity of these polymers depends on water and hence fuel cell operations are restricted to below 100 °C.

Considering the disadvantages of sulfonated polymers and advantages of polymer electrolyte capable of operating at high temperature, presently, the research focus has been on the development of high temperature stable polymer ionomers capable of transporting protons in presence of high boiling proton vehicles without water. As a result, basic heterocyclic polymers, which have higher thermal stability, emerged as material of choice for proton conduction.

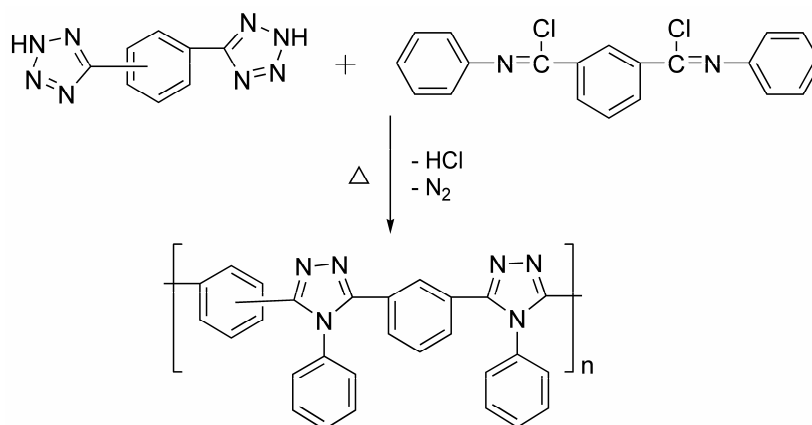
Thus, high performance, thermally stable basic polymers such as polybenzimidazoles (PBI),<sup>40,41</sup> polyoxadiazole (POD)<sup>42,43</sup> and polytriazoles (PT)<sup>44</sup> belonging azole group of polymers attracted attention of many researchers for the development of high temperature polymer electrolytes for fuel cells. These polymers as such have poor conductivity. However, on doping with strong acids, such as sulfuric or phosphoric acid, form acid-base complexes with these acids and conduct protons in absence of water.

Polybenzimidazole (PBI) is one of the most promising candidates as high temperature (>120 °C) proton-exchange membranes. It exhibits good proton conductivity after doping with H<sub>2</sub>SO<sub>4</sub> or H<sub>3</sub>PO<sub>4</sub>. But it has poor solvent solubility, inadequate electrochemical stability, low proton conductivity at low temperature compared to Nafion<sup>®</sup> and tendency for the loss of efficiency due to leaching of dopant by water/methanol.

Polytriazoles and polyoxadiazoles are another class of thermally stable high performance heterocyclic polymers known for their high thermal stability and good chemical resistance. 1,2,4 triazoles and polyoxadiazoles transport protons similar to polybenzimidazoles on complexing with acids, and have enough electrochemical stability to be used in fuel cells conditions as polymer electrolyte. However, the main problem of these polymers is poor processability. These polymers have high softening point and poor solubility in organic solvents. As a result, little attention has been paid towards the application of polymers containing triazole and oxadiazole groups as polymer electrolyte for fuel cells. The present work is focused on synthesis of polybenzimidazoles containing triazole and oxadiazole groups in main and side chain to assess possible application of these polymers, as electrolytes for fuel cells.

## 1.2 Polytriazoles

Polytriazoles are important class of heterocyclic high performance polymers, which have high thermal stability, good chemical stability, excellent mechanical properties and good flame resistant properties. They are used in many applications such as thermally stable resins, coating materials, aerospace applications, membrane materials for separation technology and as hole blocking material in organic light emitting diodes. Polytriazoles are polymers with recurring three nitrogen atoms as an integral part in the main chain giving rise to basic nature to the polymers. The first polytriazole was synthesized by C.S. Marval in 1961 and further development in the polytriazoles chemistry resulted in the synthesis of a variety of polytriazoles that provide a wide range of materials. Low molecular weight polytriazole synthesized by Marval is derived from the reaction of either m- or p-phenylene bistetrazole with N,N'-diphenylisophthalimidoyl chloride<sup>45</sup> (Scheme 1.1). High-molecular weight polytriazoles were synthesized by Holsten and Lilyquest in 1965 by reacting precursor polyhydrazide with aniline in PPA, which were soluble in only formic acid and sulfuric acid.<sup>46</sup>



**Scheme 1.1** Synthesis of polytriazoles from bistetrazole and N,N'-diphenylisophthalimidoyl chloride

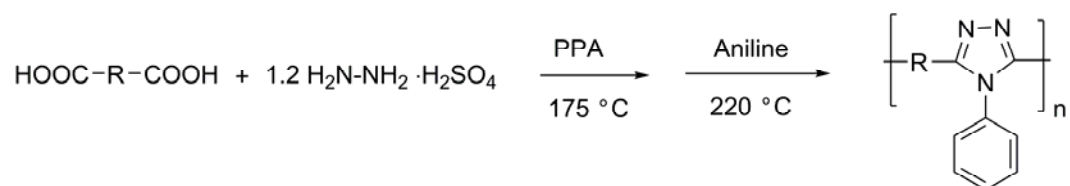
### 1.2.1 Synthetic methods for the preparation of polytriazoles

Since 1961 considerable research work has been carried out to explore the different routes for the synthesis of polytriazoles and now, a number of synthetic methods are available and the most important are:

- One-step polycondensation
- Two-step polycondensation

### 1.2.1.1 One-step polycondensation

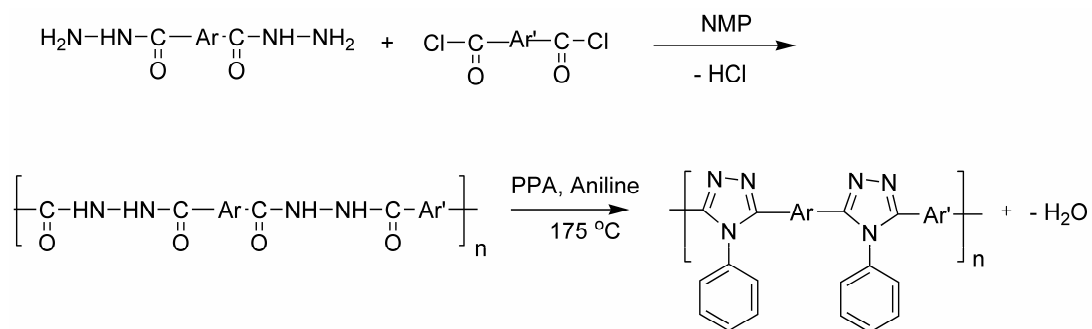
Korshak et al.<sup>47,48</sup> reported the synthesis of polytriazoles through one-step process, which involves a reaction of a dicarboxylic acid with hydrazine sulfate followed by addition of aniline to the reaction mixture and heating in PPA with constant stirring at temperatures between 215 °C and 220 °C for 7-12 h. The resulting polymer was insoluble in organic solvents and soluble in conc. sulfuric acid. The reduced viscosity in sulfuric acid was between 2.7-5.1 dL/g. The residual hydrazide groups were present in polytriazoles (Scheme 1.2).



**Scheme 1.2** Synthesis of polytriazoles by one step-polycondensation

### 1.2.1.2 Two-step polycondensation

This method involves synthesis of precursor polymer, polyhydrazide, which is subsequently cyclocondensed with aniline.



**Scheme 1.3** Synthesis of polytriazoles by two-step polycondensation

Scheme 1.3 describes a two-step process for the synthesis of an aromatic poly(phenylene)4-phenyle-1,2,4-triazole. Preparation of a prepolymer, an aromatic polyhydrazide, is provided by a polycondensation reaction of terephthaloyl-chloride and isophthaloyl-dihydrazide. The polyhydrazide is cyclocondensed at temperatures between 175 °C and 260 °C with aniline in PPA. The time for reaction varied between 24 -140 h. At low temperatures, a molecular weight between 20,000 and 29,000 is achieved. The highest inherent viscosities are obtained when the reaction is carried out at 175 °C for 140 h. A shorter reaction time with higher temperatures results in polymers with lower

viscosity. At high temperature (300 °C) cross-linked polymers is obtained, which is not soluble in sulfuric acid also. The polymers obtained by this method found to contain open chain aniline-polyhydrazide adduct.<sup>46,49</sup>

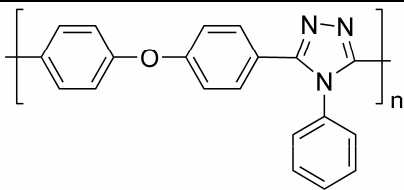
Apart from the above, other numerous methods were tried for the synthesis of polytriazoles.<sup>50-53</sup>

Hergenrother<sup>53</sup> reported synthesis of polytriazoles in two steps. In the first step, arylenedihydrazide is reacted with aromatic dicarboxylic acid chloride to form soluble poly-N-acylhydrazidine and in second step, poly-N-acylhydrazidine was cyclized at 280-300 °C under inert atmosphere or by refluxing in solvents such as m-cresol, NMP or Hexamethylphosphoramide (HMPA). High molecular weight polymer was obtained by this method. The serious drawback of this method is, polytriazoles contain polyoxadiazole as an impurity and films become brittle after thermal treatments.

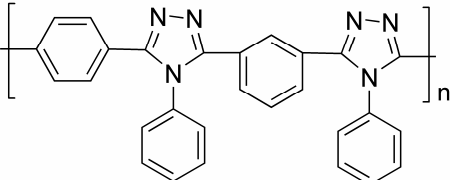
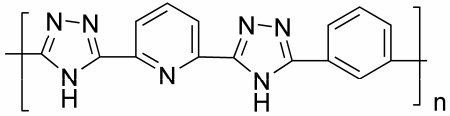
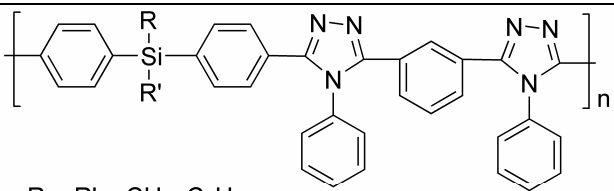
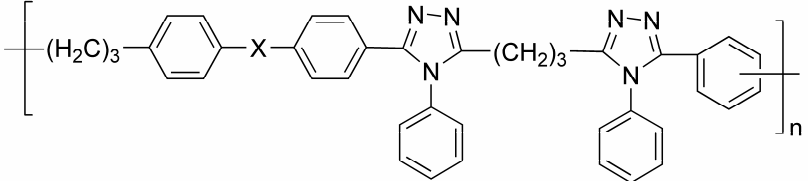
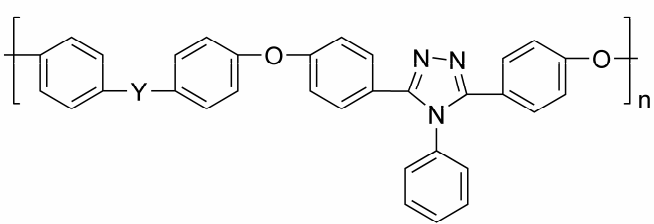
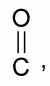
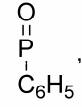
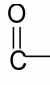
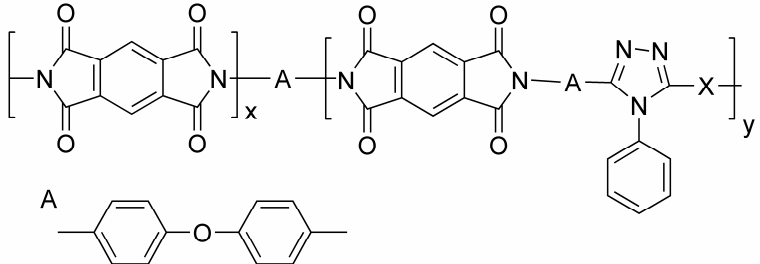
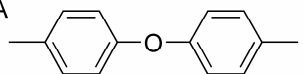
### 1.2.2 Polymers containing triazole groups

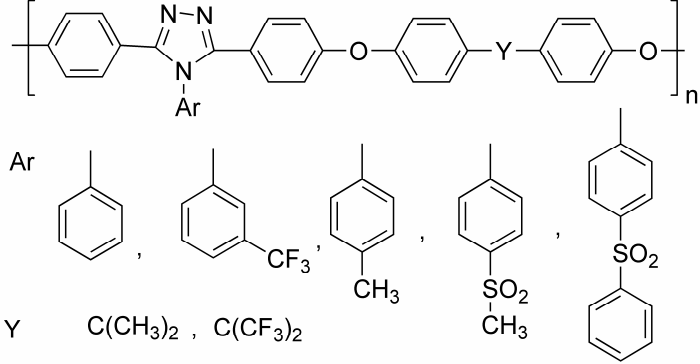
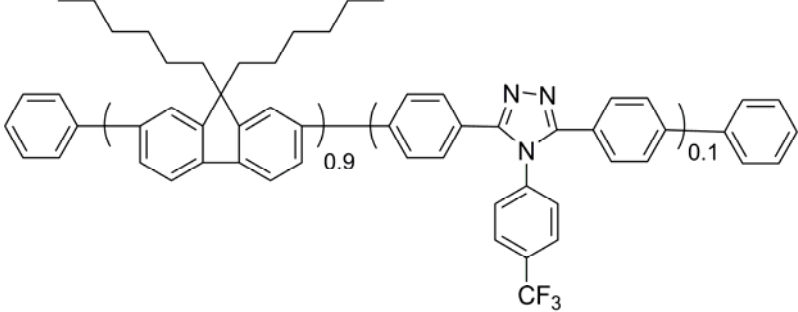
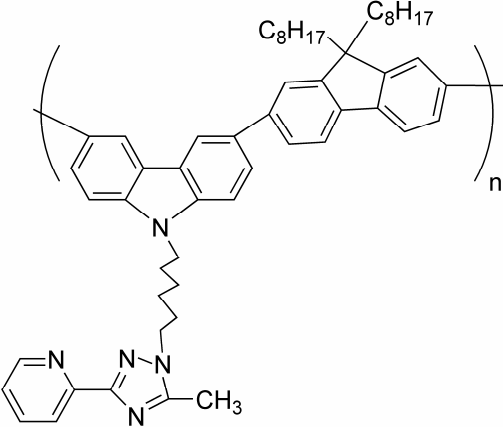
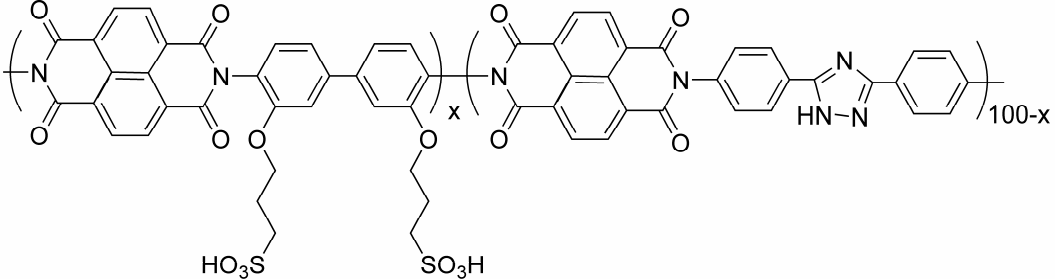
Polytriazoles are not easily processable due to their extreme structural rigidity. The processability is an important criterion without which the polymer becomes merely a laboratory curiosity. Several structural modifications were envisaged i.e. poly(aryl ethers) containing 1,2,4-triazole units,<sup>54</sup> imide-aryl ether 1,2,4-triazole copolymers,<sup>55</sup> 1,2,4-triazole/thiophene alternating copolymers by using palladium-catalyzed polycondensation (Stille-coupling),<sup>56</sup> triazole (triphenyl-1,2,4-triazole derivative) via Suzuki coupling polymerization<sup>57</sup> to overcome these limitations. There is an interest in preparing polytriazoles that are soluble in organic solvents and contain no residual hydrazide groups. The synthesis conditions such as lower reaction times and temperatures, leading to high molecular weight and retaining their chemical and thermal stability are desired. Some polymers containing 1,2,4-triazole groups are summarized below.

**Table 1.2** Structurally modified polytriazoles

Structure of polytriazole	Refs
	48



	58
	53
 <p style="text-align: center;">R = R' = CH<sub>3</sub>, C<sub>6</sub>H<sub>5</sub></p>	59
	60
 <p style="text-align: right;">Y = SO<sub>2</sub>, , ,</p> <p style="text-align: right;"></p>	61
 <p style="text-align: center;">A </p>	55

 <p>Ar</p> <p>Y <math>C(CH_3)_2</math>, <math>C(CF_3)_2</math></p>	54
 <p>CF<sub>3</sub></p>	57
 <p>C<sub>8</sub>H<sub>17</sub></p> <p>C<sub>8</sub>H<sub>17</sub></p> <p>CH<sub>3</sub></p>	62
 <p>HO<sub>3</sub>S</p> <p>SO<sub>3</sub>H</p>	63

### 1.2.3 Applications of polytriazoles to PEM fuel cells

Polytriazoles are basic in nature and form acid-base complexes capable of conducting protons, which are emerging as new candidates for high-temperature polymer electrolyte membrane fuel cells. Recently, there are few reports on polymers containing 1,2,4-triazole, which are used as polymer electrolyte membrane for fuel cell applications.

The introduction of imidazole has generated much excitement in recent years with the hope that the imidazole-based electrolytes may meet the requirements of a new generation PEM fuel cells. However, the electrochemical stability appears to be not enough for fuel cell applications due to high electronic density of imidazole ring. The triazoles are electrochemically stable due to their low electron density. In this view, Siwen Li et al showed that 1*H*-1,2,4-triazole behaves as better proton conductor compared to imidazole. They synthesized and compared the proton conductivity and electrochemical stability of the membranes with composition of Bis(3-methyldimethoxysilyl)polypropylene Oxide) (MDSPPPO), tetraethoxysilane (TEOS), alkoxysilanes with grafted triazole or imidazole (SiHc) and phosphoric acid [2MDSPPPO-2TEOS-2SiHc-5H<sub>3</sub>PO<sub>4</sub>, Hc = 4Tri and Im] .<sup>64</sup> Triazole and imidazole containing above hybrid inorganic-organic polymers showed the proton conductivity in the range of 10<sup>-3</sup> and 10<sup>-6</sup> S/cm respectively at 140 °C under anhydrous conditions. For the electrochemical stability, the cyclic voltammograms (CV) results showed, a large irreversible oxidation peak at +1.0V (vs Ag/Ag+) for imidazole, whereas no such redox peaks were observed for 1*H*-1,2,4-triazole.<sup>64</sup>

Subbaraman et al.<sup>65</sup> reported 4,5-Dicyano-1*H*-[1,2,3]-triazole (DCTz) blended with polyacrylonitrile (PAN) as a proton transport facilitator for polymer electrolyte membrane fuel cells. In the fuel cell testing they found that DCTz have no drastic poisoning effect on platinum and electrochemically stable compound. The proton conductivity of DCTz-PAN blend membranes containing *p*-toluenesulfonic acid (*p*-TsOH) (1:1 molar ratio of *p*-TsOH to DCTz *p*-TsOH) showed in the range of 10<sup>-3</sup> S/cm.

Saito et al.<sup>63</sup> reported a series of sulfonated polyimide copolymers containing 1*H*-1,2,4-triazole groups in the main chains as proton-conducting membranes for fuel cell applications. These triazole containing polyimide ionomer membranes showed better thermal, hydrolytic & oxidative stability, and mechanical properties compared to other polyimide membranes. These ionomer membranes showed low hydrogen and oxygen permeability under dry and wet conditions. The highest proton conductivity (0.3 S/cm at 88% RH) was obtained for the high IEC (2.68 mequiv/g) ionomer membrane.

Surangkha et al.<sup>66</sup> reported random copolymer and terpolymers of 1,2,3-triazole-containing acrylates and poly(ethylene glycol)methyl ether acrylate (PEGMEA), doped with strong acid such as trifluoroacetic acid (TFA), exhibiting the proton conductivity in the order of 0.0005 S/cm at 200 °C. It is believed that proton conductivity increases as the backbone's glass transition temperature decreases and combination of a

low  $T_g$  backbone with a smaller, more mobile, weakly basic heterocyclic motif, such as 1,2,3-triazole increases the proton mobility within the resulting polymer membrane.

Recently, Nunes's group reported a series of papers on sulfonated (oxadiazole-triazole) copolymers as emerging candidates for proton exchange membranes for fuel cell applications.<sup>67,68</sup> More recently, they described sulphonated poly(oxadiazole-triazole) copolymer (SPOD-SPT) membrane doped with 1H-benzimidazole-2-sulphonic Acid (BiSA) as proton conductors at 120 °C and low humidity. The membranes showed high proton conductivities, up to  $4 \times 10^{-3}$  S/cm at 120 °C and low relative humidity (5 and 10%). The membranes also had good mechanical properties and high thermal stability with  $T_g$  up to around 420 °C. They proposed that proton transfer facilitation between protonated (donors) and non-protonated (acceptors) nitrogen and sulphonic groups in BiSA and in the polymer (Scheme 1.3).<sup>69</sup>

Thus, polymers containing triazole groups are identified as possible proton conductors for applications as polymer electrolytes for fuel cells.

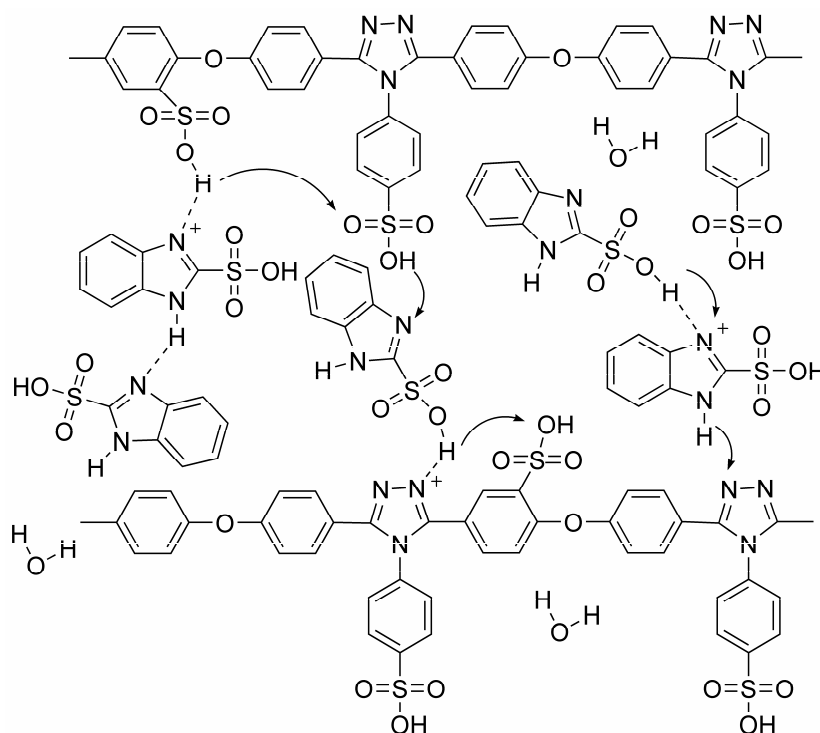


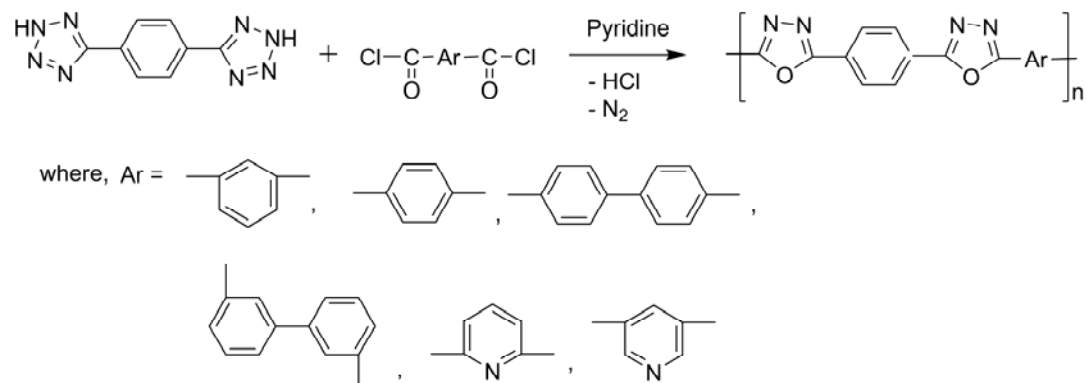
**Figure 1.3** Proton-conducting mechanism in SPOD-SPT/BiSA membranes<sup>69</sup>

### 1.3 Polyoxadiazoles

Aromatic polyoxadiazole are rigid-rod like heterocyclic polymer similar to polybenzimidazole, polybenzoxazoles, polyquinoline and poly(phenyleneterephthalamide) (PPTA) (Kevlar). Polyoxadiazoles are condensation polymers incorporating five membered oxadiazole rings in their polymer repeating units and are generally derived from the reaction of carboxylic diacids or dichlorides with hydrazine sulphate or dihydrazides. Aromatic polyoxadiazole are conjugated in form, basic in nature. The oxadiazole rings are generally strong electron-withdrawing in nature.

Aromatic polyoxadiazoles have been the focus of considerable interest with regard to the production of high-performance materials, because these polymers have high thermal stability up to 450 °C. Besides their excellent resistance to high temperature, polyoxadiazoles have many desirable characteristics, such as good hydrolytic stability, high glass transition temperatures, low dielectric constants, and good mechanical properties. Owing to these excellent physico-mechanical properties and film-forming and fiber-forming capabilities they are considered for use as heat-resistant reinforcing fibers for advanced composite materials.

In 1961, Abshire and Marvel<sup>45</sup> reported first time the preparation of polyoxadiazoles by reaction between ditetrazoles and diacid chlorides in pyridine, as shown in Scheme 1.4 based on the previous work of Huisgenj and co-workers.<sup>70,71</sup> However the obtained polymer was low-molecular weight (IV ~ 0.2 dL/g) and insoluble in organic solvents and soluble in only conc. sulphuric acid.



**Scheme 1.4** Synthesis of polyoxadiazoles by C. J. Abshire and C.S. Marvel method

#### 1.3.1 Synthetic methods for the preparation of polyoxadiazoles

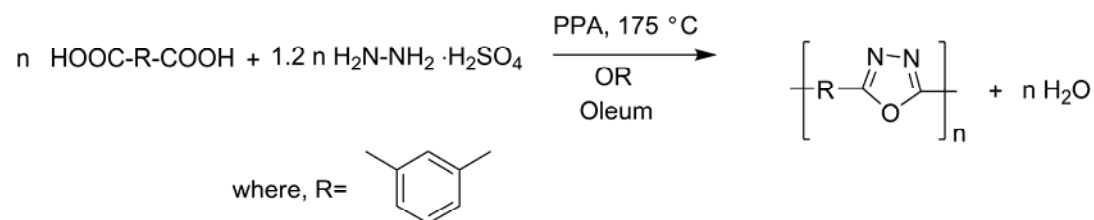
Since 1961, wide varieties of oxadiazole group-containing polymers have been synthesized to improve upon solubility, processability and physico-mechanical

properties. As a result a number of synthetic methods are available and the most important ones are<sup>72</sup>

- One-step polycondensation
- Two-step polycondensation

### 1.3.1.1 One-step polycondensation

This method is extensively used for the synthesis of polyoxadiazoles and involves the polymerization of dicarboxylic acids and hydrazine or hydrazine sulfate in polyphosphoric acid (PPA)<sup>73,74</sup> or fuming sulfuric acid (oleum),<sup>75</sup> which acts as solvent as well as condensing agent.<sup>76</sup> Although, in polycondensation reactions, the equimolar ratio of starting materials is mandatory, excess hydrazine sulfate and a ratio of dicarboxylic acid : hydrazine sulfate (1:1.2) are required to obtain high molecular weight polymers.<sup>76</sup> In presence of oleum, polycondensation is influenced by many reaction parameters such as free SO<sub>3</sub> concentration, concentration of monomers, molar ratio of dicarboxylic acid and hydrazine sulfate and temperature. Using 20-30% excess hydrazine gives the good molecular weight of polymer at reaction temperature between 85-200 °C within 3 h. It is assumed that, high and reproducible viscosities were obtained, when the solid monomers homogenously mixed before the reaction (Scheme 1.5).<sup>75</sup>

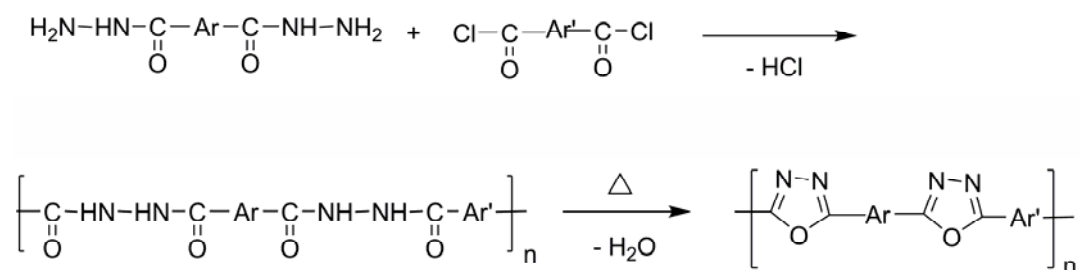


**Scheme 1.5** Synthesis of POD from hydrazine sulfate by one-step polycondensation method

Generally oleum is used in large scale synthesis of POD and shown to be a better solvent than PPA.<sup>75,77</sup> Iwakura et al.<sup>76</sup> and recently Gomes et al.<sup>78</sup> showed that PPA is a better solvent than oleum and can be used for synthesis of high-molecular weight POD. Some of the main advantages being (i) PPA is less hazardous (ii) lower degradation of monomers and polymers during the course of reaction.

### 1.3.1.2 Two-step polycondensation

In this method, POD synthesis is carried out in two stages. Soluble polyhydrazide as a precursor polymer is prepared by the reaction of dicarboxylic acids with diacid chloride which is then converted to the desired POD by heating in dehydrating agents such as PPA or POCl<sub>3</sub> or heating up to 300 °C under vacuum.<sup>49,79-81</sup> (Scheme 1.6). This method was first reported by A. H. Frazer and F. T. Wallenberger<sup>82</sup> in 1964 and provides high molecular weight POD. As polyhydrazides are soluble in many common organic solvents such as DMSO, NMP, DMAc, it offers easy way for formation of desired POD in the form of film or fiber by casting or spinning respectively.



**Scheme 1.6** Synthesis of POD from dihydrazide by two-step polycondensation method

The major drawbacks of this cyclodehydration reaction are (i) prolonged heating at 300 °C for extended periods (100 h) is required to convert polyhydrazide films or fibres into corresponding POD<sup>78,83</sup> (ii) properties of resulting product are strongly influenced by the cyclization temperature and polymer become brittle<sup>49</sup> (iii) residual hydrazide as impurity (iv) cross-linking or side reactions during cyclization (v) shrinkage of final product due to reduction of hydrazide linkages during the ring closure.<sup>84,85</sup> Other methods are attempted to prepare the polyoxadiazoles such as by polycondensation of dicarboxylic acid with hydrazine sulfate in a phosphorus pentoxide/methanesulfonic acid (PPMA) in a weight ratio of 1 : 10. As stated earlier PPMA acts as both condensing agent and as solvent for preparation of polyoxadiazoles.<sup>86</sup> This method has not been investigated further, may be due to drastic degradation of monomers in high acidic PPMA medium. Another method reported in literature to prepare polyoxadiazoles involves the reaction of aromatic dihalides with aromatic dihydrazides and carbon dioxide in the presence of palladium catalyst. However, low molecular weight polymers are obtained by this route.<sup>87</sup>

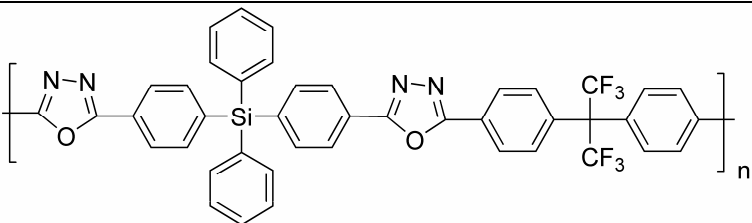
### 1.3.2 Structure-property relationship of aromatic polyoxadiazoles

Aromatic polyoxadiazoles are high performance polymers having high thermo-oxidative stability, excellent mechanical properties, good flame resistance and electrical properties and good chemical resistance. However, these polymers are not easily processable due to their extreme structural rigidity. The processability is an important criterion without which the polymer becomes merely a research interest. The fabrication of most of the unsubstituted aromatic polyoxadiazoles is difficult as a result of their high softening temperatures and their insolubility in common organic solvents. Recently, there has been an increasing demand for new processable engineering plastics having a moderately high softening temperature and solubility in organic solvents. To alleviate this problem a number of strategies were adopted to synthesize soluble/processable polyoxadiazoles without significantly affecting the thermo-mechanical properties as listed below.

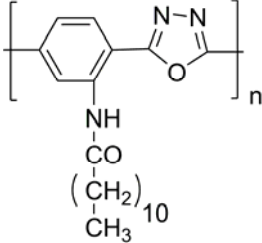
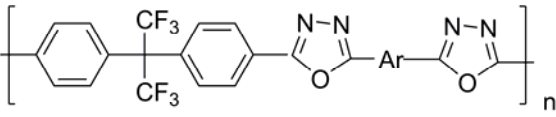
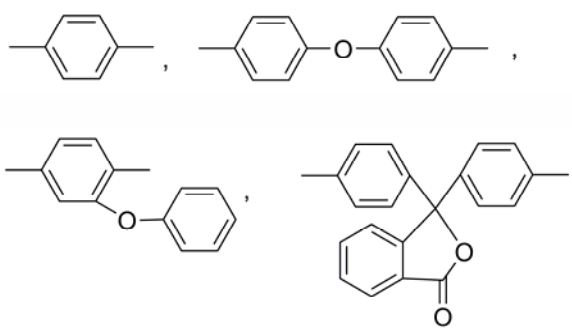
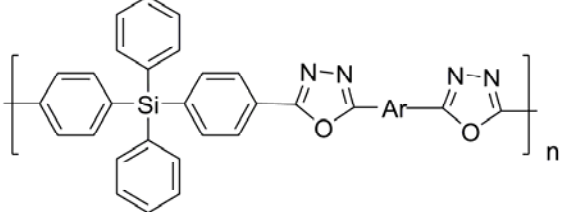
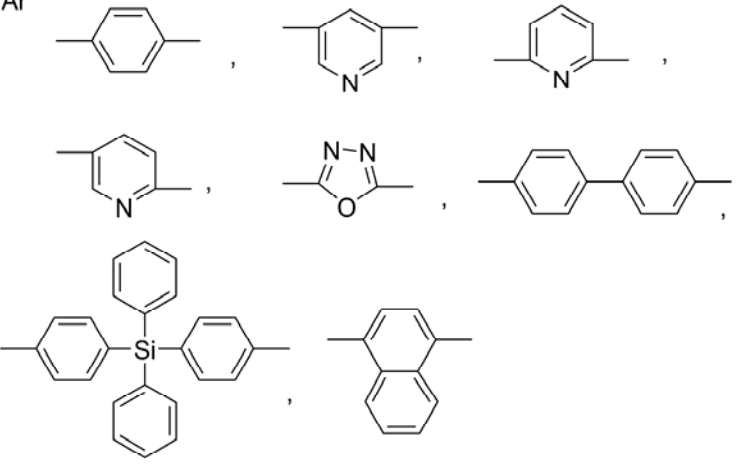
- Introduction of flexible segments or flexible groups, which reduce the chain stiffness
- Incorporation of bulky side substituents, which help for the separation of polymer chains and hinder the molecular packing and crystallization
- Use of such monomers, which suppress coplanar structures
- Use of 1,3-substituted (instead of 1,4-substituted) monomers, and/or asymmetric monomers, which reduce regularity and molecular ordering
- Preparation of copolyoxadiazoles from two or more dicarboxylic acids

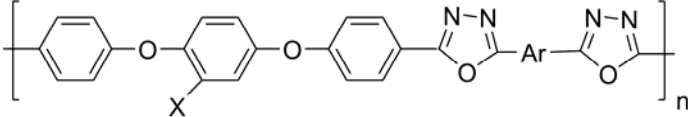
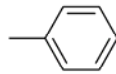
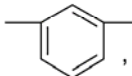
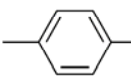
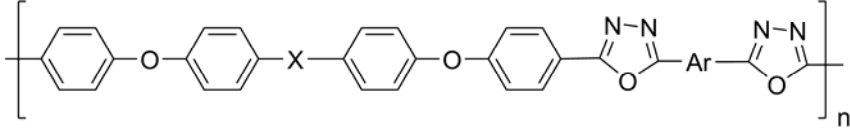
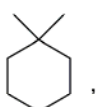
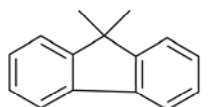
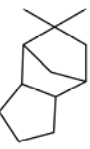
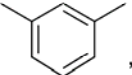
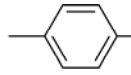
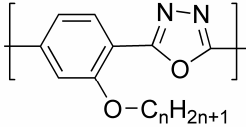
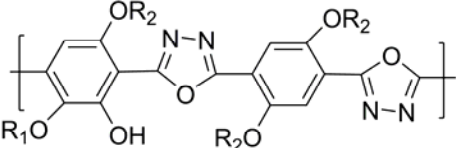
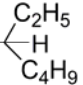
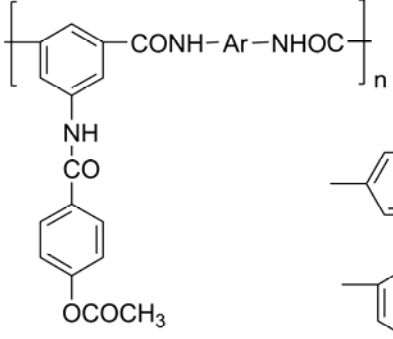
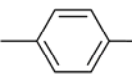
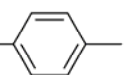
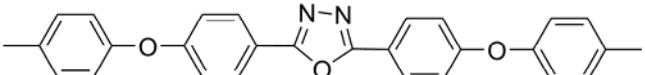
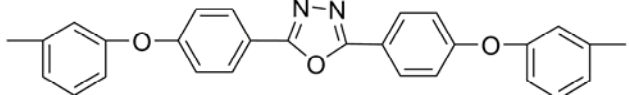
A large variety of oxadiazole polymers have been synthesized from a combination of numerous monomers of dicarboxylate derivatives by one-step polycondensation or two-step polycondensation method. Chosen examples of polyoxadiazole derivatives are summarized in the Table 1.3

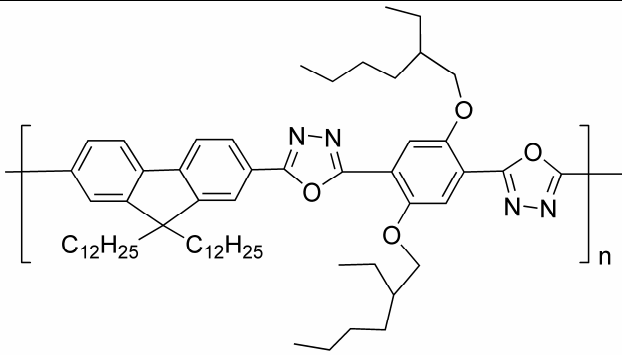
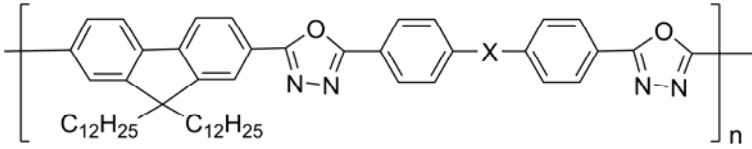
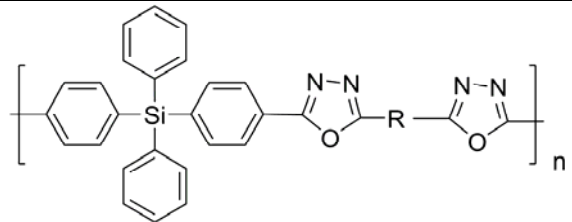
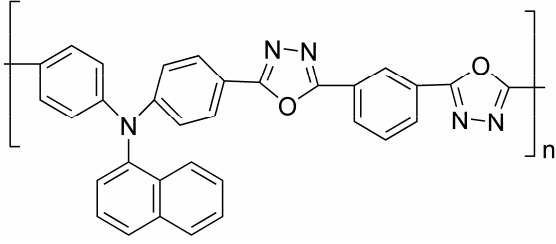
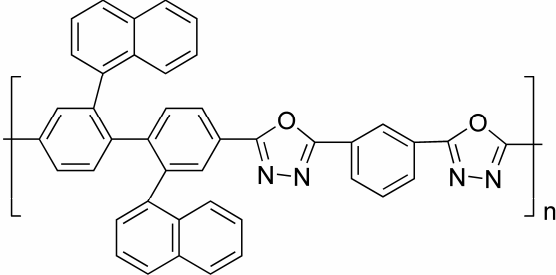
**Table 1.3** Structurally modified polyoxadiazoles

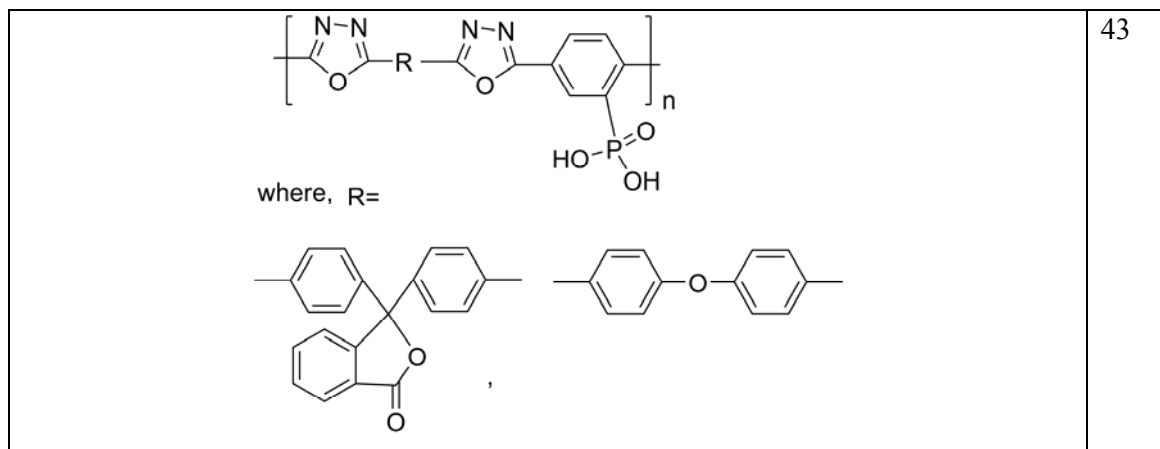
Structures of polyoxadiazoles	Refs
	88



	89
 <p>where, Ar</p> 	90
 <p>where, Ar</p> 	90

 <p>where, X H, -CH<sub>3</sub>, -C(CH<sub>3</sub>)<sub>3</sub>, </p> <p>Ar , </p>	91
 <p>where, X , , </p> <p>Ar , </p>	92
 <p>n = 2, 5, 8, 10</p>	93
 <p>R<sub>1</sub> = CH<sub>3</sub> ; R<sub>2</sub> = H<sub>2</sub>C </p>	94
 <p>where, Ar ,   </p>	95

	96
 <p>where, X = <math>-\text{C}(\text{CF}_3)_2-</math>, <math>-\text{O}-</math></p>	97
 <p>where, R = <math>-\text{C}\equiv\text{C}-</math>, <math>-\text{C}_6\text{H}_4-\text{C}(\text{H})_2-\text{C}_6\text{H}_4-</math>, <math>-\text{C}_6\text{H}_4-\text{C}(\text{H})_2-\text{C}_6\text{H}_4-</math></p>	98
	99
	100



### 1.3.3 Application of polyoxadiazoles to PEM fuel cells

Aromatic polyoxadiazoles are of great interest as high performance materials because of their excellent oxidative, thermal and mechanical properties. Films and fibers of aromatic polyoxadiazoles represent the largest end-use area for the polyoxadiazoles, because of their useful properties over an extremely broad temperature range, such as gas separation and reverse osmosis, flexible printed-circuit boards, electric automobiles, filtration of hot gases, fire-resistant cloths, insulating material in electronic devices, light-emitting diodes for color displays, preparation of high-quality graphite, polymer electrolyte membrane for fuel cells.<sup>42-44,49,72</sup>

Oxadiazole-based polymers have recently attracted considerable attention as polymer electrolyte membranes due to their proton conductivity at high-temperature. The conjugated five member oxadiazole rings contains two nitrogen atoms with lone pair of electrons and one oxygen atom. Like PBI, polyoxadiazoles are basic in nature and capable of conducting protons on doping with phosphoric acid without water and these polymers have drawn attention of many researchers working in this field. Many exploratory investigations are being conducted to examine suitability of polyoxadiazole, doped with strong acids, for the application as polymer electrolyte membrane for fuel cells. The first phosphoric acid doped polyoxadiazole membrane is reported by Zaidi et al.,<sup>42</sup> in 2000. Due to restricted solubility of polyoxadiazoles in organic solvents they prepared the membranes from sulfuric acid by phase inversion method. The membranes were doped in 85% phosphoric acid for 3-4 days. High proton conductivities were obtained ( $10^{-1}$  S/cm at 150 °C) for uncompressed polyoxadiazole membranes, doped with phosphoric acid. It was assumed that the high-proton conductivity is due to acid plugging of the macropores in the membranes providing a conduction pathway through

the liquid phase.<sup>42</sup> More recently, Gomes et al.<sup>67</sup> have published a series of papers on sulfonated polyoxadiazole and poly (oxadiazole-triazole) copolymers based on 4,4'-diphenyl ether dicarboxylic diacid. The resulting polymers were found to be soluble in NMP may be due to the flexibility of diphenyl ether groups. The partial sulfonation (~17%) of poly oxadiazole-triazole copolymer was performed in PPA solutions using hydrazine sulfate. Polymers are in the molecular weight range up to 470,000 g/mol, which showed high-proton conductivity  $10^{-2}$  S/cm at 80 °C exhibiting highly oxidative & mechanical stability.<sup>67</sup>

The same group of researchers<sup>101</sup> also optimized a single-step method for the synthesis of sulfonated polyoxadiazoles from hydrazine sulfate in PPA. The obtained polymer have high-molecular weight about 400,000 g/mol, high thermal stability with  $T_g$  ranging from 364 to 442 °C in sodium salt form and 304 to 333 °C in acid form and good mechanical properties. The ion exchange capacity (IEC) ranged from 1.26 to 2.7 mequiv  $g^{-1}$  with good oxidative stability and proton conductivity in the range of  $10^{-1}$ - $10^{-2}$  S/cm at 80 °C with relative humidity in the range of 100 to 20%.<sup>101</sup>

Polyoxadiazole doped with phosphoric acid for operation at temperatures above 100 °C and low humidity was reported by the same group. It was observed that there is no decrease in the molecular weight when the polymer was exposed to sulfuric acid and oleum mixture for a period of 19 days. Proton conductivity with low doping level (0.34 mol of phosphoric acid per polyoxadiazole repeat unit, 11.6 wt. %  $H_3PO_4$ ) at 120 °C and RH=100% was in the range of up to  $10^{-2}$  S/cm. At lower external humidity (1%) and at 150 °C, proton conductivity values dropped to  $6 \times 10^{-3}$  S/cm. To improve proton conductivity, acid doping and water uptake, they also prepared nano composite with sulfonated silica containing oligomeric fluorinated-based oxadiazole segments. The method improved the doping level and water uptake exhibiting proton conductivity in the order of magnitude of  $10^{-3}$  S/cm at 120 °C and 100% relative humidity compared to the plain membrane<sup>102</sup> in the order of magnitude of  $10^{-5}$  S/cm. In search of better membranes for PEM fuel cells, they prepared nano composite membranes of sulfonated silica (MCM-41) and sulfonated polyoxadiazole polymers based on 4,4-diphenyl ether dicarboxylic acid, which showed good proton conductivity 0.034 S/cm at 120 °C and 25% RH.<sup>103</sup>

Roeder et al.<sup>104</sup> have reported the sulfuric acid doped sulfonated polyoxadiazoles based on the 4,4'-diphenyl ether dicarboxylic acid. The protonation of oxadiazole ring by sulfuric acid (the interaction between the nitrogen atoms of the oxadiazole ring and sulfate anions,  $SO_4^{2-}$ , and  $HSO_4^-$ ) was confirmed by FTIR spectroscopic analysis. They

proposed that, the proton transport is both by dissociation from counter anions and adduct of protonated oxadiazole ring by sulfuric acid. The obtained proton conductivity of sulfonated polyoxadiazole doped with sulfuric acid adduct was 13.3 mS/cm at 50 °C.<sup>104</sup>

Shang et al.<sup>105</sup> have reported fluorene-containing sulfonated poly (arylene ether 1,3,4-oxadiazole) as proton-exchange membrane. They measured the proton conductivity at different temperature at 100% relative humidity and highest proton conductivity was obtained at 100 °C was 0.00413 S/cm. Recently, Shaplov et al.<sup>43</sup> have synthesized pendant phosphonic acid groups containing poly(1,3,4-oxadiazole)s by direct polycondensation of dicarboxylic acids containing phosphonic acid group and their dihydrazides in ionic liquid and thermal cyclization at 350 °C. The resulting polymer membranes showed very low proton conductivity in the range of  $4 \times 10^{-7}$  to  $5 \times 10^{-6}$  S/cm, which is three orders of magnitude lower than that of Nafion<sup>®</sup>

Thus, efforts are being made to develop polymer electrolyte membrane, based on POD, for fuel cells, for high temperature applications. Further inputs are desired for successful applications of POD for PEMFC.

#### 1.4 Polybenzimidazoles

Amongst azole group of polymers, polybenzimidazole (PBI) is extensively studied polymer. After the Second World War, the demand for thermally stable polymers was increased for high-temperature applications, particularly, in aerospace and military segments. To meet the needs of aerospace industries for light-weight materials, a great amount of research was devoted to the synthesis and evaluation of aromatic heterocyclic polymers from 1960s through 1980s. PBI, one of the most successful aromatic polymers, was in focus. The first aromatic analog of polybenzimidazoles was synthesized by Vogel and Marvel<sup>106</sup> in the Noyes Chemical Laboratory, University of Illinois. Before that in 1959, Brinker and Robinson<sup>107</sup> synthesized the first aliphatic analog of polybenzimidazoles.

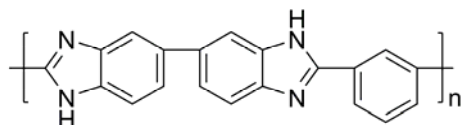


**Figure 1.4** Structure of PBI (Poly 2,2'-(m-phenylene)-5,5' bibenzimidazole)

PBIs are polymers composed of recurring imidazole groups as an integral part of the main polymer chain. It is an amorphous thermoplastic polymer with good chemical

resistance and excellent fiber properties. They have the highest thermal stability among the synthetic heterocyclic polymers, high glass transition temperature, ( $T_g$  420–440 °C), high flame resistance, high chemical resistance and excellent mechanical properties. Hence PBIs, have received much attention for use in modern technologies e.g. in blood dialysis and reverse osmosis at high-temperature and harsh environmental conditions, fire resistant garments and many others.

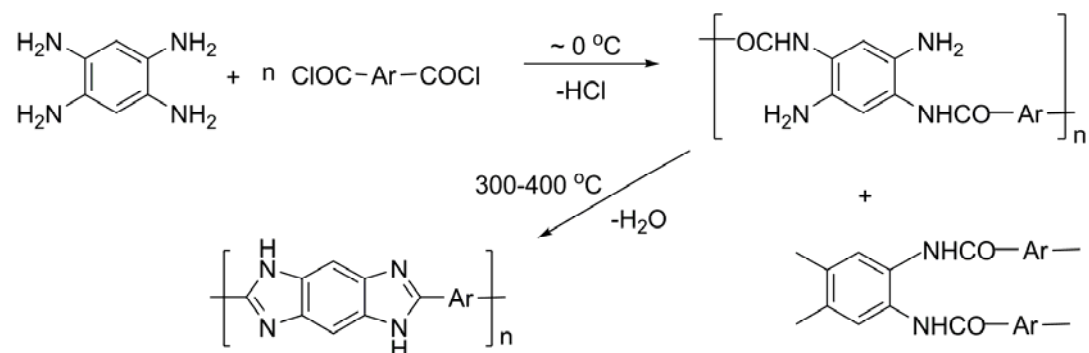
#### 1.4.1 Synthetic methods for the preparation of aromatic PBI

Several synthetic methods for preparation of aromatic PBI have been reported in literature which include,

- Interfacial polycondensation of tetraamines and acid chlorides of diacids
- Polycondensation of tetraamines and dialdehydes
- Polycondensation of dinitro dichlorobenzene with diamine
- Two stage solid/melt polycondensation of tetraamines and dicarboxylic acid esters
- Solution polycondensation of tetraamines and dicarboxylic acid in PPA

##### 1.4.1.1 Interfacial polycondensation of tetraamines and diacid chlorides

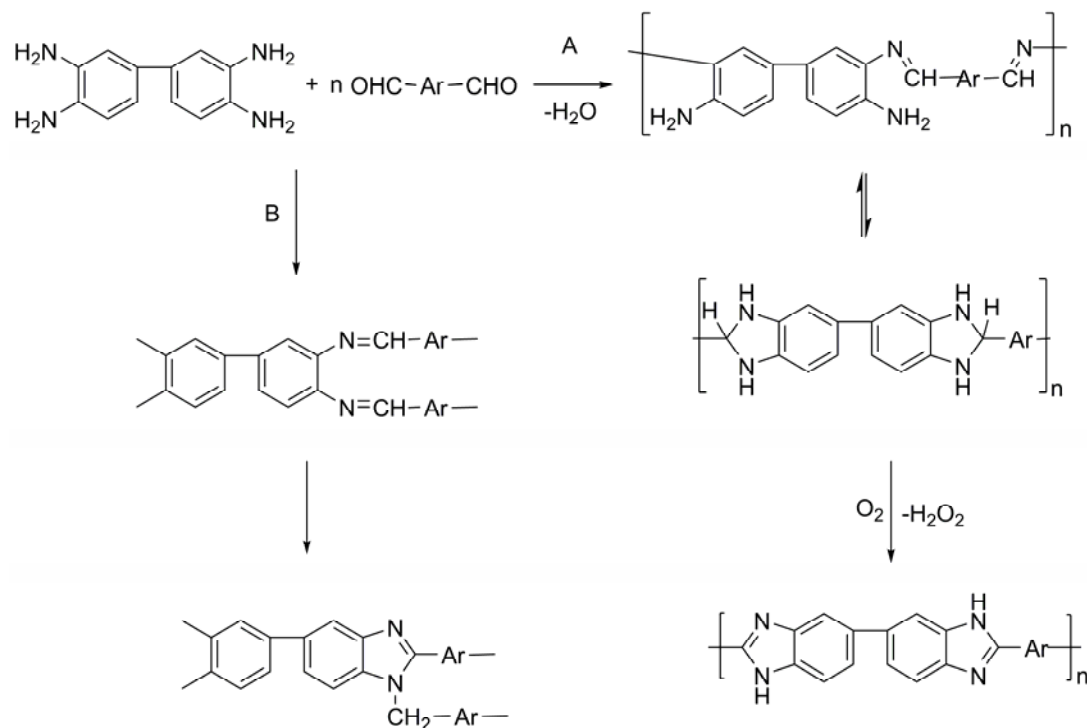
Preparation of PBIs by interfacial polycondensation involves two steps. In first step, polycondensation of tetraamines with diacid chlorides of dicarboxylic acid to form poly (aminoamide) and thermal cyclization of poly(aminoamide) in second step. The isolation of pure poly (aminoamide) is extremely difficult, as there is formation of three-dimensional cross linked polymers (Scheme 1.7).<sup>108</sup>



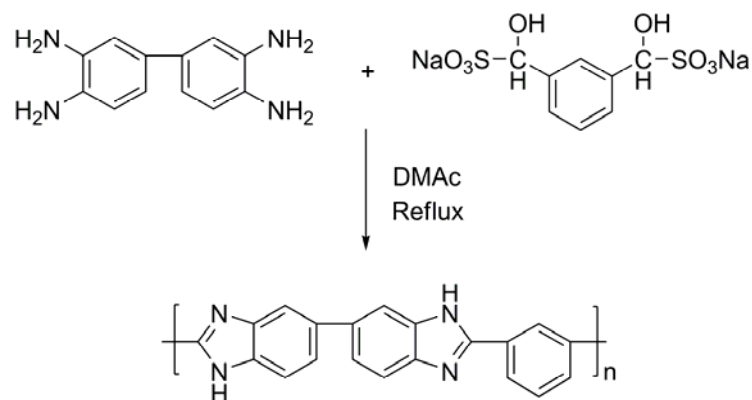
**Scheme 1.7** Synthesis of PBI by interfacial polycondensation

##### 1.4.1.2 Polycondensation of tetraamines and dialdehyde

Tetraamines and dialdehydes are reacted together to yield polyimine that undergoes cyclization on reaction with oxygen with the evolution of hydrogen peroxide as byproduct (Scheme 1.8 path A). Another possibility of this reaction is the formation of disubstituted benzimidazoles (aldehydines), which leads to branching and crosslinking of polymers (Scheme 1.8 path B).<sup>109</sup>



**Scheme 1.8** PBI synthesis from tetraamines and dialdehydes



**Scheme 1.9** PBI Synthesis from tetraamines and isophthalaldehyde bis bisulfite adduct

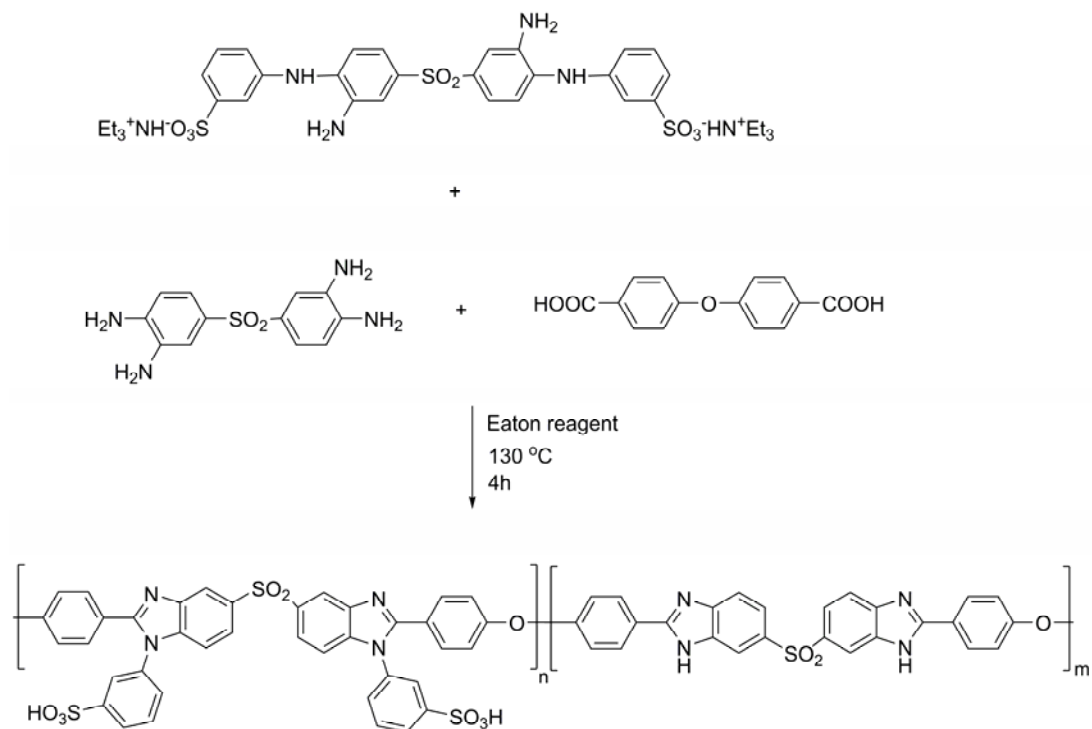
Higgins and Marvel<sup>110</sup> reported the successful synthesis of PBI by the same method, using aromatic tetraamines with isophthalaldehyde bis bisulfite adduct in organic solvents (DMF, DMAc, DMSO) with inherent viscosities in the range of 0.3-



0.5dL/g in formic acid. The cyclization was carried out at refluxing temperature of solvents and completed within 3-5 h (Scheme 1.9).

### 1.4.1.3 Polycondensation of dinitro dichlorobenzene with diamine

Poly (N-phenylbenzimidazole) was prepared by condensation of diamine and dinitro dichlorobenzene followed by reduction of nitro groups in polyamine, to yield poly (o-aminoamine). After benzylation and thermal cyclodehydration poly (N-phenylbenzimidazole) is formed.<sup>109</sup> Recently Mercer et al.<sup>111</sup> have synthesized bis-3-amino-4-[3-(triethylammoniumsulfonato)phenylamino]phenyl sulfone (BASPAPS), monomer for the synthesis of sulfonated polybenzimidazoles by following the above method without benzylation and thermal cyclodehydration. Sulfonated polybenzimidazoles were synthesized further by condensation of BASPAPS, tetraamine and dicarboxylic acid by using Eaton reagent (Scheme 1.10)

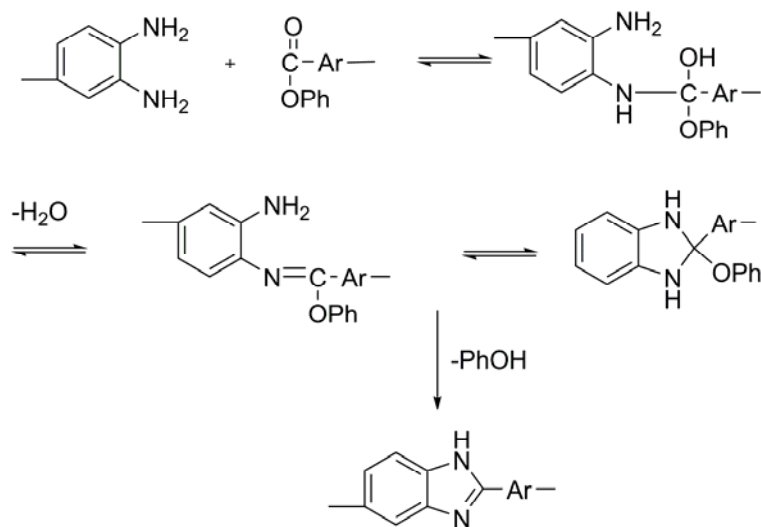


**Scheme 1.10** Synthesis of PBI starting from bis-3-amino-4-[3-(triethylammoniumsulfonato)phenylamino]phenyl sulfone(BASPAPS)

#### 1.4.1.4 Two stage solid/melt polycondensation of tetraamines and dicarboxylic acid esters

Two stage solid/melt polycondensation is an industrial method for synthesis of polybenzimidazoles. In 1983 Celanese, USA commercialized PBI by using diphenyl isophthalate and 3,3',4,4'-tetra-amino biphenyl (TAB) by using this method. Vogel and Marvel<sup>106</sup> have reported the synthesis of aromatic PBI for the first time by two stage solid/melt polycondensation of tetraamines and dicarboxylic acid esters by heating an equimolar mixture of bis(o-diamine)s and the phenyl esters of different dicarboxylic acids. A typical synthesis procedure is briefly described below.

In first stage, a mixture of euqimolar amount of TAB and the phenyl esters of dicarboxylic acids were taken in a flask; the flask was completely deoxygenated by purging with continuous flow of nitrogen. Flask was heated at 250-280 °C for 1-3 h, at that temperature large foam was produced and the byproduct (water and phenol) distilled out. The inherent viscosity of polymer is in the range of 0.1- 0.2 dL/g. In second stage, powdered polymer was heated in inert atmosphere at 400 °C for 5-6 h. High-molecular weight polymer was formed with inherent viscosity ranging from 0.6-1.0 dL/g in H<sub>2</sub>SO<sub>4</sub>. Any residual air in the reaction flask causes formation of insoluble polymer due to cross-linking.



**Scheme 1.11** Proposed mechanism of PBI synthesis by solid stage polymerization

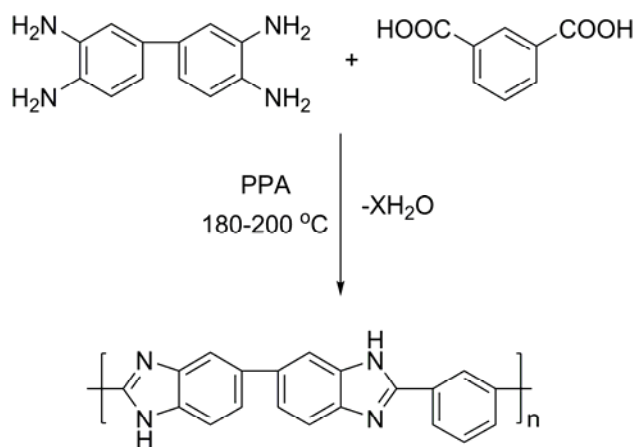
It is interesting to note the mechanism of two-stage solid polycondensation reaction (Scheme 1.11). Nucleophilic amine attacks on the ester carbonyl to form tetrahedral intermediate. On the basis of first elimination of water or phenol, the possible mechanism is decided. However, it has been shown that water is evolved before

phenol to form an imine intermediate, subsequently addition of the second amino group to the carbon-nitrogen double bond gives the imidazole. Elimination of phenol is the rate determining step.

#### 1.4.1.5 Solution polycondensation of tetraamines and dicarboxylic acid in PPA

Solution polycondensation for PBI synthesis can be carried out in high-boiling solvents such as DMAc, DMSO, DMF, NMP,<sup>109</sup> mixture of phosphorus pentoxide ( $P_2O_5$ ) and methanesulfonic acid,<sup>111</sup> PPA,<sup>112</sup> [sulfolane(tetrahydrothiophene-1,1-dioxide)] or phenyl sulfone.<sup>113</sup>

Amongst all the solvents, the use of PPA was found to be most suitable to achieve high molecular weight PBI by reacting tetraamines with dicarboxylic acid. The role of PPA in solution polycondensation is both as solvent and condensing agent. The high-molecular weight polymer was obtained in PPA at 180-200 °C within 8-12 h. Lobato et al.<sup>112</sup> have studied in detail the influence of changes in the dosage of polycondensing agent, catalyst and drying agent on molecular weight. The presence of catalyst and the drying agent did not show any marked effect on molecular weight, whereas there is a significant effect of PPA dosage (optimum dosage for PPA/TAB ratio close to 11 g PPA/mmol TAB). The higher ratio of PPA/TAB may dilute the reaction mixture. However, small amount of PPA may unacceptably increase the viscosity of reaction mixture (Scheme 1.12).



**Scheme 1.12** Synthesis of PBI by Solution polycondensation of tetraamines and dicarboxylic acid in PPA

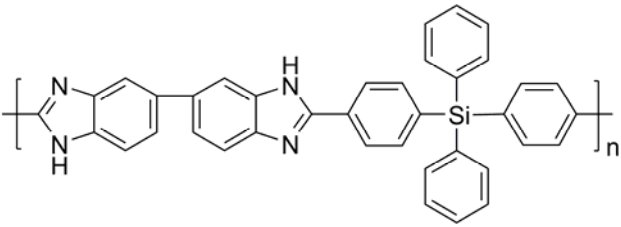
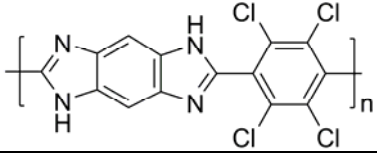
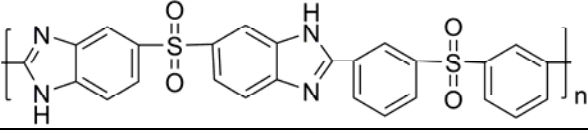
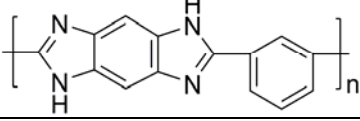
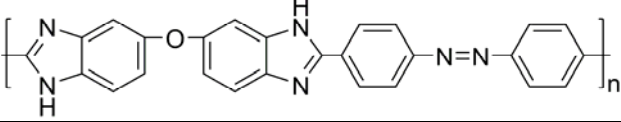
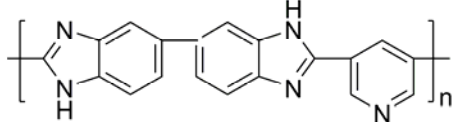
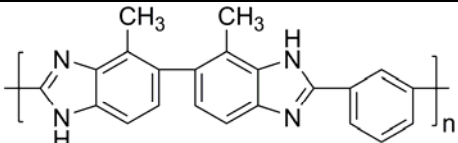
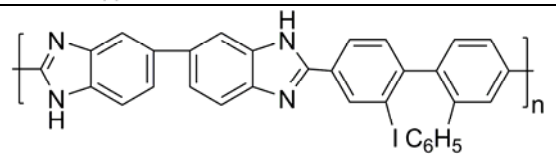
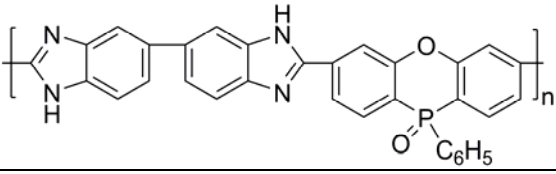
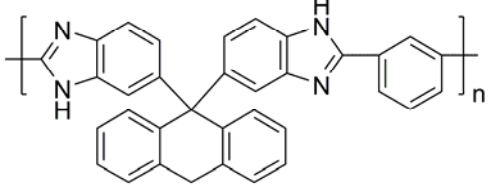
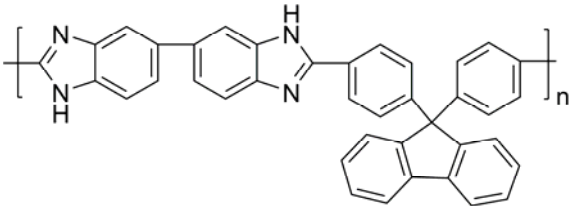
#### 1.4.2 Structural modification of PBI

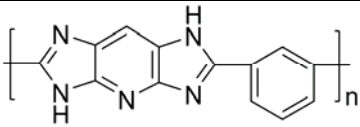
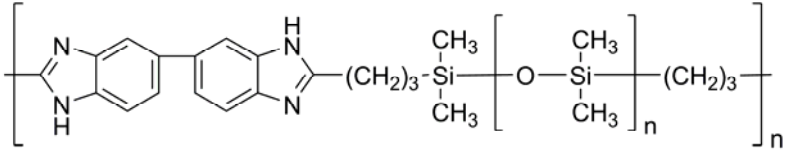
Polybenzimidazoles, due to their unique thermal properties, have received significant attention of several researchers in 1970s. PBIs form miscible blends with

various polyimides, polysulfone, polyarylates, high modulus aramids, and poly (vinyl pyridine) and poly(ether imide).<sup>114</sup> The most commonly used and commercially available PBI is synthesized from TAB and isophthalic acid. Because of high  $T_g$  and poor solvent solubility processing of PBI is difficult. Targeting various applications and improve upon processability, the structure of PBI has been modified by incorporating different functional groups in last five decades and time to time the procedures have been reviewed.<sup>109,115,116</sup> Introduction of an oxygen, siloxane,<sup>117,118</sup> silane,<sup>119</sup> phosphorous,<sup>120</sup> cardo<sup>121</sup> sulfone bridge<sup>122</sup> between aromatic units generally enhance polymer solubility and processability but reduces the thermal stability. Generally incorporation of aliphatic groups reduces the thermal stability and alicyclic groups cyclohexane, cyclopropane, and spiro [3:3]heptane rings, adamantane units<sup>123</sup> in the PBI backbone maintain the thermal stability. Some of the selected examples of reported polybenzimidazoles are summarized in the Table 1.4

**Table 1.4** Chemical structures of selected examples of PBI derivatives

PBI Structures	Refs
	106
	106
	106
	124
	125
	109
	125

	119
	126
	122
	106
	127
	128
	129
	130
	120
	120
	121

	131
	132

### 1.4.3 Applications of PBI

PBI are special class of high-performance polymers and used in specific high-temperature applications. Initially in 1960s and 1970s PBIs received significant attention due to their extraordinary thermal properties and were used in space program for fabrication of break parachute, tether lines, and non-flammable protective suits for astronauts.<sup>133</sup> Presently, PBIs are considered as future candidate as a polymer electrolyte membrane and for high-temperature separation technologies at harsh environmental conditions. Some of the selected applications are summarized below.

#### (i) Fiber and fabrics

PBI fibers are made by dry-spinning in DMAc (20-23% solution) containing 2-3% lithium chloride for improving the solubility. PBI is the only textile fiber, either commercial or developmental, which under normal conditions is nonflammable in air, emits little or no smoke, resists in oxidative environments and produces virtually no toxic gases up to 560 °C. PBI has a useful temperature limit of 560 °C, which is about 200 °C higher than commercial high-temperature organic fibers. PBI fibers show outstanding moisture regain and shrinkage less than 10% between room temperature and 600 °C. These are generally used for protective clothing e.g., in special fire-fighting suits and in light crew clothing for military and space missions.<sup>109</sup>

#### (ii) Matrix resin

PBI has been used as a matrix resin for composite preparation. Pre-impregnated materials of PBI are made by using graphite, quartz and ceramic in fabric, tow and tape forms. PBI composite laminate (PBI/Celion G30-500 8HS) has been potentially used in the tactical missile structures as nose cones, radomes, fins, nozzles casting high speed projectiles, air craft brake assemblies and radiation-resistant structures.<sup>134</sup>

#### (iii) Foams

PBI foams are prepared by heating appropriate amount of diphenyl isophthalate with tetraamines by solid state polycondensation. The prepolymer powder can be combined with reinforcing fibres, such as graphite. The cross-linking can be achieved

thermally or by introducing higher functionality in the reactants. PBI foams have better thermal stability compared to polyisocyanate and polyimide based foams. These materials possess excellent mechanical properties at high and low temperature and display low flame spread, self-ignition, and smoke generation characteristics. Foams are generally used as thermo-insulating materials in autoclaves, aircraft, and aerospace vehicles, jet engine nacelles.<sup>135</sup>

#### **(iv) Separation technology**

PBI membranes have been used as semi permeable membranes for reverse osmosis process such as sea water desalination,<sup>136</sup> ultrafiltration,<sup>137</sup> nanofiltration (removal of chromate from waste water),<sup>138</sup> gas permeability<sup>139</sup> such as H<sub>2</sub>, O<sub>2</sub>, CO<sub>2</sub> etc and blood dialysis.<sup>140</sup>

#### **(v) Adhesives**

PBI has been used as structural adhesive in metal joining specifically in aircraft and space design oriented organization due to the excellent bonding characteristics at high-temperature and even in the cryogenic region below -196 °C.<sup>109</sup>

#### **(vi) Electro-insulation materials**

Plane PBI is not conducting material. It retains its dielectric properties at high-temperature, and have good thermo-oxidative stability at high-temperature and harsh environment and has been used as an insulating material in special cables and wires, circuit boards and radomes for supersonic aircrafts, battery and electrolyte cells.<sup>109</sup>

#### **(vii) Polymer electrolyte membrane for fuel cell**

Recently, it has been shown that acid-doped PBI membrane is considered promising future candidate as a polymer electrolyte for PEMFCs at high-temperature (>120 °C) range. Recent developments of acid-doped PBI membranes are summarized in the following section.

### **1.4.4 Phosphoric acid doped PBI membranes for PEMFCs**

PEMFC technology is presently based on Nafion.<sup>®</sup> Apart from high cost, the main disadvantage of this electrolyte is low operation temperature (<80 °C) as described in detail in Section 1.1.4.1. To overcome this critical problem, Wainright et al.<sup>40</sup> in 1995 successfully developed phosphoric acid or sulfuric acid doped PBI. Undoped PBI is an electronic and ionic insulator,<sup>141-144</sup> which becomes very good ionic conductor when it is doped with acids in proper conditions and remains an electronic insulator after doping. PBI is a basic polymer (pKa ~ 5.5) possessing both proton donor (-NH-) and proton acceptor (-N=), and hydrogen-bonding sites that can easily be doped. The acid-doped

PBI membranes exhibit good proton conductivity and good mechanical and thermal properties at high temperature (200 °C). The unique feature of acid-doped poly (2,2'-(*m*-phenylene)-5,5'-bibenzimidazole) (PBI) membranes over Nafion<sup>®</sup> are:

- (i) Phosphoric acid doped PBI membranes can be operated up to 200 °C with good proton conductivity.
- (ii) Near zero electro-osmotic drag, means water management is not necessary for proton conduction.
- (iii) Low gas permeability and low methanol permeability.
- (iv) Excellent thermal and good mechanical stability up to 200 °C.

These features have made PBI a material of choice for application as membrane material for polymer electrolyte for fuel cells. More details on investigation of PBI as polymer electrolyte membranes for fuel cells are given below.

#### 1.4.4.1 Methods for preparation of acid doped PBI membranes

The acid doped membranes are prepared by several methods described below. (1) Casting from DMAc solution: N,N-dimethyl acetamide (DMAc) is the most widely used solvent for PBI. Generally, 2-5 wt% PBI solutions are prepared in inert atmosphere above the boiling point of DMAc containing 2-3% LiCl for enhancing the solubility. The obtained solution is concentrated to 20 wt% by evaporation. The concentrated solution is poured on a clean glass plate using a Gardner knife or in Petri dish and the majority of the solvent is evaporated in a ventilated oven at 60 to 120 °C. The membranes are then washed with hot water in order to remove the LiCl and residual DMAc. A final drying of membranes is carried out at 200 °C under vacuum and doped by immersion in phosphoric acid solution. (2) Casting from polyphosphoric acid: recently, Xiao et al.<sup>145, 128</sup> have developed a sol-gel process to fabricate PBI-H<sub>3</sub>PO<sub>4</sub> membranes directly from PPA solution obtained after polymerization at 200 °C, without isolation or re-dissolution of the polymer after synthesis. Upon casting, the hydrolysis of PPA to phosphoric acid by moisture induces a sol-gel transition that results in phosphoric acid-doped PBI membranes. (3) Casting from NaOH/ ethanol solution: membranes of PBI, dissolved in NaOH/ ethanol solution, are prepared by solution casting method under nitrogen atmosphere. The films obtained after solvent evaporation are washed with water until pH 7.<sup>146</sup> (4) Membranes in trifluoroacetic acid (TFA): PBI is dissolved in TFA containing phosphoric acid content of desired doping level. The solution is filtered and cast into membranes on a Petri dish under a nitrogen atmosphere.<sup>146</sup> The membrane is then dried at room temperature under vacuum. Most of the PBI membranes reported in the



literatures were prepared by DMAc method; films are observed to be mechanically strong than membranes cast from TFA. To cast films by TFA method, high-molecular weight PBI is necessary. The membranes cast in TFA solution, are softer, rubbery, and more crystalline compared to membranes cast in DMAc.<sup>147</sup>

#### 1.4.4.2 Proton conductivity of acid doped PBI

Wainright et al.<sup>40</sup> first demonstrated PBI, doped with strong acids (i.e., phosphoric acid or sulfuric acid) as a promising electrolyte for high-temperature fuel cells. Most of the published work on doping studies are based on isophthalic acid based polybenzimidazoles, (poly(2,2'-(*m*-phenylene)-5,5'-bibenzimidazole), commonly referred as PBI, which exhibits good proton conductivity, low gas permeability, excellent thermal stability, and good mechanical flexibility at elevated temperatures. PBI doped with other acids such as H<sub>2</sub>SO<sub>4</sub>,<sup>148-152</sup> HClO<sub>4</sub>,<sup>151</sup> HNO<sub>3</sub>,<sup>151</sup> HCl,<sup>151</sup> HBr<sup>149</sup> as well as organic acids like CH<sub>3</sub>SO<sub>3</sub>H, C<sub>2</sub>H<sub>5</sub>SO<sub>3</sub>H<sup>153</sup> also gives good performance for PEMFCs at elevated temperatures. Protonation of acid-doped PBI membranes was studied by different analytical methods such as NMR,<sup>154</sup> IR<sup>150</sup> and Raman spectroscopy.<sup>155</sup> Bouchet and Siebert et al.,<sup>149</sup> have showed that when PBI is doped with phosphoric acid, a very broad absorption band appears at 2500 to 3000 cm<sup>-1</sup>, corresponding to the protonation of nitrogen of imidazole by the transfer of one or more protons from H<sub>3</sub>PO<sub>4</sub> to imidazole groups. As the doping level increases, the intensity of this new band increases at the expense of absorption of both N-H groups at 3415 and the N-H---H groups at 3145 cm<sup>-1</sup>. The intensive absorption bands in the 400-1300 cm<sup>-1</sup> spectral region are characteristic of the anions, predominantly by H<sub>2</sub>PO<sub>4</sub><sup>-1</sup>

The proton conductivity of acid-doped PBI membranes is an important property, which is generally dependent on the acid doping level, temperature and atmospheric humidity. Proton conductivity increases with increasing doping level temperature and humidity. The proton conductivity also depends on method used for doping membranes. Proton conductivity of PBI membranes cast from TFA, direct PPA and DMAc process demonstrate different proton conductivity at high-temperature. Even though the doping level is similar, the properties and proton conductivity of the membranes prepared by different methods vary significantly.<sup>41</sup>

Wide variations are observed in conductivity data of PBI published by various groups. Probably method used for preparing acid doped PBI or cell used for determining conductivity may be responsible for observed variations. At a lower doping levels (< 2 mol H<sub>3</sub>PO<sub>4</sub> per each repeat unit), the conductivity is about 2.5 × 10<sup>-2</sup> S/cm and at higher

doping level 5.7 mol  $\text{H}_3\text{PO}_4$  the proton conductivity is  $7.9 \times 10^{-2}$  S/cm, at 200 °C. It appears that free or unbound acid is necessary to improve the conductivity.<sup>41</sup>

Proton transport in polymer matrix takes place either by vehicular or hopping (Grotthus) mechanism<sup>41</sup> and proton conduction in Nafion<sup>®</sup> is mainly by vehicular mechanism.<sup>18</sup> The proton conductivity in doped PBI follows the Arrhenius law, suggesting a hopping-like conduction mechanism (Figure 1.5). Proton hopping from one N-H site to another contributes little to the conductivity, but proton hopping from one N-H site to phosphoric acid anions contributes significantly through  $\text{H}_2\text{PO}_4^-/\text{HPO}_4^{2-}$ . (Figure 1.5)<sup>41</sup>

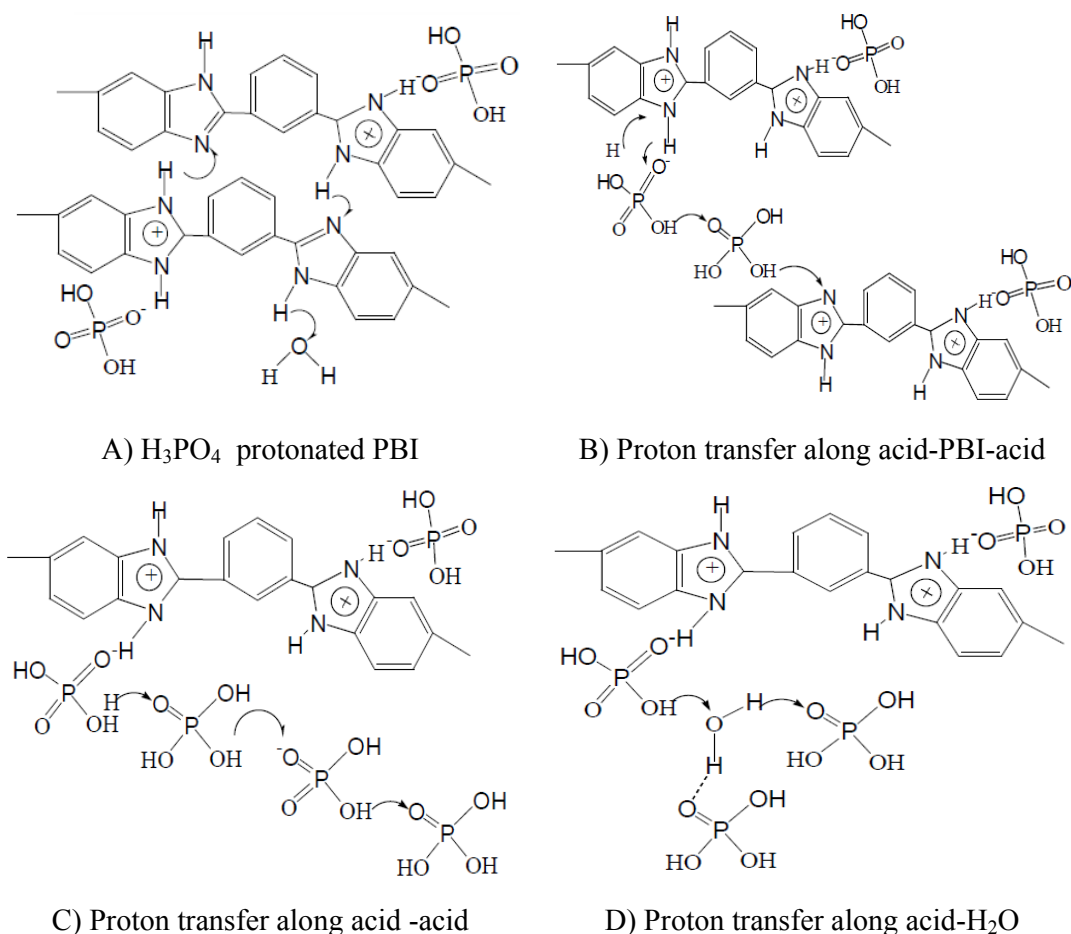


**Figure 1.5** Schematic presentation of proton conduction in acid-doped PBI membranes<sup>41</sup>

Various approaches have been suggested to improve the proton conductivity of acid-doped PBI with respect to different doping level, humidity, temperature as well as incorporating different functional groups in the polymer backbone or in side chain.

Many experimental methods have been investigated in an effort to increase the amount of acid held by PBI. Li et al.<sup>156</sup> showed that PBI doped with 16 moles PA/PRU (phosphoric acid per repeat unit) gives high proton conductivity, 0.13 S  $\text{cm}^{-1}$  at 160 °C.

Generally, it is believed that higher doping levels lead to enhanced proton conductivity and, hopefully, enhance the fuel cell performance. However, at high acid doping level, membranes become mechanically poor and unstable for MEA preparation. Based on their experimental results they suggested that doping level should be within 3.5 to 7.5 mole PA/PRU of PBI to balance reasonably good proton conductivity and mechanical strength.

Lobato et al.<sup>112</sup> studied in detail the physicochemical properties of phosphoric acid doped polybenzimidazole membranes of different molecular weight. They concluded that there is no influence of molecular weight on proton conductivity of membranes. They observed that high-molecular weight of polymer improves both the mechanical resistance and chemical resistance (degradation rate in the Fenton test). Li et al.<sup>157</sup> have found that covalently cross-linked PBIs have better proton conductivity, mechanical strength and chemical resistance than pristine PBI. They used p-xylene dibromide as cross-linking agent to adjust degree of cross-linking between, 1.1 to 13.0. The cross-linked PBI improved the mechanical properties, compared to doped pristine PBI. The oxidative stability of 13% cross-linked PBI was also improved compared to pristine PBI and Nafion<sup>®</sup> 117.

Xiao et al.<sup>145</sup> have developed a new approach for phosphoric acid doped-PBI membrane made by the sol-gel process. The PBI membranes were directly cast in PPA at 200-220 °C without isolation or redissolution of the polymers. They showed that these membranes have high phosphoric acid-doping levels (~32 mole PA/PRU of PBI), good mechanical properties (average tensile strength 1.0 to 3.5 MPa), excellent conductivities (0.26 S/cm at 200 °C), and long-term stabilities, even when operating at over 150 °C.

Mecreyes et al.<sup>158</sup> have prepared porous PBI membranes doped with phosphoric acid, where high doping level up to 14.6 mole PA/PRU of PBI could be obtained. The porous membranes were prepared by the PBI solution containing porogen. The proton conductivity with high levels of doping was up to  $10^{-2}$  S/cm at 140 °C. It is believed that phosphoric acid adsorbed in pores is ultimately responsible to increase the proton conductivity.

Various structural modification in PBI were also tried to enhance proton conductivity of PBI. Xiao et al.<sup>128</sup> have, synthesized PBI containing pyridine group in the main chain. The incorporation of the pyridine group increased the base content of polymer, which in turn increased the solubility, thermo-oxidative stability, acid-uptake capacity and ultimately proton conductivity. Acid-doped membranes were prepared by

sol-gel process with high doping levels (15 to 25 mole of PA per PBI repeat unit). The PBI based on 2,5 pyridine dicarboxylic acid showed high proton conductivity (0.2 S/cm at 200 °C) at high doping levels (20.4 mole PA/PRU of polymer). Xu et al.<sup>159</sup> have synthesized the amine-terminated hyper branched polybenzimidazoles (HBPBIs) by condensation polymerization of aromatic dicarboxylic acids at 190 °C and membranes were cross-linked by using ethylene glycol diglycidyl ether (EGDE) and terephthaldehyde (TPA). The membranes were fabricated by solution cast method. The cross-linked membranes showed better phosphoric acid uptake (572/100g) and proton conductivity (0.064 S/cm) at 170 °C and 0% RH.

Poly (2,5-benzimidazole), or AB-PBI (Figure 1.6) is another polybenzimidazole derivative that has been investigated as an alternative fuel cell membrane material. AB-PBI is directly synthesized from single monomer, 3,4-diaminibenzoic acid in PPA.

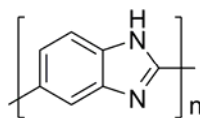


**Figure 1.6** Structure of AB-PBI

Asensio et al.<sup>160</sup> have prepared phosphoric acid doped AB-PBI membranes by casting from methanesulfonic acid followed by doping with phosphoric acid. The appropriate doping was achieved in 70-80% phosphoric which led to high proton conductivity. (PBI  $3.4 \times 10^{-2}$  S/cm 71%  $H_3PO_4$ , 5% RH and for AB-PBI  $3.9 \times 10^{-2}$  S/cm 72%  $H_3PO_4$ , 5% RH at 180 °C).<sup>41</sup> The same group has reported direct casting of AB-PBI membranes from poly (2,5-benzimidazole/phosphoric acid/methanesulfonic acid ) solution. They found that the proton conductivity of AB-PBI 3.0  $H_3PO_4$  PA/PRU was  $1.5 \times 10^{-2}$  S/cm at 180 °C in dry condition.

Uchida et al.<sup>161</sup> have prepared phosphoric acid doped AB-PBI membranes following acid bath doping procedure. Very high proton conductivity (as high as 0.12 S/cm) was observed at below 120 °C, whereas it decreased to 0.025 S/cm above 150 °C, which was attributed to dehydration of the doped acid.

Kim et al.<sup>162</sup> have also developed membranes following a direct casting method from a mixture of AB-PBI, methanesulfonic acid, and  $P_2O_5$ . The proton conductivities ranged from 0.02 to 0.06 S/cm at 110 °C with 0% RH, and doping levels ranged from 1.6 to 3.7 moles PA/PRU of ABPBI.

Thus, effect of various parameters, such as method of doping, doping level, temperature, structure of polybenzimidazole polymer, molecular weight of polymer etc.

on proton conductivity of phosphoric acid doped PBI membranes has been extensively studied, significant literature is available on performance of PBI membranes in H<sub>2</sub>/O<sub>2</sub> fuel cell stacks.

#### 1.4.5 Polybenzimidazoles in H<sub>2</sub>/O<sub>2</sub> fuel cells

The application of H<sub>3</sub>PO<sub>4</sub> doped PBI in H<sub>2</sub>/O<sub>2</sub> fuel cells has been investigated extensively. Wang et al.<sup>163</sup> first demonstrated the use of H<sub>3</sub>PO<sub>4</sub> doped PBI membranes in high temperature H<sub>2</sub>/O<sub>2</sub> fuel cells. They used E-Tek electrodes with a platinum (Pt) loading of 0.5 mg/cm<sup>2</sup> on carbon as electrodes. The results showed no membrane deterioration after a 200 h test at 150 °C. The maximum power was 0.25 W/cm<sup>2</sup> at 700 mA/cm<sup>2</sup> current with H<sub>2</sub> and O<sub>2</sub> gas feed at atmospheric pressure and room temperature humidification. Recent H<sub>2</sub>/O<sub>2</sub> fuel cell results presented by Samms<sup>164</sup> using lower Pt loadings (0.35mg Pt/cm<sup>2</sup> on each electrode) and TFA-cast films (3 mil, 0.0075 cm thick), evaluate the effects of temperature and anode feed gas composition H<sub>2</sub>/25% CO<sub>2</sub>/1% CO) at atmospheric pressure and without humidification. The maximum power density reported was *ca.* 0.4W/cm<sup>2</sup> at 0.5V. The power output rose with temperature, reaching a broad plateau between 175 and 225 °C. The addition of 1% CO to the hydrogen stream decreased the cell potential by 17 mV at 600 mA/cm<sup>2</sup> at 200 °C.

Savadogo and Xing<sup>165</sup> have reported H<sub>2</sub>/O<sub>2</sub> fuel cell results between 50-185 °C at atmospheric pressure with non-humidified gases using sulfuric and phosphoric acid doped PBI membranes. A maximum power output of 0.65 W/cm<sup>2</sup> was reported. They found that the addition of 3% CO to the hydrogen feed had no effect on the polarization curves at 185 °C. Li et al.<sup>166</sup> reported a power density of nearly 0.5 W/cm<sup>2</sup> (at 0.5V), on a H<sub>2</sub>/O<sub>2</sub> fuel cell based on PBI·6.5H<sub>3</sub>PO<sub>4</sub> membrane operating at 190 °C with H<sub>2</sub> and O<sub>2</sub> stream at atmospheric pressure. The power output increased substantially as the temperature was increased from 55 to 190 °C. Furthermore, Li et al.<sup>14</sup> studied the effects of temperature on CO poisoning in PEMFC based on PBI·5.3 H<sub>3</sub>PO<sub>4</sub> membrane operating at temperatures from 125 to 200 °C. By defining CO tolerance as a voltage loss less than 10 mV, it was found that 3% CO in hydrogen could be tolerated at current densities up to 0.8 A/cm<sup>2</sup> at 200 °C, compared to the tolerance of only 0.0025% CO (25 ppm) at 80 °C at current densities up to 0.2 A/cm<sup>2</sup>. Uchida et al.<sup>161</sup> reported the H<sub>2</sub>/O<sub>2</sub> fuel cell performance of ABPBI·1.0 H<sub>3</sub>PO<sub>4</sub> membrane, which was operated at 120 °C and ambient pressure with H<sub>2</sub> and O<sub>2</sub> humidified at room temperature. The performances were not satisfactory with low open circuit potential.

Asensio et al.<sup>167</sup> investigated H<sub>2</sub>/O<sub>2</sub> fuel cell using ABPBI·2.8H<sub>3</sub>PO<sub>4</sub> membrane as electrolyte, which was prepared by casting membranes from (DMAc) solution followed by H<sub>3</sub>PO<sub>4</sub> acid bath doping. The fuel cell showed the best performance at 130 °C with the maximum power densities of 175 mW/cm<sup>2</sup> with humidified gases at room temperature, which was comparable to the maximum power density of 185 mW/cm<sup>2</sup> from PBI·6.4H<sub>3</sub>PO<sub>4</sub> membranes obtained at the same conditions. The fuel cell operating at higher temperatures up to 180 °C showed a small decrease in the maximum power density.

Xiao et al.<sup>128</sup> reported H<sub>2</sub>/O<sub>2</sub> fuel cell using pyridine-based PBI (PPBI) membrane as electrolyte, which was prepared by casting membranes directly from PPA polymerization solution followed by hydrolysis of PPA to PA by atmospheric moisture. The fuel cell showed the best performance at 160 °C with the maximum power density 500 mW/cm<sup>2</sup> without any humidification or external pressure. Seland et al.<sup>168</sup> described the testing of the gas-diffusion electrodes for polymer electrolyte membrane fuel cells utilizing phosphoric acid doped polybenzimidazole (PBI) electrolyte, which allows for an operating temperature as high as 200 °C. In order to determine the optimum structure of anodes and cathodes, they varied the platinum content in the Pt/C catalyst and catalyst loading, as well as the loading of the PBI electrolyte dispersed in the catalyst layer. They tested different MEAs in terms of their performance by recording polarization curves using pure oxygen and hydrogen. It was found that a high platinum content and a thin catalyst layer on both anode and cathode, gave the overall best performance. They attributed it to the different catalyst surface areas, the location of the catalyst in relation to the electrolyte membrane and particularly the amount of PBI dispersed in the catalyst layer. The best performance they obtained was 250 mW/cm<sup>2</sup> at 125 °C and 550 mW/cm<sup>2</sup> at 175 °C of power densities using a catalyst of 50% Pt/C and a relative high PBI loading in the catalyst layer on both anode (0.4 mg cm<sup>-2</sup> Pt, 0.36 mg cm<sup>-2</sup> PBI) and cathode (0.6 mg cm<sup>-2</sup> Pt, 0.6 mg cm<sup>-2</sup> PBI), respectively. Thus, significant work has been conducted on performance of H<sub>3</sub>PO<sub>4</sub> doped PBI membrane in fuel cell stack under fuel cell operational conditions of H<sub>2</sub>/O<sub>2</sub> fuel cells. The results are encouraging. In order to enhance overall performance PBI as PEM for fuel cells, various methods have been tried including structural modifications of PBI. Some of these are given below.

### 1.4.6 Modification of PBI

PBIs are modified in different ways, introducing either sulfonic or phosphoric acid groups via substitution of NH group of imidazole or by incorporating functional groups in the backbone of PBI. The functional modifications of PBI by introducing the sulfonic groups or phosphoric group into the PBI main chain as well as side chain were particularly attractive due to their potential applications in PEM fuel cells.

#### 1.4.6.1 Sulfonated PBI

Three main approaches have been developed to prepare the sulfonated polybenzimidazoles (sPBI): (a) post-sulfonation of PBI or ABPBI by heat treatment with sulfuric acid at high temperatures (450-475 °C)<sup>169-171</sup> (b) chemical grafting of functional monomers (e.g. propanesultone, butanesultone, and sodium (4-bromomethyl) benzenesulfonate) onto PBI chain<sup>37,172</sup> via substitution of NH of imidazole groups and (c) direct polymerization of sulfonated dicarboxylic acid monomers (e.g., 5-sulfoisophthalic acid and 2-sulfoterephthalic acid) with tetraamine.<sup>173-175</sup>

##### 1.4.6.1(a) Post sulfonation of PBI

Post sulfonation of PBI is generally carried out by immersing in dilute sulfuric acid solution, wherein the sulfuric acid protonates the imidazole group of PBI molecule, forming a sulfate ionic salt. After heating, the ionic bond is converted to a permanent, covalent C-S bond. Post sulfonation of PBI depends on both the concentration of sulfuric acid and temperature.<sup>176</sup> Higher sulfonation levels upto about 2.2 SO<sub>3</sub>H/PBI repeat unit are achieved by dissolving PBI powder in a mixture of 96 wt% H<sub>2</sub>SO<sub>4</sub>/P<sub>2</sub>O<sub>5</sub>.<sup>177</sup>

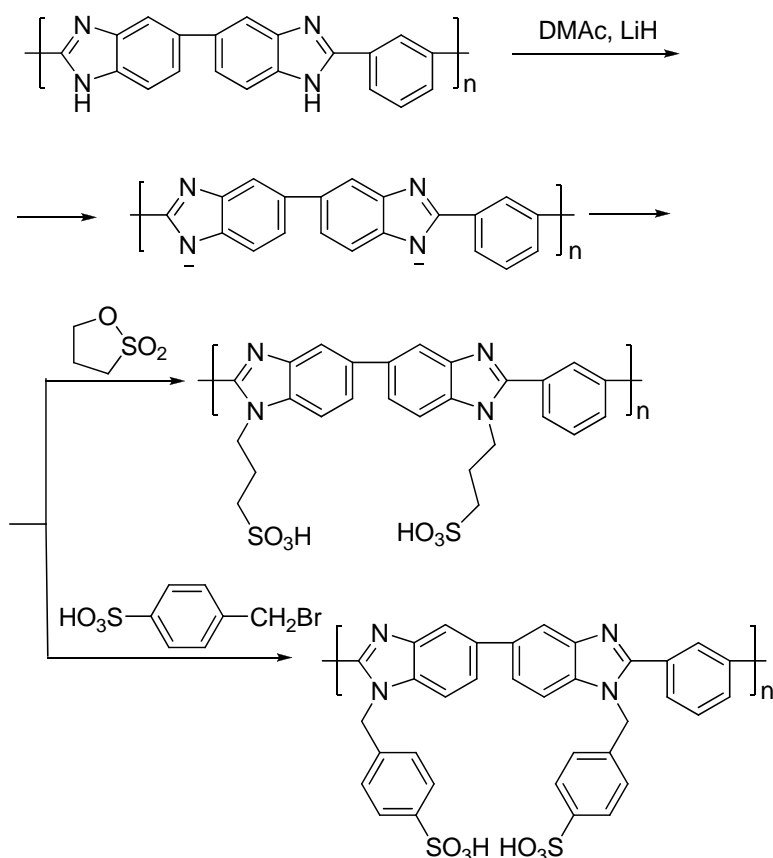
Very low proton conductivity (in the range of 10<sup>-6</sup> S/cm) is reported for sulfonated PBI, containing ~24% of sulfonic acid group/PBI monomer unit.<sup>170</sup> After doping with 4.6 mole of H<sub>3</sub>PO<sub>4</sub>/PRU, 41% sulfonated AB-PBI membranes showed fairly high proton conductivity (3.5×10<sup>-2</sup> S/cm) at 185 °C in dry condition.<sup>178</sup> Xu et al.<sup>179</sup> have carried out sulfonation of poly[2,2'-(p-oxydiphenylene)-5,5'-bibenzimidazole] (SOPBI) using a mixture of concentrated and fuming sulfuric acid at 80 °C and further cross-linked by thermal treatment at 180 °C in vacuo for 20 h. The resulting cross-linked membranes displayed improved radical oxidative and water stability compared to the corresponding uncross-linked polymers. Very high proton conductivity (150 mS/cm at 120 °C) in water could be achieved. Sulfonated PBI prepared by immersing in dilute H<sub>2</sub>SO<sub>4</sub> for 1 h and then heating at 475 °C for 2 min. showed low proton conductivity (7.5 × 10<sup>-5</sup> S/cm at 160 °C and 100% RH).<sup>171</sup>

#### 1.4.6.1 (b) Chemical grafting of PBI

Thermostable proton-conducting polymers may be prepared by introducing alkyl or aryl sulfonated substituents into the PBI backbone and their electrochemical properties can be controlled by varying the number of substituents and the length of alkyl chains. The chemical grafting of N-H in imidazole ring is made easily possible due to its slight acidic nature (N-H group which behaves as a Bronsted acid). PBI can thus be metallated by using the corresponding alkali metal hydrides. This reaction produces hydrogen gas and nucleophilic anionic nitrogens on PBI which may be grafted by reactions with, e.g., sultone and alkyl halides bearing sulfonic acid group (Scheme 1.13). The polymer main-chain retains its rigidity after substitution of the –NH- units because of its fully aromatic nature. The degree of sulfonation can be controlled by the extent of activation of the polymer (number of N-H groups ionized) and the degree of grafting on the activated sites.<sup>172</sup>

The degree of sulfonation could be controlled by the feed ratio and concentration of ionomers. The proton conductivity of membranes at 75% sulfonation level was  $1 \times 10^{-2}$  S/cm (50 °C and 100% RH), which was very close to that of Nafion<sup>®</sup> 117, measured under identical conditions.<sup>172</sup> One major limitations with sulphonated membranes is that they tend to shrink and lose the flexibility and conductivity at low levels of humidity.<sup>148</sup> The dehydration of the membranes leads to the formation of a hydrogen-bonded network, which contributes to the cross linking of the polymer and hence modifies its proton transportation and mechanical properties. In practice, these materials are not suitable in high temperature fuel cells (120-200 °C), where the level of membrane hydration would be very low.<sup>180</sup>





**Scheme 1.13** Synthetic route to sulfonated PBI by chemically grafting of 1,3-propane sultone and 4-bromobenzyl sulfonic acid respectively

Glipta et al.<sup>148</sup> have reported the proton conductivity of  $2 \times 10^{-2}$  S/cm (at 25 °C and 100% relative humidity) for base-doped *N*-benzylsulfonate-grafted PBI. Their contention was after immersing in aqueous organic or inorganic base the network is disrupted leading to rehydration and return to a swollen and flexible state. Rikukawa et al.<sup>37</sup> have synthesized the sulfopropylated PBI (PBI-PS) and observed that water uptake of PBI-PS films increased with increasing in relative humidity and sulfoalkylation level, and the maximum value of water uptake reached 11.3 H<sub>2</sub>O per sulfonic acid group (H<sub>2</sub>O/SO<sub>3</sub>H) at 90% RH. The proton conductivity was fairly high in the range of  $10^{-3}$  at 100-140 °C which was higher than Nafion<sup>®</sup> under similar conditions. They further correlated with sulfobutylated PBI (PBI-BS) and found that fuel cell based on PBI-BS membrane and commercial electrodes showed a maximum power density of 200 mW/cm<sup>2</sup> at 80 °C (H<sub>2</sub>/O<sub>2</sub>, 0.4 mg Pt/cm<sup>2</sup> E-Tek electrode, 0.7A/cm<sup>2</sup> at 0.3V, 100% R.H., ambient pressure).<sup>37</sup> Phosphoethylated PBI was also synthesized by following the same procedure and the resulting polymer was insoluble in organic solvents and membranes could not be casted. The proton conductivity of Phosphoethylated PBI were measured in pressed

pellets form and the value was as high as  $10^{-3}$  S/cm.<sup>20</sup> Sukumar et al.<sup>181</sup> have reported the preparation of soluble form of ethyl phosphonic acid grafted PBI and the proton conductivity of  $H_3PO_4$  doped membrane was as high as  $10^{-1}$  S/cm at 160 °C. They also synthesized the poly (vinyl phosphonic acid)/PBI network by graft-through technique. The maximum proton conductivity achieved was as high as  $2.8 \times 10^{-2}$  S/cm at 160 °C in anhydrous condition for the membrane containing 12 vinyl phosphonic acids per benzimidazole unit.

#### 1.4.6.1 (c) Direct polymerization of sulfonated monomer units

Sulfonated PBI are, in general, synthesized by direct polymerization of sulfonated dicarboxylic acid monomers (e.g. 5-sulfoisophthalic acid and 2-sulfoterephthalic acid) with aromatic tetraamines. The degree of sulfonation can be controlled by using the various stoichiometric ratios of sulfonated and non-sulfonated dicarboxylic acid monomers. Preparations of PBI with sulfonic acid groups directly attached on the aromatic backbone were reported in several papers.<sup>182,183</sup> Asensio et al.<sup>174</sup> have prepared the poly[*m*-(5-sulfo)-phenylenebenzobisimidazole (SMPPBBI) by using 1,2,4,5-tetraaminobenzene tetrahydrochloride 5-sulfoisophthalic acid mono-sodium salt in PPA. They correlated the proton conductivity of sulfonated (SMPPBBI) and non-sulfonated PBI (MPPBBI) with same doping level of phosphoric acid (3.6  $H_3PO_4$ /PRU of polymer). SMPPBBI showed better proton conductivity ( $2 \times 10^{-6}$  S/cm), which was two orders of magnitude higher than that of the nonsulfonated PBI ( $9 \times 10^{-8}$  S/cm). Qing et al.<sup>184</sup> have prepared sulfonated dicarboxylic acid, 4,8-disulfonyl-2,6-naphthalenedicarboxylic acid (DSNDA) monomer, from 2,6-naphthalenedicarboxylic acid by direct sulfonation. Sulfonated PBI (sPBI-NF) were further synthesized from DSNDA, 2,2-bis(4-carboxyphenyl)hexafluoropropane (BIS-B-AF) and 3,3-diaminobenzidine in PPA. They found that polymers were soluble in polar aprotic solvents (e.g. DMF, DMSO and DMAc) and they have good thermal stabilities ( $T_5 > 453$  °C), high glass-transition temperatures ( $T_g > 220$  °C) and high tensile strength (~ 95 MPa). They also measured the proton conductivity of sulfonated PBI prepared from molar feed ratios of DSNDA /BIS-B-AF (60/40) and the value was  $2.7 \times 10^{-3}$  S/cm (90 °C, 100% RH). They ascribed the low proton conductivity due to the strong ionic interaction between the sulfonic acids and basic imidazole groups. The same group also reported the synthesis of sulfonated PBI, by using 5-sulfoisophthalic acid mono-sodium salt, but the proton conductivity and fuel cell applicability of polymer was not reported.<sup>175</sup>

Mercier et al. have synthesized high molecular weight sulfonated PBI from new sulfonated tetraamine by using Eaton reagent (Scheme 1.10) to study the effect of polymer architecture on membrane morphology and proton conduction. They established that sequenced copolymer has 10 times higher proton conductivity than random copolymers. However, the proton conductivity was low ( $10^{-6}$  to  $10^{-4}$  S/cm at room temperature in the hydrated state).<sup>111</sup>

#### 1.4.6.2 Blends of PBI with other polymers

Another method of modification of the properties of polybenzimidazoles is the preparation of blends of PBI with other miscible polymers. PBI is a basic polymer (pKa 5.5) and it possesses both proton donor (-NH-) and proton acceptor (-N=) hydrogen bonding sites. Various polymers having carbonyl and sulfonyl functionality in their backbone can easily take part in the specific interaction with the available hydrogen-bonding sites of the PBI chain and result in miscible blends. A large number of PBI blends with several polymers such as polyimide, poly(ether imide), sulfonated polysulfone, sulfonated poly ether ketone are studied in the literature by various authors in regards to the specific hydrogen bonding interactions involved between the proton donating (-NH-) site of PBI with the proton accepting site of the other polymers.<sup>111,114,134, 185-188</sup>

The concept developed by Kerres et al.<sup>189</sup> is very similar to that of acid/base complexes which consists of mixing strong acids with polymers bearing basic sites. These promising new ionomer blend membranes are synthesised by combining polymeric nitrogen-containing bases (N-bases) with polymeric sulfonic acids. The sulfonic acid groups interact with the N-bases either to form hydrogen bonds or by protonation of the basic N-sites.

The polymer blends of PBI with sulfonated polysulfone (SPSF) for fuel cells was prepared by Hasiotis et al.<sup>190,191</sup> The proton conductivity of the blends was found to be higher than that of pure PBI under the same doping conditions. They obtained conductivity up to  $10^{-1}$  S/cm with  $H_3PO_4$  doping level of  $x = 5$ , at 160 °C and 80% RH for 75%PBI-25%SPSF (70% degree of sulfonation) as compared to  $2.7 \times 10^{-2}$  S/cm for a PBI- $5H_3PO_4$  at 150 °C and 80% RH. At high temperature (150 °C), the mechanical properties were improved for the blend membranes.

Pu et al.<sup>192</sup> studied the blends of PBI/P4VP doped with  $H_3PO_4$ . The thermal stabilities of the blends are lower than that of PBI. The mechanical stability of the blends

at high temperatures is questionable. No fuel cell performance based on these membranes has been shown. They also prepared the blends of PBI/polyimide (PI) and PBI/polyvinylpyrrolidone (PVP). They found that, proton conductivity of H<sub>3</sub>PO<sub>4</sub> doped PBI/PVP and PBI/PI blends increases with increase in temperature, while proton conductivity of H<sub>3</sub>PO<sub>4</sub> doped PBI/PVP and PBI/PI blends decreases with increase in content of PI or PVP in the blend.<sup>193</sup>

Zaidi et al.<sup>194</sup> reported the composite membranes prepared from acid–base polymer blend and solid inorganic proton conductive boron phosphate (BPO<sub>4</sub>). The blends are composed of sulfonated polyetheretherketone (SPEEK) as the acidic component and PBI as the basic component. The contents of solid boron phosphate (BPO<sub>4</sub>) in the composite membrane varied from 10 to 40 wt%. The conductivity of the composite membranes was found to increase with the incorporation of BPO<sub>4</sub> particles into blend membranes. The highest conductivity of  $6 \times 10^{-3}$  S/cm was observed for composite membrane at room temperature

Wycisk et al.<sup>195</sup> reported blends of Nafion<sup>®</sup> and polybenzimidazole (PBI). The dependence of membrane proton conductivity and methanol permeability on the extent of proton substitution of Nafion<sup>®</sup> during blending and on the PBI content of the final membrane was studied. It was found that membrane selectivity (the ratio of proton conductivity to methanol permeability) was the highest (four times that of Nafion<sup>®</sup> 117) when fully protonated Nafion<sup>®</sup> was used during blending and when the PBI content was 8%. DMFC performance of Nafion<sup>®</sup>–PBI membranes (approximately 60 μm in thickness) was found to be superior to that of Nafion<sup>®</sup> 117 at 1.0 and 5.0 M methanol feeds.

Lee et al.<sup>196</sup> also reported proton exchange membranes prepared from blends of PBI and sulfonated poly(arylene thioether)s and investigated in terms of water uptake, swelling, proton conductivity and oxidative chemical stability. PBI-sulfonated polymer blend membranes had a room temperature proton conductivity in the range 0.12–0.22 S/cm and exhibited lower water uptakes and better chemical stability against hydrogen peroxide treatment as compared to that of pure sulfonated polymer membranes. The membrane prepared from the blend of sulfonated poly(arylene thiosulfone)s and PBI showed excellent oxidative stability, displaying no weight loss for 45 h in 5 wt% hydrogen peroxide solution at 60 °C.

## 1.5 Summary

From the foregoing discussions it is undoubtedly clear that the state-of-the-art-material, Nafion<sup>®</sup> is the benchmark for synthesis of the new membranes for PEMFC applications. The major drawback of Nafion<sup>®</sup>, besides high cost, is low proton conductivity at high-temperature and/or it suddenly drops above 90 °C. On the other hand, polybenzimidazoles (PBI), polyoxadiazoles (POD) and polytriazoles have excellent thermal, chemical and mechanical properties and the polymers also display low gas permeability. H<sub>3</sub>PO<sub>4</sub>-doped PBI membranes exhibit good proton conductivity at high temperature (>120 °C) in anhydrous conditions retaining their mechanical properties. Similarly, other acid-base complexes of polyoxadiazole or polytriazole with strong acids also display good proton conductivity at high temperature.

## 1.6 Scope and objective of the present work

Foregoing literature review reveals that acid-doped PBI is one of the most promising candidates for the application as polymer electrolytes for high temperature (>120 °C) proton-exchange membrane fuel cells and presently, it is considered as a material of future, alternative to expensive Nafion<sup>®</sup> type polymers. However, there are still some shortcomings of PBI, such as low solvent solubility, low proton conductivity, compared to Nafion<sup>®</sup>, particularly at low temperature (<80 °C), low electrochemical stability under fuel cell operational condition, fear of leaching out of dopant from polymer matrix by water/methanol loading to loss of efficiency with time, etc. which require further improvements. Various methods such as incorporation of basic pyridine groups and sulfonic acid groups in polymer, blends with sulfonated and other polymers, and synthesis of hyper-branched and cross-linked polymers have been investigated, which met with some success. Parallely, other thermally stable polymers belonging to azole groups of polymers such as polyoxadiazoles or polytriazoles are also under considerations and investigations are under progress to assess possibility of application of these polymers as high temperature polymer electrolyte for fuel cells. However, poor processability is main hurdle of these polymers. Some times combining two types of polymers as copolymers helps to modify the properties. A copolymer of sulfonated poly (oxadiazole-triazole) is one such example. In this respect copolymer containing benzimidazole and oxadiazole groups or copolymer containing benzimidazole and triazole groups have not been investigated as polymer electrolytes for fuel cell, although all these groups interact with strong acids under similar conditions to conduct protons.

As a part of on going research work, to modify the properties of PBI by incorporating other groups, the present work is undertaken to study the effect of oxadiazole and triazole groups on the properties of polybenzimidazole.

Thus, objective of this work is to synthesize polybenzimidazole containing oxadiazole and N-phenyl 1,2,4-triazole groups in main chain and side chain to study the effect of these groups on physical and electro-chemical properties of PBI. Although, polybenzimidazole containing oxadiazole or triazole groups in main chain can be synthesized by condensing dihydrazide, a diacid and a tetraamine or a dihydrazide, a diacid and tetraamine followed by aniline respectively in PPA at high temperature, it is extremely difficult to know the exact composition of resultant polymers due to possible incomplete cyclization. This feature made us to synthesize diacid monomers containing preformed oxadiazole or N-phenyl 1,2,4-triazole groups, shown below.

To compare properties of polybenzimidazole containing 1,2,4-oxadiazole groups in main chain, synthesized by condensation of preformed acid, 3,3'-(1,3,4-oxadiazole-2,5-diyl)dibenzoic acid (ODBA), and those prepared by other method, copolymers containing benzimidazole and 1,2,4-oxadiazole groups were prepared by condensation of dihydrazide, a diacid and a tetraamine in PPA.

Thus present work describes synthesis of and characterization of four diacid monomer, namely, 3,3'-(4-phenyl-4H-1,2,4-triazole-3,5-diyl) dibenzoic acid (PTDBA), 5-(4,5-diphenyl-4H-1,2,4-triazol-3-yl) isophthalic acid (DTIA), 5-(5-phenyl-1,3,4-oxadiazol-2-yl) isophthalic acid (POIA) and 3,3'-(1,3,4-oxadiazole-2,5-diyl) dibenzoic acid (ODBA) (as shown in figures), three of which are new.

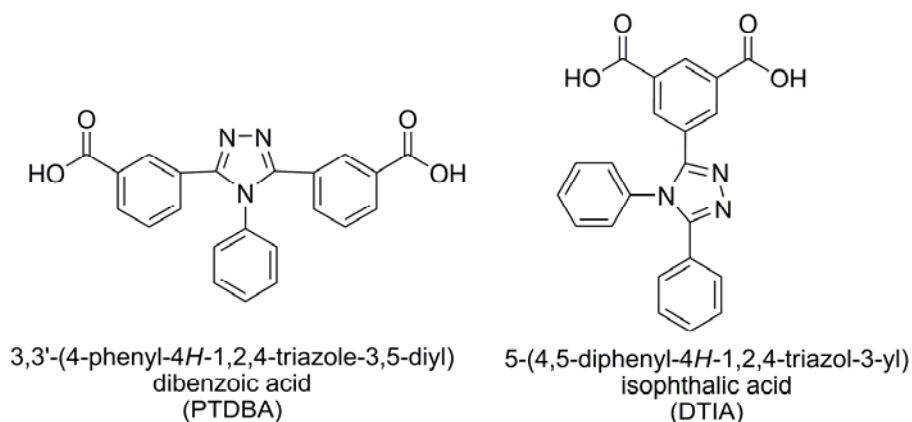


**Figure 1.7** Dicarboxylic acids having triazole group

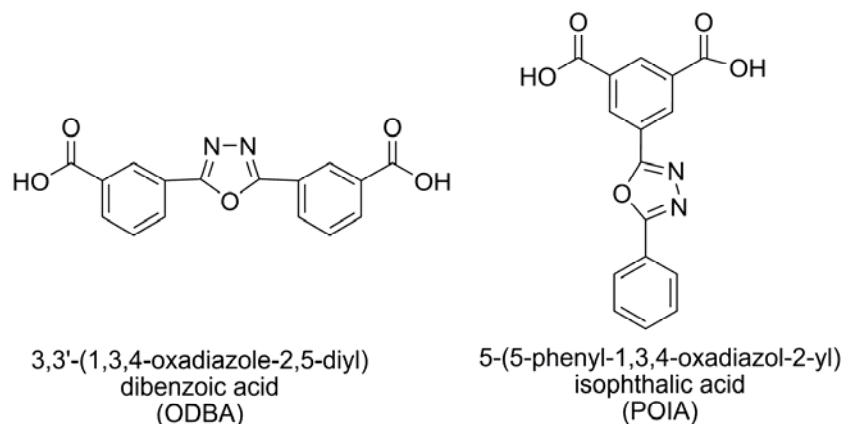


**Figure 1.8** Dicarboxylic acids having oxadiazole group

Further, this work also describes synthesis, characterization and application as polymer electrolyte for fuel cell of novel polybenzimidazoles containing oxadiazole and N-phenyl 1,2,4-triazole groups in main and side chain, based on these diacid monomers and study of polybenzimidazoles containing 1,2,4-oxadiazole groups in main chain, synthesized by two different routes.

## References

- Grove, W. R. *Philos. Mag. J. Sci.*, Ser.3, **1839**, 14, 127-30.
- Mond, L.; Langer, C. *Proc. R. Soc. London Ser. B* **1889**, 46, 296– 308.
- [www.rexresearch.com/jacques/jacques.htm](http://www.rexresearch.com/jacques/jacques.htm)
- Bauer, E.; Ehrenberg, H. E. *Z. Electrochem.* **1912**, 18, 1002.
- Davytan, O. K. *Bull. Acad. Sci. URSS Classe. Sci. Technol.* **1946**, 1, 107–14.
- Broers, G. H. J.; Ketelaar, J. A. A. *Ind. Eng* **1960**, 52, 303-306.
- Bacon, F. T. The high-pressure hydrogen oxygen fuel cell. *Fuel Cells*, ed. GJ Young, **1960**, 5, 51–77. New York: Reinhold
- Zawodzinski, T. A.; Derouin, C.; Radzinski, S.; Sherman, R. J.; Smith, V. T.; Springer, T.E.; Gottesfeld, S. *J Electrochem Soc* **1993**, 140, 1041-1047..
- Gottesfeld, S. *J Electrochem Soc* **1993**, 140, 1041-1047.
- Devanathan, R. *Energy Environ. Sci.*, **2008**, 1, 101–119.
- Fuel Cell Today, Johnson Matthey Public Limited Company. [www.fuelcelltoday.com](http://www.fuelcelltoday.com) (accessed Jan 2005).
- PEM Fuel Cells: Theory and Practice, Barbir, F. Elsevier Academic press, **2005**.
- Winter, M.; Brodd, R.J. What Are Batteries, Fuel Cells, and Supercapacitors? *Chem. Rev.* **2004**, 104, 4245-4270.
- Li, Q.; He, R.; Gao, J.-A.; J. Jensen, O.; Bjerrum, N. J. *Journal of The Electrochemical Society*, **2003**, 150, A1599-A1605.
- DuPont Fuel Cells, Information on Nafion<sup>®</sup> membranes from [www.fuelcells.dupont.com](http://www.fuelcells.dupont.com)

16. Kerres, J. A. *J. Membr. Sci.* **2001**, 185, 3.
17. Savadogo, O. *J. New Mater. Electrochem. Syst.* **1998**, 1, 47.
18. Kreuer, K. D. *J. Membr. Sci.* **2001**, 185, 29.
19. Jones, D. J.; Roziere, J. *J. Membr. Sci.* **2001**, 185, 41.
20. Rikukawa, M.; Sanui, K. *Prog. Polym. Sci.* **2000**, 25, 1463.
21. Inzelt, G.; Pineri, M.; Schultze, J. W.; Vorotyntsev, M. A. *Electrochem. Acta* **2000**, 45, 2403.
22. Kreuer, K. D. In Handbook of Fuel Cells; Vielstich, W., Lamm, A., Gasteiger, H. A., Eds.; John Wiley & Sons Ltd.: New York, **2003**; 3, 420.
23. Hickner, M.A.; Ghassemi, H.; Kim, Y.S. *Chemical Reviews*, **2004**, 104, 4587–4611.
24. Genies, C.; Mercier, R.; Sillion, B.; Cornet, N.; Gebel, G.; Pineri, M. *Polymer* **2001**, 42, 359-373.
25. Guo, X.; Fang, J.; Watari, T.; Tanaka, K.; Kita, H.; Okamoto, K.I. *Macromolecules* **2002**, 35, 6707-6713.
26. Bauer, B.; Jones, D. J.; Roziere, J.; Tchicaya, L.; Alberti, G.; Massinelli, M.; Peraio, A.; Besse, S.; Ramunni, E. *J. New Mater. Electrochem. Syst.* **2000**, 3, 93.
27. Trotta, F.; Drioli, E.; Moraglio, G.; Poma, E. B. *J. Polym. Sci.* **1998**, 70, 477.
28. Shibuya, N.; Porter, R. S. *Macromolecules* **1992**, 25, 6495-6499.
29. Kobayashi, T.; Rikukawa, M.; Sanui, K.; Ogata, N. *Solid State Ionics* **1998**, 106, 219-225.
30. Ise, M.; Kreuer, K. D.; Maier, J. *Solid State Ionics* **1999**, 125, 213-223.
31. Kerres, D.; Cui, W.; Reichle, S. *J. Polym. Sci. Polym. Chem. Part A* **1996**, 34, 2421.
32. Chen, M. H.; Chiao, T.; Tseng, T. W. *J. Appl. Polym. Sci.* **1996**, 61, 1205-1209.
33. Kerres, J.; Cui, W.; Disson, R.; Neubrand, W. *J. Membr. Sci.* **1998**, 139, 211-225.
34. Deimede, V.; Voyiatzis, G. A.; Kallitsis, J. K.; Li, Q.; Bjerrum, N. J. *Macromolecules* **2000**, 33, 7609-7617.
35. Hasiotis, C.; Deimede, V.; Kontoyannis, C. *Electrochim. Acta* **2001**, 46, 2401-2406.
36. Lufrano, F.; Squadrito, G.; Patti, A.; Passalacqua, E. *J. Appl. Polym. Sci.* **2000**, 77, 1250-1256.
37. Bae, J.-M.; Honma, I.; Murata, M.; Yamamoto, T.; Rikukawa, M.; Ogata, N. *Solid State Ionics* **2002**, 147, 189-194.
38. Child, A. D.; Reynolds, J. R. *Macromolecules* **1994**, 27, 1975-1977.
39. Kosmala, B.; Schauer, J. *J. Appl. Polym. Sci.* **2002**, 85, 1118-1127.
40. Wainright, J. S.; Wang, J. T.; Savinell, R. F. and Litt, M. H. *J. Electrochem. Soc.*, **142**, L121, 1995.
41. Ma, Y. L., Wainright, J. S., Litt, M. H., and Savinell, R. F., *J of the Electrochemical Society* **2004**, 151, A8-A16.
42. Zaidi, S. M. J.; Chen, S. F.; Mikhailenko, S. D. and Kaliaguine, S. *J. New Materials Electrochem. Syst.* **2000**, 3, 27-32.
43. Shaplov, A. S.; Lozinskaya, E. I.; Odinets, I. L.; Lyssenko, K. A.; Kurtova, S. A.; Timofeeva, G. I.; Iojoiu, C.; Sanchez, J.-Y.; Abadie, M. J. M.; Voytekunas, V. Y.; Vygodskii, Y. S. *Reactive & Functional Polymers* **2008**, 68, 208-224.
44. Kumagai, M.; Takeoka, Y.; Rikukawa, M. Abs. 190, 204<sup>th</sup> Meeting, © 2003 The Electrochemical Society, Inc.
45. Abshire, C. J. and Marvel, C. S. *Macromol chem.* **1961**, 44-66, 388.



46. Holsen, J. R.; Lilyquist, M. R. *J. Polym. Sci.: Part A* 1965, 3, 3905-3917.
47. Virpsha, Z. O.; Travnikova, A.P.; Krongauz, Y. S. and Korshak, V. V. *Vysokomol. Soyed.* **1969**, A11/1, 69-72.
48. Korshak, V. V.; Dyachenko, A. V.; Krongauz, Y. S. and Berestneva, G. L. *Vysokomol. Soyed.* **1969**, A11/1, 7-10.
49. E. R. Hensema, M. E. R. Sena, M. H. V. Mulder and C. A. Smolders *J. Polym. Sci.: Part A polym. Chem.* **1994**, 32, 527-537.
50. Bates, H.; Fisher, J. W. and Wheatly, E. W. U. S. Pats. 2,512,599; 2,512,600;2,512,601 ; 2,512,624; 2,512,625; 2,512,626; 2,512,627; 2,512,628; 2,512,629; 2,512,630 (1950); assigned to Celanese Corporation of America.
51. Weidinger, H. and Kranz, J. *Chem. Ber.* **1963**, 96, 1064.
52. Saga M. and Shono, T. *J. polym. Sci. Part B* **1966**, 4, 869.
53. Hergenrother, P. M. *Macromolecules* **1970**, 3, 10-16.
54. Carter, K. R.; Miller, R. D. and Hedrick, J. L. *Macromolecules* **1993**, 26, 2209-2215.
55. Carter, K. R.; Miller, R. D. and Hedrick, J. L. *Polymer* **1993**, 34, 843-848.
56. Yasuda, T.; Namekawa, K.; Iijima, T.; Yamamoto, T. *Polymer* **2007**, 48, 4375-4384.
57. Chen, S.-H.; Shiau, C.-S.; Tsai, L.-R.; Chen Y. *Polymer* **2006**, 47, 8436-8443.
58. Gebben, B.; Mulder M. H. V. and Smolders, C. A. *J. Membr. Sci.* **1989**, 46, 29-41.
59. Ghatge, N. D.; Jadhav, J. Y.; and Shinde, B. M. and Mishra, B. M. *J. of Polym Sci. Polym Chem.Part A* **1986**, 24, 103-107.
60. Padma, S.; Mahadevan, V. ; Srinivasan, M. *J. of Polym Sci. Polym Chem.Part A* **1989**, 27, 729-731.
61. Connell, J. W.; Hergenrother, P. M. and Wolf, P. *Polymer* **1992**, 33, 3507-3511.
62. Du, B. Liu, R.; Zhang, Y.; Yang, W.; Sun, W.; Sun, M.; Peng, J.; Cao, Y. *Polymer* **2007**, 48, 245-254.
63. Saito, J.; Miyatake, K. and Watanabe, M. *Macromolecules* **2008**, 41, 2415-2420.
64. Li, S.; Zhou, Z.; Zhang, Y. and Liu, M. *Chem. Mater.* **2005**, 17, 5884-5886.
65. Subbaraman, R.; Ghassemi, H. and Zawodzinski Jr., T. A. *J. Am. Chem. Soc.* **2007**, 129, 2238-2239.
66. Martwiset, S.; Woudenberg, R. C.; Granados-Focil, S.; Yavuzcetin, O.; Tuominen, M. T.; Coughlin, E. B. *Solid State Ionics* **2007**, 178,1398-1403.
67. Gomes, D.; Roeder, J.; Ponce, M.L.; Nunes, S. P. *J. Membr. Sci.* **2007**, 295, 121-129.
68. Ponce, M. L.; Gomes, D.; Nunes, S. P. *J. Membr. Sci* **2008**, 319, 14-22.
69. Ponce, M. L.; Boaventura, M.; Gomes, D.; Mendes, A.; Madeira, L. M. and Nunes S. P. *Fuel Cells* **2008**, 8, 209-216.
70. Huisgenj, R.; Sauer, J.; Sturm, H. J. *Angew Chem.* **1958**, 70, 272.
71. Huisgenj, R. *Angew. Chem.* **1960**, 72, 359.
72. Schulz, B.; Bruma, M. and Brehmer, L. *Advanced Materials* **1997**, 9, 601-613.
73. Souza, F. G.; Sena, Jr. M. E.; Soares, B.G. *J of Appl Polym Sci.* **2004**, 93, 1631-1637.
74. Gomes, D.; Borges, C. P.; Pinto, J. C. *Polymer* **2001**, 42, 851-865.
75. Schulz, B.; Leibnitz E. *Acta Polymerica* **1992**, 43, 343-347.
76. Iwakura, Y.; Uno, K. and Hara, S. *J. of Polym Sci. Polym Chem.Part A* **1965**, 3, 45-54.

77. Iwakura, Y. Uno, K.; Die, S. H. *Macromol Chem* **1966**, 94, 103-113.
78. Gomes, D.; Borges, C. P.; Pinto, J. C *polymer* **2004**, 45, 4997-5004.
79. Sava, I.; Schulz, B.; Zhu, S.; Bruma, M. High Perform. Polym. **1995**, 7, 493,
80. Chernikov, A. Y.; Petrov, G. N.; Bulai, A. K.; Yakovlev, M. N.; Urman, Y. G.; Slonim, Y.; Korshak, V. V.; Vysokomol. Soedin.. Ser. B **1988**, 28, 205.
81. Frazer, A. H. and Reed, T. A. *J. of Polym Sci. Part C* **1967**, 19, 89-94.
82. Frazer, A. H.; Wallenberger, F. T. *J. of Polym Sci. Polym Chem. Part A* **1964**, 2, 1181.
83. Wallenberger, F. T. *Angew. Chimi. Internat. Edit.* **1964**, 3, 460-470.
84. Gebben, B.; Rolevink, E.; Mulder, M. H. V. and Smolders, C. A. *J. of Polym Sci. Polym Chem. Part A* **1989**, 27, 4129-4141,
85. Gebben, B.; Rolevink, E.; Mulder, M. H. V. and Smolders, C. A., *J. of Polym Sci. Polym Chem. Part A* **1988**, 26, 1757-1768.
86. Ueda M. and Sugita, H. *J. of Polym Sci. Polym Chem. Part A* **1988**, 26, 159-166 .
87. Imai, Y.; Kakimoto, M.; Yoneyama M.; Koho J. K. Tokkyo JP02279727, 1990 (Chem. Abstr. **1991**, 114, 208041u
88. Fitch, J. W.; Cassidy, P. E.; Weikel, W. J.; Lewis, T. M.; Trial, T.; Burgess L.; March J. L.; Glowe D. E. and Rolls, G. C. *Polymer*, **1993**, 34, 4796-4798.
89. Schulz, B.; Kaminorz, Y.; Brehmer, L. *Synthetic Metals* **1997**, 84, 449-450.
90. Zhu, S.; Schulz, B.; Bruma, M. and Brehmer L. *Polymers for Advanced Technologies* **1996**, 7, 879-887.
91. Hsiao, S.-H.; Dai, L.-R.; He, M.-H. *J. of Polym Sci. Polym Chem. Part A* **1999**, 37, 1169-1181.
92. Hsiao, S.-H.; He, M.-H. *Macromol. Chem. Phys.* **2001**, 202, 3579-3589.
93. Gillo, M.; Iannelli, P.; Laurienzo, P.; Malinconico, M.; Roviello, A.; Mormile, P. and Petti, L. *Chem. Mater.* **2002**, 14, 1539-1547.
94. Janietz, S.; Anlauf, S. *Macromol. Chem. Phys.* **2002**, 203, 427-432.
95. Iosip, Ion, S.; Maria, M.-D.; Corneliu, B.; Hamciuc, Robison, J.; Okrasa, L.; Tadeusz, P. *European Polymer Journal* **2003**, 39, 725-738.
96. Yang, N. C.; Chang, S.; Yang, N. C.; *Polymer* **2003**, 44, 2143-2148.
97. Yang, N. C.; Park, Y. H. Yang, N. C.; *J. of Polym Sci. Polym Chem. Part A* **2003**, 41, 674-683.
98. Hamciuc, E.; Bruma, M.; Kopnick, T.; Kaminorz, Y.; Schulz B. *Polymer* **2001**, 42, 1809-1815.
99. Liou, G.-S.; Hsiao, S.-H.; Chen, W.-C.; and Yen, H.-J. *Macromolecules* **2006**, 39, 6036-6045.
100. Liou, G.-S.; Hsiao, S.-H.; Fang Y.-K. *J. of Polym Sci. Polym Chem. Part A* **2006**, 44, 6466-6483.
101. Gomes, D.; Roeder, J.; Ponce, M. L.; Nunes, S. P. *Journal of Power Sources* **2008**, 175, 49-59.
102. Gomes, D.; Nunes, S. P. *J. of Membr. Sci.* **2008**, 321, 114-122.
103. Gomes, D.; Marschall, R.; Nunes, S. P.; Wark M. *J. of Membr. Sci.* **2008**, 322, 406-415.
104. Roeder, J.; Gomes, D.; Ponce, M. L.; Abetz, V.; Nunes S. P. *Macromol. Chem. Phys.* **2007**, 208, 467-473.

105. Shang, X. Y.; Shu, D.; Wang, S. J.; Xiao, M.; Meng, Y. Z. *J. of Membr. Sci.* **2007**, 291, 140-147.
106. Vogel, H. and Marvel, C. S. *J. Polym. Sci* **1961**, 1, 511-539.
107. Brinker, K. C.; Cameron D. D.; Robinson I. M. U.S. Patent 2904537, 1959.
108. Gerber A H. US pat. 3943125 (**1976**).
109. Neuse, E. W. *Advances in Polymer Science* **1982**, 47, 1- 42.
110. Higgins, J. and Marvel, C. S. *J. of Polym Sci. Polym Chem.Part A* **1970**, 8, 171-177.
111. Jouanneau, J.; Mercier, R.; Gonon, L. and Gebel, G. *Macromolecules* **2007**, 40, 983-990.
112. Lobato, J.; Canizares, P.; Rodrigo, M .A. ; . Linares, J. J.; Aguilar J. A. *J. of Membr. Sci.* **2007**, 306, 47–55.
113. Hedberg, F. L. and Marvel, C. S. *J. of Polym Sci. Polym Chem.Part A* **1974**, 12, 1823-1828.
114. Musto, P.; Karasz, F. E. and MacKnight, W. J. *Macromolecules* **1991**, 24, 4762-4769.
115. Chung, T.-S. *Polymer Reviews* **1997**, 37, 277–301.
116. Arnold Jr., F. E. and . Arnold, Fred. E *Advances in Polymer Sciences* **1994**, 117, 257-295.
117. Iyakajihia, T. and Marvel, C. S. *J of Polym Sci: Part A-I* **1969**, 7, 1295-1298.
118. Breed, L. W. and Willy Jr, J. C. *Journal of Polymer Science* **1976**, 14, 83-92.
119. Kovacs, H. N.; Delman, A. D. and Simms, B. B *J. of Polym Sci. Polym Chem.Part A* **1968**, 6, 2103-2115.
120. Ato, M.; Yokoyama, M. *J. of Polym Sci. Polym Chem.Part A* **1981**, 19, 591-594.
121. Srnivasan, P. R.; Mahadevan, V. and Srnivasan M. *J. of Polym Sci. Polym Chem.Part A* **1982**, 20, 3095-3105.
122. Lakshmi Narayan, T. V. and Marvel, C. S. *J. of Polym Sci. Polym Chem.Part A* **1967**, 5, 1113-1118.
123. Arthur, S. M.; Schwartz L. *Journal of Polymer Science* **1970**, 3665-3666.
124. Varma, I. K. and Veena *J. of Polym Sci. Polym Chem.Part A* **1976**, 14, 973-980.
125. Foster, R. T. and Marvel, C. S. *Journal of Polymer Science* **1965**, 3, 417-421.
126. Neuse, E. W. and Loonat, M. S. *Macromolecules* **1983**, 16, 128-136.
127. Srnivasan, P. Mahadevan, R. V. and Srnivasan, M. *J of Polym Sci Polym Chem Edition* **1982**, 20, 1145-1150.
128. Xiao, L.; Zhang, H.; Jana, T.; Scanlon, E.; Chen, R.; Choe, E-W.; Ramanathan, L. S.; Yu, S. and Benicewicz, B.C. *Fuel Cells* **2005**, 5, 287-295.
129. Korshak, V. V.; Teplyakov, M. M. and Fedorova, R. D. *J. of Polym Sci. Polym Chem.Part A* **1971**, 9, 1027-1043.
130. Banihashemi, A.; Kiaizadeh, F. *Makromol. Chem.* **1980**, 181, 325 -331.
131. Gerber, A. H. *J. of Polym Sci. Polym Chem.Part A* **1973**, 11, 1703-1719.
132. Mulvaney J. E. and Marvel, C. S. *Journal of Polymer Science* **1961**, L, 541-547.
133. Jackson, R..H. *Textile Research Journal* **1978**; 48: 314-319.
134. Salamone, J. C *Polymeric Materials Encyclopedia Vol 7*, **1996**.
135. Hardy, E.E. and Saunders, J. H. Chapter 14, New High Temperature Resistant Plastic Foams, Part-II, Edited by K. C. Frisch and J. H. Saunders, Marcel Dekker, New York (**1973**).
136. Belohlav, L. R. *Angew Makromol Chem* **1974**, 40/41, 465-483.

137. Presently Available Membranes for Liquid Separation Edited by S. P. Nunes and K.-V. Peinemann 2001 Wiley-VCH Verlag GmbH.
138. Wang, K. Y.; Chung, T.-S. *J. of Membr. Sci.* **2006**, 281 307–315.
139. Kumbharkar, S. C.; Karadkar, P. B.; Kharul, U. K. *J. of Membr. Sci.* **2006**, 286, 161–169.
140. *Encyclopedia of Chemical Processing and Design* Edited by Lee, S. **2005**, 1, 1096.
141. Pohl, H. A.; Chartoff, R. P. *J. Polym. Sci. Part A* **1964**, 2, 2787.
142. Aharoni, S. M.; Litt, M.H. *J. Polym. Sci. Polym. Chem. Ed.* **1974**, 12,,639.
143. Hoel,D., Grunwald, E. *J. Phys. Chem.* **1977**, 81, 2135.
144. Aharoni, S. M.; Signoreli, A. *J. Appl. Polym. Sci.* **1979**, 23, 2653.
145. Xiao, L., Zhang, H.; Scanlon, E.; Ramanathan, L.S.; Choe, E.-W.; Rogers, D.; Apple, T. and Benicewicz, B.C. *Chemistry of Materials*, **2005**, 17, 5328.
146. Litt, M.; Ameri, R.; Wang, Y.; Savinell, R and Wainwright, *J. Materials Research Society*, **1999**, 548, 313.
147. Ameri, R. PhD Thesis, Case Western Reserve University, Cleveland, **1997**.
148. Glipta, X.; Hadda, M. E.; Jones, D. J.; Roziere, J. *Solid State Ionics* **2001**, 145, 61-68.
149. Bouchet, R.; Siebert, E. *Solid State Ionics* **1999**, 118, 287.
150. Glipta, X.; Bonnet, B.; Mula, B.; Jones, D. J.; Roziere, J. *J. Mater. Chem.* **1999**, 9, 3045.
151. Xing, B.; Savadogo, O. *J. New Mater. Electrochem. Syst.* **1999**, 2, 95.
152. Kawahara, M.; Morita, J.; Rikukawa, M.; Sanui, K.; Ogata, N. *Electrochim. Acta* **2000**, 45, 1395.
153. Hiroshi, A.; Masao, I.; Katsutoshi, N.; Hiroyuki, O.; Masaru, I. US 6124060 (**2000**), EP 967674 (**1999**).
154. [Wasmus, S.; Dauch, B. A.; Moaddel, H. Rinaldi, P. L.; Litt, M. H.; Rogers, C.; Valeriu, A.; Mateescu, G. D. and Savinell, R. F. Electrochemical Society Meeting, Reno, NV, May 21-26, **1995**; p 716.
155. Li Q.; Ronghuan, H.; Rolf, W.; Berg, H.; Hjuler, A.; Bjerrum N. J. *Solid State Ionics* 2004, **168**, 177–185.
156. Li Q.; Hjuler H. A. and Bjerrum N. J. *Journal of Applied Electrochemistry* **2001**, 31, 773-779.
157. [Li Q.; Pan, C.; Jensen, J. O.; Noye, P. and Bjerrum N. J. *Chem. Mater.* **2007**, 19, 350-352.
158. Mecerreyes, D.; Grande, H.; Miguel, O.; Ochoteco, E.; Marcilla, R. and Cante, I. *Chem. Mater.* **2004**, 16, 604-607.
159. Xu, H.; Chen, K.; Guo, X.; Fang, J.; Yin J. *J. of Membr. Sci.* **2007**, 288, 255–260.
160. Asensio, J. A.; Borros S. and Gomez-Romero, P. *J. of Membr. Sci.* **2004**, 241, 89-93.
161. Uchida, H.; Yamada, Y.; Asano, N.; Watanabe, M.; Litt, M. *Electrochemistry* **2002**, 70 , 943-945.
162. Kim, H.-J.; Cho, S. Y.; An, S. J.; Eun, Y. C.; Kim, J.-Y.; Yoon, H.-K.; Kweon, H.-J.; Yew, K. H. *Macromol. Rapid Commun.* **2004**, 25, 894–897.
163. Wang, J. T.; Savinell, R. F.; Wainwright, J.; Litt, M. and Yu, H. *Electrochim. Acta* **1996**, 41, 193.
164. Samms, S. Kinetics in an Internal Reforming Fuel Cell, High Temperature PEM Fuel Cell Performance, and a Fundamentals Based Impedance Model, PhD, Case Western Reserve University, Cleveland, OH, **2001**.

165. Savadogo, O. and Xing, B. *J. New Mat. Electrochem. Syst.* **2000**, 3, 345 .
166. Li, Q. F.; Hjuler, H. A. and Bjerrum, N. *J. Electrochim. Acta* **2000**, 45, 4219.
167. Asensio, J. A.; Borros, S. and Gomez-Romero, P. *J. Electrochem. Soc.* **2004**, 151, A304.
168. Seland, F.; Berning, T.; Børresen, B. and Tunold, R. *Journal of Power Sources* **2006**, 160, 27.
169. Asensio, J. A.; Borros, S.; Gomez-Romero, P. *Electrochim Acta* **2004**, 49, 4461–4466.
170. Ariza, M.J.; Jones, D. J.; Roziere, J. *Desalination* **2002**, 147, 183–189.
171. Staiti, P.; Lufrano, F.; Arico, A. S.; Passalacqua, E.; Antonucci, V. *J. of Membr. Sci.* **2001**, 188, 71–78.
172. Glipa, X.; Haddad, M.; Jones, D.J.; Roziere, J. *Solid State Ionics* **1997**, 97, 323–31.
173. Sakaguchi, Y.; Kitamura, K.; Nakao, J.; Hamamoto, S.; Tachimori, H.; Takase, S. *Polym Mater Sci Eng* **2001**, 84, 899–900.
174. Asensio, J.A.; Borros, S.; Gomez-Romero P. *J Polym Sci Part A Polym Chem* **2002**, 40, 3703–10.
175. Qing, S.; Huang, W.; Yan, D. *European Polymer Journal* **2005**, 41, 1589–1595.
176. Wainright, J. S.; Litt, M. and Savinell, R. F. eds., High Temperature Membranes, Handbook of Fuel cell, Fundamentals, Techonology, and Application, Vol. 3, John Wiley & Sons, 2003.
177. Hu, H. Novel Polymer Electrolytes for Rechargeable Lithium Batteries, MS, case Western Reserve University, Cleveland, OH, 1996.
178. Asensio, J. A.; Borros, S.; Gomez-Romero, P. *Electrochemistry Communications* **2003**, 5, 967–972.
179. Xu, H.; Chen, K.; Guo, X.; Fang, J.; Yin, J. *Polymer* 2007, 48, 5556-5564
180. Hogarth, M. and Glipa, X. High temperature membranes for solid polymer fuel cells; ETSU F/02/00189/REP; Johnson Matthey Technology Centre: **2001**.
181. Sukumar, P. R.; Wu, W.; Markova, D.; Unsal, O.; Klapper, M.; Mullen K. *Macromol. Chem. Phys.* **2007**, 208, 2258–2267.
182. Dang, T. D.; Bai, S. J.; Heberer, D. P.; Arnold, F. E. and Spry R. J. *J of Polym Sci: Part B Polym Phy.* **1993**, 31, 1941-1950.
183. Uno, K.; Niume, K.; Iwata, Y.; Toda, F. and Iwakura Y. *J Polym Sci Polym Chem Edition* **1977**, 15, 1309-1318.
184. Qing, S.; Huang, W.; Yan, D. *Reactive & Functional Polymers* **2006**, 66, 219–227.
185. Shogbon, C. B.; Brousseau, J.-L.; Zhang, H.; Benicewicz, B. C.; Akpalu, Y. *Macromolecules* **2006**, 39, 9409.
186. bung, L.; Williams, D. J.; Karasz, F. E. and MacKnight, W. J. *Polym. Bd.*, 1986, 16,457
187. Guerra, G.; Williams, D. J.; Karasz, F. E.; MacKnight, W. J. *Journal of Polymer Science Part B: Polymer Physics* **1988**, 26, 301.
188. Ahn, T. K.; Kim, M. and Choe, S., *Macromolecules* **1997**, 30, 3369.
189. Kerres, J.; Ullrich, A.; Meier, F.; Häring, T. *Solid State Ionics* **1999**, 125, 243.
190. Hasiotis, C.; Qingfend, L.; Deimede, V.; Kallitsis, J. K.; Kontoyannis, C. G. and Bjerrum, N. *J. J. Electrochem. Soc.* **2001**, 148, A513.
191. Hasiotis, C.; Deimede, V. and Kontoyannis, C. G. *Electrochim. Acta* **2001**, 46, 2401.
192. Pu, H. *Polymer International* **2003**, 52,1540

193. Pu, H. Liu Q.; Qiao L.; Yang, Z. *Polymer Engineering & Science* 2005, 45, 1395..
194. Zaidi, S. M. J *Electrochimica Acta* **2005**, 50, 4771-4777.
195. Wycisk, R.; Chisholm, J.; Lee, J.; Lin, J.; Pintauro, P. N. *Journal of Power Sources* **2006**, 163, 9-17.
196. Lee, J. K. and Kerres, J. *Journal of Membrane Science* **2007**, 294, 75.

# Chapter **2**

**Synthesis and characterization of  
monomers**

## 2.1 Introduction

Polymers, in general, are built from monomer units and large numbers of them are made by polycondensation of monomers having functional groups. Carboxylic diacids (CDA) belong to this category of monomers and these diacids or their derivatives, under proper conditions, can react quantitatively with dihydroxy compounds or diamines to give, polyesters or polyamides respectively, having broad range of applications in different fields. Using these reactions, a variety of polymers such as polyhydrazides, polyamide imides, polyarylates, polybenzimidazoles (PBI), polyoxadiazoles (POD), polytriazoles (PT), polyoxazoles, etc. have been synthesized. Some of these polymers are used as specialty polymers for high temperature applications. Polybenzimidazoles are, nitrogen containing heterocyclic polymers, known for their high temperature stability, excellent mechanical properties and high chemical and fire resistance. They are used in a variety of applications such as high temperature mechanical and electrical parts,<sup>1-3</sup> protective clothing for military,<sup>4</sup> desalination, gas separation and reverse osmosis,<sup>5-8</sup> aerospace,<sup>2</sup> sensors<sup>9</sup> and nanofiltration.<sup>10</sup> High thermal stability, amphoteric nature and capability to interact with strong acids or alkalies to conduct protons on doping, have made PBI a prospective candidate as membrane material for polymer electrolyte fuel cell, particularly, at high temperature, and presently, it is considered as an alternative to expensive Nafion.<sup>®</sup> Polyoxadiazole and polytriazole also belong to azole group of polymers and they conduct protons on doping, suitable for high temperature polymer electrolyte membranes for fuel cell applications.<sup>11-15</sup>

However, these heterocyclic polymers synthesized from *isophthalic* and *terephthalic* acids can not be easily processed and therefore are not useful for industrial applications.<sup>16</sup> To improve processibility, synthesis of these polymers with structurally modified diacid including substituents (either in main chain or side chain) has been followed without sacrificing their thermal properties.

In this context, PBI containing, POD and PT groups which can also conduct protons on doping with acid, assume importance as polymer electrolyte membrane for fuel cell applications. With this view, in the present work, we synthesized diacids containing N-phenyl triazole and oxadiazole groups to prepare novel PBI containing these groups in main chain and side chain, for application as polymer electrolyte for fuel cells.

Synthesis of diacids is performed typically by oxidation of  $-\text{CH}_2\text{OH}$ ,  $-\text{CHO}$ ,  $-\text{COCH}_3$  with suitable oxidizing reagents. Disproportionation of an aldehyde by



Cannizzaro reaction, benzilic acid rearrangement, halogenation followed by hydrolysis of methyl ketones in haloform reaction and hydroformylation of an alkene followed by its hydrolysis in the Koch reaction have widely been attempted for diacid synthesis. However among these methods oxidation of  $-\text{CH}_3$  group has been well acknowledged due to its reliable oxidation process. In general, stoichiometric reagents such as  $\text{KMnO}_4 + \text{H}_2\text{O} + \text{pyridine}$ ,  $\text{CrO}_3 + \text{H}_2\text{SO}_4$ ,  $\text{Na}_2\text{Cr}_2\text{O}_7 + \text{aq. H}_2\text{SO}_4$  are used for oxidation of  $-\text{CH}_3$  to  $-\text{COOH}$ . Among these reagents  $\text{KMnO}_4$  with oxidation state of (+VII) act as powerful oxidizing agent. This reagent can be used in acidic, alkaline or neutral medium and pH maintained determines its reactivity. In acid solution it changes its oxidation state from (+VII) to (+II) adding five electrons, while in neutral state and basic medium it changes from (+VII) to (+IV) with the gain of three electrons. Thus, oxidation by  $\text{KMnO}_4$  in acidic medium is the most powerful technique. Being inorganic compound,  $\text{KMnO}_4$  is insoluble in organic solvents and highly soluble in water. So to carry out oxidation of organic compounds, water miscible organic solvents with high resistance to oxidation are preferred and solvents such as pyridine, acetic acid, *t*-butanol and dry acetone are found more suitable.<sup>17</sup> Therefore, the oxidation of  $-\text{CH}_3$  to  $-\text{COOH}$  with  $\text{KMnO}_4 + \text{H}_2\text{O} + \text{pyridine}$  system has attracted large attention because of its controlled oxidation and easy to handle.

Carboxylic diacid (CDA) monomers used for making various condensation polymers are usually prepared by initially synthesizing intermediates possessing methyl groups followed by their oxidation to corresponding carboxylic acid. Such intermediates can easily be synthesized from simple condensation reaction of appropriate compounds containing single or two methyl groups or hydrazides.<sup>18</sup> Most of the polymers, synthesized from carboxylic diacids, such as polybenzimidazoles, polyoxadiazoles, polytriazoles have already been discussed in Chapter-1.

The first step towards synthesis of aromatic diacids is to prepare methyl group containing intermediates having triazole moiety or oxadiazole. The synthesis of this derivative was designed in such a fashion that the resulting polymer would have 1,2,4-triazole and 1,2,4-oxadiazole groups either in main chain or as a side chain. To achieve this objective, we initially used organic compounds such as 3-methyl benzoic acid and 3,5-dimethyl benzoic acid, which are easily available in the market. Thus, four aromatic diacids viz., 3,3'-(4-phenyl-4H-1,2,4-triazole-3,5-diyl) dibenzoic acid (PTDBA), 5-(4,5-diphenyl-4H-1,2,4-triazol-3-yl)isophthalic acid (DTIA), 5-(5-phenyl-1,3,4-oxadiazol-2-yl) isophthalic acid (POIA) and 3,3'-(1,3,4-oxadiazole-2,5-diyl)dibenzoic acid (ODBA)

were synthesized. The synthesis of ODBA has already been reported.<sup>19-21</sup> This chapter describes synthesis and characterization of these four aromatic diacids in detail.

## 2.2 Experimental

### 2.2.1 Materials

3,5-dimethyl benzoic acid and calcium hydride (CaH<sub>2</sub>) were purchased from Aldrich chemicals and used without further purification. *N,N*-dimethylacetamide (DMAc) and *N,N*-dimethylformamide (DMF) were purchased from S.D. fine-Chem. India Ltd. and used after distillation over CaH<sub>2</sub>. Methanol, potassium permanganate (KMnO<sub>4</sub>), 3-methyl benzoic acid, pyridine, hydrazine hydrate (99%), toluene, H<sub>2</sub>SO<sub>4</sub> (96%), dimethyl sulfoxide (DMSO), benzoic acid, sodium carbonate, sodium sulfate anhydrous, glacial acetic acid and hydrochloric acid (HCl), were purchased from S.D. fine-Chem. India Ltd. and used as such. Thionyl chloride (SOCl<sub>2</sub>), phosphorous trichloride (PCl<sub>3</sub>), phosphorous oxychloride (POCl<sub>3</sub>) and aniline were purchased from Loba Chem. India Ltd. and distilled prior to use. Methyl, 3-methylbenzoate was synthesized from 3-methyl benzoic acid while for the synthesis of 3-methylbenzohydrazide, reported procedure was followed.<sup>22</sup>

### 2.2.2 Analytical methods

Elemental analysis was performed on Elementar vario-EL. FTIR spectra, were recorded in KBr pellets using Perkin Elmer 16 PC FTIR spectrophotometer. <sup>1</sup>H NMR spectra, were scanned either in DMSO-d<sub>6</sub> or CDCl<sub>3</sub> depending on the solubility on a Bruker NMR spectrometer, operating at 200 MHz proton frequency.

### 2.2.3 Synthesis of new substituted aromatic diacids

#### 2.2.3.1 Synthesis of 3,3'-(4-phenyl-4H-1,2,4-triazole-3,5-diyl) dibenzoic acid (PTDBA)

This diacid was synthesized in three steps. Initially, 3-methyl benzohydrazide was condensed with 3-methyl benzoyl chloride yielding 3-methyl-N'-(3-methylbenzoyl) benzohydrazide (MBH). MBH was further reacted with aniline in orthodichlorobenzene (ODCB) in presence of PCl<sub>3</sub> to obtain 4-phenyl-3,5-dim-tolyl-4H-1,2,4-triazole (PDT). The dicarboxylic acid, 3,3'-(4-phenyl-4H-1,2,4-triazole-3,5-diyl) dibenzoic acid (PTDBA), was finally synthesized by alkaline oxidation of methyl groups of PDT with

potassium permanganate, pyridine and water. The various steps involved in the synthesis of this diacids are outlined in Scheme 2.1.

**(i) Synthesis of 3-methyl-N'-(3-methylbenzoyl) benzohydrazide (MBH)**

A solution of 25 g (0.166 mol) of 3-methylbenzohydrazide in dry 100 mL N, N-dimethylacetamide contained in a 500 mL three necked round bottom flask, equipped with a magnetic stirrer, thermo well and dropping funnel, cooled to 0 °C. 28.25 g (0.183 mol) of 3-methylbenzoyl chloride was added to it by drop-wise for 30 min with stirring. 2 mL of pyridine was then added to this solution. The reaction mixture was stirred for 4 h at 0 °C and directly precipitated in ice water and then filtered. The solid was washed with deionised water and treated with 10% sodium bicarbonate solution to remove free acid formed. The solid was filtered, washed with water, dried in vacuum oven at 100 °C and recrystallized from methanol to obtain the pure MBH in white colour.

Yield: 35.55 g (80%). m.p. 218.3 - 219.6 °C.

FTIR (KBr,  $\text{cm}^{-1}$ ): 3208 (N-H str.); 1643 (C=O str.); 1537 (N-H def.). (Figure 2.1)

$^1\text{H}$  NMR (DMSO- $d_6$ , 200 MHz,  $\delta$ , ppm): 10.44 (s, 2H); 7.75 (s, 2H); 7.72 (d, 2H); 7.39 (d, 4H); 2.38 (s, 6H). (Figure 2.2)

$^{13}\text{C}$  NMR (DMSO- $d_6$ , 200 MHz,  $\delta$ , ppm): 165.9 (q, 2C); 137.8 (q, 2C); 132.6 (q, 2C); 132.4 (2C); 128.4 (2C); 128.1(2C); 124.6 (2C); 21.1 (2C). (Figure 2.3)

Anal. Calculated for ( $\text{C}_{16}\text{H}_{16}\text{N}_2\text{O}_2$ , %): C, 71.62; H, 6.01; N, 10.44. Found C, 71.46; H, 5.97; N, 10.80.

**(ii) Synthesis of 4-phenyl-3, 5-di-m-tolyl-4H-1, 2, 4-triazole (PDT)**

A solution of 21.24 g (0.228 mol) aniline, 50 mL ODCB and 5.74 g (0.04181 mol) of  $\text{PCl}_3$  was prepared in a 250 mL three necked round bottom flask equipped with thermowell, stirrer, reflux condenser was heated to 100 °C for 1 h. Then 10.2 g (0.0380 mol) of MBH was added to this reaction mixture while stirring and the solution was heated to ~195 °C for 3 h and then ODCB and  $\text{PCl}_3$  were distilled out. The reaction mixture was cooled to room temperature and poured in to 500 mL water to obtain the precipitate, which was collected by filtration. The obtained crude product was recrystallized from a mixture of ethanol water (80:20) to get white shining crystals.

Yield: 9.535 g (73%). m.p. 174.6 °C.

FTIR (KBr,  $\text{cm}^{-1}$ ): 3052 (Aromatic C-H Str.); 2957, 2921 (Aliphatic C-H Str.); 1605, 1495, 1170 (C=N). (Figure 2.4)

$^1\text{H}$  NMR ( $\text{CDCl}_3$ , 200 MHz,  $\delta$ , ppm): 2.26 (s, 6H); 7.05(d, 2H); 7.14 (m, 6H); 7.37-7.43(m, 5H). (Figure 2.5)

$^{13}\text{C}$  NMR ( $\text{CDCl}_3$ , 200 MHz,  $\delta$ , ppm): 154.8 (q, 2C); 138.2 (q, 2C); 135.2 (q, 1C); 130.4 (2C); 129.9 (2C); 129.7 (2C); 129.5 (1C); 128.1(2C); 127.8 (2C); 126.4 (q, 2C); 125.7 (2C); 21.3 (2C). (Figure 2.6)

Anal. Calculated for ( $\text{C}_{22}\text{H}_{19}\text{N}_3$ , %): C, 81.20; H, 5.89; N, 12.91 Found C, 80.92; H, 5.85; N, 13.09.

### (iii) Synthesis of 3, 3'-(4-phenyl-4H-1,2,4-triazole-3,5-diyl) dibenzoic acid (PTDBA)

A three necked 1 L round bottom flask, equipped with a mechanical stirrer, thermo well and reflux condenser, was charged with 10 g (0.0307 mol) of PDT, 150 mL of each pyridine and water at room temperature. This solution was then heated to 120 °C and 29.14 g (0.1843 mol) of  $\text{KMnO}_4$  as oxidizing agent was subsequently added portion wise with stirring. This solution was refluxed for 8 h and then 50 mL of methanol was added to it to destroy excess permanganate. The  $\text{MnO}_2$  formed, was immediately filtered and washed with hot distilled water repeatedly. Filtrate and washings were combined and the pyridine was removed by vacuum distillation. After cooling, the solution was slowly acidified by acetic acid and the crude product PTDBA precipitated, was then subsequently filtered and washed with large amount of distilled water. PTDBA in crude form was dissolved in 150 mL of 10%  $\text{Na}_2\text{CO}_3$  solution and stirred for 15 min. The solution was heated to 100 °C for a 30 min and treated with 0.2 g activated charcoal. The solution was filtered and the filtrate was acidified by acetic acid to precipitate the PTDBA. The PTDBA was washed with deionised water until neutral to pH and then dried in vacuum oven at 125 °C for 24 h.

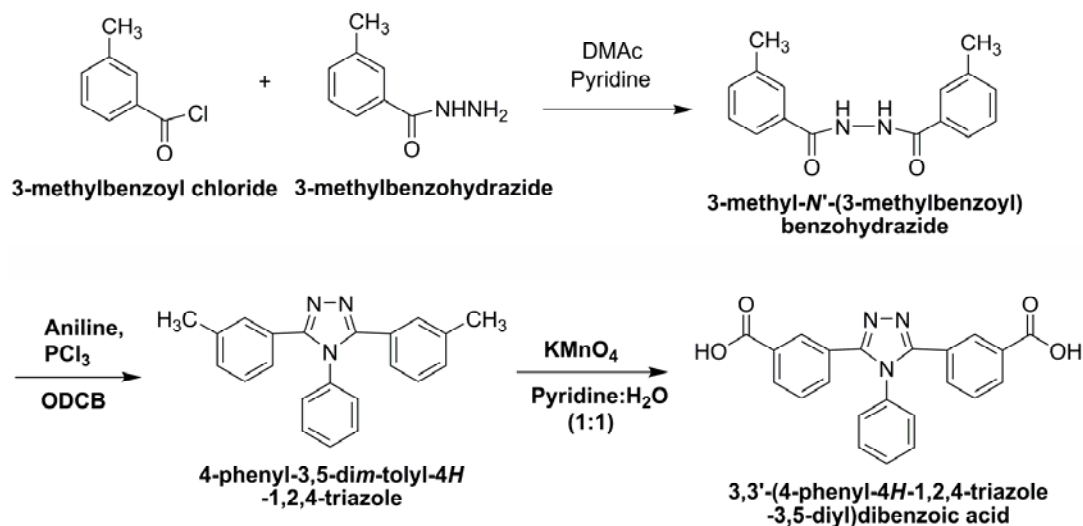
Yield: 10.9 g (92.06%). m.p. 318.4 - 320.5 °C.

FTIR ( $\text{KBr}$ ,  $\text{cm}^{-1}$ ): 3300-2500 (Broad O-H str.); 1717 (C=O str.); 1611, 1498, 1170 (C=N str.). (Figure 2.7)

$^1\text{H}$  NMR ( $\text{DMSO-d}_6$ , 200 MHz,  $\delta$ , ppm): 7.47-7.57 (m, 7H); 7.61-7.65 (dt, 2H); 7.95-7.99 (dt, 2H); 8.03(s, 2H). (Figure 2.8)

$^{13}\text{C}$  NMR ( $\text{DMSO-d}_6$ , 200 MHz,  $\delta$ , ppm): 171.8 (q, 2C); 159 (q, 2C); 139.6 (q, 1C); 137.7 (2C); 136.4 (q, 2C); 135.7 (2C); 135.3 (2C); 135.2 (2C); 134.6 (2C); 134.2 (2C); 133.4 (2C); 132.3 (q, 2C). (Figure 2.8)

Anal. Calculated for ( $\text{C}_{22}\text{H}_{15}\text{N}_3\text{O}_4$ , %): C, 68.57; H, 3.92; N, 10.90 Found C, 68.72; H, 3.92; N, 10.96.



**Scheme 2.1** Synthesis of 3,3'-(4-phenyl-4H-1,2,4-triazole-3,5-diyl) dibenzoic acid (PTDBA)

### 2.2.3.2 Synthesis of 5-(4,5-diphenyl-4H-1,2,4-triazol-3-yl) isophthalic acid (DTIA)

N'-benzoyl-3,5-dimethylbenzohydrazide (BDBH), obtained by the simple condensation reaction of benzoyl hydrazide and 3,5-dimethyl benzoyl chloride was reacted with aniline in ODCB in presence of  $\text{PCl}_3$  to yield 3-(3,5-dimethylphenyl)-4,5-diphenyl-4H-1,2,4-triazole (DPDT). 5-(4,5-diphenyl-4H-1,2,4-triazol-3-yl)isophthalic acid (DTIA) was obtained by the alkaline oxidation of methyl groups of DPDT to carboxylic acid groups by using potassium permanganate, pyridine and water. The various steps involved in the synthesis of this diacid are outlined in Scheme 2.2.

#### (i) Synthesis of N'-benzoyl-3,5-dimethylbenzohydrazide (BDBH)

In a three necked 500 mL round bottom flask, equipped with a magnetic stirrer, thermo well and dropping funnel, 25 g (0.183 mol) of benzoyl hydrazide was dissolved in dry 100 mL DMAc and the solution was cooled to 0 °C. To this cooled solution, 30.87 g (0.183 mol) of 3,5-dimethyl benzoyl chloride was added drop-wise for 30 min followed by addition 2 mL pyridine. The reaction mixture was stirred for 4 h at 0 °C and then precipitated in ice water and filtered. The obtained crude product was treated with 10% sodium bicarbonate solution to remove any formed free acid. The product obtained was filtered, washed with distilled water, dried and finally purified by recrystallization in methanol.

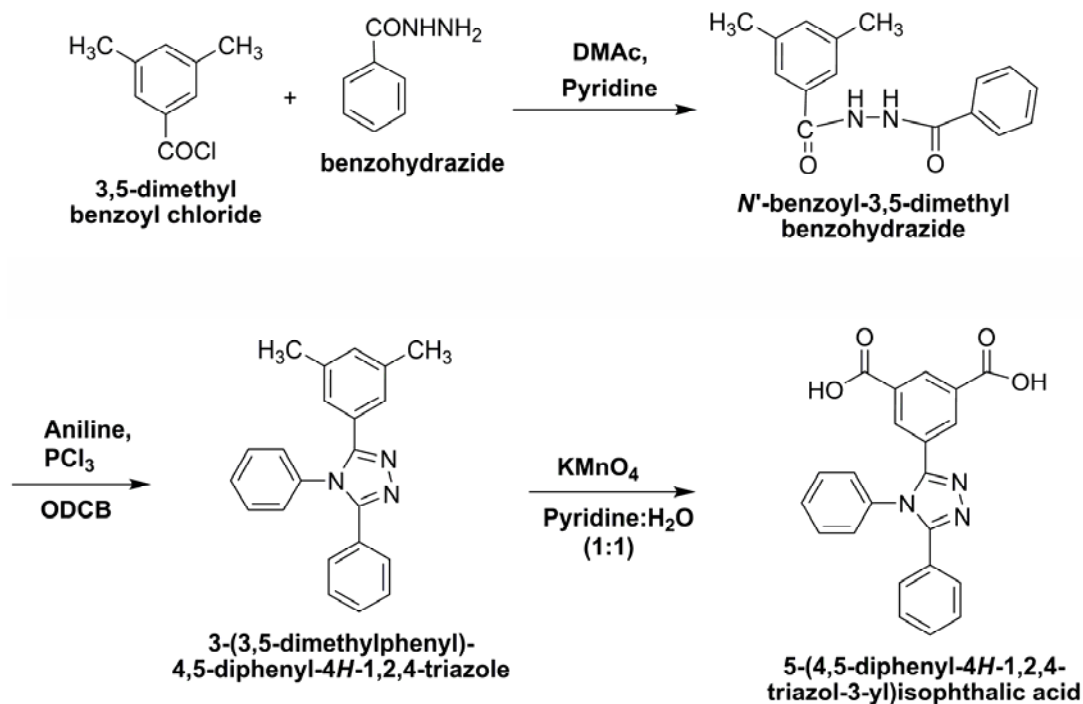
Yield: 40.39 g (82%). m.p. 218 °C.

FTIR (KBr,  $\text{cm}^{-1}$ ): 3210 (N-H str); 1674, (C=O str.); 1526 (N-H def.). (Figure 2.9)

$^1\text{H}$  NMR (DMSO- $d_6$ , 200 MHz,  $\delta$ , ppm): 2.34 (s, 6H); 7.23 (s, 1H); 7.52-7.55 (m, 5H); 7.90-7.94(d, 2H); 10.38(s, 1H); 10.48(s, 1H). (Figure 2.10)

$^{13}\text{C}$  NMR (DMSO- $d_6$  200 MHz,  $\delta$ , ppm): 166.24 (q, 1C); 165.89 (q, 1C); 137.71 (q, 2C); 133.17 (1C); 132.66 (q, 2C); 131.92 (1C); 128.58 (2C); 127.57 (2C); 125.33 (2C); 20.94 (2C). (Figure 2.11)

Anal. Calculated for ( $\text{C}_{16}\text{H}_{16}\text{N}_2\text{O}_2$ , %): C, 71.62; H, 6.01; N, 10.44 Found C, 71.66; H, 5.27; N, 10.60



**Scheme 2.2** Synthesis of 5-(4,5-diphenyl-4H-1,2,4-triazol-3-yl)isophthalic acid (DTIA)

### (ii) Synthesis of 3-(3,5-dimethylphenyl)-4,5-diphenyl-4H-1,2,4-triazole (DPDT)

A solution 41.65 g (0.4477 mol) of aniline, 100 mL of ODCB and 11.25 g (0.08205 mol)  $\text{PCl}_3$  contained in 250 mL three necked round bottom flask, equipped with thermowell, stirrer, reflux condenser was heated to 100 °C for 1 h. To this reaction mixture 20 g (0.0745 mol) of BDBH was added with stirring and heated to 190-200 °C for 3 h. ODCB and  $\text{PCl}_3$  were distilled out, the reaction mixture was cooled to room temperature and precipitated in 500 mL distilled water. The obtained crude product was washed with water and recrystallized from a mixture of ethanol:water (80:20) to obtain white shining crystals.

Yield: 19.2 g (79.2%). m.p. 249.9-250.6 °C.

FTIR (KBr,  $\text{cm}^{-1}$ ): 3052 (Aromatic C-H Str.); 2957, 2921 (Aliphatic C-H Str.); 1606, 1496, 1172 (C=N). (Figure 2.12)

$^1\text{H}$  NMR ( $\text{CDCl}_3$ , 200 MHz,  $\delta$ , ppm): 2.18 (s, 6H); 6.97.0 (s, 1H); 7.0 (s, 2H); 7.14 (d, 2H); 7.26-7.3 (m, 3H); 7.4-7.43 (m, 5H). (Figure 2.13)

$^{13}\text{C}$  NMR ( $\text{CDCl}_3$ , 200 MHz,  $\delta$ , ppm): 155.05 (q, 1C); 154.61 (q, 1C) 137.9 (q, 2C); 135 (1C); 131.27 (1C); 129.18 (2C); 129.58 (1C); 129.46 (1C); 128.79 (2C); 128.37 (2C); 128.37 (2C); 127.81 (2C); 126.98 (1C); 126.59 (1C(q), 2C); 21.18 (6C). (Figure 2.14)

Anal. Calculated for ( $\text{C}_{22}\text{H}_{19}\text{N}_3$ , %): C, 81.20; H, 5.89; N, 12.91 Found C, 81.68; H, 5.72; N, 12.67.

### (iii) Synthesis of 5-(4,5-diphenyl-4H-1,2,4-triazol-3-yl)isophthalic acid (DTIA)

A solution of 10 g (0.0307 mol) of DPDT in 150 mL pyridine and 65 mL water contained in 500 mL three necked round bottom flask, equipped with a mechanical stirrer, thermo well and reflux condenser was heated to reflux. To this reflux solution 29.14 g (0.1843 mol) solid  $\text{KMnO}_4$  was added portion wise. Distilled water was added occasionally to wash down the permanganate. This oxidation process of methyl groups was carried out for 8 h. To destroy excessive permengate, 50 mL of methanol was added afterwards in the reflux condition. The formed insoluble  $\text{MnO}_2$  filtered followed by washing with hot distilled water. The filtrate along with washing was vacuum distilled to remove excess pyridine. Then, at ambient temperature the resultant solution was slowly acidified by  $\text{CH}_3\text{COOH}$ . This crude DTIA was filtered and washed several times with distilled water to remove any  $\text{CH}_3\text{COOH}$  and dissolved in 100 mL 10%  $\text{Na}_2\text{CO}_3$  solution by stirring at 100 °C for 30 min. The solution was filtered hot and kept for overnight at room temperature without disturbing. The fine white crystalline Na-salt of DTIA was filtered. To obtain the final diacid, Na-salt of DTIA was dissolved in 250 mL of distilled water, treated with small amount of charcoal, stirred for 10-15 min and then filtered. The filtrate was again acidified with  $\text{CH}_3\text{COOH}$  to obtain the precipitate of pure DTIA. The solid was washed with water, filtered and dried at 125 °C for 24 h.

Yield: 8.5 g (72%). m.p. 329-330 °C.

FTIR (KBr,  $\text{cm}^{-1}$ ): 3300-2500 (Broad O-H str.); 1691 (C=O str); 1601, 1497 (C=N str.). (Figure 2.15)

$^1\text{H}$  NMR ( $\text{DMSO-d}_6$ , 200 MHz,  $\delta$ , ppm): 7.4 (m, 5H); 7.5 (s, 5H); 8.17 (s, 2H); 8.45 (s, 1H). (Figure 2.16)

$^{13}\text{C}$  NMR (DMSO- $d_6$  200 MHz,  $\delta$ , ppm): 166.15 (q, 2C); 155 (q, 1C); 153.17 (q, 1C); 134.84 (q, 1C); 133.09 (2C); 132.01 (q, 2C); 130.98 (2C); 130.37 (2C); 130.11 (2C); 128.86 (3C); 128.55 (2C); 128.23 (1C); 127.08 (1C). (Figure 2.17)

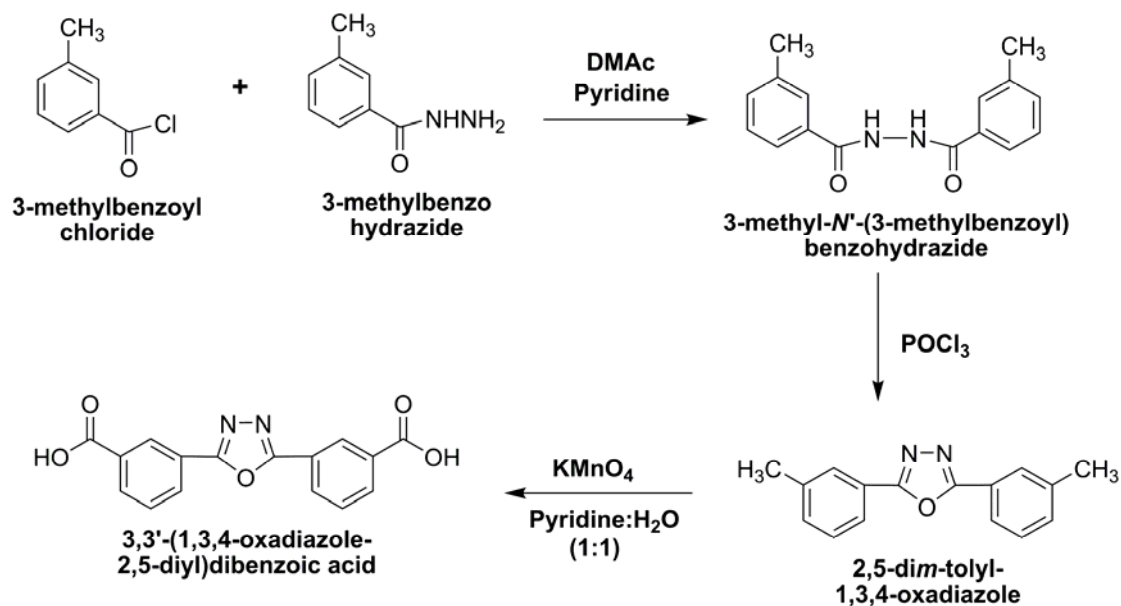
Anal. Calculated for ( $\text{C}_{22}\text{H}_{15}\text{N}_3\text{O}_4$ , %): C, 68.57; H, 3.92; N, 10.90 Found C, 68.72; H, 4.05; N, 9.66.

### 2.2.3.3 Synthesis of 3,3'-(1,3,4-oxadiazole-2,5-diyl)dibenzoic acid (ODBA)

It is synthesized according to the reported procedure.<sup>21</sup> The various steps involved in the synthesis of this diacids are outlined in Scheme 2.3.

#### (i) Synthesis of 3-methyl-N'-(3-methylbenzoyl)benzohydrazide (MBH)

MBH was synthesized by the same procedure as described in section 2.2.3.1(i).



**Scheme 2.3** Synthesis of 3,3'-(1,3,4-oxadiazole-2,5-diyl)dibenzoic acid (ODBA)

#### (ii) Synthesis of 2,5-dim-tolyl-1,3,4-oxadiazole (DTO)

25 g (0.0805 mol) of MBH was added to 250 mL of  $\text{POCl}_3$  contained in a 500 mL three necked round-bottom flask, equipped with thermowell, stirrer, reflux condenser and heated to 80 °C for 16 h with stirring. Subsequently,  $\text{POCl}_3$  was distilled off and the residue was poured into distilled water for precipitation. The solid was filtered and dissolved in 250 mL of DMSO. The resultant solution in DMSO was again precipitated in distilled water, filtered and washed several times with distilled water. The obtained



product was purified by column chromatography (80:20, petroleum benzene: ethyl acetate). Whitish solid product was obtained at the end.

Yield 6.3 g (85%).

FTIR (KBr,  $\text{cm}^{-1}$ ): 1594, 1543 (C=N str.); 1277, 1071 (C-O-C str.). (Figure 2.18)

$^1\text{H}$  NMR ( $\text{CDCl}_3$ ,  $\delta$ , ppm): 2.38 (s, 6H); 7.26-7.29(d, 2H); 7.34-7.38 (t, 2H); 7.84 (s, 2H); 7.89 (2H, d). (Figure 2.19)

Anal. Calculated for ( $\text{C}_{16}\text{H}_{14}\text{N}_2\text{O}$ , %) C, 76.78; H, 5.64; N, 11.19 Found C, 77.01; H, 5.78; N, 11.10.

### (iii) Synthesis of 3,3'-(1,3,4-oxadiazole-2,5-diyl)dibenzoic acid (ODBA)

To a three necked 1 L round bottom flask, equipped with a mechanical stirrer, thermo well and reflux condenser was added 20 g (0.0796 mol) of DTO, 300 mL pyridine, and 300 mL water. The reaction mixture was then heated to 130 °C and to the refluxing solution, 82.04 g (0.516 mol) solid  $\text{KMnO}_4$  was added portion wise to maintain a slow reflux. Water was added occasionally to replace the loss by evaporation and to wash down the permanganate. The solution was then refluxed for 10 h before the addition of methanol (150 mL) to destroy excess permanganate. The  $\text{MnO}_2$  was suction filtered while hot and washed with boiling distilled water. Filtrate and washings were combined and the pyridine was removed by vacuum distillation. After cooling, the solution was acidified with acetic acid. ODBA in crude form was dissolved in 150 mL of 10%  $\text{Na}_2\text{CO}_3$  solution and stirred for 15 min. The solution was heated to 100 °C for a 30 min and treated with 0.2 g activated charcoal. The solution was filtered and the filtrate was acidified by acetic acid to precipitate the ODBA. The obtained solid product was purified by redissolving in  $\text{Na}_2\text{CO}_3$  solution, treated with small amount of charcoal, and reprecipitating with acetic acid after filtration. The solid after filtration was purified by heating in 300 mL boiling deionised water for 30 min followed by filtration while hot and washing with hot water. The solid was dried in vacuum oven at 125 °C for 24 h.

Yield: 18 g (72 %). m.p. 367-369 °C.

FTIR (KBr,  $\text{cm}^{-1}$ ): 3300-2500 (Broad O-H str.); 1684 (C=O str); 1611, 1543 (C=N str.); 1264, 1086 (C-O-C str.). (Figure 2.20)

$^1\text{H}$  NMR ( $\text{DMSO-d}_6$ ,  $\delta$ , ppm): 7.74-7.82 (t, 2H); 8.17-8.21 (d, 2H); 8.35-8.39 (d, 2H); 8.6 s, 2H). (Figure 2.21)

$^{13}\text{C}$  NMR ( $\text{DMSO-d}_6$ ,  $\delta$ , ppm): 123.87 (2C, 6); 127.43 (2C, 4); 130.11(2C, 3); 130.91(2C, 1); 132.12 (2C, 5); 132.72 (2C, 2); 163.79 (2C, 7); 166.58 (2C, 8). (Figure 2.22)

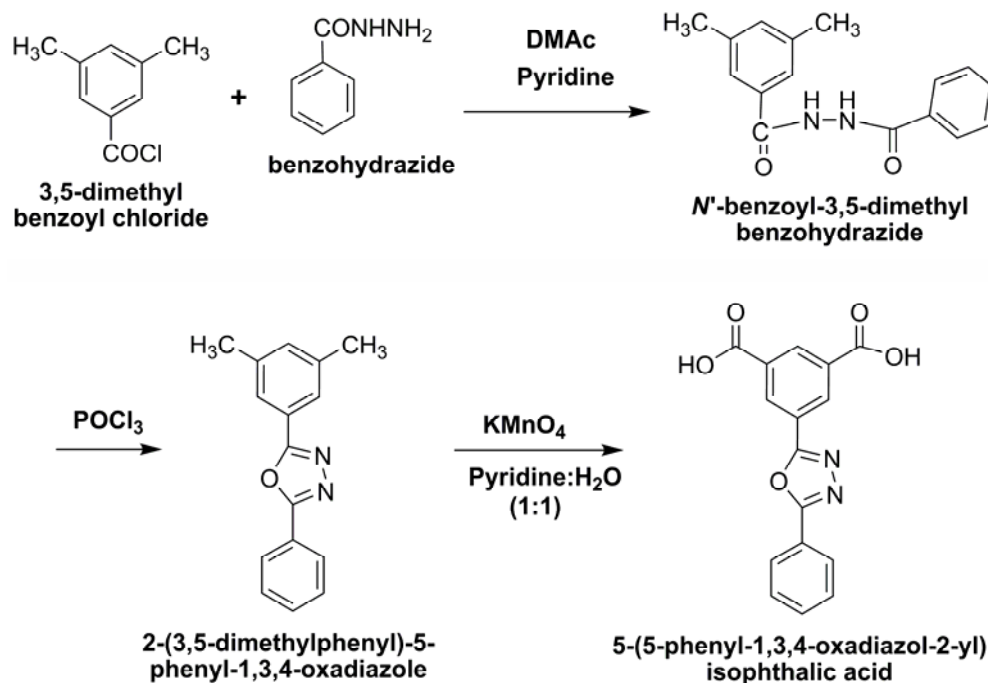
Anal. Calculated for (C<sub>16</sub>H<sub>10</sub>N<sub>2</sub>O<sub>5</sub>, %): C, 61.94; H, 3.25; N, 9.03 Found C, 61.20; H, 3.03; N, 8.80.

### 2.2.3.4 Synthesis of 5-(5-phenyl-1,3,4-oxadiazol-2-yl) isophthalic acid (POIA)

It is synthesized from 3,5-dimethyl benzoic acid in three steps. In the first step, 3,5-dimethyl benzoyl chloride was condensed with benzoyl hydrazide in DMAc and pyridine to obtain N'-benzoyl-3,5-dimethylbenzohydrazide (BDBH), which was cyclized by POCl<sub>3</sub> to yield 2-(3,5-Dimethyl Phenyl)-5-Phenyl-1,3,4-Oxadiazole (DPPO). In the last step, methyl group of DPPO was oxidized to -COOH by using potassium permanganate, water and pyridine. The various steps involved in the synthesis are outlined in Scheme 2.4.

#### (i) Synthesis of N'-benzoyl-3,5-dimethylbenzohydrazide (BDBH)

BDBH was synthesized by the same procedure as described in section 2.2.3.2(i).



**Scheme 2.4** Synthesis of 5-(5-phenyl-1,3,4-oxadiazol-2-yl) isophthalic acid (POIA)

#### (ii) Synthesis of 2-(3,5-Dimethyl Phenyl)-5-Phenyl-1,3,4-Oxadiazole (DPPO)

10 g (0.03727 mol) of BDBH was added to 100 mL of POCl<sub>3</sub> contained in a 250 mL three necked round-bottom flask, equipped with thermowell, stirrer, reflux condenser and heated to 80 °C for 16 h with stirring. Subsequently, POCl<sub>3</sub> was distilled off and the residue was poured into distilled water for precipitation. The solid was filtered and

dissolved in 100 mL of DMSO. The resultant solution in DMSO was again precipitated in distilled water, filtered and washed several times with distilled water. Crude product was recrystallized from methanol, to obtain white shining crystals.

Yield: 7.21 g (77%). m.p. 160°C.

FTIR (KBr,  $\text{cm}^{-1}$ ): 1604, 1550 (C=N str.); 1231, 1070 (C-O-C str.).(Figure 2.23)

$^1\text{H}$  NMR ( $\text{CDCl}_3$ ,  $\delta$ , ppm): 2.34 (s, 6H); 7.15 (s, 1H); 7.55 (m, 3H); 7.75(s, 2H); 8.15(d, 2H). (Figure 2.24)

$^{13}\text{C}$  NMR ( $\text{DMSO-d}_6$ ,  $\delta$ , ppm): 164.84 (1C, 7); 164.27 (1C, 8); 138.79 (2C, 2&4); 133.45 (1C, 1); 131.6 (1C, 12); 129.01 (2C, 11&13); 126.87 (2C, 10&14); 124.6 (2C, 3&5); 124.01 (1C, 9); 123.63 (1C, 4); 21.09 (2C, 15&16). (Figure 2.25)

Anal. Calculated for ( $\text{C}_{16}\text{H}_{14}\text{N}_2\text{O}$ , %): C, 76.80 ; H, 5.60; N, 11.20 Found C, 75.95; H, 6.30; N, 12.50.

### (iii) Synthesis of 5-(5-phenyl-1,3,4-oxadiazol-2-yl) isophthalic acid (POIA)

A three necked 1 L round bottom flask, equipped with a mechanical stirrer, thermo well and reflux condenser, was charged with 10 g (0.040 mol) of DPPO, 150 mL pyridine and 150 mL water at room temperature. This solution was then heated to 120 °C with stirring and 37.92 g (0.240 mol) of solid  $\text{KMnO}_4$  was subsequently added portion wise. Occasional addition of distilled water was performed to sustain the least by evaporation of solvent and to wash down permanganate. This solution was refluxed for 10 h and then 50 mL of methanol added to destroy excess permanganate. The  $\text{MnO}_2$  was suction filtered while hot and then successively washed with hot distilled water. The filtrate and washings were combined and vacuum distilled to remove pyridine. After cooling, the solution was slowly acidified by acetic acid and the crude product, precipitated, was then subsequently filtered and washed with large amount of distilled water. POIA in crude form was dissolved in 150 mL of 10%  $\text{Na}_2\text{CO}_3$  solution and stirred for 15 min. The solution was heated at 100-120 °C for 30 min and treated with 0.2 g activated charcoal. The resultant solution was then filtered and the filtrate was acidified by acetic acid to precipitate POIA. The product was purified by treating with 150 mL methanol at room temperature for 12 h. It is observed that impurity was dissolved in methanol. The resultant product was filtered and washed with methanol. It was dried in vacuum oven at 125 °C for 24 h.

Yield: 8.5 g (69%). m.p. > 300°C.

FTIR (KBr,  $\text{cm}^{-1}$ ): 3300-2500 (Broad O-H str.); 1773, 1697 (C=O str); 1544 (C=N str.); 1245, 1025 (C-O-C str.). (Figure 2.26)

$^1\text{H}$  NMR (DMSO- $d_6$ ,  $\delta$ , ppm): 7.64 (m, 3H); 8.12(d, 2H); 8.59(s 1H); 8.71(s, 2H).

( Figure 2.27)

$^{13}\text{C}$  NMR (DMSO- $d_6$ ,  $\delta$ , ppm): 165.65 (2C, 15 & 16); 164.45 (1C, 8); 162.81 (1C, 7); 132.56 (3C, 2,6 &1); 132.23 (1C,12); 130.65 (2C, 3 & 5); 129.65 (2C, 10 & 14); 126.87 (2C, 11 & 13); 124.39 (1C, 4); 123.14 (1C, 9). (Figure 2.28)

Anal. Calculated for ( $\text{C}_{16}\text{H}_{10}\text{N}_2\text{O}_5$ , %): C, 61.94; H, 3.22; N, 9.03 Found C, 61.65; H, 3.10; N, 8.85.

## 2.3 Results and Discussion

### 2.3.1 Synthesis and characterization of 3, 3'-(4-phenyl-4H-1,2,4-triazole-3,5-diyl) dibenzoic acid (PTDBA)

Diacid PTDBA was synthesized in three steps as described earlier (**Scheme 2.1**). In the first step, 3-methylbenzoyl chloride and 3-methylbenzohydrazide were condensed in dry DMAc to form MBH. The obtained product was recrystallized from methanol and 80% yield could be achieved. The structure of MBH was confirmed by usual characterization techniques such as FTIR,  $^1\text{H}$  NMR,  $^{13}\text{C}$  NMR and elemental analysis.

FTIR spectrum of MBH (Figure 2.1) showed absorption band at  $3208\text{ cm}^{-1}$  and  $1537\text{ cm}^{-1}$  corresponding to the  $-\text{N-H}$  stretching and deformation, respectively. Specific absorption of carbonyl ( $-\text{C=O}$ ) group in amide linkage observed at  $1643\text{ cm}^{-1}$ .

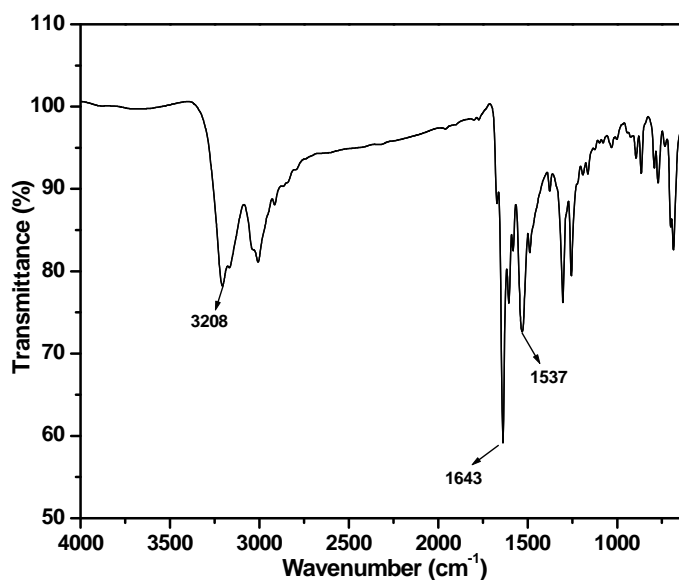


**Figure 2.1** FTIR spectrum of 3-methyl-N'-(3-methylbenzoyl)benzohydrazide (MBH) in KBr

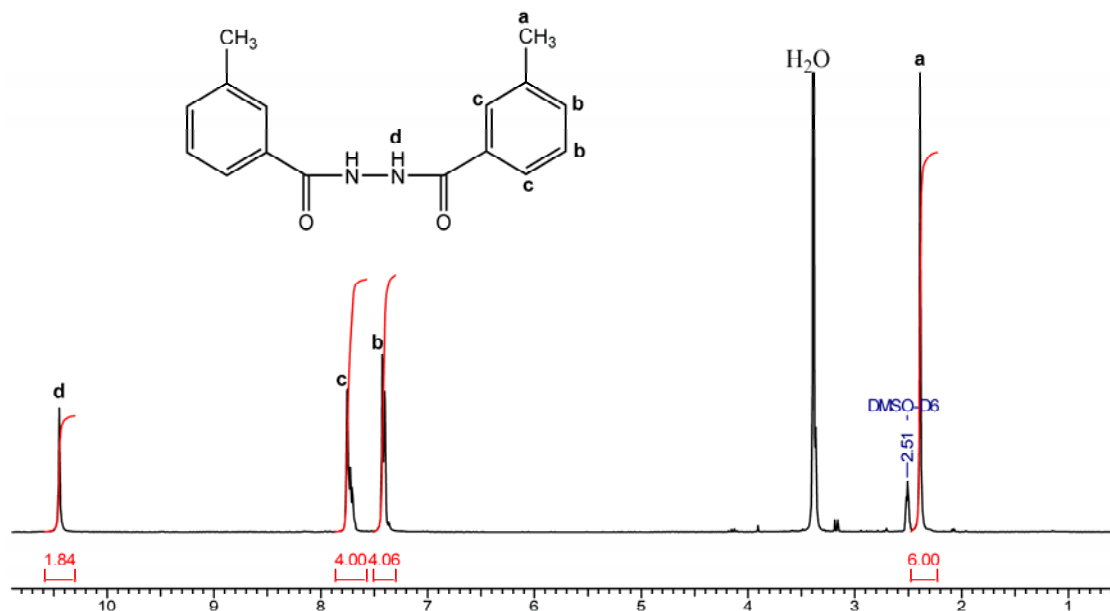


**Figure 2.2**  $^1\text{H}$  NMR spectrum of 3-methyl-N'-(3-methylbenzoyl)benzohydrazide (MBH) in  $\text{DMSO-d}_6$

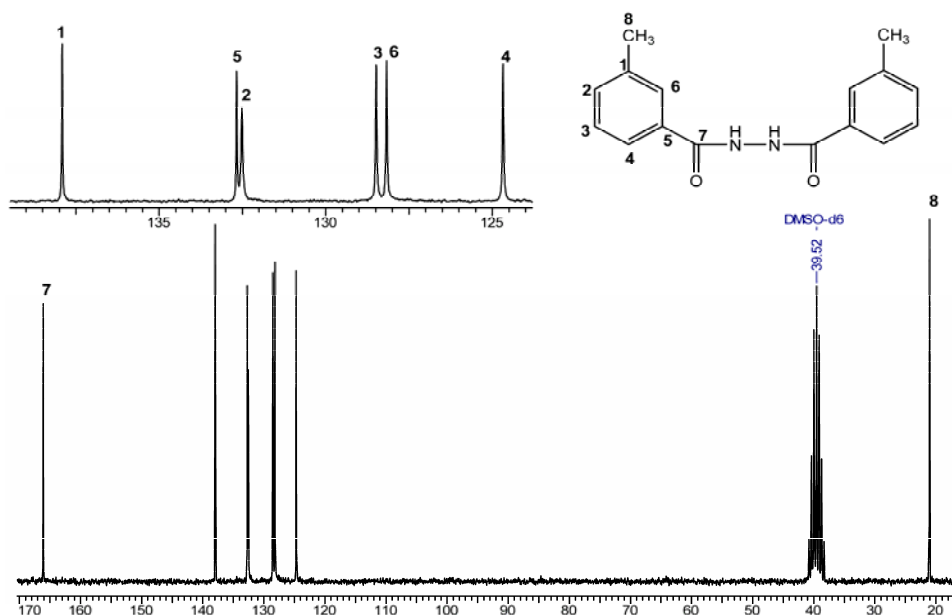


**Figure 2.3**  $^{13}\text{C}$  NMR spectrum of 3-methyl-N'-(3-methylbenzoyl)benzohydrazide (MBH) in  $\text{DMSO-d}_6$

The  $^1\text{H}$  NMR spectrum (Figure 2.2) of MBH showed a singlet at 10.44 ppm corresponding to the  $-\text{N-H}$  proton and singlet at 2.38 ppm corresponded to protons of methyl groups. Singlet at 7.75 ppm, doublet at 7.72 ppm and 7.39 ppm corresponded to protons present in the aromatic region.  $^{13}\text{C}$  NMR spectrum (Figure 2.3) showed aromatic carbons in the region 165.9–124.6 ppm with expected peak values. It also exhibited the

characteristic peak at 21.1 ppm corresponding to the  $-\text{CH}_3$  groups. Moreover, observed elemental analysis values were in good agreement with calculated values.

In second step, MBH was cyclized with aniline to obtain 4-phenyl-3,5-di-*m*-tolyl-4H-1,2,4-triazole (PDT) and the compound was characterized by FTIR,  $^1\text{H}$  NMR,  $^{13}\text{C}$  NMR, and elemental analysis. In FTIR spectrum, peaks at N-H stretching ( $3208\text{ cm}^{-1}$ ) and carbonyl group ( $1643\text{ cm}^{-1}$ ) present in MBH completely disappeared. Various new peaks at  $1605\text{ cm}^{-1}$  and  $1495\text{ cm}^{-1}$  corresponding to C=N of triazole were observed, indicating complete cyclization in the resultant PDT as shown in (Figure 2.4).

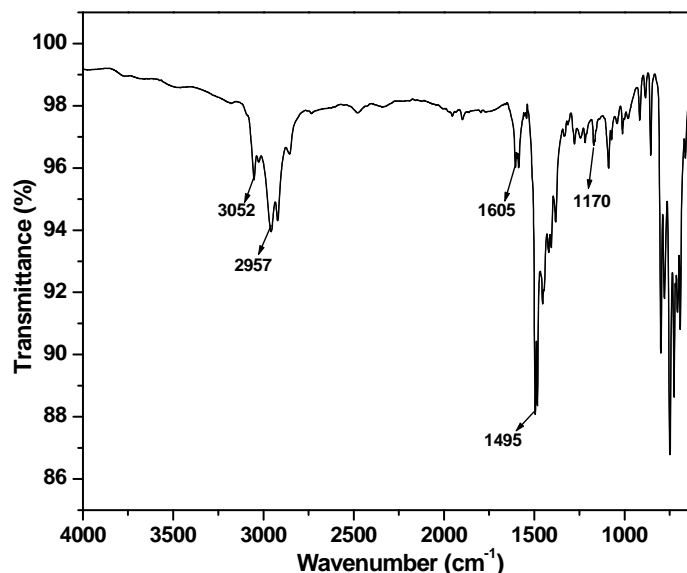


**Figure 2.4** FTIR spectrum of 4-phenyl-3, 5-di-*m*-tolyl-4H-1, 2, 4-triazole (PDT) in KBr

In  $^1\text{H}$  NMR spectrum (Figure 2.5), the presence of a singlet corresponding to six protons of two methyl groups was observed at 2.26 ppm. Various aromatic protons were observed at 7.05 ppm (doublet), 7.14 ppm (multiplet) and 7.37 ppm (multiplet) as indicated by b,c and d respectively in Figure 2.5. Moreover two protons corresponding to secondary amine (N-H) of MBH at 10.44 ppm were absent, indicating formation of cyclic triazole moiety.  $^{13}\text{C}$  NMR spectrum (Figure 2.6) of PDT also showed different peaks of corresponding aromatic carbons in the range 154.8–125.7 ppm and methyl carbons at 21.3 ppm. In addition, the anticipated values of elemental analysis further confirmed the structure of PDT.

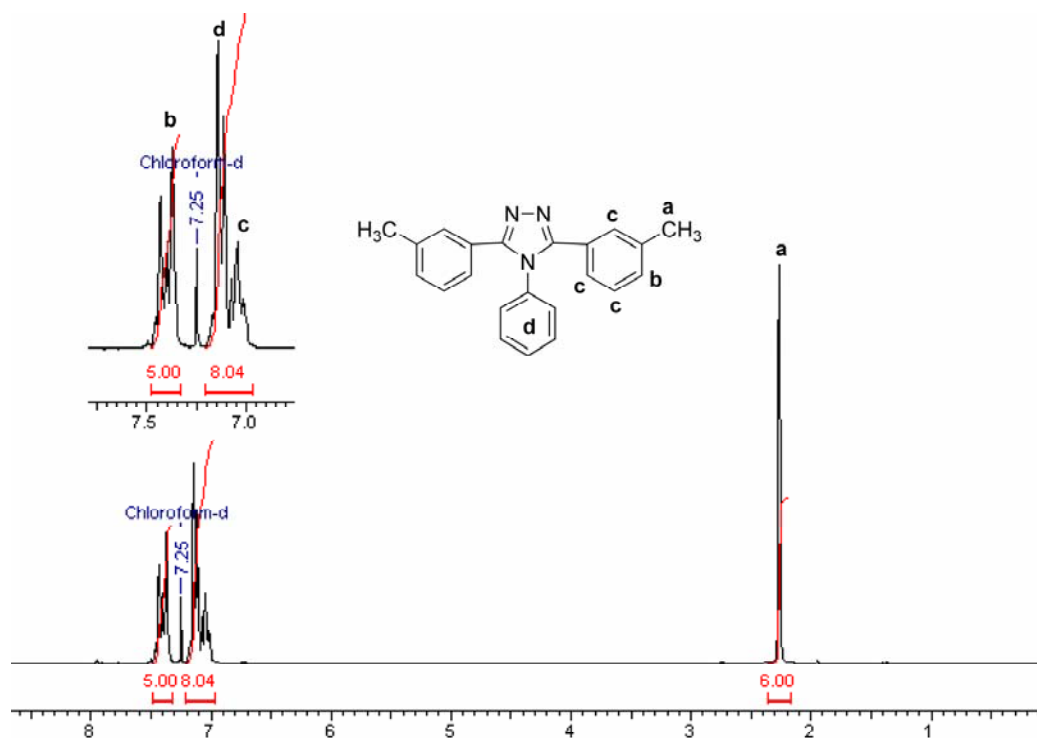


**Figure 2.5**  $^1\text{H}$  NMR spectrum of 4-phenyl-3, 5-di-m-tolyl-4H-1, 2, 4-triazole in  $\text{CDCl}_3$

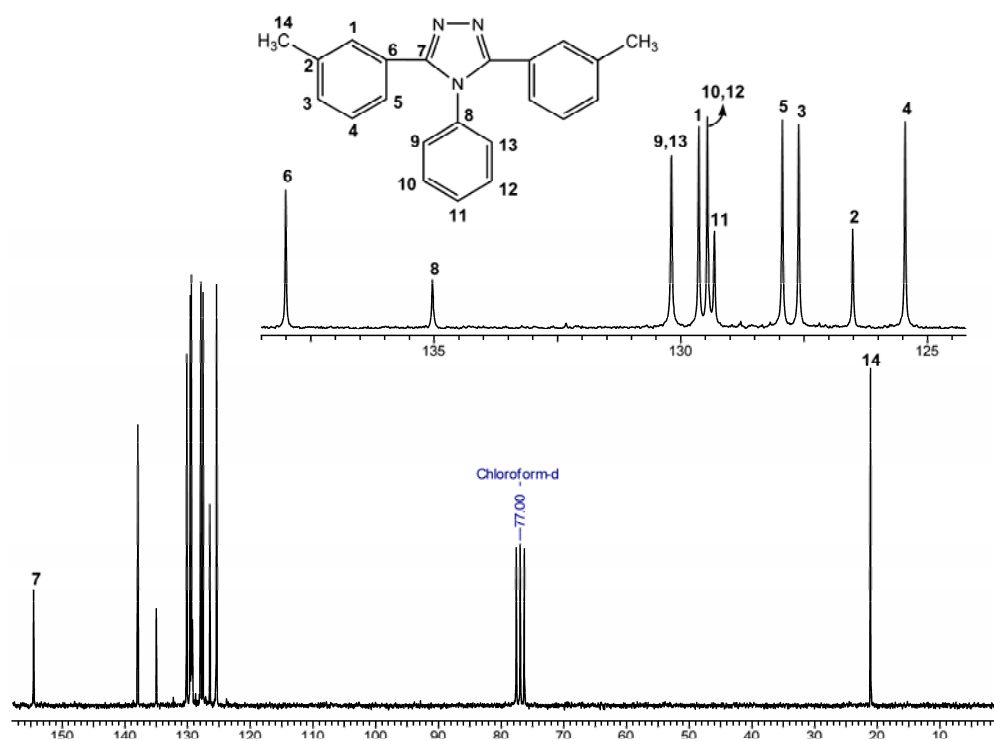


**Figure 2.6**  $^{13}\text{C}$  NMR spectrum of 4-phenyl-3, 5-di-m-tolyl-4H-1, 2, 4-triazole (PDT) in  $\text{CDCl}_3$

The third step involves the synthesis of monomer viz., 3,3'-(4-phenyl-4H-1,2,4-triazole-3,5-diyl) dibenzoic acid (PTDBA). It was synthesized by alkaline oxidation of

the intermediate viz. PDT using aqueous  $\text{KMnO}_4$ -pyridine system. The formed potassium salt of PTDBA was obtained in corresponding dicarboxylic acid by neutralizing with acetic acid. In the oxidation step excess  $\text{KMnO}_4$  had to be used to ensure the complete oxidation of the methyl groups (up to the point where the color of  $\text{KMnO}_4$  did not lose on refluxing). The diacid was purified by dissolving in aqueous sodium carbonate solution and filtering the solution after charcoal treatment. In this procedure the unoxidised reactant, if remained any, was removed. The precipitate of PTDBA was obtained by acidifying its sodium salt with acetic acid and the product was characterized by FTIR,  $^1\text{H}$  NMR,  $^{13}\text{C}$  NMR and elemental analysis. Elemental analysis values were in good agreement with the calculated values.

The FTIR spectrum of PTDBA (Figure 2.7) showed broad band from  $3300\text{ cm}^{-1}$  to  $2500\text{ cm}^{-1}$  of  $-\text{OH}$  of  $-\text{COOH}$  group, while band at  $1717\text{ cm}^{-1}$  was due to carbonyl ( $\text{C}=\text{O}$ ) stretching. These observation confirmed the presence of carboxyl groups ( $-\text{COOH}$ ) in PTDBA.

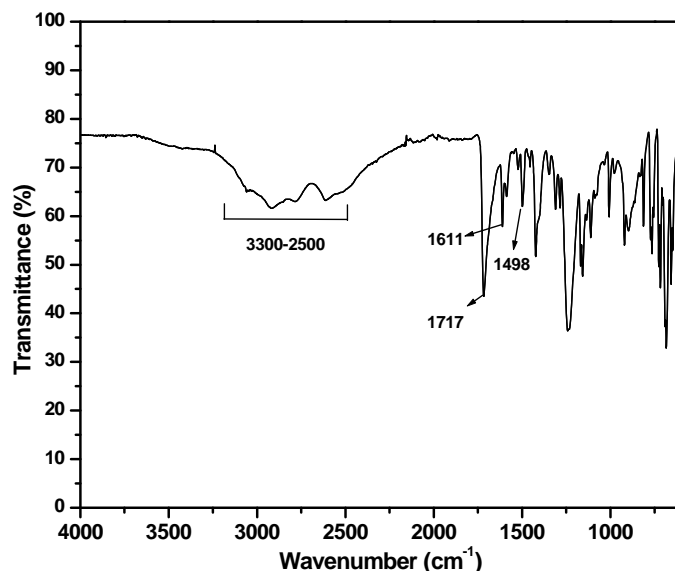


**Figure 2.7** FTIR spectrum of 3, 3'-(4-phenyl-4H-1,2,4-triazole-3,5-diyl) dibenzoic acid (PTDBA) in KBr

The structure of PTDBA was elucidated by  $^1\text{H}$  NMR spectrum (Figure 2.8). The observed multiplet at 7.47-7.57 ppm, double triplet at 7.61 ppm and 7.99 ppm and a singlet at 8.03 ppm corresponded to various aromatic protons. The complete disappearance of the peak at 2.26 ppm corresponding to methyl group in the PDT further indicated its oxidation to carboxyl group.  $^{13}\text{C}$  NMR (Figure 2.8) also confirmed the structure of PTDBA exhibiting aromatic carbons in the range 171.8–132.3 ppm with expected values. There were no peaks of carbon of methyl groups (21.30 ppm) and



appearance of new peaks at 171.8 ppm, corresponding to carbonyl group of -COOH functionality, further confirmed its complete oxidation and expected structure (PTDBA).

Thus, the chemical structure of intermediates as well as diacid (PTDBA) was confirmed by FTIR and  $^1\text{H}$  NMR,  $^{13}\text{C}$  NMR spectra and elemental analysis.

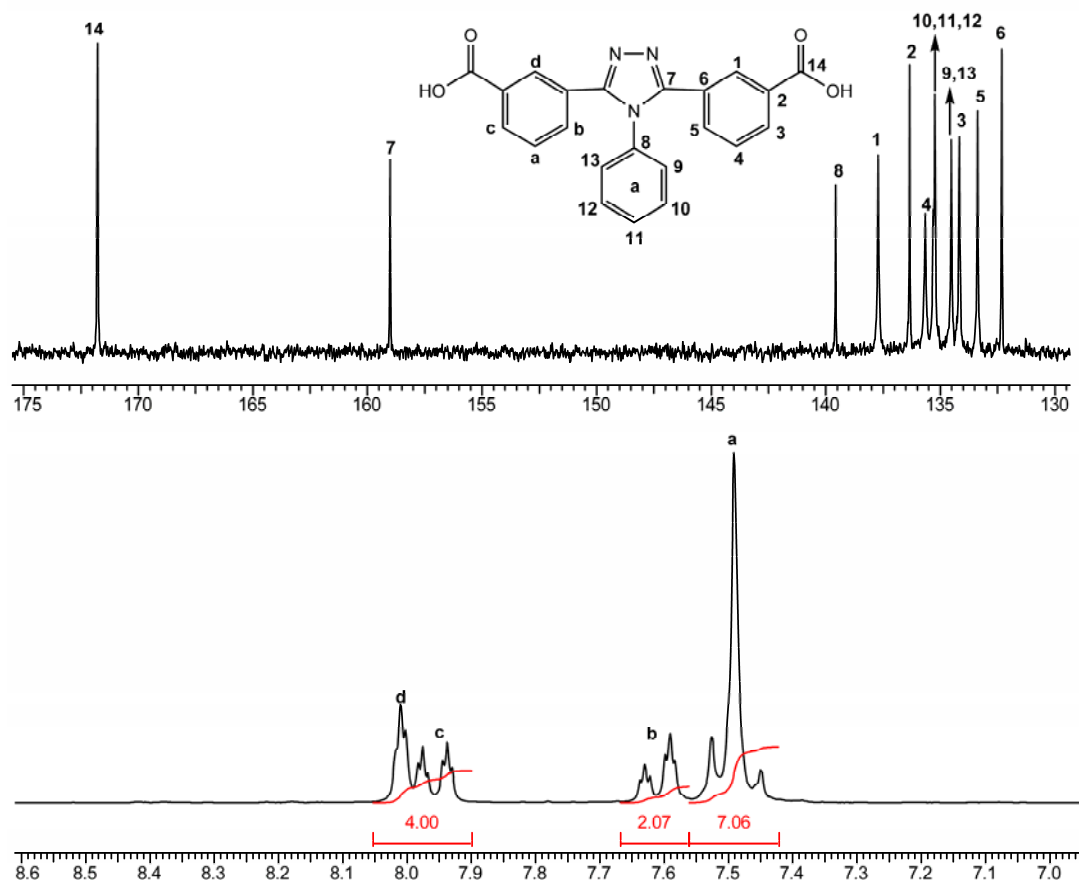


**Figure 2.8**  $^1\text{H}$  and  $^{13}\text{C}$  NMR spectra of 3, 3'-(4-phenyl-4H-1,2,4-triazole-3,5-diyl) dibenzoic acid (PTDBA) in  $\text{DMSO-d}_6$

### 2.3.2 Synthesis and characterization of 5-(4,5-diphenyl-4H-1,2,4-triazol-3-yl)isophthalic acid (DTIA)

The diacid, DTIA, was synthesized in three steps (Scheme 2.2). 3,5-dimethyl benzoyl chloride was obtained from 3,5-dimethyl benzoic acid by using thionyl chloride. Other intermediate viz., methyl benzoate was synthesized by esterification of benzoic acid with excess methanol. Benzohydrazide was synthesized by condensing hydrazine hydrate with methyl benzoate in dry toluene. N'-benzoyl-3,5-dimethylbenzohydrazide (BDBH) was prepared by condensing benzohydrazide with 3,5-dimethyl benzoyl chloride in dry DMAc. Later on, BDBH and aniline were subjected to subsequent cyclization to triazole in *ortho*-dichlorobenzene (ODCB) using  $\text{PCl}_3$  catalyst. The cyclized

product DPDT could be recrystallized from a mixture of ethanol:water (80:20) with 80% yield. In the final step, alkaline oxidation of DPDT was performed with  $\text{KMnO}_4$ -water-pyridine system. The crude monomer DTIA was crystallized in sodium salt form in aqueous sodium carbonate solution. It was further treated with charcoal in deionised water solution and subsequent acidification by acetic acid yielded the white shining crystalline diacid. It was finally dried in vacuum oven at  $125\text{ }^\circ\text{C}$  for 24 h. The usual characterization techniques such as FTIR,  $^1\text{H}$  NMR,  $^{13}\text{C}$  NMR and elemental analysis were carried out to elucidate the corresponding structures of monomer and intermediates.

FTIR spectrum of the intermediate BDBH (Figure 2.9) showed absorption at  $3210\text{ cm}^{-1}$  and  $1674\text{ cm}^{-1}$  corresponding to  $-\text{N-H}$  stretching and carbonyl ( $-\text{C}=\text{O}$ ) deformation occurred in the amide linkage, respectively. The deformation of secondary amine  $-\text{N-H}$  in the same amide linkage was observed at  $1526\text{ cm}^{-1}$ . Further characterization of BDBH by  $^1\text{H}$  NMR spectrum (Figure 2.10) showed two singlets at  $10.38\text{ ppm}$  and  $10.48\text{ ppm}$  corresponding to the protons of secondary amine. Singlet at  $2.34\text{ ppm}$  was due to protons of methyl group. Aromatic peaks occurred as singlet, multiplet and doublet at  $7.23\text{ ppm}$ ,  $7.52\text{ ppm}$  and  $7.9\text{ ppm}$ , respectively.  $^{13}\text{C}$  NMR spectrum of the same intermediate (Figure 2.11) showed peaks of aromatic carbons in the range  $166.24\text{--}125.33\text{ ppm}$  and the peak at  $20.94\text{ ppm}$  was due to the  $-\text{CH}_3$ . Elemental analysis is in good agreement with the theoretical values. Thus, FTIR spectrum,  $^1\text{H}$  NMR,  $^{13}\text{C}$  NMR and elemental analysis confirmed the structure of the BDBH.

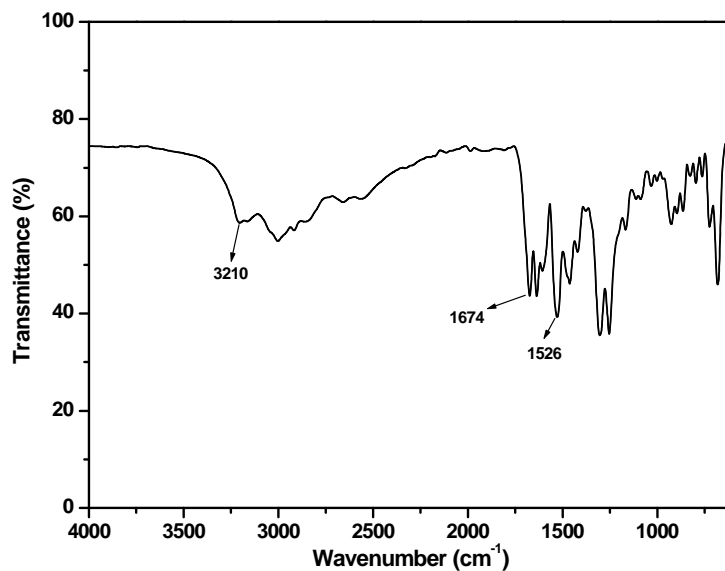


**Figure 2.9** FTIR spectrum of N'-benzoyl-3,5-dimethylbenzohydrazide (BDBH) in KBr

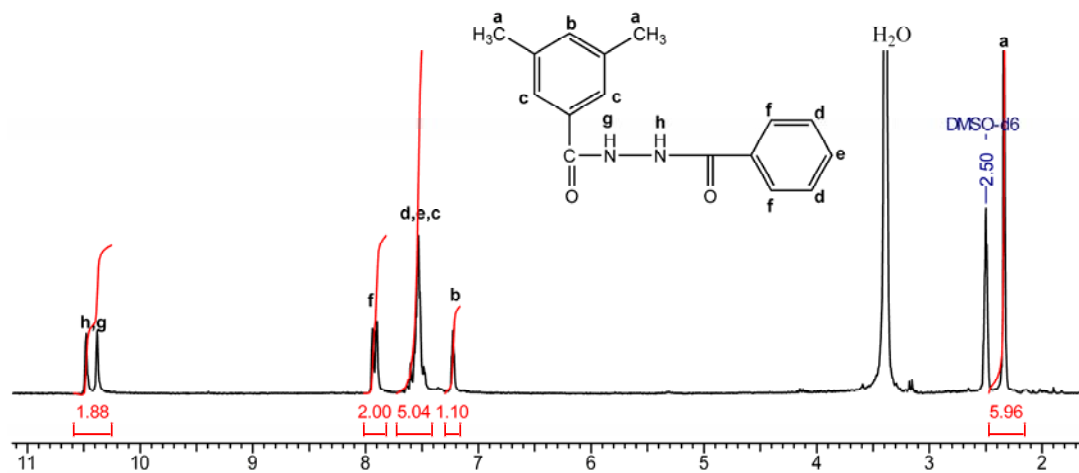


**Figure 2.10** <sup>1</sup>H NMR spectrum of N'-benzoyl-3,5-dimethylbenzohydrazide (BDBH) in DMSO-d<sub>6</sub>

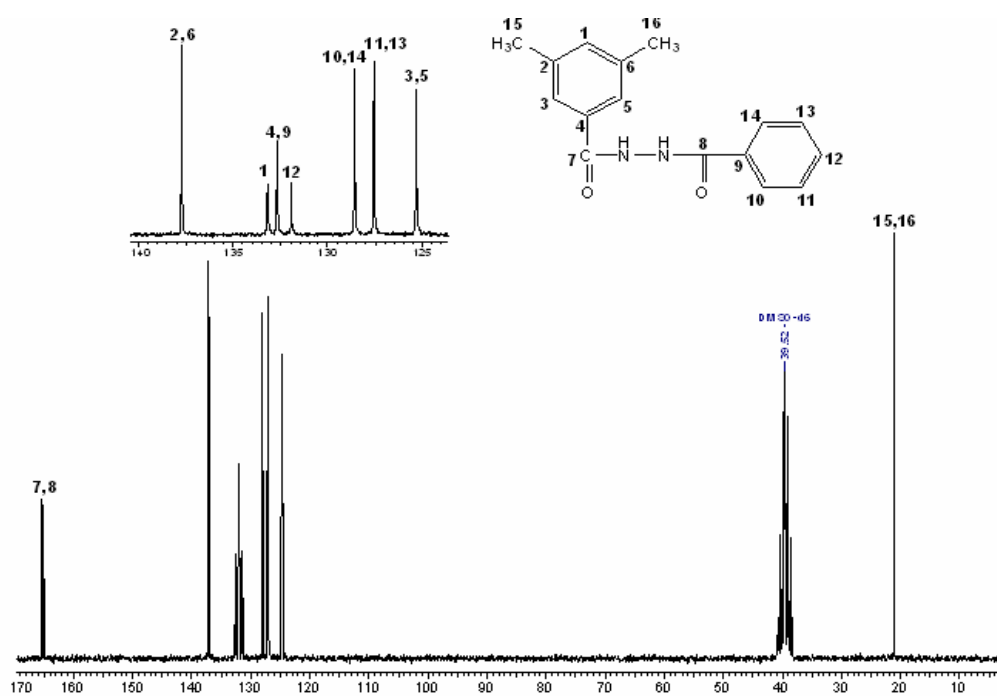


**Figure 2.11** <sup>13</sup>C NMR spectrum of N'-benzoyl-3,5-dimethylbenzohydrazide (BDBH) in DMSO-d<sub>6</sub>

The FTIR spectrum of the second step, cyclized intermediate DPDT, exhibited complete disappearance of characteristic peak of -N-H stretching and (C=O) deformation at 3210 cm<sup>-1</sup> and 1674 cm<sup>-1</sup>, respectively which were present in the BDBH. The various characteristic peaks of (C=N) were observed at 1606 cm<sup>-1</sup>, 1496 cm<sup>-1</sup>, and 1172 cm<sup>-1</sup> (Figure 2.12) indicating complete cyclization.

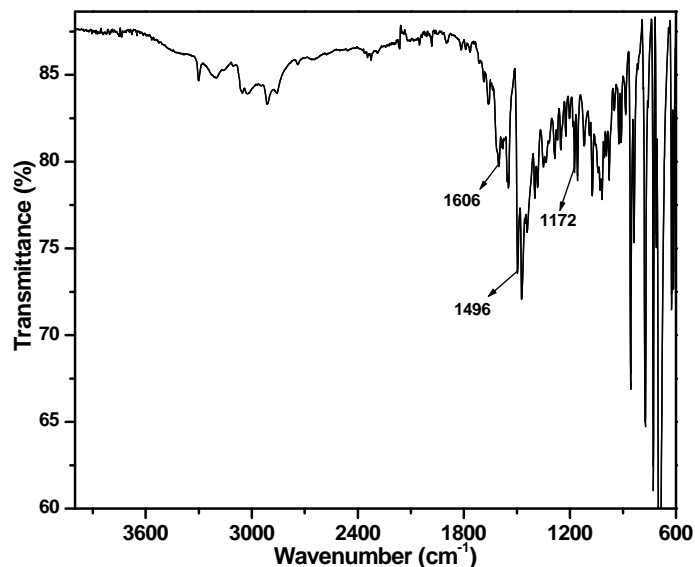


**Figure 2.12** FTIR spectrum of 3-(3,5-dimethylphenyl)-4,5-diphenyl-4H-1,2,4-triazole (DPDT) in KBr

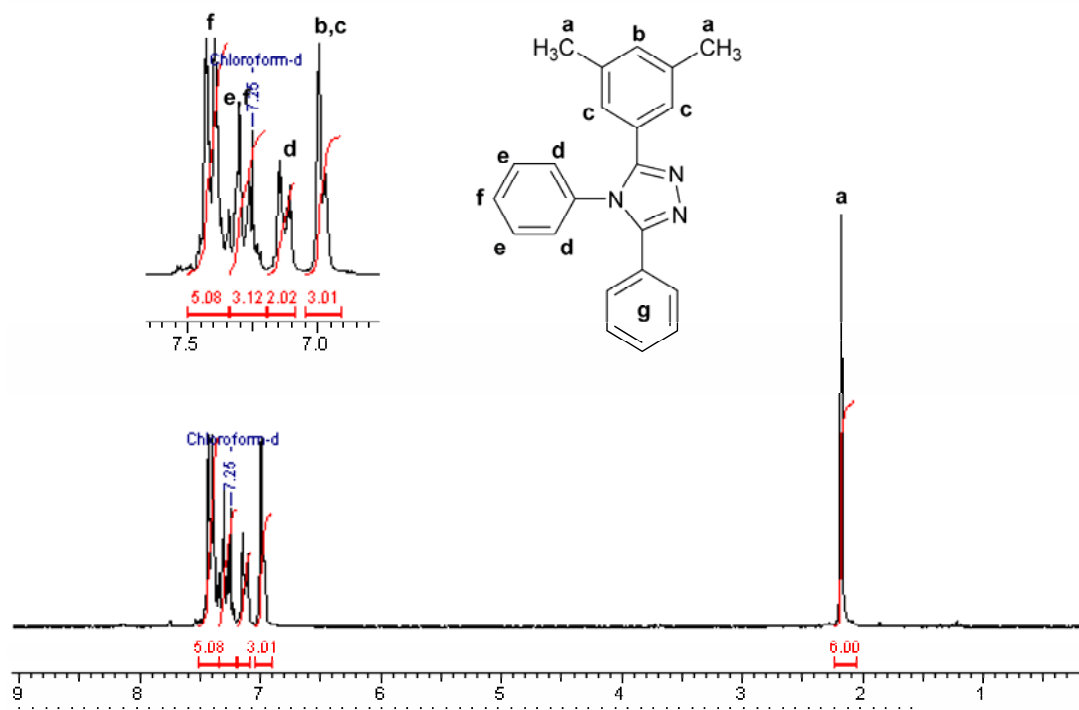


**Figure 2.13**  $^1\text{H}$  NMR spectrum of 3-(3,5-dimethylphenyl)-4,5-diphenyl-4H-1,2,4-triazole (DPDT) in  $\text{CDCl}_3$

In  $^1\text{H}$  NMR spectrum (Figure 2.13), the presence of a singlet at 2.18 ppm can be assigned to protons of methyl groups, while aromatic protons b, c, d, e, f and g showed expected integration and multiplets in the region 6.97-7.4 ppm. The complete cyclization in DPDT was further confirmed by the absence of two proton singlets of secondary amine (-N-H) which was present in the precursor, BDBH.  $^{13}\text{C}$  NMR spectrum (Figure

2.14) of DPDT showed different peaks of respective aromatic carbons in the range between 155.05-126.59 ppm. The methyl carbons appeared at 21.18 ppm.

Thus, good agreement in observed and calculated elemental analysis values, FTIR,  $^1\text{H}$  NMR and  $^{13}\text{C}$  NMR analysis confirm expected structure of DPDT.

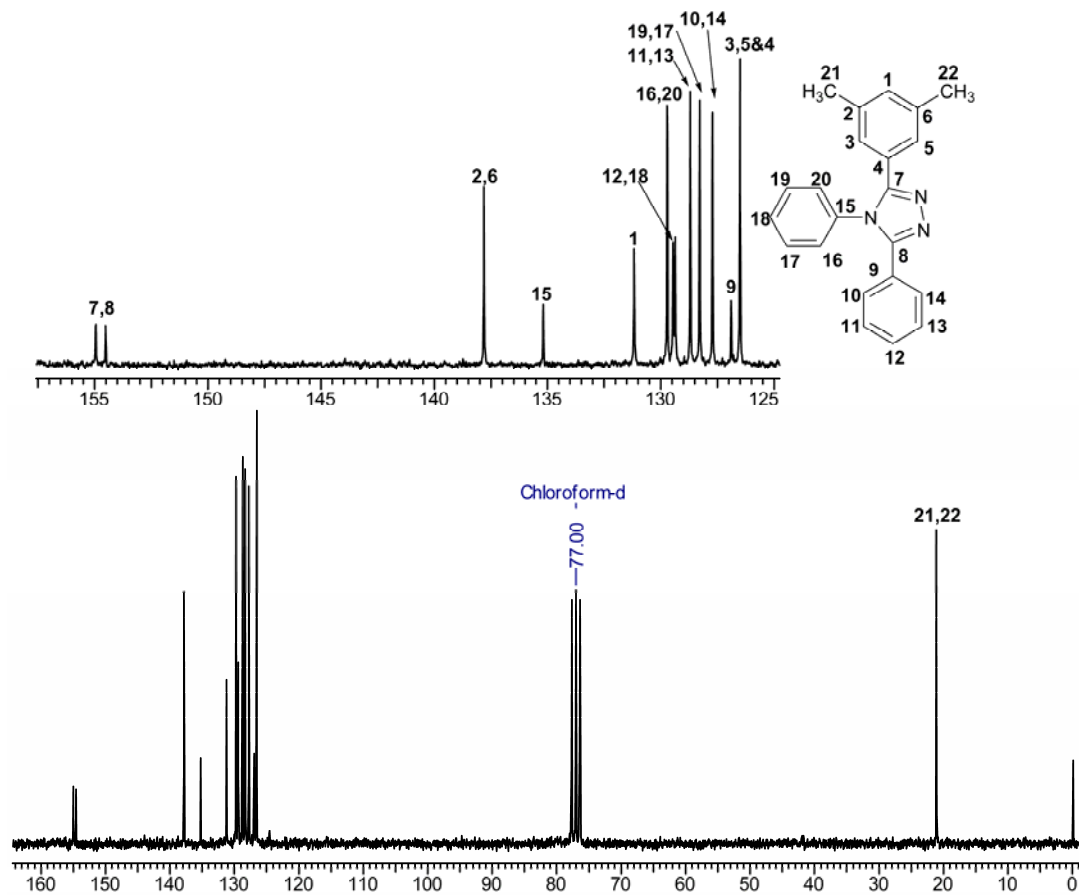


**Figure 2.14**  $^{13}\text{C}$  NMR spectrum of 3-(3,5-dimethylphenyl)-4,5-diphenyl-4H-1,2,4-triazole (DPDT) in  $\text{CDCl}_3$

The final step constituted oxidation of the intermediate DPDT to the desired 5-(4,5-diphenyl-4H-1,2,4-triazol-3-yl)isophthalic acid (DTIA) by using aqueous  $\text{KMnO}_4$ -pyridine system as mentioned earlier. The product was characterized by FTIR,  $^1\text{H}$  NMR,  $^{13}\text{C}$  NMR and elemental analysis. Elemental analysis values are in good agreement with the calculated values.

The FTIR spectrum of DTIA (Figure 2.15) showed broad band from  $3300\text{ cm}^{-1}$  to  $2500\text{ cm}^{-1}$  indicating the presence of  $-\text{COOH}$  group. The characteristic peak of  $\text{C}=\text{O}$  stretching in carboxyl group appeared at  $1691\text{ cm}^{-1}$ .  $^1\text{H}$  NMR spectrum revealed various peaks from 7.4-8.45 ppm within which aromatic protons are present (Figure 2.16). The complete disappearance of the methyl protons appeared at 2.18 ppm in the earlier intermediate DPDT in the  $^1\text{H}$  NMR, confirms its complete oxidation to carboxylic acid.

However, carboxylic acid peaks could not be located in the present spectrum since protons become more detachable in the highly polar DMSO-d<sub>6</sub> solvent.

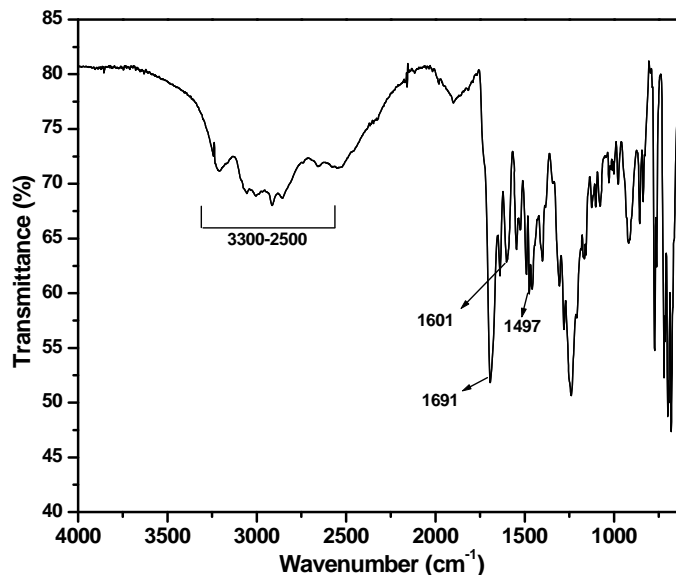


**Figure 2.15** FTIR spectrum of 5-(4,5-diphenyl-4H-1,2,4-triazol-3-yl)isophthalic acid (DTIA) in KBr

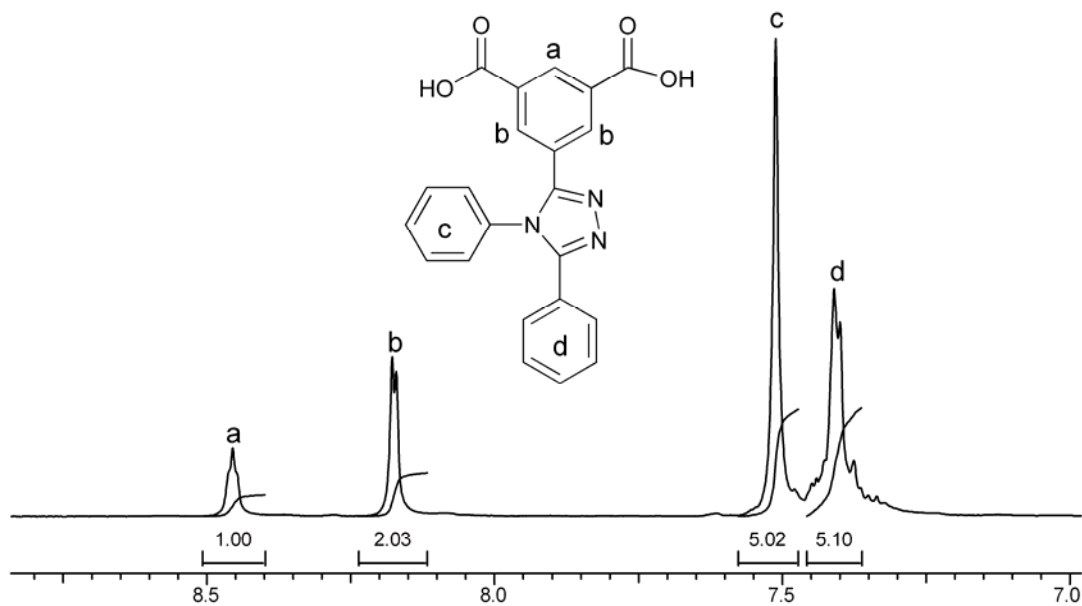


**Figure 2.16** <sup>1</sup>H NMR spectrum of 5-(4,5-diphenyl-4H-1,2,4-triazol-3-yl)isophthalic acid (DTIA) in DMSO-d<sub>6</sub>

The peak appearance at 166.15 ppm in <sup>13</sup>C NMR (Figure 2.17) corresponding to carbonyl carbon (carbon no. 22 in Figure 2.17) attached to aromatic ring supports the complete oxidation of methyl groups and confirms the presence of –COOH groups. It is well known that <sup>13</sup>C NMR of IPA exhibits the chemical shift at 167 ppm in the same

solvent viz. DMSO- $d_6$ .<sup>23</sup> The remaining aromatic carbons appeared within the range 155–127.08 ppm. It is interesting to note that, there were no peaks belonging to methyl carbons at 21.18 ppm as appeared in its intermediate DPDT (Figure 2.14). It is therefore concluded the complete oxidation ( $-CH_3$  to  $-COOH$ ) And the results confirm the structure of DTIA.

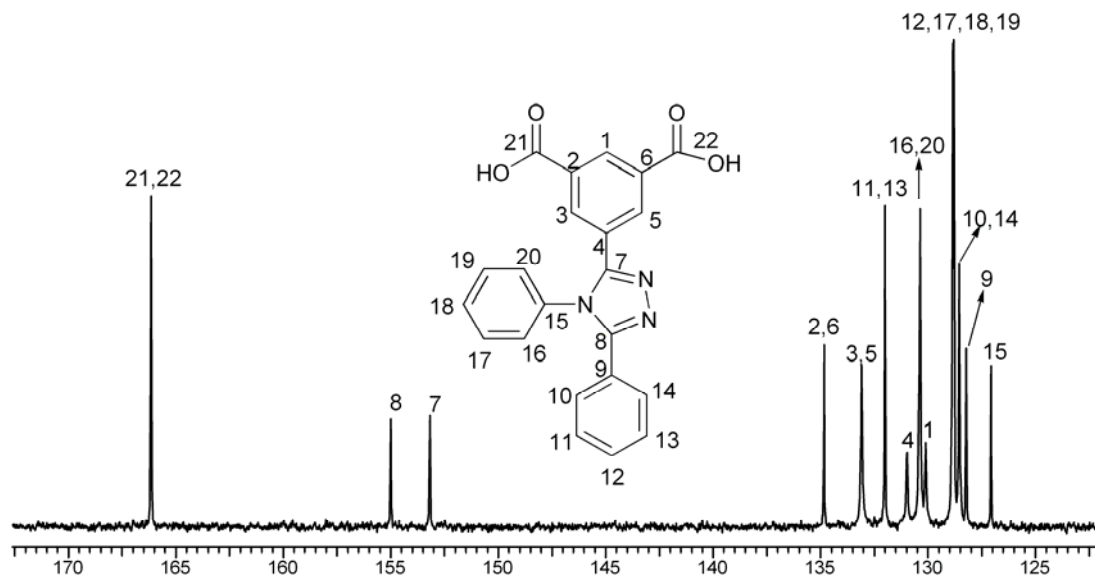


**Figure 2.17** <sup>13</sup>C NMR spectrum of 5-(4,5-diphenyl-4H-1,2,4-triazol-3-yl)isophthalic acid (DTIA) in DMSO- $d_6$

### 2.3.3 Synthesis and characterization of 3,3'-(1,3,4-oxadiazole-2,5-diyl)dibenzoic acid (ODBA)

The diacid ODBA was also synthesized in three steps as shown in Scheme 2.3. The 2,5-dim-tolyl-1,3,4-oxadiazole (DTO) was synthesized from the same intermediate (MBH) used to obtain PTDBA. The synthesis and characterization of MBH has already been discussed in Section 2.3.1. The cyclization step towards oxadiazole in DTO was achieved by heating the intermediate MBH with phosphorous oxy chloride ( $POCl_3$ ) at 80 °C for 16 h. The DTA was purified by column chromatography technique with 80:20 petroleum benzene : ethyl acetate. The subsequent oxidation of the DTO yielded the desired end product 3,3'-(1,3,4-oxadiazole-2,5-diyl)dibenzoic acid (ODBA). The oxidation was performed by the same reagent viz. aqueous  $KMnO_4$ -pyridine system, which had earlier been used for the novel diacids; PTDBA and DTIA. The product obtained was found to contain impurities difficult to separate by crystallization. During the oxidation to diacid (ODBA), isophthalic acid was thought to be generated due to the probable hydrolysis of oxadiazole. Hence to remove this undesired IPA, the obtained crude ODBA was heated in boiling deionised water for 30 min and then immediately

filtered. The IPA remained soluble in hot deionised water in filtrate while the desired ODBA was obtained as the whitish solid. The solid in filtrate was recovered and analysis proved it to be IPA.

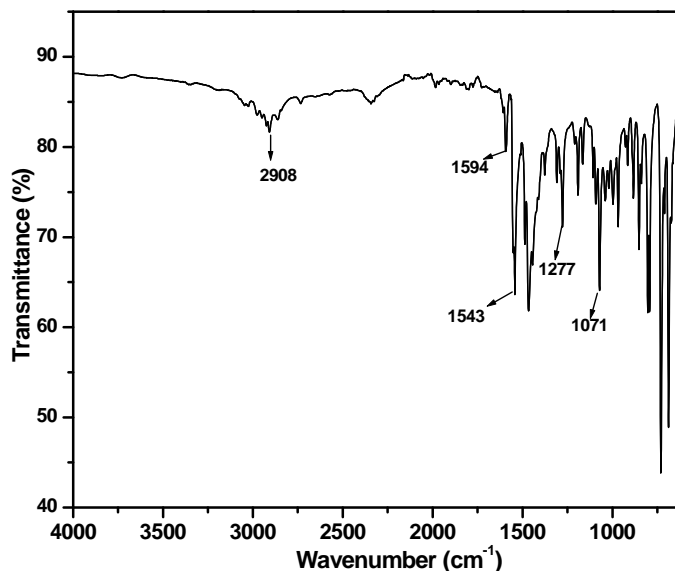


**Figure 2.18** FTIR spectrum of 2,5-dim-tolyl-1,3,4-oxadiazole (DTO) in KBr

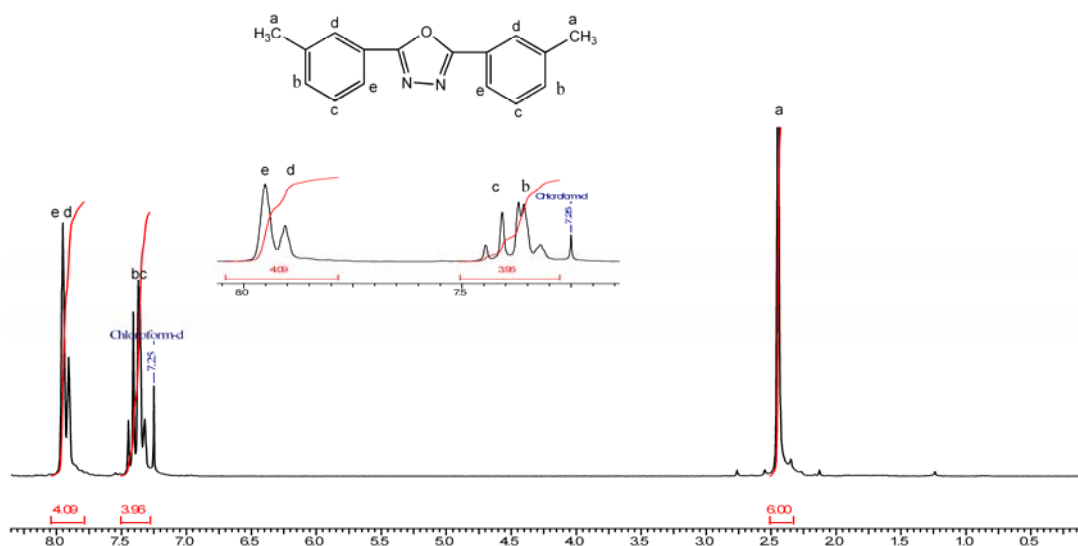


**Figure 2.19**  $^1\text{H}$  NMR spectrum of 2,5-dim-tolyl-1,3,4-oxadiazole (DTO) in  $\text{CDCl}_3$

The intermediates and the final diacid (ODBA) were characterized by FTIR,  $^1\text{H}$  NMR, and elemental analysis. The characterization of the first intermediate MBH was discussed in Section 2.3.1. The FTIR spectrum of DTO (Figure 2.18) showed bands at  $1071\text{ cm}^{-1}$  and  $1277\text{ cm}^{-1}$  corresponding to  $-\text{C}-\text{O}-\text{C}-$  linkage in the oxadiazole moiety as symmetric and asymmetric stretching, respectively. The appearance of new bands at  $1594\text{ cm}^{-1}$  and  $1543\text{ cm}^{-1}$  due to the  $\text{C}=\text{N}$  stretching and the disappearance of bands at  $3208\text{ cm}^{-1}$  and  $1643\text{ cm}^{-1}$  corresponding to  $-\text{N}-\text{H}$  and carbonyl stretching of hydrazide,



respectively confirm the formation of cyclization in DTO. The  $^1\text{H}$  NMR spectrum (Figure 2.19) of DTO displayed the singlet in the upfield at 2.38 ppm corresponding to protons of *meta* linked  $-\text{CH}_3$  groups. The remaining aromatic protons located in the region 7.26-7.89 ppm also showed expected peak integration. The observed and calculated values in the elemental analysis were also in good agreement.

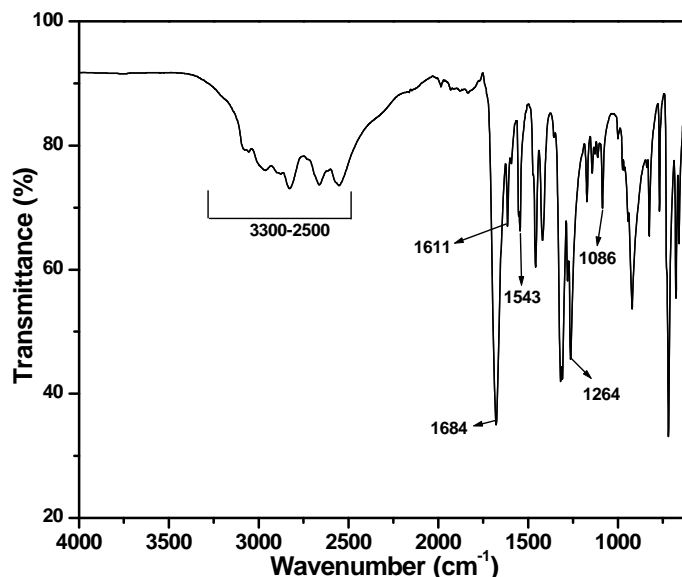


**Figure 2.20** FTIR spectrum of 3,3'-(1,3,4-oxadiazole-2,5-diyl)dibenzoic acid (ODBA) in KBr

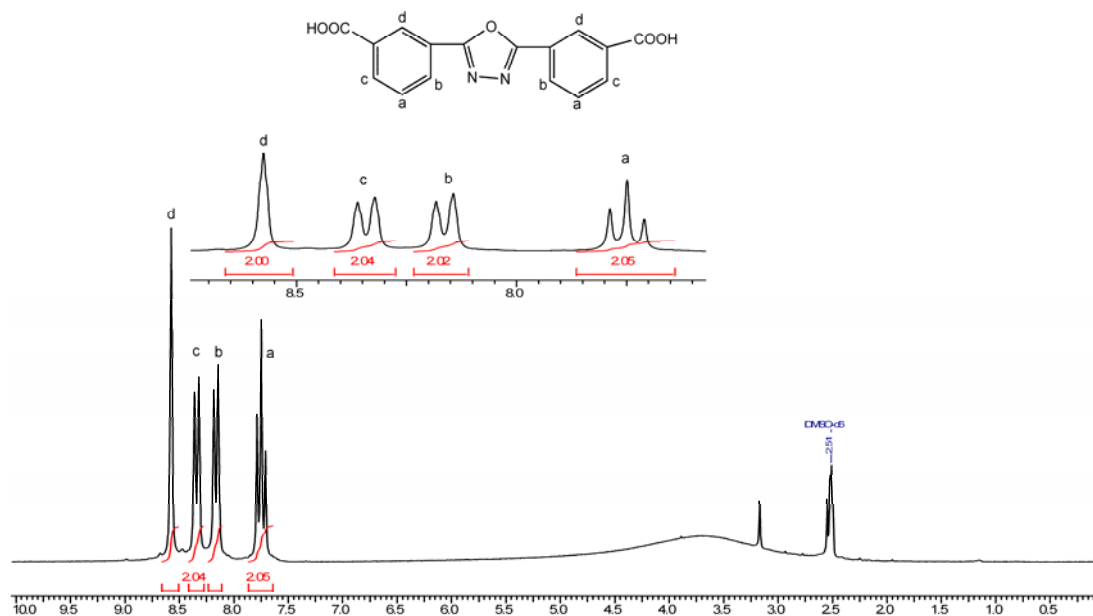


**Figure 2.21**  $^1\text{H}$  NMR spectrum of 3,3'-(1,3,4-oxadiazole-2,5-diyl)dibenzoic acid (ODBA) in  $\text{DMSO-d}_6$

The characterization of ODBA by FTIR (Figure 2.20) showed broad absorption in the region  $3300\text{-}2500\text{ cm}^{-1}$  which assigned to the hydrogen bonded hydroxyl group.

The presence of carbonyl group in the acid functionality was confirmed by the appearance of a band at  $1684\text{ cm}^{-1}$ . It should be noted that the frequency corresponding to the symmetric ( $1086\text{ cm}^{-1}$ ) and asymmetric ( $1264\text{ cm}^{-1}$ ) stretching of -C-O-C- linkage has also been retained, thus confirming the presence of cyclized structure of oxadiazole in the final diacid, too. Further characterization of ODBA by  $^1\text{H}$  NMR (Figure 2.21) exhibited the singlet at 8.6 ppm corresponding to proton d which appeared at the most downfield among all the aromatic protons, as expected since proton d was near to the electron withdrawing carboxyl group. Protons b and c showed the expected doublets at 8.17 and 8.36 ppm respectively, since they could ortho-coupled with only proton a. A proton a also showed the triplet (7.74-7.82 ppm) as it was flanked by two ortho positioned protons b and c.  $^{13}\text{C}$ -NMR spectrum (Figure 2.22) of the ODBA showed various eight carbons in the range 123.87-166.58 ppm, within which respective peaks corresponding to carbonyl as well as aromatic carbons appeared. The observed elemental analysis was also in good agreement with calculated values.

Thus, the chemical structure of intermediates as well as diacid (ODBA) was confirmed by FTIR and  $^1\text{H}$  NMR,  $^{13}\text{C}$  NMR spectra and elemental analysis.

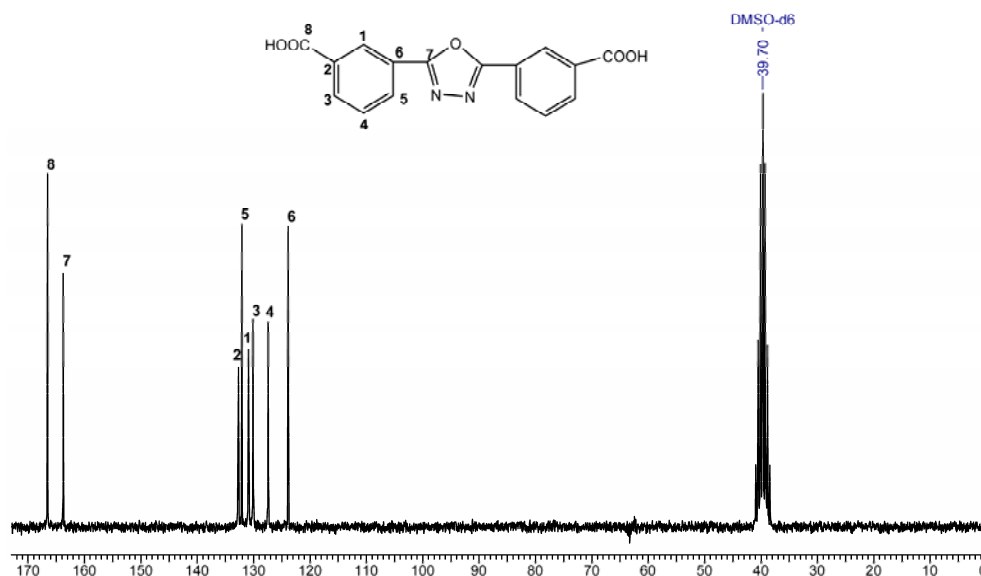


**Figure 2.22**  $^{13}\text{C}$  NMR spectrum of 3,3'-(1,3,4-oxadiazole-2,5-diyl)dibenzoic acid (ODBA) in  $\text{DMSO-d}_6$

### 2.3.4 Synthesis and characterization of 5-(5-phenyl-1,3,4-oxadiazol-2-yl)isophthalic acid (POIA)

POIA, was synthesized in three steps as shown in Scheme 2.4, starting from 3,5-dimethyl benzoic acid. Starting from 3,5-dimethyl benzoic acid through various steps gave an intermediate BDBH and the detailed procedure for the synthesis of BDBH explained

in Section 2.2.3.2.(i). BDBH was then cyclized to DPPO containing oxadiazole moiety by using  $\text{POCl}_3$ . The procedure for cyclization of DPPO and DTO was almost the same except in the purification step, the latter being purified through column chromatography. On the other hand, DPPO was purified by crystallization in methanol. Obtained yield of the purified DPPO was 77 % with white shining crystals. The attainment of oxidation of DPPO to POIA was accomplished with aqueous  $\text{KMnO}_4$ -pyridine system by similar procedure followed for oxidation of DTO to corresponding ODBA, with the exception in purification. Purification of POIA was observed to be extremely tedious and attempted by recrystallization in various polar aprotic solvents (DMF, DMAc, DMSO, NMP) as well as polar protic solvents (acetic acid, formic acid, methanol, ethanol, isopropanol, water) including binary solvent system of polar aprotic and polar protic solvents. This diacid could not be crystallized in any solvents. Finally, the diacid was purified by repeated washing with methanol to remove the impurities. Various intermediates and the final product were characterized by FTIR,  $^1\text{H}$  NMR,  $^{13}\text{C}$  NMR and elemental analysis.

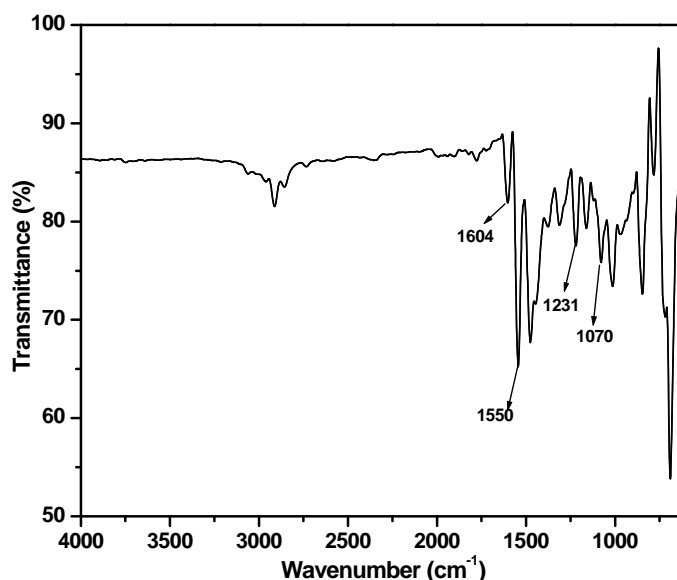


**Figure 2.23** FTIR spectrum of 2-(3,5-Dimethyl Phenyl)-5-Phenyl-1,3,4-Oxadiazole (DPPO) in KBr

The characterization of BDBH was explained earlier in the Section 2.3.2. Characterization of DPPO by FTIR (Figure 2.23) spectroscopy technique revealed peaks at  $1070\text{ cm}^{-1}$  and  $1231\text{ cm}^{-1}$  due to the symmetric and asymmetric stretching, respectively of  $-\text{C}-\text{O}-\text{C}-$  linkage in the oxadiazole moiety. Peaks appeared at  $1604\text{ cm}^{-1}$  and  $1550\text{ cm}^{-1}$  were due to  $\text{C}=\text{N}$  stretching. Absence of  $-\text{N}-\text{H}$  peak at  $3210\text{ cm}^{-1}$  and carbonyl group at  $1674\text{ cm}^{-1}$  confirmed complete cyclization to oxadiazole in DPPO.

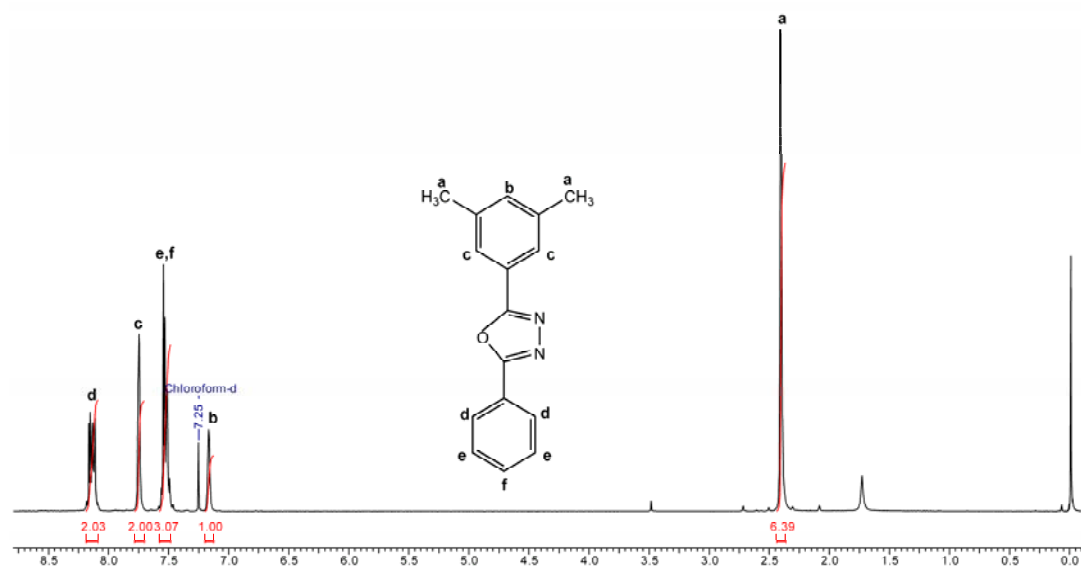


**Figure 2.24**  $^1\text{H}$  NMR spectrum of 2-(3,5-Dimethyl Phenyl)-5-Phenyl-1,3,4-Oxadiazole (DPPO) in  $\text{CDCl}_3$

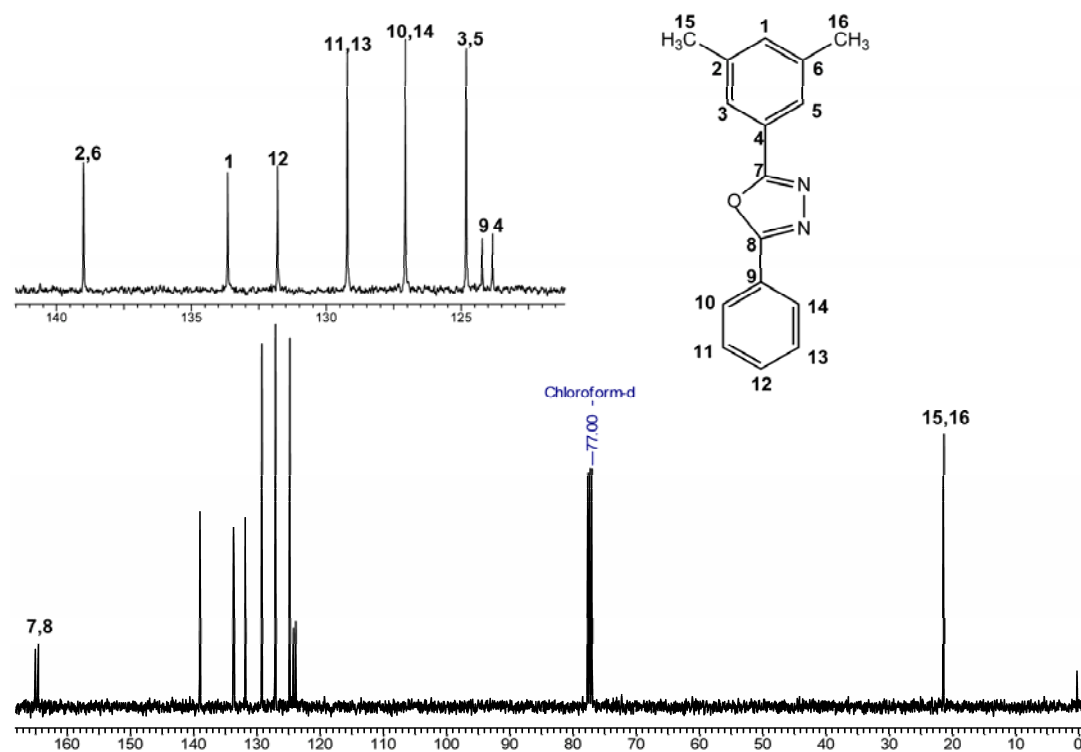


**Figure 2.25**  $^{13}\text{C}$  NMR spectrum of 2-(3,5-Dimethyl Phenyl)-5-Phenyl-1,3,4-Oxadiazole (DPPO) in  $\text{CDCl}_3$

$^1\text{H}$  NMR spectrum (Figure 2.24) of 2-(3,5-Dimethyl Phenyl)-5-Phenyl-1,3,4-Oxadiazole (DPPO) showed singlet at 2.34 corresponding to  $-\text{CH}_3$  protons. In the aromatic region, singlet at 7.15 ppm, multiplet at 7.55 ppm, singlet at 7.75 ppm and doublet of doublet at 8.15 ppm corresponding to the one, three, two, two protons,

respectively with expected multiplicity and integration are observed.  $^{13}\text{C}$  NMR spectrum (Figure 2.25) showed aromatic carbons at 164.84-123.63 ppm with expected values and peak at 21.09 ppm corresponding to the  $-\text{CH}_3$  group. With these observations along with good agreements of elemental analysis values confirmed the structure of the product (DPPO).

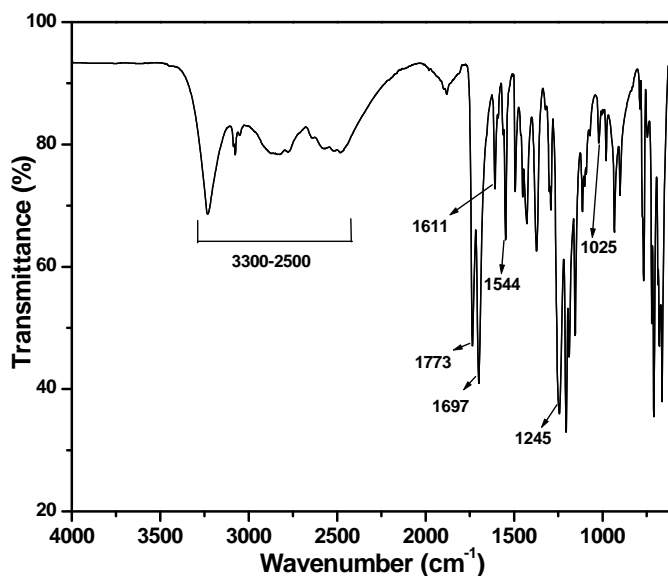


**Figure 2.26** FTIR spectrum of 5-(5-phenyl-1,3,4-oxadiazol-2-yl) isophthalic acid (POIA) in KBr

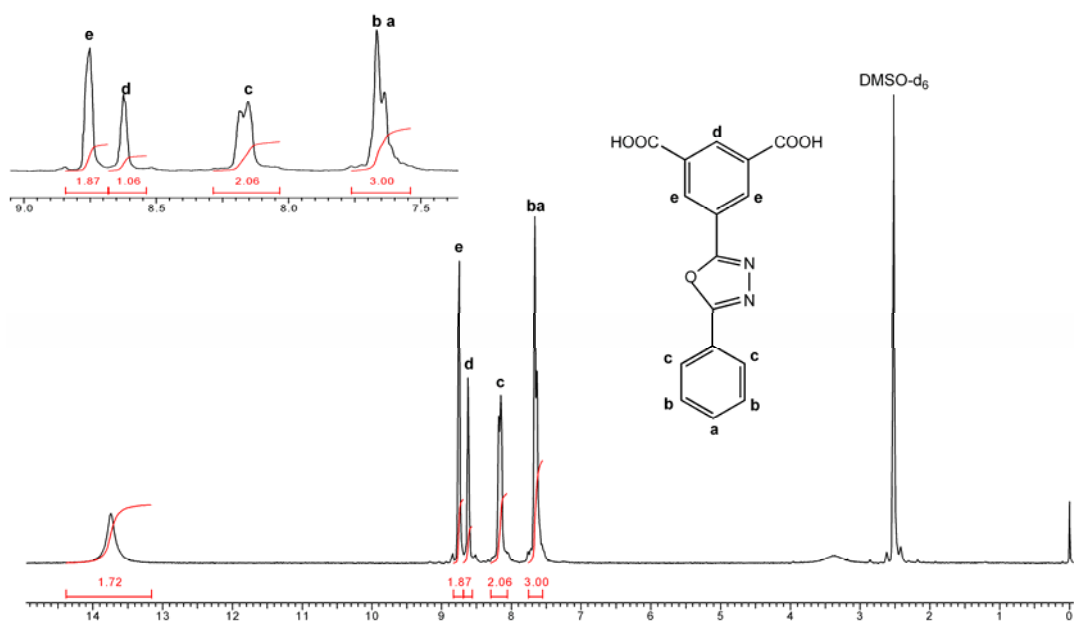


**Figure 2.27**  $^1\text{H}$  NMR spectrum of 5-(5-phenyl-1,3,4-oxadiazol-2-yl) isophthalic acid (POIA) in  $\text{DMSO-d}_6$

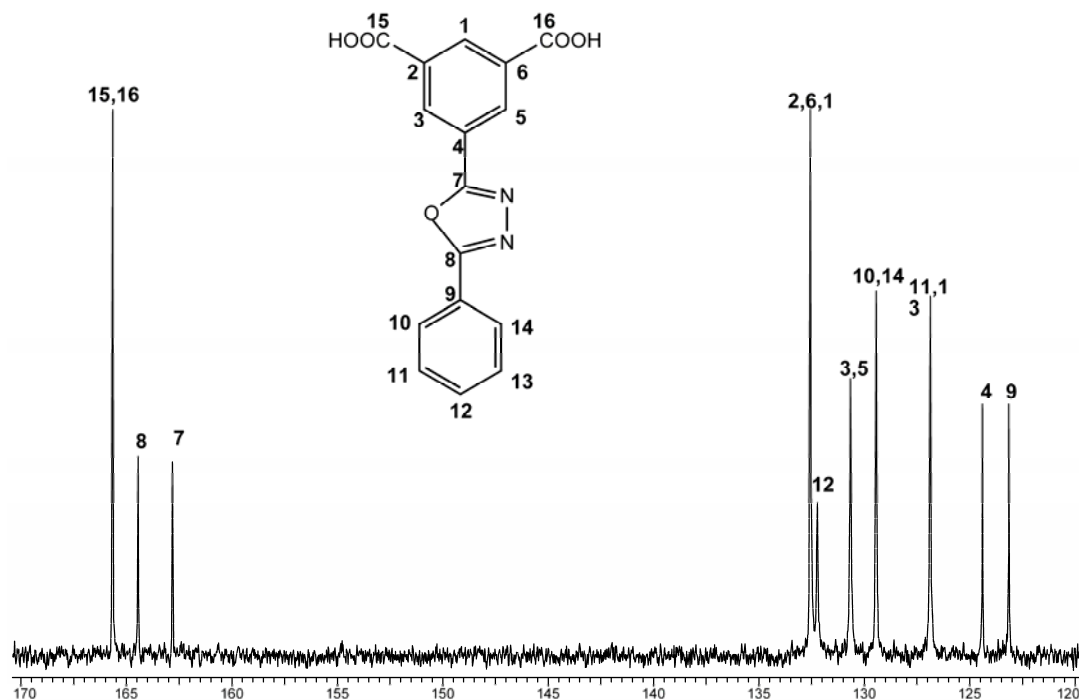


**Figure 2.28**  $^{13}\text{C}$  NMR spectrum of 5-(5-phenyl-1,3,4-oxadiazol-2-yl) isophthalic acid (POIA) in  $\text{DMDO-d}_6$

FTIR spectrum (Figure 2.26) of 5-(5-phenyl-1,3,4-oxadiazol-2-yl) isophthalic acid (POIA) showed a broad absorption in the region  $3300\text{-}2500\text{ cm}^{-1}$  corresponding to the hydrogen bonded hydroxyl group. The absorptions due to  $>\text{C}=\text{O}$  group appeared at  $1773\text{ cm}^{-1}$  and  $1697\text{ cm}^{-1}$  due to inter- and intramolecular hydrogen bonding, respectively. The specific peak of  $-\text{C}-\text{O}-\text{C}-$  stretching in oxadiazole group appeared at  $1025\text{ cm}^{-1}$  and  $1245\text{ cm}^{-1}$  due to symmetric and asymmetric stretching, respectively.  $^1\text{H}$  NMR (Figure 2.27) showed various peaks in the region  $7.67\text{-}8.75\text{ ppm}$  due to different aromatic protons consistent with structure of POIA. The absence of a singlet at  $2.34\text{ ppm}$  corresponding  $-\text{CH}_3$  protons of DPPO proved its complete oxidation. In  $^{13}\text{C}$ -NMR spectrum, (Figure 2.28) various peaks of aromatic carbons appeared between  $165.65\text{-}123.14\text{ ppm}$  consistent with structure as shown in Figure 2.28, in which the most downfield peak at  $165.65\text{ ppm}$  was due to the carbon of carboxyl group.

Thus, the chemical structure of intermediates as well as diacid (POIA) was confirmed by FTIR,  $^1\text{H}$  NMR,  $^{13}\text{C}$  NMR spectral analysis and elemental analysis.

## 2.4 Conclusions

- Three new diacids namely, 3,3'-(4-phenyl-4H-1,2,4-triazole-3,5-diyl) dibenzoic acid (PTDBA), 5-(4,5-diphenyl-4H-1,2,4-triazol-3-yl)isophthalic acid and 5-(5-phenyl-1,3,4-oxadiazol-2-yl) isophthalic acid were successfully synthesized by simple condensation reactions with high purity and good yields, by using the less expensive commercially available starting materials.
- A oxadiazole group containing diacid 3,3'-(1,3,4-oxadiazole- 2,5-diyl)dibenzoic acid was also synthesized with high purity and good yields.
- The structures of all diacid monomers and intermediate compounds were fully characterized and confirmed by FTIR, <sup>1</sup>H NMR, <sup>13</sup>C NMR analysis and elemental analysis.

## References

1. Neuse, E. W. *Advances in Polymer Sciences* **1982**, 47, 1-42.
2. Tsunoda, S.; Koezuka, H.; Kurata, T.; Yanaura, S.; Ando, T. *J. Polym. Sci.B: Polym. Phys.* **1988**, 26, 1697.
3. Hardy, E. E. and Saunders, J. H. Chapter 14, *New High Temperature Resistant Plastic Foams, Part-II*, Edited by K. C. Frisch and J. H. Saunders, Marcel Dekker, New York (**1973**).
4. Chung, T.-S. *Polymer Reviews* **1997**, 37, 277 – 301.
5. Belohlav, L. R. *Angew Makromol Chem.* **1974**, 40/41, 465-483.
6. Kumbharkar, S. C.; Karadkar, P. B.; Kharul, U. K. *J. Membr. Sci.* **2006**, 286, 161–169.
7. Sena, M. E.; Andrade, C. T. *Polymer Bulletin* **1995**, 34, 643-648.
8. Leibnitz, E.; Eisold, C.; Paul, D. *Angew. Mukromol. Chem.* **1993**, 210, 197.
9. Yang, N. C.; Chang, S.; Suh, D. H. *Polymer* **2003**, 44, 2143–2148.
10. Wang, K.Y.; Chung, T.-S. *J. Membr. Sci.* **2006**, 281, 307–315.
11. Rikukawa, M. and Sanui, K. *Prog. Polym. Sci.* **2000**, 25, 1463.
12. Devanathan, R. *Energy Environ. Sci.* **2008**, 1, 101–119.
13. Ma, Y.-L.; Wainright, J. S.; Litt, M. H. and Savinella, R. F. *Journal of the Electrochemical Society* **2004**, 151, A8-A16.
14. Zaidi, S. M. J.; Chen, S. F.; Mikhailenko, S. D. and Kaliaguine, S. *J. New Materials Electrochem. Syst.* **2000**, 3, 27-32.
15. Shaplov, A. S.; Lozinskaya, E. I.; Odinets, I. L.; Lyssenko, K. A.; Kurtova, S. A.; Timofeeva, G. I.; Iojoiu, C.; Sanchez, J-Y.; Abadie, M. J. M.; Voytekunas, V. Y.; Vygodskii, Y. S. *Reactive & Functional Polymers* **2008**, 68, 208-224.
16. Schulz, B.; Bruma, M. and Brehmer, L. *Advanced Materials* **1997**, 9, 601-613.

17. Carruthers, W. Modern methods of organic synthesis 3<sup>rd</sup> edition, Cambridge University Press, **1996**.
18. Kim, S. W.; Shim, S. C.; Jung, B.-J.; Shim, H.-K. *Polymer* **2002**, 43, 4297-4305.
19. Preston, J. *Heterocyclic Chem* **1965**, 2, 441.
20. Siegrist, A. E. and Moergeli, E. U.S. Patent 2,765,304 (**1956**).
21. Javaid, K. and Smith, D. M. *J. Chem. Research (S)* **1984**, 118-119.
22. Tod, W.; Campbelv, E.; Roniksa, F. S. and Arago, J. *J. of Appl Polym. Sci.* **1959**, 11, 155-162.
23. <http://www.sigmaaldrich.com/spectra/fnmr/FNMR010732.PDF>.



# Chapter **3**

**Synthesis and characterization  
of polybenzimidazoles and  
copolybenzimidazoles containing triazole  
groups and their application as polymer  
electrolyte membranes for fuel cells**

### 3.1 Introduction

The proton exchange membrane fuel cells (PEMFCs) have received wide attention of researchers due to their high power density and possible applications in vehicular transportation, electric utility and others requiring clean, quiet and portable power. Polymer electrolyte membrane (PEM) is the key component of PEMFCs and presently, perfluorosulfonic acid polymers, such as Nafion,<sup>®</sup> are the state-of-the-art materials for PEM. However, high cost, difficult water management, high fuel cross-over, low operational temperature, sensitivity to presence of carbon monoxide impurities for catalyst poisoning, are among other draw backs of Nafion<sup>®</sup> have prompted researchers to look for alternative less expensive polymer membrane, preferably, operating above 120 °C for proton transport. Polybenzimidazoles (PBIs) are considered as promising alternative materials for Nafion among the various polymeric materials investigated.<sup>®</sup> It is a thermally stable basic polymer having hydrogen donor and acceptor sites, which on doping with strong acids conduct protons.<sup>1</sup> The PBI, widely investigated as proton-exchange membranes, is poly [2,2-(*m*-phenylene)-5,5-benzimidazole]. It has poor tractability, poor oxidative stability at operational conditions, low proton conductivity at less than 100 °C compared to Nafion<sup>®</sup> and tendency to loose efficiency due to leaching out of dopant by water/methanol.

Several approaches have been explored to modify the properties of PBI to overcome these limitations. These include addition of inorganic fillers,<sup>2</sup> heteropolyacid based composites,<sup>3-9</sup> acid-base blends with sulfonated polymers,<sup>10</sup> such as sPEEK,<sup>11</sup> sulfonated poly(arylene-thioether)s,<sup>12</sup> sulfo-fluorinated poly (arylene-sulfo-ethers),<sup>13</sup> sulfonated polysulfones<sup>14</sup> and insitu doping during casting process.<sup>15</sup> Sulfonation of pristine PBI is another method studied extensively.<sup>16-22</sup> PBIs with structural variations have also been reported, which include poly(2,5-benzimidazole) (i.e.AB-PBI),<sup>23</sup> PBI based on 1,2,4,5-tetraaminobenzene,<sup>24</sup> pyridine dicarboxylic acids,<sup>25</sup> naphthalene dicarboxylic acid<sup>26</sup> and sulfonated isophthalic acid,<sup>27,28</sup> sulfonated PBI,<sup>29</sup> fluorine group containing PBI<sup>30</sup> and hyperbranched PBI.<sup>31</sup> These methods met with limited success.

Poly (N-phenyl-1,2,4-triazole) is another class of thermally stable high performance heterocyclic polymers known for their high glass transition temperature, high thermal stability, good mechanical strength and good chemical resistance. Triazole, like imidazole, is basic in nature capable of interacting with strong acids and used as a viable proton transport facilitator.<sup>32-34</sup> They have adequate capability to conduct the protons and better electrochemical stability. Polytriazoles, doped with phosphoric acid

have been found to exhibit good proton conductivity.<sup>35</sup> Recently, Ponce et al.<sup>36,37</sup> have synthesized sulfonated poly (oxadiazole-triazole) copolymers and demonstrated that the benzimidazole sulfonic acid doped sulfonated poly(oxadiazole-triazole) copolymers are promising candidates as a proton exchange membranes. However, there is no report on the synthesis of PBI tethered with N-Phenyl 1,2,4-triazole (NPT) groups. Since, both benzimidazole and triazole groups support proton conduction on doping with phosphoric acid, a polymer having both these groups should behave as a good polymer electrolyte for fuel cells. Properties of polymers containing alternate benzimidazole and NPT groups in main chain and a polymer containing all benzimidazole groups in main chain and pendant NPT groups in side chain are expected to be different. With this view we designed and prepared two new diacids for the synthesis of PBI containing NPT groups in main and side chain to study the behavior of these two types of polymers.

Thus, in this chapter, the synthesis of polybenzimidazoles containing NPT groups from two new dicarboxylic acids, namely, 3'-(4-phenyl-4H-1,2,4-triazole-3,5-diyl) dibenzoic acid (PTDBA) and 5-(4,5-diphenyl-4H-1,2,4-triazol-3-yl)isophthalic acid (DTIA) is illustrated and discussed. In addition, copolymers were synthesized with other diacids, namely, pyridine dicarboxylic acid, terephthalic acid, sebacic acid, adipic acid and isophthalic acid (IPA) for the structure-property relationship studies. Copolymers containing varying extents of NPT groups in main chain as well as in side chain were also synthesized by condensing a mixture of IPA and PTDBA and a mixture of DTIA and IPA respectively, in different mole ratio (90:10, 70:30, 50:50, 30:70 and 10:90) with TAB to study the effect of NPT groups on properties of polybenzimidazoles. Polybenzimidazoles were synthesized by high-temperature polycondensation method by using polyphosphoric acid (PPA) as a solvent and condensation agent. The synthesized polybenzimidazoles were investigated in terms of chemical structure, polymer and electrochemical properties.

## 3.2 Experimental

### 3.2.1 Materials

Isophthalic acid (IPA), terephthalic acid (TPA), pyridine 2,6-dicarboxylic acid (PDCA), adipic acid (AA), sebacic acid (SA), 3,3',4,4',-tetra-amino biphenyl (TAB), calcium hydride (CaH<sub>2</sub>), polyphosphoric acid (115%) and trifluoro acetic acid (TFA) were purchased from Aldrich chemicals. AA, SA and IPA were purified by crystallization from methanol, while TAB and PDCA were recrystallized from water and water:HCl

(1:1) respectively. N-methyl-2-pyrrolidinone (NMP), N, N-dimethylacetamide (DMAc), N, N-dimethylformamide (DMF) were distilled over  $\text{CaH}_2$ . Methanol, ortho phosphoric acid (85%), mohr's salt  $[(\text{NH}_4)_2\text{Fe}(\text{SO}_4)_2 \cdot 6\text{H}_2\text{O}]$ , sulfuric acid (96%), methane sulfonic acid (MSA), formic acid (FA), dimethyl sulfoxide (DMSO) and hydrogen peroxide (30%, w/v) were purchased from S.D. fine-chem. India Ltd. and used without further purification. The diacids 3'-(4-phenyl-4H-1,2,4-triazole-3,5-diyl) dibenzoic acid (PTDBA) and 5-(4,5-diphenyl-4H-1,2,4-triazol-3-yl)isophthalic acid (DTIA) were synthesized as per procedure given in Chapter 2.

### 3.2.2 Analytical methods

Elemental analysis was performed on Elementar vario-EL. Inherent viscosity (IV) measurements of all polymers were carried out in DMAc (0.5 g/dL) at 30 °C using a Ubbelohde viscometer (model F725). The FTIR spectra were recorded on a Perkin Elmer 16 PC spectrophotometer. Films of 20  $\mu\text{m}$  thickness were used for recording FTIR spectra.  $^1\text{H}$  NMR spectra were obtained on a Bruker NMR spectrometer operating at a proton frequency of 200 MHz in  $\text{DMSO-d}_6$  at room temperature. Thermogravimetric analyses (TGA) were recorded using Perkin Elmer TGA-7 instrument from 50 to 900 °C with a scanning rate of 10 °C  $\text{min}^{-1}$  in  $\text{N}_2$  atmosphere. Glass transition temperature ( $T_g$ ) was measured using DSC Q-10 (TA) instrument. For the DSC measurements, approximately 5-7 mg of sample was taken in an aluminum pan that was tightly crimped and then scanned from 50 to 450 °C in  $\text{N}_2$  atmosphere at a flow rate 20 mL/min and heating rate of 20 °C/min. The wide-angle X-ray diffraction spectra (WAXD) were obtained using Rigaku Dmax 2500 diffractometer with  $\text{Cu-K}\alpha$  (1.589 Å) radiation source at ambient temperature. Tensile properties of polymer films were determined on Instron tensile tester series IX using film strips (1.5 x 7 cm and 100  $\mu\text{m}$  thick) at a shear rate of 5 mm/min at room temperature.

#### ➤ Solubility measurement

The solubility of polymers in various solvents was determined by dissolving 50 mg of the polymer in 5 mL solvent. A dry sample in powder form was kept in desired solvent for 24 h at ambient temperature with occasional shaking. If necessary, the sample was heated to reflux temperature of low boiling solvents or at 150 °C for high boiling solvents for 10-15 h.

➤ **Membrane casting**

Dense membranes were prepared by solution casting method. A 3% (w/v) polymer solution in DMAc was filtered through G-0 sintered funnel on a clean and smooth glass Petri dish. The samples were kept overnight in an oven at 85 °C to remove the solvent. The films were peeled-off by immersing in water and soaked in water for 2 days in order to remove the residual DMAc. Such films were finally dried in vacuum oven at 125 °C for 2 days to remove the last traces of solvent.

➤ **Water uptake**

The water uptake capacity of all membranes was measured at room temperature by immersing accurately weighed dried membranes (40-45 mg) into deionized water for 24 h. The wet membranes were taken out, wiped with tissue paper and weighed immediately on a microbalance. The water uptake capacity was calculated using following equation (1).

$$WU = \frac{(W_w - W_d)}{W_d} \times 100 \quad (1)$$

where  $W_d$  and  $W_w$  are the weights of dry and wet membrane respectively.

➤ **Oxidative stability**

Oxidative stability was evaluated by the Fenton test.<sup>38</sup> Three pieces of membranes of 2 cm × 2 cm were immersed in 3% H<sub>2</sub>O<sub>2</sub> containing 4 ppm of Fe<sup>2+</sup> [Mohr's salt, (NH<sub>4</sub>)<sub>2</sub>Fe(SO<sub>4</sub>)<sub>2</sub>·6H<sub>2</sub>O] at 70 °C. The samples were taken out from the solution after desired time, washed thoroughly with distilled water, dried at 120 °C for 6 h and weighed. The Fenton solution was replaced with fresh stock solution after every 24 h. Stability was evaluated from the weight losses after each Fenton test.

➤ **Acid doping**

To determine the H<sub>3</sub>PO<sub>4</sub> uptake, accurately weighed dry samples of membranes (size 2 cm × 2 cm and 100 μm thick) were immersed in different molar concentrations of H<sub>3</sub>PO<sub>4</sub> for various time intervals at ambient temperature. The samples were taken out from the dopant after intended time and the excess of phosphoric acid adhered to samples was removed by blotting with tissue paper and weighed again. The weight gain due to both water and phosphoric acid was obtained by comparing the weight change before and after doping. For determining the acid-uptake by membranes, these membrane samples were further dried at 100 °C under vacuum until an unchanged weight was obtained. The acid-uptake was calculated in wt % by equation:

$$PU = \frac{(W_w - W_d)}{W_d} \times 100 \quad (2)$$

Where  $W_d$  and  $W_w$  are the initial weight of dry membrane and after removal of water from doped membrane samples respectively.

➤ **Conductivity measurements**

The proton conductivity was measured using an Auto Lab PGSTST 30 impedance analyzer with FRA software in the frequency range of 0.1-10<sup>5</sup> Hz with amplitude of 10 mV. To measure the conductivity at different temperatures, the cell was placed in a sealed glass vessel and the temperature was recorded in close proximity to the membrane sample with a K-type thermocouple. Films of 100 μm thickness were sandwiched between two stainless steel plates and measurements were carried out in a conductivity cell at temperatures ranging from 25 to 175 °C without humidification. The conductivity ( $\sigma$ ) was calculated by the formula:

$$\sigma = \frac{L}{RA} \quad (3)$$

Where R, L, and A are the measured resistance, thickness, and cross-sectional area of the membrane, respectively.

➤ **Fuel cell performance tests**

The electrodes were prepared by brushing the catalyst ink on the gas diffusion layers (GDL), prepared by applying slurry of Vulcan XC-72, PTFE, water and cyclohexane. The slurry was brushed until a carbon coating of 4 mg cm<sup>-2</sup> was achieved. The GDL was heat treated at 350 °C for 30 minutes before applying the catalyst ink. The catalyst ink was prepared by mixing 20% Pt/C, Nafion, water and isopropyl alcohol using a homogenizer (Cole Parmer, Model: CV33) for 2 minutes on 20 second on off basis. The amount of Pt and Nafion loading were 0.5 and 0.6 mg cm<sup>-2</sup> respectively. Finally, a thin layer of PBI was applied on the electrode surface before uni-axially pressing them with the membrane (at 100 °C and 1 ton for 3 minutes) to prepare the membrane electrode assembly (MEA). Single fuel cell experiments of the MEAs were tested on an Arbin fuel cell test station (Model: Arbin-001 MITS Pro-FCTS 5.0-FCTS) at 100, 125 and 150 °C. The single cell was of 5 cm<sup>2</sup> apparent area with serpentine flow fields (Electrochem ink). Prior to the testing, the MEA was conditioned at OCV conditions for 30 min followed by 15 min operation at 0.2 V, after which polarization measurements were carried out with a flow of 0.2 slpm (standard liters per minute) H<sub>2</sub> and O<sub>2</sub>.

### 3.2.3 Synthesis of polybenzimidazoles

Polybenzimidazoles were synthesized from diacids 3'-(4-phenyl-4H-1,2,4-triazole-3,5-diyl) dibenzoic acid (PTDBA) (Scheme 3.1) and 5-(4,5-diphenyl-4H-1,2,4-triazol-3-yl)isophthalic acid (DTIA) (Scheme 3.2) by condensing them with 3,3',4,4',-tetra-amino biphenyl (TAB) by high-temperature solution polycondensation procedure in PPA. The copolymers of these diacids were synthesized by using isophthalic acid, or pyridine dicarboxylic acid, or terephthalic acid, or sebacic acid, or adipic acid as comonomer. A typical procedure for high-temperature solution polycondensation in PPA is described below.

#### 3.2.3.1 Synthesis of PBI having NPT group in main chain and side chain

##### ➤ Synthesis of homo polymer (TM-100)

A mixture of TAB, 1 g (0.00466 mol) and PPA 30 g contained in a 50 mL three necked round bottom flask, equipped with a mechanical stirrer, nitrogen gas inlet and a guard tube was heated at 140 °C with stirring under a stream of nitrogen. PTDBA, 1.79 g (0.00466 mol) was added slowly with stirring to the solution and the temperature was raised to 170 °C in 2 h to give homogeneous solution. The solution was further heated to 200 °C and maintained at this temperature for 12 h under nitrogen purge. The viscous solution was then poured into 500 mL water to precipitate the polymer. The polymer was filtered and washed repeatedly with water. To remove residual phosphoric acid, the polymer was stirred in 10% sodium bicarbonate solution overnight and washed with water to neutrality followed by repeated hot water wash to eliminate sodium bicarbonate, if any. The polymer was dried at 100 °C for 24 h and 150 °C for another 24 h in vacuum oven. A brown color polymer was obtained. The yield of the polymer was about 97%.

Other copolybenzimidazoles PTDBA and PBI of DTIA having NPT groups in side chain were also synthesized by a similar procedure and their yields and viscosity values are given in Table 3.1. and Table 3.2 respectively.

**Table 3.1** Inherent viscosity (IV), yield, film appearance and film nature of Polybenzimidazoles having NPT groups in main chain

Polymer	Diacid used	Inherent	Yield	Film Appearance	Film
---------	-------------	----------	-------	-----------------	------

Code	(% mole ratio)	Viscosity $\eta_{inh}$ (dL/g) <sup>a</sup>	(%)	(Translucent ) film	Nature
TM-100	PTDBA 100	0.99	97	Light brown	Flexible
TM-90	PTDBA /IPA 90:10	0.97	95	Light brown	Flexible
TM-70	PTDBA /IPA 70:30	1.01	98	Light brown	Flexible
TM-50	PTDBA /IPA 50:50	0.99	95	Light brown	Flexible
TM-30	PTDBA /IPA 30:70	1.08	98	Light brown	Flexible
TM-10	PTDBA /IPA 10:90	0.99	99	Brown	Flexible
TM-T	PTDBA /TPA 50:50	1.30	97	Brown	Flexible
TM-P	PTDBA /PDCA 50:50	0.94	94	Brown	Flexible
TM-S	PTDBA / SA 50:50	0.97	92	Light brown	Flexible
TM-A	PTDBA / AA 50:50	0.65	93	Brown	Flexible
PBI	IPA 100	1.2	98	Brown	Flexible

PTDBA: 3'-(4-phenyl-4H-1,2,4-triazole-3,5-diyl) dibenzoic acid; IPA: Isophthalic acid; AA: Adipic acid; SA: Sebacic acid; PDCA: Pyridine dicarboxylic acid; TPA: terephthalic acid;

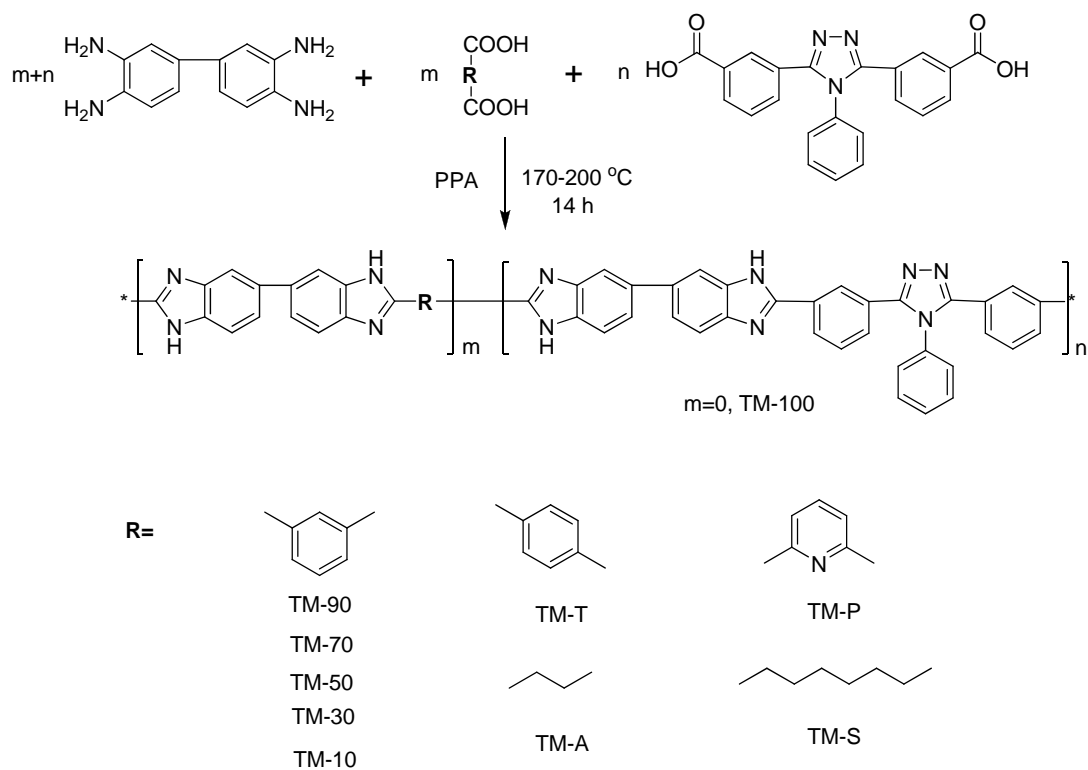
<sup>a</sup>Inherent viscosity measured in DMAc (0.5 g/dL concentration) at 30 °C

**Table 3.2** Inherent viscosity, yield, film appearance and film nature of Polybenzimidazoles having NPT groups in side chain

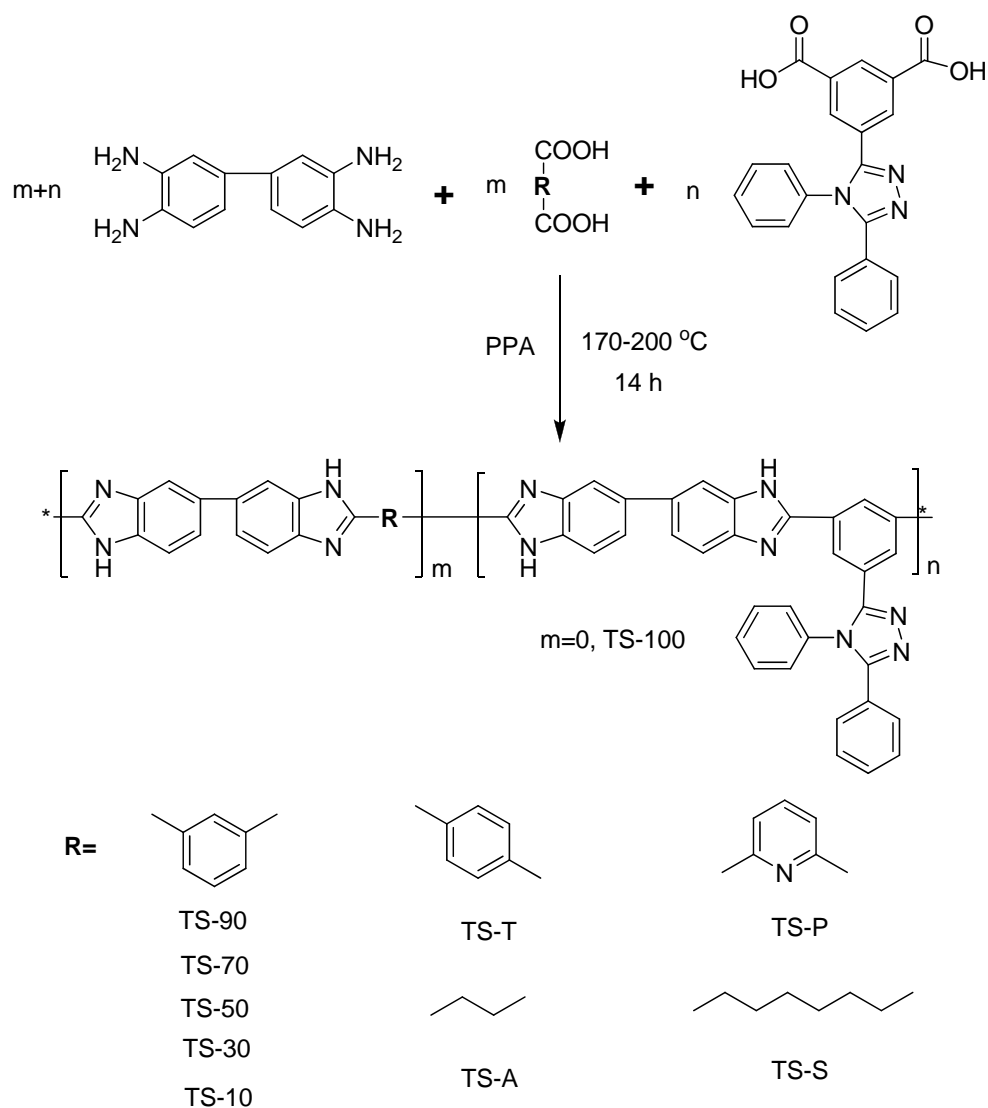
Polymer Code	Diacids used (% mole ratio)	Inherent Viscosity $\eta_{inh}$ (dL/g) <sup>a</sup>	Yield (%)	Film Appearance (Translucent )film	Film Nature
TS-100	DTIA 100	0.80	97	Light brown	Flexible
TS-90	DTIA /IPA 90:10	0.65	96	Light brown	Flexible
TS-70	DTIA /IPA 70:30	0.93	98	Light brown	Flexible
TS-50	DTIA /IPA 50:50	0.91	97	Light brown	Flexible
TS-30	DTIA /IPA 30:70	1.05	97	Light brown	Flexible
TS-10	DTIA /IPA 10:90	1.16	98	Light brown	Flexible
TS-T	DTIA /TPA 50:50	1.40	96	Light brown	Flexible
TS-P	DTIA /PDCA 50:50	0.86	95	Golden yellow	Flexible
TS-S	DTIA / SA 50:50	0.70	93	Light brown	Flexible
TS-A	DTIA / AA 50:50	0.52	91	Brown	Brittle

DTIA: 5-(4,5-diphenyl-4H-1,2,4-triazol-3-yl)isophthalic acid; <sup>a</sup>Inherent viscosity measured in DMAc (0.5 g/dL concentration) at 30 °C





**Scheme 3.1** Synthesis of polybenzimidazoles from PTDBA



**Scheme 3.2** Synthesis of polybenzimidazoles from DTIA

### 3.3 Results and Discussion

#### 3.3.1 Synthesis and structural characterization of polybenzimidazoles

Literature reports on the synthesis of polybenzimidazoles *via* different synthetic routes are discussed in Chapter 1, Section 1.4.1. Among them the widely used methods are: (1) two stage solid/melt polycondensation (2) solution polycondensation. It was found that two stage solid/melt polycondensation methods was not useful for this study since only low molecular weight polybenzimidazoles obtained. It is known that, synthesis of polybenzimidazoles by solution polymerization, especially, in PPA is an excellent method to prepare high-molecular weight polymer. The role of PPA in solution polycondensation is both as solvent as well as condensing agent. Thus, a new class of

modified polybenzimidazoles was synthesized, in this study, by this method using newly prepared diacids PTDBA, DTIA and other commercially available diacids such as IPA, TPA, PDCA, SA and AA with TAB. Copolymers containing varying extents of N-phenyl 1,2,4-triazole (NPT) groups in main chain were synthesized by condensing a mixture of PTDBA and IPA in different mole ratios (90:10, 70:30, 50:50, 30:70 and 10:90) with TAB (Schemes 3.1). Similarly copolymers containing varying extents of N-Phenyl 1,2,4-triazole (NPT) groups in side chain were synthesized by condensing a mixture of DTIA and IPA in different mole ratios (90:10, 70:30, 50:50, 30:70 and 10:90) with TAB (Schemes 3.2).

In general, synthetic route to polymers containing NPT groups is by the reaction of aniline with polymers containing hydrazide/oxadiazole<sup>40</sup> groups in PPA at high temperature. Often the polymers obtained by these methods are not well defined due to the presence of some uncyclised hydrazide or unreacted oxadiazole groups. To avoid such ambiguity, in the present work, the polymers were synthesized by reacting TAB with a newly synthesized diacid monomer, PTDBA, and DTIA containing preformed NPT group.

The polybenzimidazoles were obtained in quantitative yields and their inherent viscosities are closed to 1 dL/g, indicative of high molecular weight (Table 3.1 and 3.2). All polymers form strong thread during precipitation in water. The homo and copolymers form strong, tough and flexible films on casting in DMAc.

The structure of polymers thus obtained, was confirmed by FTIR and <sup>1</sup>H NMR spectroscopy. Before recording the IR spectra, all the film samples were soaked in hot water and dried at 150 °C for 2 days in a vacuum oven to remove last traces of solvent, which is confirmed by the absence of C-H stretching at 2940 cm<sup>-1</sup> for DMAc. PBI is hygroscopic and thus absorbs water, which is evident from the peak at 3615 cm<sup>-1</sup>. PBI shows absorption at 3409 and 3140 cm<sup>-1</sup> due to free non-hydrogen-bonded N-H stretching and self-associated N-H stretching, respectively. Due to absorption of moisture the above peaks could not be observed distinctively for PBI containing NPT groups, instead a broad peak was observed in this region. The presence of benzimidazole group was confirmed by several characteristic bands at 1445 cm<sup>-1</sup> (in plane deformation of benzimidazole), 1280 cm<sup>-1</sup> (breathing mode of the imidazole ring), and peaks at 1611 cm<sup>-1</sup>, 1596 cm<sup>-1</sup>, 1177 cm<sup>-1</sup> for C=N stretching.

The FTIR spectrum of polybenzimidazoles derived from PTDBA (Figure 3.1) and DTIA (Figure 3.2) showed an additional absorption at 1497 cm<sup>-1</sup> due to triazole group. The characteristic band of C=N stretching in triazole moiety<sup>41</sup> at 1497 cm<sup>-1</sup> in all

the polymers confirmed the presence NPT groups in PBI. The intensity of the characteristic peak of triazole group at  $1497\text{ cm}^{-1}$  in copolymers of PTDBA and IPA increases systematically with increase in the mol% PTDBA (dotted line in Figure-3.3). In pristine PBI, this peak is absent.

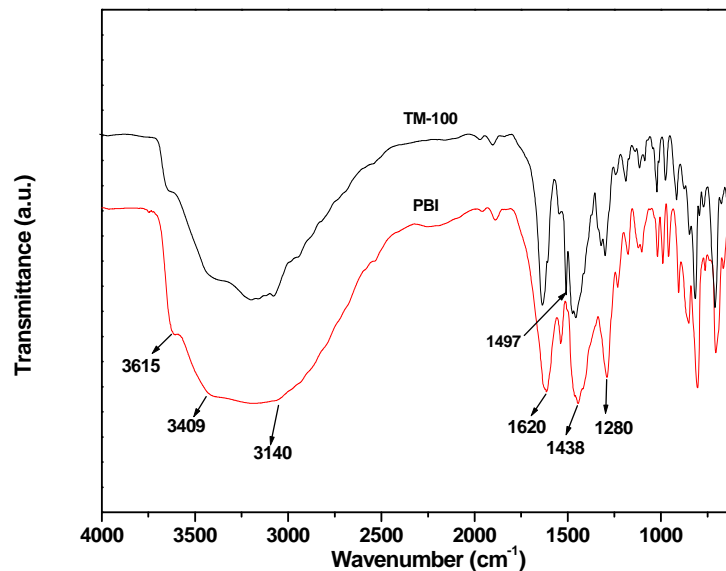


**Figure 3.1** FTIR spectra of NPT group containing PBI in main chain (TM-100) and PBI (film)

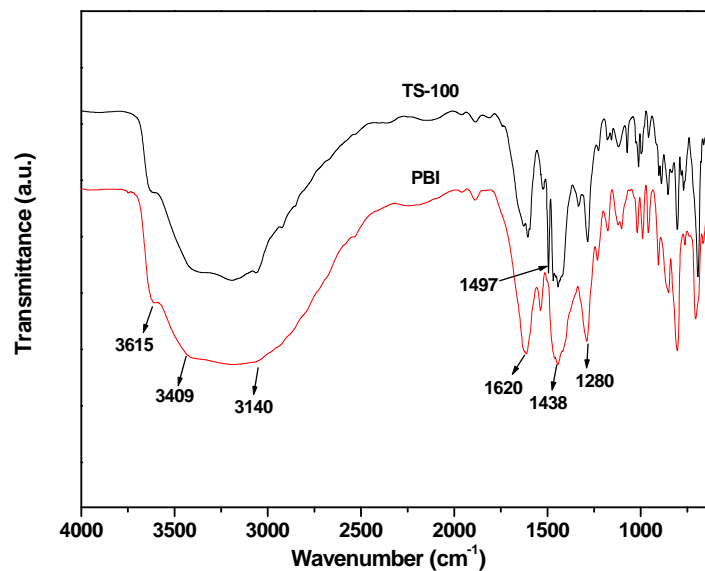


**Figure 3.2** FTIR spectra of NPT group containing PBI in side chain (TS-100) and PBI (film)

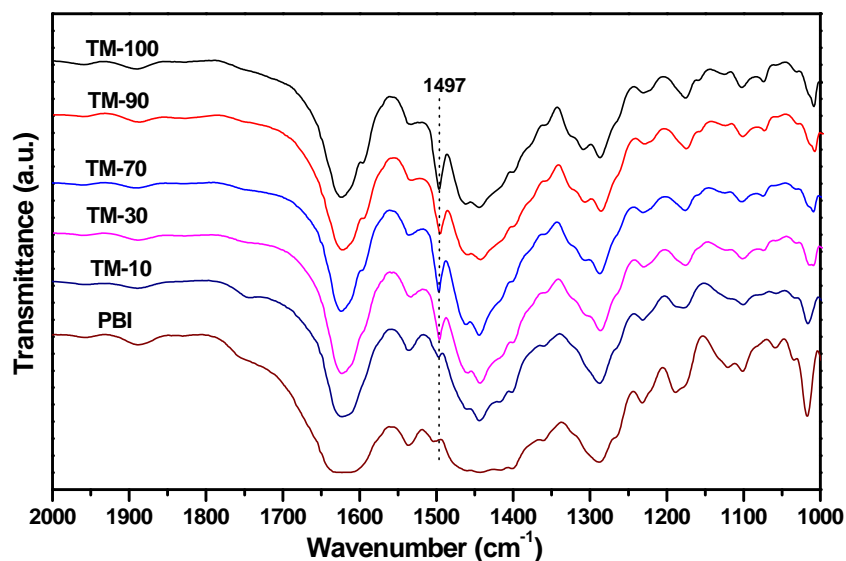


**Figure 3.3** FTIR spectra of polymer films of copolymers of PTDBA and IPA

Figure 3.4 shows  $^1\text{H}$  NMR spectrum of TM-100. The imidazole proton peak at 13.21 ppm, and all the aromatic protons at 7.26 – 8.66 ppm with expected integrations were observed. Figure 3.5 shows  $^1\text{H}$  NMR spectrum of TS-100 wherein similar observations are noticed (imidazole proton peak at 13.4 ppm and aromatic protons at 7.45 – 9.12 ppm).

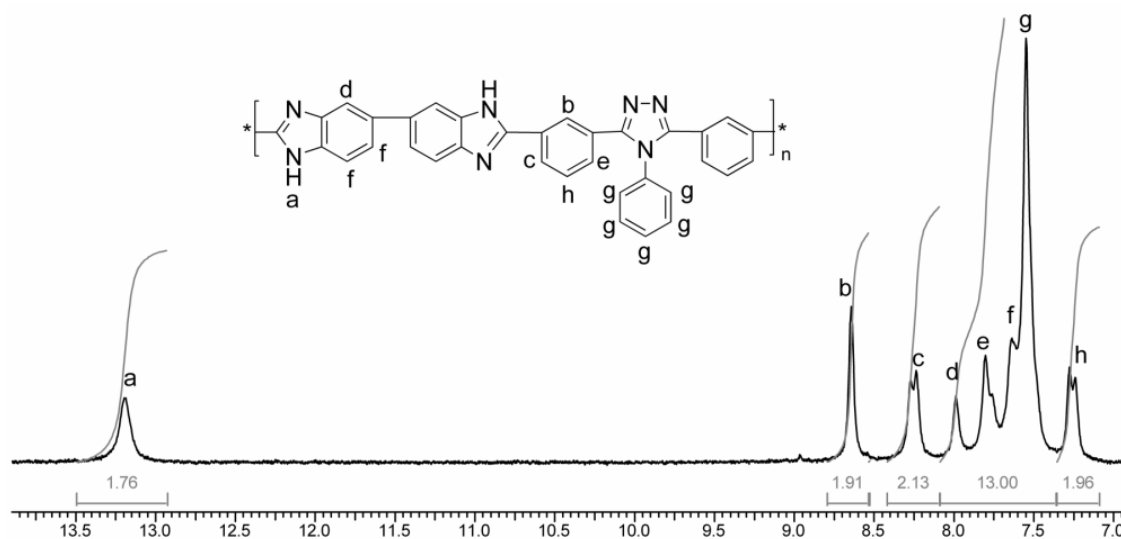


**Figure 3.4**  $^1\text{H}$ -NMR spectrum of homo polymer (TM-100) in  $\text{DMSO-d}_6$

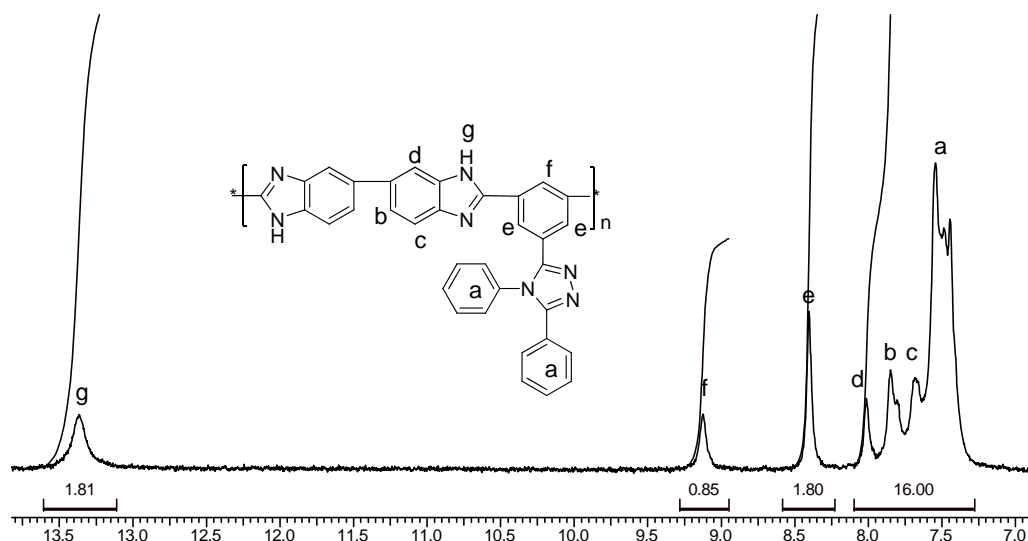


**Figure 3.5**  $^1\text{H}$ -NMR spectrum of homo polymer (TS-100) in  $\text{DMSO-d}_6$

### 3.3.2 Properties of polybenzimidazoles

The polybenzimidazoles were characterized by solubility measurements, X-ray diffraction, DSC, TGA and mechanical strength. Other studies such as oxidative stability, water uptakes, phosphoric acid uptake and proton conductivity of membranes were also carried out.

#### 3.3.2.1 Polymer solubility

Solubility in solvents is one of the important properties of polymers and good solubility is desired for many polymer applications. PBIs are rigid polymers with high softening point and one of the major barriers to their extensive application has been their infusibility and poor solubility leading to poor processability.<sup>42</sup> They are soluble in polar aprotic solvents such as DMAc only after heating at high temperature for several hours in presence of lithium chloride. Incorporation of additional nitrogen atom in the polymer backbone is known to enhance the solubility of polymer.<sup>25</sup> Incorporation of bulky group in polymer also enhances the solubility due to disruption of rigid structure and reduction in cohesive energy. This is reflected in high solubility of NPT group containing PBI. These polymers are easily soluble in polar aprotic solvents such as DMF, DMAc, NMP and DMSO to give 3-8% solution at room temperature under stirring (Table 3.3 and 3.4). They are also readily soluble in strong acids such as  $\text{H}_2\text{SO}_4$ , trifluoroacetic acid (TFA), formic acid (FA), methane sulfonic acid (MSA) etc. However, these polymers are not soluble in common solvents such as chloroform, toluene, dioxane, tetrahydrofuran & acetic acid due to their polar nature. Thus, NPT group in the main chain as well as side chain in both homo and copolymers improves the solubility.

**Table 3.3** Solubility behavior of Polybenzimidazoles having NPT groups in main chain (PTDBA-based polymers)

Polymer Code	Solvents							
	TFA	MSA	FA	H <sub>2</sub> SO <sub>4</sub>	DMF	DMSO	DMAc	NMP
TM-100	++	++	++	++	++	++	++	++
TM-90	++	++	++	++	++	++	++	++
TM-70	++	++	++	++	++	++	++	++
TM-50	++	++	++	++	++	++	++	++
TM-30	++	++	++	++	++	++	++	++
TM-10	++	++	++	++	++	++	++	++
TM-T	++	++	++	++	++	++	++	++
TM-P	++	++	++	++	++	++	++	++
TM-S	++	++	++	++	++	++	++	++
TM-A	++	++	++	++	++	++	++	++
PBI	++	++	++	++	+	+	+	+

Concentration: 5mg/mL

++, Soluble at room temperature; +, Soluble on heating;

TFA: Trifluoro acetic acid; H<sub>2</sub>SO<sub>4</sub>: conc. sulfuric acid; DMF: N,N-dimethylformamide; DMAc: N,N-dimethyl acetamide; DMSO: dimethyl sulfoxide; NMP: N-methyl-2-pyrrolidone; MSA: methane sulfonic acid; FA: formic acid; TFA: terephthalic acid; PDCA: pyridine 2,4-dicarboxylic acid; SA: sebacic acid and AA: adipic acid.

**Table 3.4** Solubility behavior of Polybenzimidazoles having NPT groups in side chain (DTIA-based polymers)

Polymer Code	Solvents							
	TFA	MSA	FA	H <sub>2</sub> SO <sub>4</sub>	DMF	DMSO	DMAc	NMP
TS-100	++	++	++	++	++	++	++	++
TS-90	++	++	++	++	++	++	++	++
TS-70	++	++	++	++	++	++	++	++
TS-50	++	++	++	++	++	++	++	++
TS-30	++	++	++	++	++	++	++	++
TS-10	++	++	++	++	++	++	++	++
TS-T	++	++	++	++	++	++	++	++
TS-P	++	++	++	++	++	++	++	++
TS-S	++	++	++	++	++	++	++	++
TS-A	++	++	++	++	++	++	++	++

Concentration: 5mg/mL

++, Soluble at room temperature; +, Soluble on heating;

### 3.3.2.2 Thermal properties

The thermal stability and glass transition temperatures ( $T_g$ ) of the polybenzimidazoles were determined by thermogravimetric analysis (TGA) and differential scanning calorimetry (DSC), respectively.

#### 3.3.2.2.1 Thermogravimetric analyses

Thermogravimetric analyses (TGA) were recorded at a heating rate of  $10\text{ }^\circ\text{C min}^{-1}$  in  $\text{N}_2$  atmosphere. To remove absorbed moisture, the samples were preheated to  $150\text{ }^\circ\text{C}$  and after holding for 10 min cooled to  $50\text{ }^\circ\text{C}$ , prior to measurements. The initial decomposition temperature (IDT), the decomposition temperature at 10% weight loss ( $T_{10}$ ) and the maximum decomposition temperature ( $T_{\text{max}}$ ) for polybenzimidazoles synthesized from PTDBA and DTIA are summarized in the Table 3.5 and 3.6 and the thermograms of polymers are shown in Figure 3.6 to 3.9

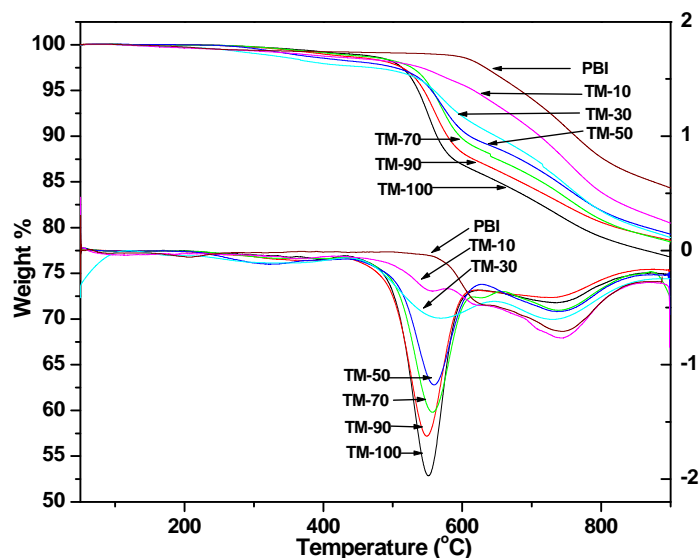


**Figure 3.6** Thermograms and derivatives of thermograms of polybenzimidazoles from PTDBA in  $\text{N}_2$  atmosphere (purging rate  $20\text{ mL/min}$ ) recorded at a heating rate  $10\text{ }^\circ\text{C/min}$

All fully aromatic polymers based on PTDBA (Figure 3.6) have high thermal stability, the initial decomposition temperature (IDT) ranging from  $514 - 528\text{ }^\circ\text{C}$  while, polymers containing aliphatic chains, TM-S and TM-A, have comparatively low thermal stability with IDT of  $475$  and  $483\text{ }^\circ\text{C}$  respectively. Low IDT of NPT group containing polybenzimidazoles compared to rigid PBI based on isophthalic acid (IDT  $603\text{ }^\circ\text{C}$ ) is due to the presence of NPT groups. Polytriazoles normally decompose around  $500\text{ }^\circ\text{C}$ .<sup>40</sup> In case of copolymers, IDT increases slightly with increasing IPA content. In copolymers containing 50 mole% of different acids, change in IDT is not significant for different



aromatic acids except for aliphatic ones. Temperature at which 10% weight loss takes place ( $T_{10}$ ) is 563 °C for homo polymer of PTDBA (TM-100) and  $T_{10}$  increases with increase in IPA content in copolymers of PTDBA and IPA.

**Table 3.5** Thermal properties of polybenzimidazoles having NPT groups in main chain (PTDBA-based polymers)

Polymer Code	IDT (°C) <sup>a</sup>	$T_5$ (°C) <sup>b</sup>	$T_{10}$ (°C) <sup>c</sup>	$T_{max}$ (°C) <sup>d</sup>	Residue (wt %) <sup>e</sup>	$T_g$ (°C) <sup>f</sup>
TM-100	515	536	563	551	77	376
TM-90	514	534	566	547	78	378
TM-70	520	544	584	556	78	390
TM-50	522	543	598	558	79	397
TM-30	520	547	638	558	78	408
TM-10	528	603	699	558	80	409
TM-T	519	520	576	548	79	390
TM-P	516	535	586	549	77	401
TM-S	475	478	492	501	45	306
TM-A	483	485	502	514	57	329
PBI	603	683	760	751	85	431

IPA: isophthalic acid; TPA: terephthalic acid; PDCA: pyridine 2,4-dicarboxylic acid; SA: sebacic acid; AA: adipic acid; <sup>a</sup>IDT: initial decomposition temperature; <sup>b,c</sup> $T_5$ ,  $T_{10}$ : temperature at which 5%, 10% wt loss observed; <sup>d</sup> $T_{max}$ : maximum decomposition temperature; <sup>e</sup> residue at 900 °C; <sup>f</sup> $T_g$ : glass transition temperature.

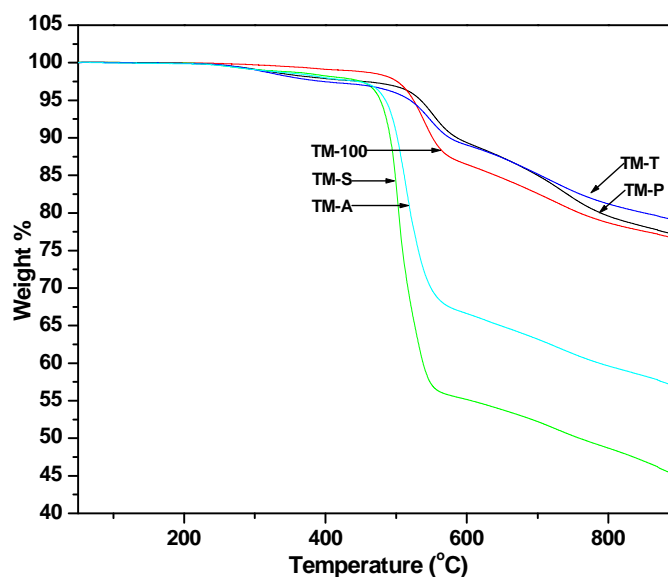


**Figure 3.7** Thermograms of other polybenzimidazoles from PTDBA in nitrogen

Thus,  $T_{10}$  of homo polymer (TM-100) is 563 °C, whereas for copolymer, TM-10, containing 90-mole% of IPA,  $T_{10}$  is 699 °C. Similarly, % residue of all polymers containing NPT groups except polymer containing aliphatic group, is in the range of 77 – 80% (Figure 3.7) revealing that the structure of diacids and copolymer composition do

not have significant effect on residue. As expected, polymers containing aliphatic groups have low thermal stability compared to aromatic copolymers.

Polybenzimidazoles bearing NPT moiety in the side chain (DTIA-based polymers) (Figure 3.8 and 3.9) also have high thermal stability, the initial decomposition temperature (IDT) ranging from 450 – 514 °C.  $T_5$ ,  $T_{10}$  and  $T_{max}$  of DTIA based polymers showed similar trend as PTDBA-based polymers. All aromatic polymers based on DTIA showed  $T_5$  and  $T_{10}$  in the range of 511-520 °C and 535-593 °C respectively. As expected the aliphatic group bearing polymers (TS-S and TS-A) have low thermal stability, IDT of TS-S and TS-A were 450 °C and 460 °C respectively.

From the above two series it is clear that the polymers with NPT groups (in main chain as well as side chain) could maintain the thermal stability of polybenzimidazoles. Fully aromatic polymers of both the series have thermal stability near about 500 °C.

**Table 3.6** Thermal properties of polybenzimidazoles having NPT groups in side chain (DTIA -based polymers)

Polymer Code	IDT (°C) <sup>a</sup>	$T_5$ (°C) <sup>b</sup>	$T_{10}$ (°C) <sup>c</sup>	$T_{Max}$ (°C) <sup>d</sup>	Residue (wt %) <sup>e</sup>	$T_g$ (°C) <sup>f</sup>
TS-100	514	520	543	541	73	417
TS-90	481	507	535	520	71	428
TS-70	499	512	550	521	71	420
TS-50	487	517	593	520	77	419
TS-30	497	537	654	524	78	429
TS-10	497	587	684	524	77	412
TS-T	486	511	577	517	73	NF
TS-P	479	521	589	522	70	NF
TS-S	450	458	472	479	49	317
TS-A	460	477	502	493	60	349
PBI	603	683	760	751	85	431

NF-not found; <sup>a</sup> IDT: initial decomposition temperature; <sup>b,c</sup>  $T_5$ ,  $T_{10}$ : temperature at which 5%, 10% wt loss observed; <sup>d</sup>  $T_{max}$ : maximum decomposition temperature; <sup>e</sup> residue at 900 °C.

<sup>f</sup>  $T_g$ : glass transition temperature.

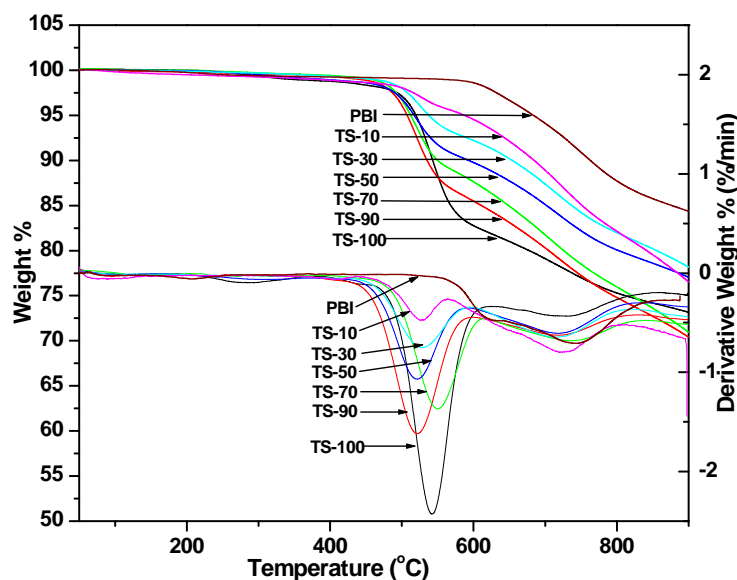


**Figure 3.8** Thermograms and derivatives of thermograms of polybenzimidazoles from DTIA in  $N_2$  atmosphere recorded at a heating rate  $10\text{ }^\circ\text{C}/\text{min}$

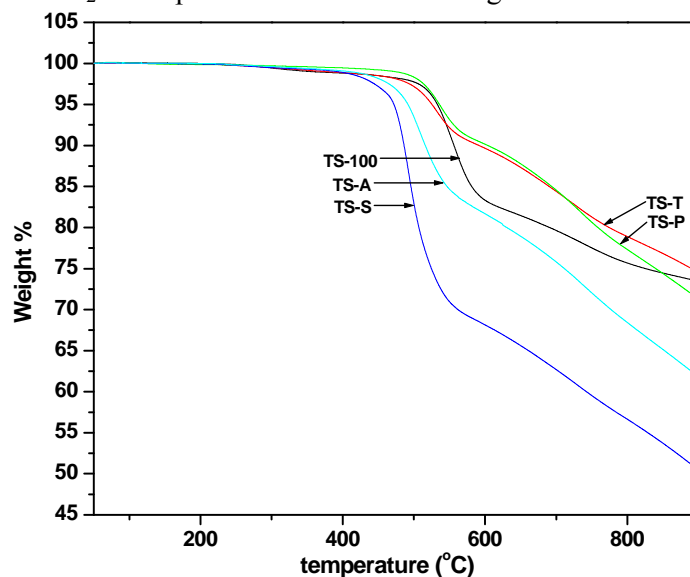


**Figure 3.9** Thermograms of other polybenzimidazoles from DTIA in nitrogen

### 3.3.2.2.2 Glass transition temperature ( $T_g$ )

The glass transition temperature ( $T_g$ ) of the polymers was measured from  $50\text{ }^\circ\text{C}$  to  $450\text{ }^\circ\text{C}$  in nitrogen atmosphere at a heating rate of  $20\text{ }^\circ\text{C}/\text{min}$  (Figure 3.10 and 3.11). The presence of NPT groups in the PBI main chain lowered  $T_g$  values (Table 3.5). Although, the bulky aromatic groups hinder the free segmental motions, the effect of chain separation due to pendant phenyl and bulky groups resulting in lower hydrogen bridge and increase in free volume seems to be dominant and eventually account for the observed decrease in  $T_g$ .<sup>43</sup> Thus, decrease in the hydrogen bonding between  $-N-H \dots N-$  groups in polymers and increase in free volume mainly contributed to reduced  $T_g$  value

(376 °C) of TM-100 compared to PBI (431 °C) (Figure 3.10). This is supported by observed high polymer solubility. However, in the copolymers,  $T_g$  values increase with increasing isophthalic units in the polymer due to increased rigidity. The  $T_g$  values of fully aromatic polymers containing NPT groups are lower compared to conventional PBI (without NPT groups), which are in the range of 376-409 °C. The copolymers based on sebacic acid and adipic acids have low  $T_g$  306 °C and 329 °C respectively due to flexible alkane chain structure (Table 3.5).

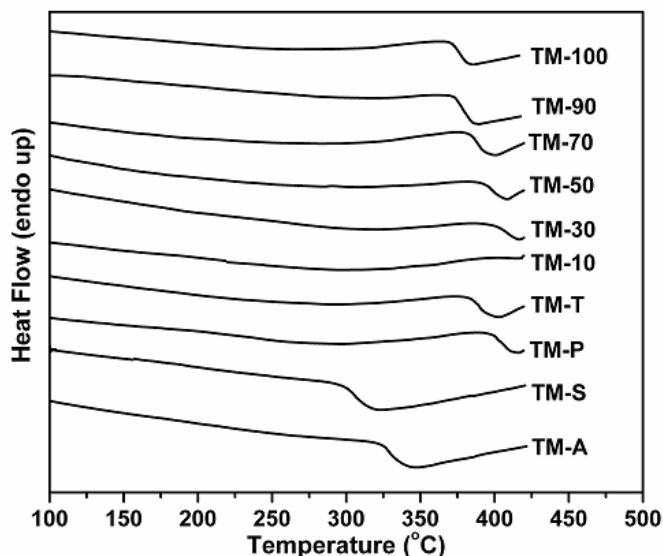


**Figure 3.10** DSC Thermograms of homo polymer and copolymers based on PTDBA in  $N_2$ , (heating rate  $20\text{ °C min}^{-1}$ )

The  $T_g$  values of fully aromatic polybenzimidazoles based on DTIA containing NPT groups in side chain is high ranging between 412 °C to 429 °C, whereas  $T_g$  of PBI, is 431 °C. Although, the  $T_g$  values of PBI containing NPT groups are slightly lower than that of PBI, the difference is not significant. Generally, bulky side groups in a polymer disrupt rigidity of the polymer and increase the free volume resulting in lowering of  $T_g$ . The high  $T_g$  of these polymers, compared to PTDBA based polymers is due to the bulky rigid pendant NPT moiety, which sterically restrict chain movement and enhance  $T_g$ .<sup>44</sup> However, slightly low  $T_g$  of these polymers, compared to PBI is, probably, due to increased free volume. As anticipated, copolymers TS-A and TS-S containing flexible aliphatic linkages have low  $T_g$  compared to aromatic polymers. Copolymer TS-S with more flexible  $C_8$  aliphatic linkages has low  $T_g$  (317 °C) compared to TS-A ( $T_g$  349 °C) with less flexible  $C_4$  aliphatic linkages. Effect of bulky side group in restricting chain movement to increase  $T_g$  could be clearly seen from the higher  $T_g$  values of DTIA based

TS-S and TS-A (Table 3.6) compared to that of PTDBA based TM-S ( $T_g$  306 °C) and TM-A ( $T_g$  329 °C) in Table 3.5.

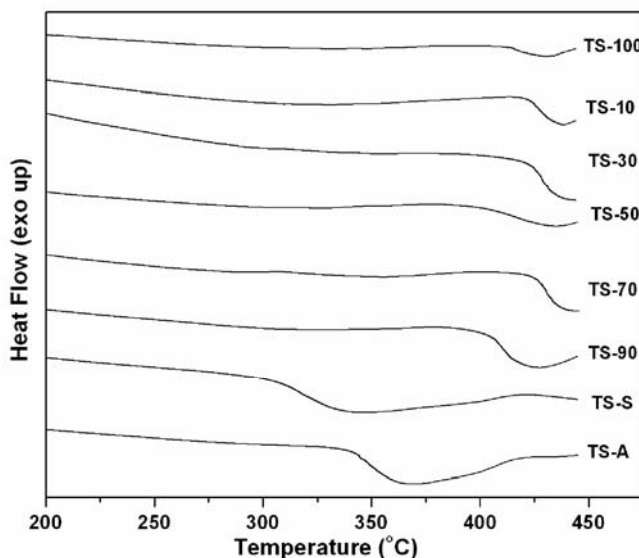


**Figure 3.11** DSC Thermograms of homo polymer and copolymers based on DTIA in  $N_2$ , (heating rate  $20\text{ }^\circ\text{C min}^{-1}$ )

### 3.3.2.3 Crystallinity

The crystallinity in the synthesized polymers is dependent on rigidity of both tetraamines and diacids employed. It is known that less symmetrical monomers<sup>45</sup> and those having pendant groups<sup>46</sup> reduce the crystallinity in polymers and improves their solubility. The degree of crystallinity in PBI is experimentally obtained from wide angle X-ray diffraction (WAXD) measurements. Even though the information from WAXD is less precise in the case of amorphous polymers than that of crystalline polymers; this information is highly useful to characterize amorphous structures. The d-spacing obtained from the X-ray diffractograms is a measure of the interchain packing in the polymers. Amorphous polymers show halos due to coherent inter- and intra-segmental diffraction of X-rays.<sup>47</sup> If the intersegmental scattering dominates the intra-segmental, the WAXD spectra can provide some information on the chain packing in amorphous polymers.

In the present study the crystallinity of all polymers (film form) were evaluated by WAXD measurements. All PBIs from diacid PTDBA showed amorphous pattern indicating loss of crystallinity with increasing bulky NPT moiety in the backbone of polymer (Figure 3.12 and 3.13). This is attributed to the flexibility of NPT group, which increases the disorder in chains, thereby causing less chain packing. Amorphous nature

of these polymers is also reflected in enhanced polymer solubility. Most of the PBIs synthesized from diacid DTIA (Figure 3.14) showed similar X-ray patterns to that of PBI derived from IPA. PBI showed a broad, amorphous pattern centered at a  $2\theta = 24^\circ$ . Among the samples between NPT groups in main chain and side chain, the samples with NPT groups in main chain are more amorphous in nature may be due to these groups in polymer backbone, which disturbs the chain packing.

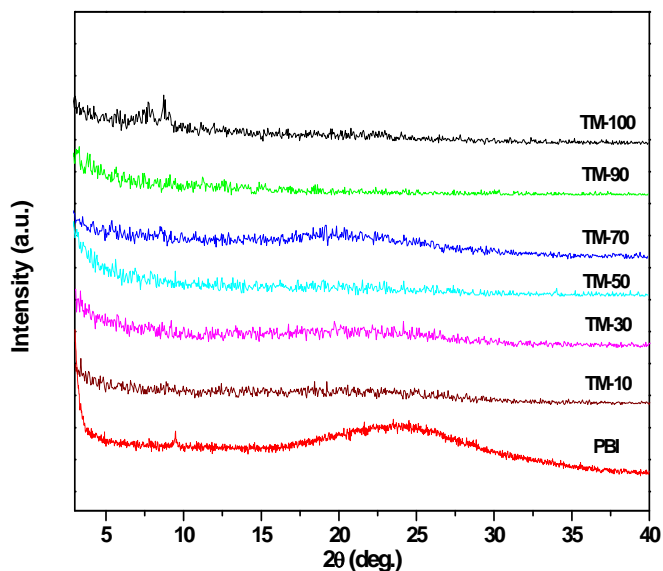


**Figure 3.12** WAXD diffractograms of PBIs from PTDBA

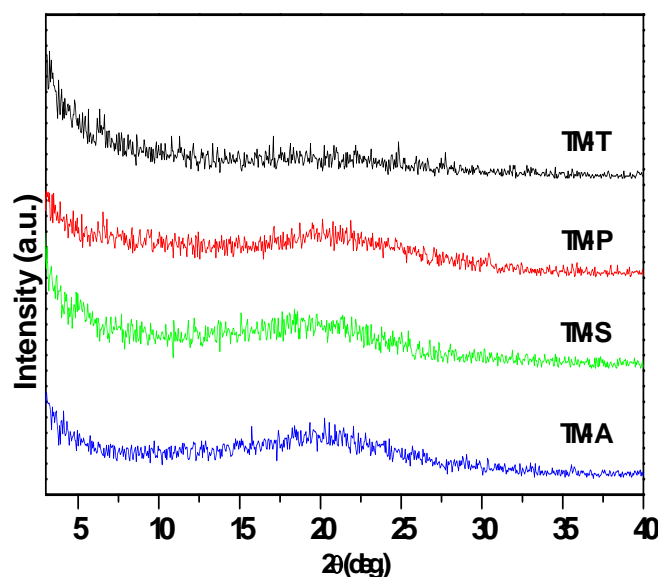


**Figure 3.13** WAXD diffractograms of other copPBIs from PTDBA

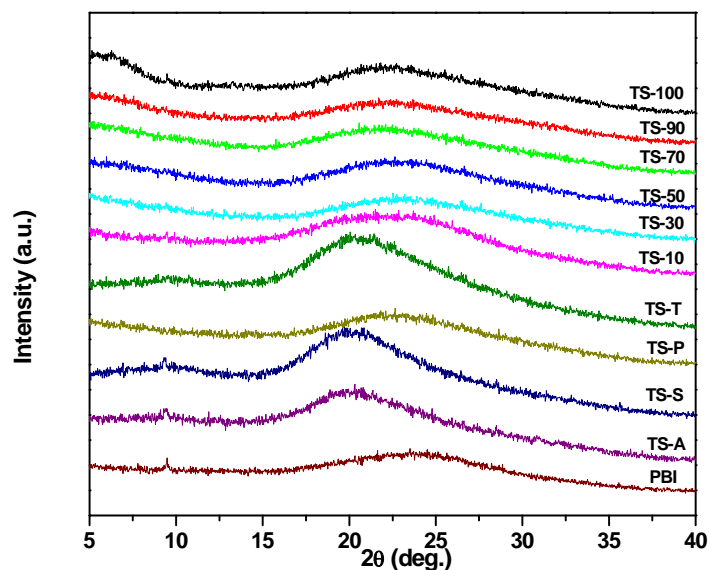


**Figure 3.14** WAXD diffractograms of PBIs from DTIA

### 3.3.2.4 Mechanical properties

Mechanical properties of all polymers were determined using tensile tester at room temperature. Figures 3.15 and 3.16 show stress vs strain curves of PTDBA and DTIA based polymers where as analytical data are summarized in Tables 3.7 and 3.8 respectively. Homopolymer based on PTDBA (TM-100) has tensile stress of 98 MPa, while tensile stress of PBI is 138 MPa. The bulky NPT group in main chain is expected to lower rigidity of polymer due to disruption of hydrogen bridging of PBI. Incorporation of IPA into PTDBA based polymer disrupts regular structure of homopolymer resulting in further lowering of tensile stress. Thus, incorporation of 10 mole% of IPA in PTDBA lowers tensile stress to 78 MPa. Modulus of copolymers of PTDBA and IPA vary in the range of 1897-2600 MPa. Toughness of homopolymer of PTDBA is 3.1 MPa. Incorporation of IPA increases the toughness of copolymers. Highest toughness value of 18.6 MPa is exhibited by copolymer containing 90 mole% of IPA. Similar trend is observed for elongation at break which increases with increase in IPA content in copolymers. The homopolymer TM-100 has 4 % elongation at break while copolymer containing 90 mole% IPA shows 23 % elongation at break. Structure of other diacids in copolymer has significant influence on tensile properties. Copolymers containing 50-mole% of terephthalic acid and 50-mole % of PTDBA have highest elongation at break of 42 %. Copolymers containing aliphatic chains, TM-S and TM-A show low tensile stress. Copolymer TM-A exhibits lowest toughness and elongation at break.

**Table 3.7** Mechanical properties PTDBA-based PBIs

Polymer Code	Tensile Stress (MPa)	Modulus (MPa)	Toughness (MPa)	Elongation at Break (%)	Water uptake (%)
TM-100	98	2467	3.0	4	15
TM-90	78	2600	2.6	4	15
TM-70	79	1897	7.3	8	16
TM-50	89	2372	8.0	8	15
TM-30	81	2230	13.8	15	18
TM-10	66	2295	18.6	23	18
TM-T	80	2052	40.9	42	14
TM-P	62	2088	1.9	4	19
TM-S	49	1955	12.4	23	12
TM-A	37	2371	0.5	2	13
PBI	138	3337	4.4	7	19

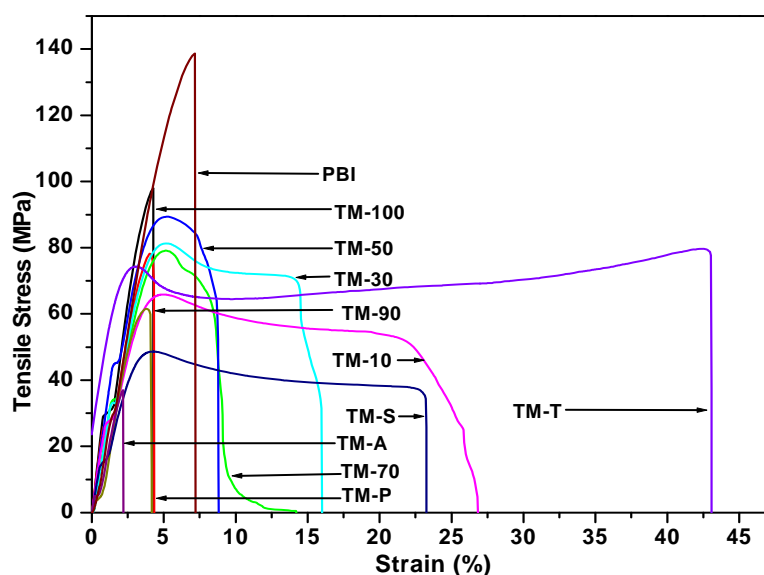


**Figure 3.15** Mechanical properties PTDBA-based PBIs

DTIA-based polymers also exhibited good tensile properties as shown in Figure 3.16. The low tensile stress of 71 MPa of homopolymer, (TS-100), compared to 138 MPa of PBI indicates that the bulky side groups disrupt rigid regular structure of PBI lowering tensile strength. Incorporation of 10 mole% NPT groups in side chain has significant effect of reducing tensile strength of PBI to 71 Mpa (e.g. copolymer TS-90). The tensile stress of all fully aromatic copolymers varies in the range 56 to 84 MPa. Except copolymer TS-10, all PBIs containing NPT groups have modulus in the range of 2225 to 3150 MPa, toughness 1.5 to 8.3 MPa and elongation at break 1.8 to 10% compared to 3337 MPa, 4.4 MPa, and 7% respectively for PBI. Significantly, TS-10 has high modulus of 3419 MPa, high toughness of 28.5 MPa and high elongation of 23.5%



compared to PBI. It appears that incorporation of small quantity (10%) of NPT groups in PBI disrupts hydrogen bonding and allowing the polymer chains to slip over each other with little resistance which gives a kind of plasticizing effect resulting in high modulus and increased elongation. However, it is clearly seen that further increasing NPT groups increases resistance to movement due to vicinal pendant bulky groups and reduces modulus and elongation. From this study, it can be inferred that the polybenzimidazoles containing NPT groups have sufficiently high mechanical properties for many applications.

**Table 3.8** Mechanical properties DTIA-based PBIs

Polymer Code	Tensile Stress (MPa)	Modulus (MPa)	Toughness (MPa)	Elongation at Break (%)	Water uptake (%)
TS-100	71	2793	5.8	4.9	15
TS-90	84	2260	4.1	3	17
TS-70	71	2426	4.8	8.1	16
TS-50	63	2225	8.3	9	16
TS-30	65	2725	7.3	10	18
TS-10	71	3419	28.5	23.5	21
TS-T	68	3151	2.5	3.6	17
TS-P	58	3069	1.5	2.3	22
TS-S	56	2271	1.0	1.8	10
TS-A	64	2372	1.2	1.9	12

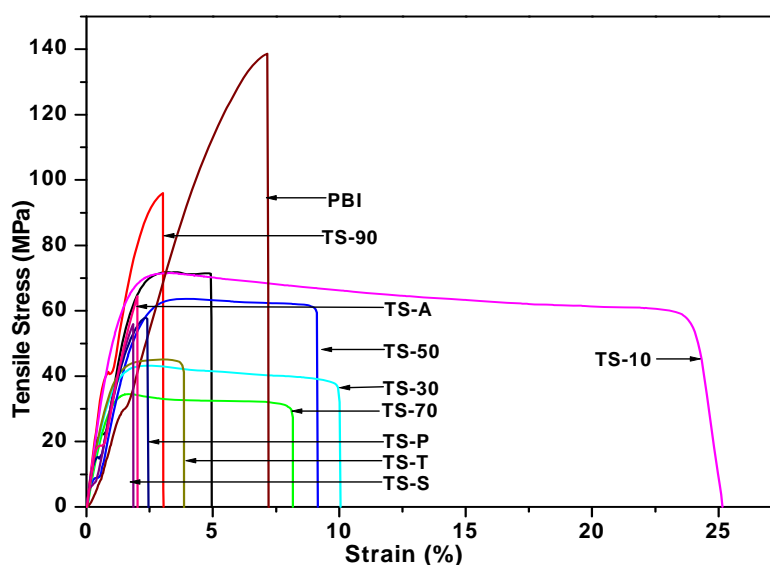


**Figure 3.16** Tensile stress versus strain graph of PBIs from PTDBA

### 3.3.2.5 Water uptake

The water uptake in PBI is due to the intermolecular hydrogen bonding between water and N and N-H groups. In PBI, the hydrogen bonding occurs in two ways. Firstly, two water molecules may attach to each imidazole ring so that one water molecule could act as a proton acceptor and other one as a proton donor and second possibility is one water molecule would act as a proton acceptor and donor. The first possibility would allow a maximum of four water molecules and second possibility would allow two water molecules to attach to each imidazole.<sup>48</sup> The water uptake results of polymer membranes are shown in Table 3.7 and 3.8 for PTDBA and DTIA based polymers respectively. PBI takes 19 wt% water, which is in good agreement with reported values in the literature.<sup>49</sup> The water uptake of NPT group containing PBI (TM-100 and TS-100) is reduced to 15 wt%. The low water uptake ability is attributed to bulky NPT groups perturbing the intermolecular and intramolecular hydrogen bonding between water and N and N-H groups. Similar observation was made in case of polyamides, wherein the equilibrium water sorption is much lower for the phenoxy group containing polyamides than for the unmodified ones.<sup>43</sup>

### 3.3.2.6 Oxidative stability

Long-term stability of a polymer electrolyte membrane is very important for the durability of fuel cells performance. Polymer electrolytes are subjected to strongly oxidizing and reducing environment in the presence platinum catalyst and they generally undergo degradation at operational conditions, which reduces the life time of fuel cell. Membrane based on PBI is known to undergo degradation by ·OH or ·OOH radicals formed by the decomposition of H<sub>2</sub>O<sub>2</sub> generated at cathode during operational conditions.<sup>49,38</sup> Cross-linking is reported to enhance oxidative stability of PBI.<sup>38</sup> Use of high molecular weight PBI is another method, which helps to prevent loss of strength of membrane due to degradation to some extent. However, high molecular weight PBI has disadvantage of poor solvent solubility making membrane preparation difficult. So it is equally important to maintain high molecular weight, good solvent solubility and better oxidative stability for the optimized performance of a membrane.

Experimentally, oxidative stability of PBI membrane is evaluated by Fenton test. Membranes of PBI and PBI containing NPT groups were evaluated for oxidative stability by Fenton test. A weight loss of 17% was observed for PBI membrane, where as, PBI containing NPT groups in main chain (TM-100) and side chain (TS-100) shows only 1% and 8% weight loss after 120 h respectively. The results obtained in a systematic study conducted with varying mole % of NPT groups (in PTDBA and DTIA

based polymers) are shown in the Figure 3.17 to 3.20 respectively. The %weight loss decreases with increasing percentage of NPT groups in IPA-based copolymers. In the case of aliphatic group containing copolymers in both series (PTDBA and DTIA based polymers); the % weight loss was observed in the range of 14 to 19%. The results show that modification of PBI by NPT groups enhances the oxidative stability of PBI, especially in NPT groups in main chain.

Exact mechanism of degradation of PBI by  $\cdot\text{OH}$  and  $\cdot\text{OOH}$  radicals in fuel cells has not been reported, though there are some reports on thermo-oxidative degradation of PBI.<sup>50, 51</sup> It appears that attack of  $\cdot\text{OH}$  and  $\cdot\text{OOH}$  radicals on PBI causes abstraction of labile hydrogen of H-N- of imidazole groups generating radical on benzimidazole groups which shifts to aromatic benzene ring as described by Musto et al.<sup>52</sup> leading to degradation of PBI. NPT groups do not support this type of mechanism due to absence of active hydrogen and reduces sites of degradation of PBI and hence enhances oxidative stability. As shown by Siwen Li, et al.,<sup>34</sup> triazole moiety has a better electrochemical stability than benzimidazole. Thus, NPT groups in PBI enhance the oxidative stability that is worth noting.

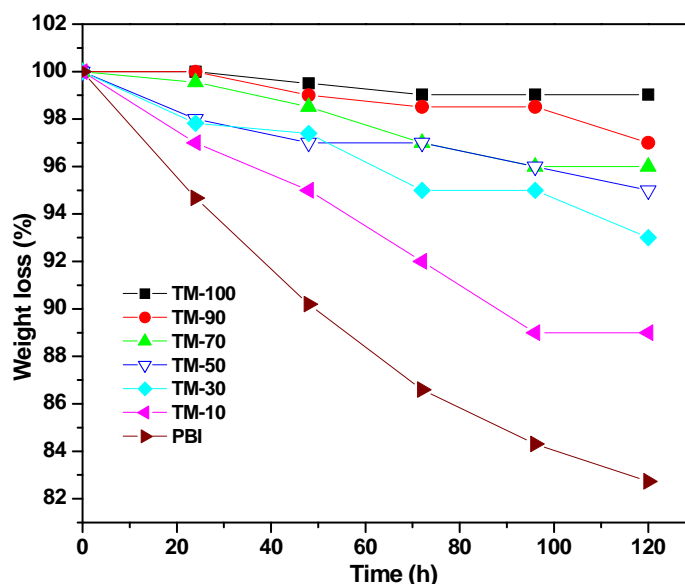


**Figure 3.17** Oxidative stability of PBI and copolymers of IPA containing NPT groups in main chain. Membrane degradation in terms of %wt. loss of a membrane measured at different time intervals. Membranes were dipped in 3%  $\text{H}_2\text{O}_2$  containing 4 ppm  $\text{Fe}^{2+}$  (Fenton solution) at 70 °C in an oven, taken out after 24 h and measured their wt loss after drying. The procedure is repeated with fresh Fenton solutions

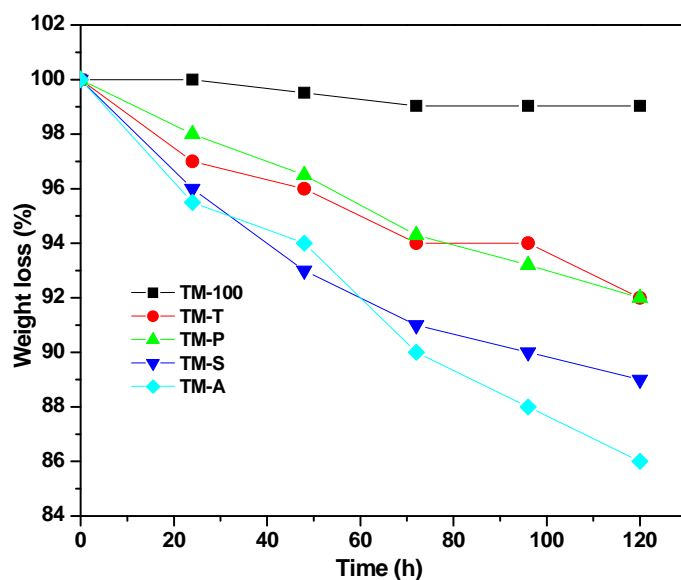


**Figure 3.18** Oxidative stability of PBI and coPBI of other diacids containing NPT groups in main chain

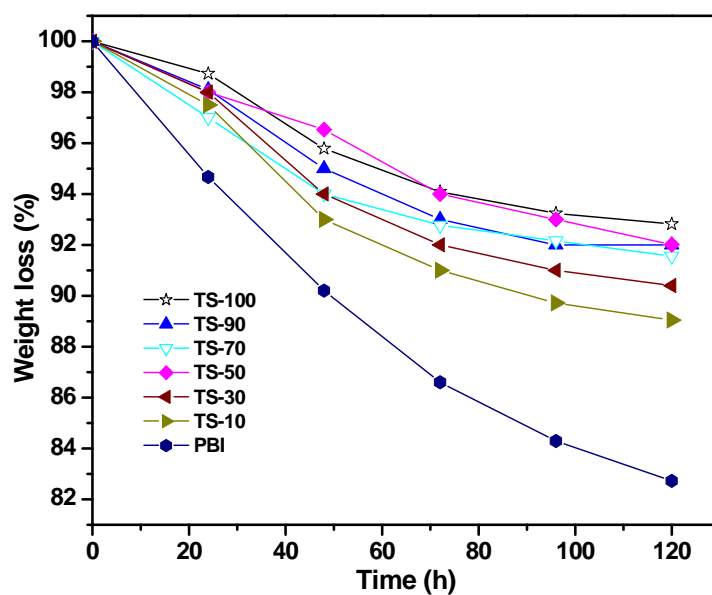


**Figure 3.19** Oxidative stability of PBI and coPBI of IPA containing NPT groups in side chain

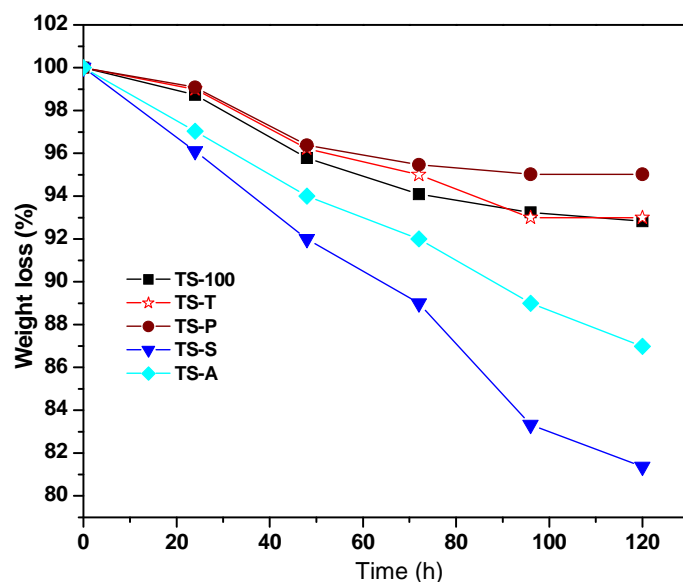


**Figure 3.20** Oxidative stability of PBI and coPBI of other diacids containing NPT groups in side chain

### 3.3.2.7 Phosphoric acid doping study

Having confirmed that the NPT group containing PBI have good film forming properties, high thermal stability and good mechanical strength for high temperature applications, work was continued further to explore possible applications of these polymers as membrane material for polymer electrolyte for fuel cells. Proton conductivity of PBI depends on phosphoric acid doping level. The acid-uptake behavior of newly synthesized polymers is anticipated to be different from commercial PBI, due to structural variations. Polymer electrolyte membranes based on PBI are generally doped with phosphoric acid and the doping level of  $\text{H}_3\text{PO}_4$  in PBI plays an important role in proton conductivity. Higher the doping level higher is the proton conductivity. However, higher doping level affects mechanical properties of the membrane and to maintain a balance between doping level and mechanical properties, a detailed study of effect of acid concentration and time of doping on acid uptake capacity of polymer membranes is essential. The acid uptake capacity of newly synthesized polymers was determined by doping membranes in various molar concentrations of  $\text{H}_3\text{PO}_4$  solutions at room temperature for different time periods. The doping level is defined as the weight percent of acid per gram of the polymer or copolymers. It is known that PBI is generally doped in 85%  $\text{H}_3\text{PO}_4$  at room temperature.

Polymers based on PTDBA, TM-100, TM-90, TM-70, TM-P, TM-S and TM-A are found to dissolve in 14 M  $\text{H}_3\text{PO}_4$  at room temperature. Therefore, a detailed study on the effect of phosphoric acid concentration (2-14 M) on doping level was undertaken.

The polymers (TM-100, TM-90, TM-70, TM-P, TM-S & TM-A) on doping with 12 M  $\text{H}_3\text{PO}_4$  are observed to take up large quantity of phosphoric acid (4-5 times its weight) within 10-15 h and got dissolved at 100 °C in absorbed phosphoric acid during drying though they are not soluble at room temperature. As expected, the doping level of polymers increases with increasing concentration of phosphoric acid (Figure 3.21 and 3.22). Acid-uptake behavior of homo-polymer, TM-100, is similar to that of PBI up to 10 M  $\text{H}_3\text{PO}_4$  solutions, though acid-uptake is slightly lower for TM-100 in 2 M solutions. Acid-uptake of other copolymers is comparatively lower. The acid-uptake of TM-10 and TM-30, TM-50, TM-T and TM-P in 12 M solutions is close to that of PBI. The equilibrium acid-uptake of TM-100, TM-90, TM-70 and TM-50, doped in 10 M  $\text{H}_3\text{PO}_4$ , is in the range of 173-195 wt% of  $\text{H}_3\text{PO}_4$ , while saturation point of acid-uptake of other copolymers, TM-10, TM-30, TM-T and TM-P doped in the 12 M  $\text{H}_3\text{PO}_4$  is 240-256 wt%. Higher acid-uptake of TM-10, TM-30, TM-50 and TM-T may be due to higher  $\text{H}_3\text{PO}_4$  acid concentration. The acid-uptake of PBI in 14 M  $\text{H}_3\text{PO}_4$  is 297 wt%. However the aliphatic group containing PBI TM-S and TM-A got dissolved in 10 M  $\text{H}_3\text{PO}_4$ , and hence these polymers had to be doped in 8 M  $\text{H}_3\text{PO}_4$ .

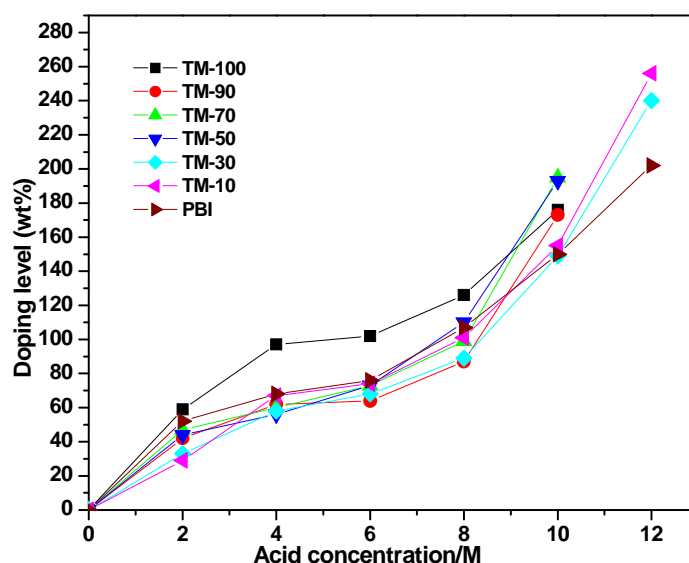


**Figure 3.21** Doping level of phosphoric acid (wt%) in PTDBA based polymers as a function of the concentration of  $\text{H}_3\text{PO}_4$

Doping level of polymers was studied by determining doping level at various time intervals (Figure 3.23 and 3.24). Doping level of polymers TM-10, TM-30, TM-T and TM-P was determined in 12 M  $\text{H}_3\text{PO}_4$ , while that of TM-100, TM-90, TM-70 and TM-50 polymers in 10 M  $\text{H}_3\text{PO}_4$  and TM-S and TM-A in 8 M  $\text{H}_3\text{PO}_4$ . Doping level of PBI was determined in 14 M  $\text{H}_3\text{PO}_4$ . Saturation point for copolymer samples is observed

to be between 15 – 20 h, while for PBI ~24 h. The doping level depends on concentration of acid. Thus, PBI containing NPT groups could not be doped at higher doping level due to solubility limitations. However, membranes of these polymers remain strong and flexible after doping with lower concentration of phosphoric acid.

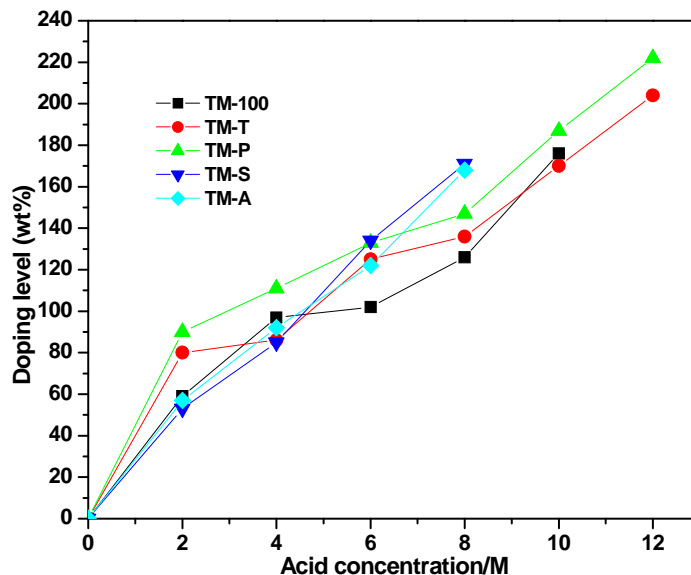


**Figure 3.22** Doping level of phosphoric acid (wt%) in PTDBA based polymers as a function of the concentration  $H_3PO_4$

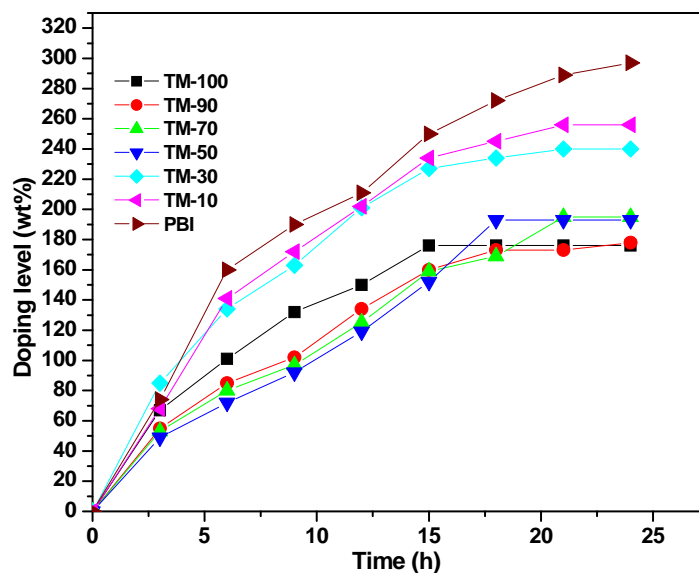


**Figure 3.23** Doping levels of PTDBA based polymers at different time intervals. Concentration of  $H_3PO_4$  for TM-100, TM-90, TM-70, TM-50 (10 M), for TM-10 and TM-30 (12M) and for PBI (14M)

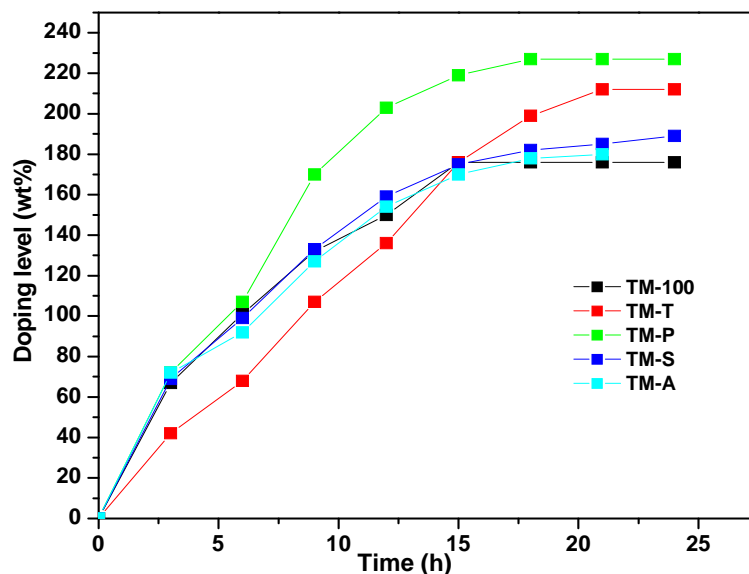


**Figure 3.24** Doping levels of PTDBA based polymers at different time intervals. Concentration of  $H_3PO_4$  for TM-100, (10 M), for TM-T and TM-P (12M) and for TM-S and TM-A (8M)

The phosphoric acid uptake behavior of polymers based on DTIA containing NPT groups in side chain was found to be similar to that of PTDBA-based polymers. Polymers TS-100, TS-90, TS-70, TS-P, TS-S and TS-A are found to dissolve in 14 M  $H_3PO_4$  at room temperature. The membranes of these polymers on doping with 12M  $H_3PO_4$ , take up a lot of phosphoric acid (4-5 times its weight) within 10-15 h and got dissolved in absorbed phosphoric acid at 100 °C during drying, though they are not soluble at room temperature. To determine the solubility and doping behavior of these polymers in phosphoric acid, the effect of phosphoric acid concentration on doping level was studied by immersing in 2-14 molar  $H_3PO_4$  for 24 h at room temperature (Figure 3.25 and 3.26). As expected, the doping level of polymers increases with increasing concentration of phosphoric acid.

$H_3PO_4$  doping level of polymers was also studied at various time intervals (Figure 3.27 and 3.28). Doping level of PBI was determined in 14 M  $H_3PO_4$  while TS-100 and TS-70, TS-50 and TS-P in 10 M and TS-10, TS-30 and TS-T in 12 M  $H_3PO_4$  and TS-S and TS-A in 8 M. Saturation point for pendant NPT group containing polymers TS-100 to TS-50 was in the range of 180 - 190 wt%, between 18 – 21 h, while for TS-10, TS-30 and TS-T was in the range of 200- 240 wt% during this period. However, it was observed that the acid uptake of aliphatic group containing PBI, TS-S and TS-A was much more even in 8 M phosphoric acid. The acid uptake capacity of TS-S and TS-A was found to be in the range of 150-200 wt% and saturation point of acid uptake was 18-



24 h. The high acid uptake of PBI (~300 wt% in 24 h) is mainly due to higher concentration of phosphoric acid. From the data, it appears that the acid uptake increases with time and time dependant acid uptake of NPT group containing polymers is controlled by concentration of dopant.

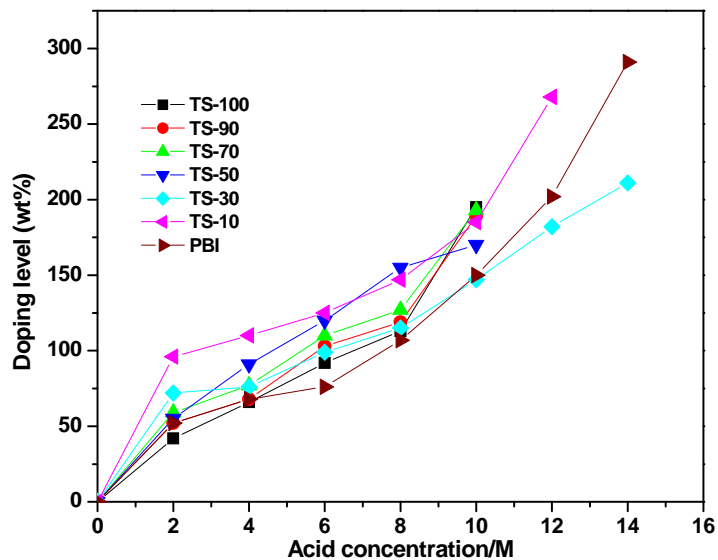


**Figure 3.25** Doping level of phosphoric acid (wt%) in DTIA based polymers and PBI polymers as a function of acid concentration

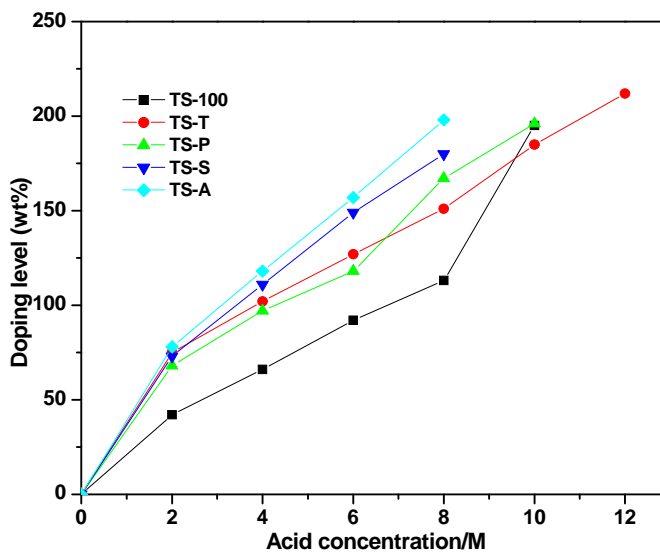


**Figure 3.26** Doping level of phosphoric acid (wt%) in DTIA based polymers as a function of acid concentration

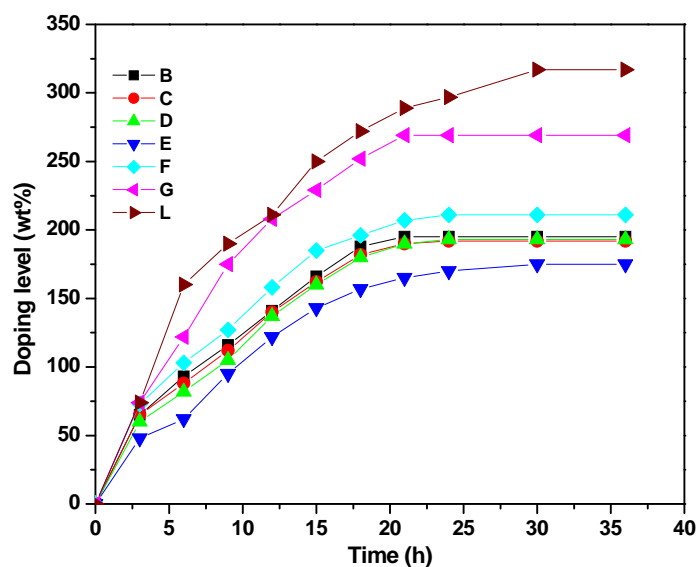


**Figure 3.27** Acid doping levels DTIA based polymers at different time intervals. Concentration of  $\text{H}_3\text{PO}_4$  for TS-100, TS-90, TS-70 and TS-50 (10 M) , for TS-10 and TS-30 (12M) and for PBI (14M)

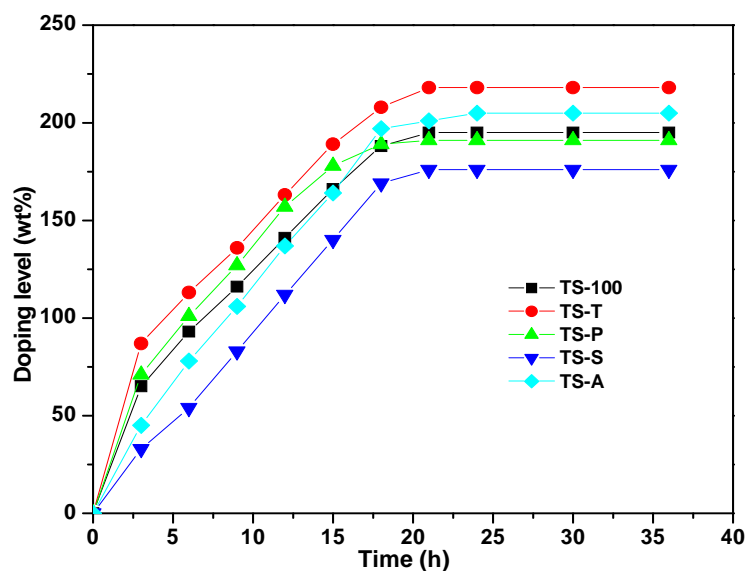


**Figure 3.28** Acid doping levels at different time intervals. Concentration of  $\text{H}_3\text{PO}_4$  for TS-100, (10 M) , for TS-T and TS-P (12M) and for TS-S and TS-A (8M)

### 3.3.2.8 Proton conductivity measurements

The proton conductivity is one of the important properties of fuel cell membranes. The proton conductivity of PBI depends on phosphoric acid-uptake, temperature and relative humidity.<sup>48,53</sup> Usually, proton conductivity increases with increasing acid-uptake, temperature and relative humidity. The proton conductivity of NPT group containing PBI membrane of thickness  $\sim 100\mu\text{m}$  was determined at different

temperatures (25-175 °C) by AC impedance spectroscopy using two-probe electrode assembly.

As mentioned in doping studies, the membranes of polybenzimidazoles of PTDBA, doped with high concentration of H<sub>3</sub>PO<sub>4</sub>, have a tendency to soften above 100 °C. So, these membranes had to be doped in lower concentration of phosphoric acid for conductivity measurements. Based on doping study, membranes TM-100, TM-90, TM-70, TM-50 and TM-P, doped in 10 M phosphoric acid, membranes TM-30, TM-10, and TM-T, doped in 12 M phosphoric acid, membranes TM-S and TM-A doped in 8 M phosphoric acid and PBI membrane doped in 14 M phosphoric acid for 24 h were used for determining proton conductivity. The temperature dependence of proton conductivity of NPT group containing PBI is shown in (Table 3.9.) As expected, the proton conductivity increases with increasing temperature. The proton conductivity of PBI is high compared to NPT group containing polymers. It is speculated that high doping level of PBI (297 wt %) compared to other polymers is one of the reasons for observed high proton conductivity. The proton conductivity of TM-100 with doping level of 175 wt % is in the range of  $4.35 \times 10^{-5}$  to  $4.70 \times 10^{-3}$  S cm<sup>-1</sup> (25 °C to 175 °C). TM-30, TM-10 and PBI with higher doping level show high proton conductivity indicating influence of doping level on proton conductivity.

**Table 3.9** Proton conductivity of PTDBA based polymers

Polymer code	Proton conductivity (S/cm) at temperature (°C)						
	25 °C	50 °C	75 °C	100 °C	125 °C	150 °C	175 °C
TM-100 (176)*	$4.35 \times 10^{-5}$	$1.12 \times 10^{-4}$	$2.34 \times 10^{-4}$	$6.74 \times 10^{-4}$	$1.30 \times 10^{-3}$	$2.15 \times 10^{-3}$	$4.70 \times 10^{-3}$
TM-90 (178)*	$1.36 \times 10^{-5}$	$4.16 \times 10^{-5}$	$1.07 \times 10^{-4}$	$2.69 \times 10^{-4}$	$1.34 \times 10^{-3}$	$2.91 \times 10^{-3}$	$5.70 \times 10^{-3}$
TM-70 (195)*	$2.79 \times 10^{-5}$	$7.76 \times 10^{-5}$	$2.13 \times 10^{-4}$	$5.49 \times 10^{-4}$	$1.02 \times 10^{-3}$	$1.99 \times 10^{-3}$	$4.93 \times 10^{-3}$
TM-50 (193)*	$2.55 \times 10^{-5}$	$6.76 \times 10^{-5}$	$1.28 \times 10^{-4}$	$3.63 \times 10^{-4}$	$1.07 \times 10^{-3}$	$2.37 \times 10^{-3}$	$5.0 \times 10^{-3}$
TM-30 (256)*	$7.02 \times 10^{-5}$	$1.94 \times 10^{-4}$	$3.71 \times 10^{-4}$	$8.51 \times 10^{-4}$	$1.74 \times 10^{-3}$	$2.63 \times 10^{-3}$	$7.12 \times 10^{-3}$
TM-10 (240)*	$2.01 \times 10^{-4}$	$4.57 \times 10^{-4}$	$1.03 \times 10^{-3}$	$2.12 \times 10^{-3}$	$3.63 \times 10^{-3}$	$6.6 \times 10^{-3}$	$1.8 \times 10^{-2}$
TM-T (204)*	$1.29 \times 10^{-3}$	$1.37 \times 10^{-3}$	$1.78 \times 10^{-3}$	$2.08 \times 10^{-3}$	$2.54 \times 10^{-3}$	$2.61 \times 10^{-3}$	$2.56 \times 10^{-3}$
TM-P (222)*	$3.34 \times 10^{-3}$	$3.89 \times 10^{-3}$	$6.45 \times 10^{-3}$	$7.69 \times 10^{-3}$	$7.85 \times 10^{-3}$	$9.54 \times 10^{-3}$	$1.27 \times 10^{-2}$
TM-S (171)*	$2.25 \times 10^{-3}$	$2.98 \times 10^{-3}$	$4.07 \times 10^{-3}$	$4.9 \times 10^{-3}$	$5.52 \times 10^{-3}$	$8.83 \times 10^{-3}$	NM
TM-A (168)*	$2.25 \times 10^{-3}$	$2.76 \times 10^{-3}$	$3.33 \times 10^{-3}$	$4.39 \times 10^{-3}$	$6.4 \times 10^{-3}$	$8.71 \times 10^{-3}$	NM
PBI (297)*	$7.42 \times 10^{-3}$	$9.6 \times 10^{-3}$	$1.4 \times 10^{-2}$	$2.05 \times 10^{-2}$	$2.69 \times 10^{-2}$	$3.00 \times 10^{-2}$	$3.17 \times 10^{-2}$

\* phosphoric acid doping level in weight % of the polymers;  
NM-not measured

The nitrogen atoms in triazole groups, being less basic compared to benzimidazole groups, should facilitate proton transfer by Grotthus mechanism due to comparatively weak hydrogen bonding, which helps to exchange protons due to less friction.<sup>37</sup> For good proton conduction, proton acceptor should exchange proton easily. Thus, presence of NPT groups besides benzimidazole groups should have helped better proton transfer resulting in enhanced proton conductivity. However, it appears that this effect is outweighed by effect due to low doping level to reduce proton conductivity and hence comparatively low proton conductivity was observed in these polymers.

Membrane of polybenzimidazoles containing NPT groups in side chain (based on DTIA) on doping with H<sub>3</sub>PO<sub>4</sub> of high concentration, tend to soften and lose mechanical integrity at high temperature. So, these membranes were doped with different concentrations of H<sub>3</sub>PO<sub>4</sub> (as described earlier), for determining proton conductivity. Thus, membranes of TS-100, TS-90, TS-70 and TS-50 were doped in 10 M phosphoric acid, membranes of TS-10, TS-30, TS-P and TS-T doped in 12 M phosphoric acid, membranes of TS-S and TS-A doped in 8 M phosphoric acid while PBI membrane doped in 14 molar phosphoric acid for 24 h. So doping level of these membranes varies considerably (Table 3.10). As such, it is difficult to correlate proton conductivity with structural variations in these polymers. The proton conductivity of homo polymers (TS-100) with doping level of 195 wt% is in the range of  $1.07 \times 10^{-4}$  to  $3.18 \times 10^{-3}$  S/cm in the temperature range of 25 °C to 175 °C which is low as compared to proton conductivity ( $3.17 \times 10^{-2}$  S cm<sup>-1</sup>) of PBI, in the same temperature range, with doping level of 297 wt%. In copolymer series of DTIA and IPA based polymers, the proton conductivity increases with increase in IPA content. It appears that NPT groups in side chain do not enhance proton conductivity of PBI. The molecular weight of DTIA being higher than IPA, on equal weight basis, the polymer of DTIA has low imidazole content compared to IPA based PBI, which reduces ionic conductivity on main chain resulting in slightly lower proton conductivity. NPT groups in side chain may not be contributing much for proton conductivity. Thus, low doping level and low protonating imidazole sites in main chain of DTIA based polymers are probable causes for observed low proton conductivity, compared to PBI, in these polymers. In copolymer series 50:50 mole% of DTIA and others diacids, polymer containing aliphatic groups (TS-A) shows high proton conductivity in the range of  $1.29 \times 10^{-3}$  to  $9.23 \times 10^{-3}$  S/cm in the temperature range 25-150 °C. In spite of low doping level of 205 wt% high proton conductivity of TS-A is probably due to flexible aliphatic groups.

Proton conductivity data show that both doping level and structural composition of polymers influences proton conductivity. Due to different doping levels of polymer series of PTDBA (Table 3.9) and DTIA (Table 3.10) based polymers it is difficult compare proton conductivity of these two series of polymers to correlate effect of NPT groups in main chain and side chain with proton conductivity.

**Table 3.10** Proton conductivity of DTIA based polymers

Polymer code	Proton conductivity (S/cm) at temperature (°C)						
	25 °C	50 °C	75 °C	100 °C	125 °C	150 °C	175 °C
TS-100 (195)*	$1.07 \times 10^{-4}$	$1.71 \times 10^{-4}$	$3.17 \times 10^{-4}$	$6.21 \times 10^{-4}$	$1.1 \times 10^{-3}$	$2.05 \times 10^{-3}$	$3.18 \times 10^{-3}$
TS-70 (193)*	$1.24 \times 10^{-4}$	$2.12 \times 10^{-4}$	$4.2 \times 10^{-4}$	$8.19 \times 10^{-4}$	$1.32 \times 10^{-3}$	$2.34 \times 10^{-3}$	$3.73 \times 10^{-3}$
TS-50 (175)*	$1.5 \times 10^{-4}$	$2.39 \times 10^{-4}$	$5.59 \times 10^{-4}$	$9.46 \times 10^{-4}$	$1.96 \times 10^{-3}$	$2.96 \times 10^{-3}$	$6.58 \times 10^{-3}$
TS-30 (211)*	$2.99 \times 10^{-4}$	$4.46 \times 10^{-4}$	$9.45 \times 10^{-4}$	$1.75 \times 10^{-3}$	$3.13 \times 10^{-3}$	$5.26 \times 10^{-3}$	$1.05 \times 10^{-3}$
TS-10 (269)*	$2.64 \times 10^{-4}$	$5.6 \times 10^{-4}$	$1.57 \times 10^{-3}$	$2.55 \times 10^{-3}$	$5.14 \times 10^{-3}$	$8.6 \times 10^{-3}$	$1.68 \times 10^{-2}$
TS-T (218)*	$1.58 \times 10^{-4}$	$2.65 \times 10^{-4}$	$7.71 \times 10^{-4}$	$1.91 \times 10^{-3}$	$2.07 \times 10^{-3}$	$3.24 \times 10^{-3}$	$4.58 \times 10^{-3}$
TS-P (191)*	$3.2 \times 10^{-4}$	$7.28 \times 10^{-4}$	$1.26 \times 10^{-3}$	$2.23 \times 10^{-3}$	$3.2 \times 10^{-3}$	$4.79 \times 10^{-3}$	$6.6 \times 10^{-3}$
TS-S (176)*	$7.91 \times 10^{-4}$	$1.29 \times 10^{-3}$	$2.0 \times 10^{-3}$	$3.5 \times 10^{-3}$	$5.4 \times 10^{-3}$	$8.2 \times 10^{-3}$	NM
TS-A (205)*	$1.29 \times 10^{-3}$	$2.42 \times 10^{-3}$	$3.17 \times 10^{-3}$	$4.4 \times 10^{-3}$	$5.87 \times 10^{-3}$	$9.23 \times 10^{-3}$	NM
PBI (297)*	$7.42 \times 10^{-3}$	$9.6 \times 10^{-3}$	$1.4 \times 10^{-2}$	$2.05 \times 10^{-2}$	$2.69 \times 10^{-2}$	$3.00 \times 10^{-2}$	$3.17 \times 10^{-2}$

\* phosphoric acid doping level in weight % of the polymers.

NM-not measured

### 3.3.2.9 Membrane electrode assembly fabrication

The method used to fabricate the catalyst layer on the gas diffusion (GDL) layer is same as used for fabricating gas diffusion layer on the wet-proofed carbon cloth. The catalyst ink was prepared using commercial Pt/C (20 wt%, Arora Matthey Ltd.). The Pt/C, 5 % Nafion solution, and isopropyl alcohol was mechanically mixed in an ultrasonic mixer and deposited by brushing method on the GDL. The Pt and Nafion loading were fixed at  $0.5 \text{ mg/cm}^2$  and  $0.6 \text{ mg/cm}^2$ , respectively. After that a thin layer of PBI was coated on the catalyst layer using a 2 wt% solution of PBI in DMAc.

Polymer electrolyte membranes, TM-100 (80  $\mu\text{m}$ ), TS-100 (80  $\mu\text{m}$ ) were doped in 10 molar phosphoric acid where as PBI membrane (90  $\mu\text{m}$ ) was doped in 14 molar phosphoric acid for 24 h. Then membranes were wiped out by tissue paper and dried at 100 °C in vacuum oven. The membrane electrode assemblies were prepared by hot-

pressing the pretreated electrode ( $5 \text{ cm}^2$ ) membrane under the conditions of  $100 \text{ }^\circ\text{C}$ ,  $130 \text{ atm}$  for 3 min.

### 3.3.2.10 Polarization study

Figures 3.29, 3.30 and 3.31 show a comparison of fuel cell performance of TM-100, TS-100 and PBI membranes, respectively in terms of polarization plots of MEAs fabricated using 20% Pt/C for both anode and cathode in a single cell experiment, at  $100$ ,  $125$  and  $150 \text{ }^\circ\text{C}$  with a dry  $\text{H}_2/\text{O}_2$  gas flow rate of  $0.2 \text{ slpm}$ . TM-100 and TS-100 membranes show lower performance than that of the PBI membrane. The open-circuit voltage (OCV) obtained using TM-100 and TS-100 membranes is  $0.7$  and  $0.75 \text{ V}$ , respectively at  $150 \text{ }^\circ\text{C}$ , whereas for PBI it is  $0.92 \text{ V}$ . The TM-100 and TS-100 membrane gives a maximum power density  $81$  and  $63 \text{ mW/cm}^2$  respectively at  $0.3 \text{ V}$ , whereas the PBI membrane gives  $210 \text{ mW/cm}^2$  at  $0.3 \text{ V}$ . The lower fuel cell performance of TM-100, TS-100 membrane can be attributed to low  $\text{H}_3\text{PO}_4$  acid content and low proton conductivity.

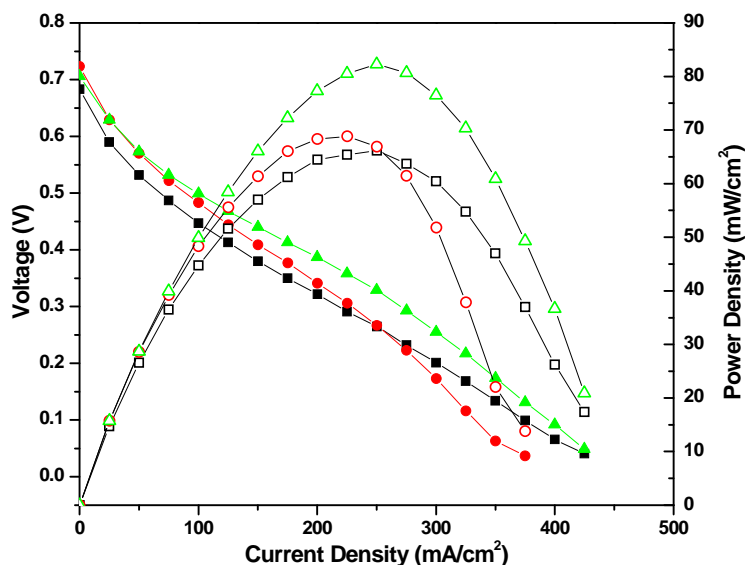


**Figure 3.29** Polarization curves obtained with TM-100 membrane fuel cell at different temperatures with dry  $\text{H}_2$  and  $\text{O}_2$  (flow rate  $0.2 \text{ slpm}$ ). The cell was conditioned for 30 min at open-circuit potential and at  $0.2 \text{ V}$  for 15 min before measurements. Key: ( $\blacksquare$ )  $100$ , ( $\bullet$ )  $125$  and ( $\blacktriangle$ )  $150 \text{ }^\circ\text{C}$

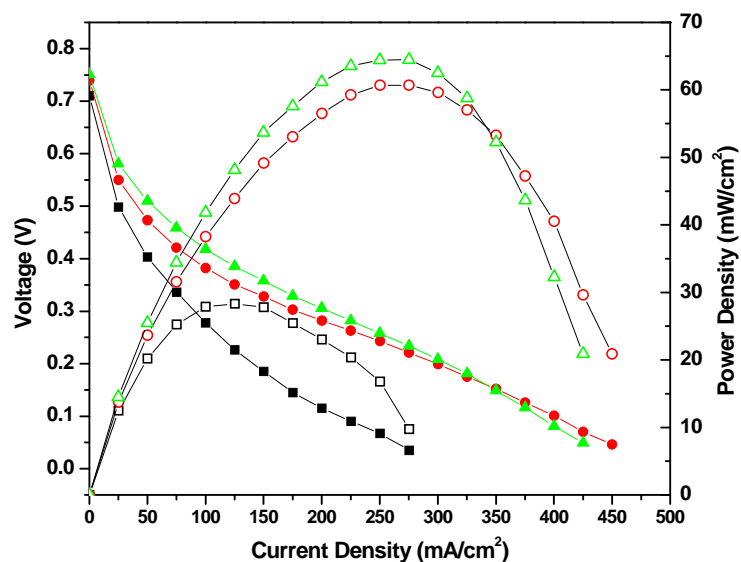


**Figure 3.30** Polarization curves obtained with TS-100 membrane fuel cell at different temperatures with dry H<sub>2</sub> and O<sub>2</sub> (flow rate 0.2 slpm). The cell was conditioned for 30 min at open-circuit potential and at 0.2 V for 15 min before measurements. Key: (■□) 100, (●○) 125 and (▲Δ) 150 °C

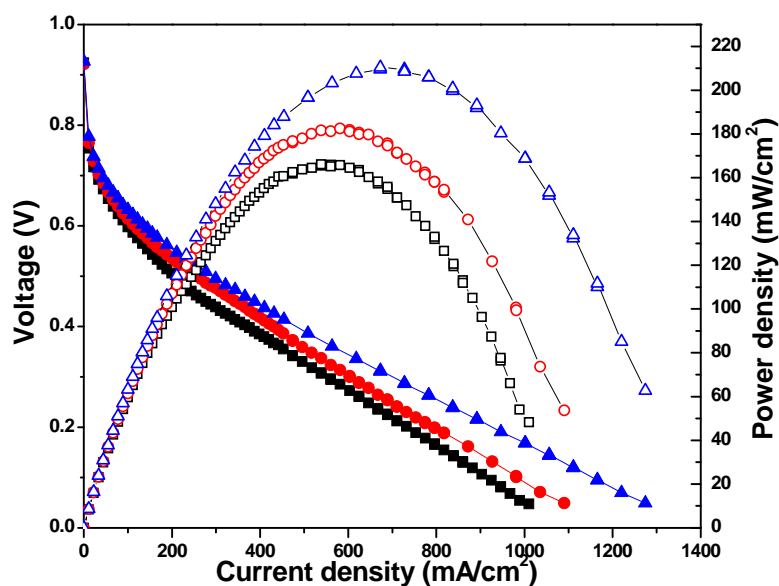


**Figure 3.31** Polarization curves obtained with PBI membrane fuel cell at different temperatures with dry H<sub>2</sub> and O<sub>2</sub> (flow rate 0.2 slpm). The cell was conditioned for 30 min at open-circuit potential and at 0.2 V for 15 min before measurements. Key: (■□) 100, (●○) 125 and (▲Δ) 150 °C

### 3.4 Conclusions

- New series of polybenzimidazoles having N-Phenyl 1,2,4-triazole (NPT) groups in main chain and side chain were synthesized from substituted diacids 3'-(4-phenyl-4H-1,2,4-triazole-3,5-diyl) dibenzoic acid (PTDBA) and 5-(4,5-diphenyl-4H-1,2,4-triazol-3-yl)isophthalic acid (DTIA) with 3,3',4,4',-tetra-amino biphenyl (TAB) using high temperature solution polycondensation in PPA.
- The polymers have high inherent viscosity and good solubility in aprotic solvents at room temperature and they form tough and flexible films.
- These polymers exhibit high thermal stability and good mechanical strength.
- Incorporation of NPT groups in polybenzimidazoles enhances the oxidative stability.
- Incorporation of NPT moiety in the polybenzimidazoles increases the phosphoric acid uptake. At higher doping level, these membranes are soluble in phosphoric acid.
- The polymers showed reasonably good proton conductivity for the applications as membrane material for high temperature polymer electrolyte for proton exchange membrane fuel cells (PEMFCs).

### References

1. Wainright, J. S.; Wang J-T.; Weng, D.; Savinell, R. F. and Litt, M. *J. Electrochem. Soc.* **1995**, 142, L121–L123.
2. Jang, M.Y.; Yamazaki, Y. *J. Power Sources* **2005**, 139, 2-8.
3. Staiti, P.; Minutoli, M. and Hocevar, S. *J. Power Sources* **2000**, 90, 231-235.
4. Staiti, P. and Minutoli, M. *J. Power Sources* **2001**, 94, 9-13.
5. Asensio, J. A.; Borros, S. and Gomez-Romero, P. *Electrochem. Commun.* **2003**, 5, 967-972.
6. Cabasso, I.; Yuan, Y. X.; Johnson, F. E. US Patent 2004, 20040028976A1.
7. Staiti, P.; Minutoli, M.; Hocevar, S. *J. Power Sources* **2000**, 90, 231-235.
8. He, R.; Li, Q. F.; Xiao, G. and Bjerrum, N. J. *J. Membr. Sci.* **2003**, 226, 169-184.
9. Jang, M.Y.; Yamazaki, Y. *Solid State Ionics* **2004**, 167, 107-112.
10. Kerres, J. A.; Ullrich, A.; Haring, T.; Baldauf, M.; Gebhard, U. and Preidel, W. *J. New Mater. Electrochem. Sys.* **2000**, 3, 229-239.
11. Kerres, J.; Ullrich, A.; Meier, F. and Häring, T. *Solid State Ionics* **1999**, 125, 243-249.
12. Lee, J. K. and Kerres, J. *J. Membr. Sci.* **2007**, 294, 75-83.
13. Schönberger, F.; Hein, M. and Kerres, J. *Solid State Ionics* **2007**, 178, 547-554.
14. Hasiotis, C.; Deimede, V. and Kontoyannis, C. G. *Electrochim Acta* **2001**, 46, 2401–2406.
15. Xiao, L.; Zhang, H.; Scanlon, E.; Ramanathan, L. S.; Choe, W-W.; Rogers, D.; Apple, T. and Benicewicz, B. C. *Chem. Mater.* **2005**, 17, 5328-5333.



16. Ariza, M. J.; Jones, D. J. and Roziere, J. *Desalination* **2002**, 147, 183-189.
17. Glipa, X.; El haddad, M.; Jones, D. J. and Roziere, J. *Solid State Ionics* **1997**, 97, 323-331.
18. Peron, J.; Ruiz, E.; Jones, D. J.; Roziere, J. *J. Membr. Sci.* **2008**, 314, 247-256.
19. Staiti, P.; Lufrano, S. F.; Arico, A. S.; Passalacqua, E. and Antonucci, V. *J. Membr. Sci.* **2001**, 188, 71-78.
20. Roziere, J.; Jones, D. J.; Marrony, M.; Glipa, X. and Mula, B. *Solid State Ionics* **2001**, 145, 61-68.
21. Bae, J. M.; Honma, I.; Murata, M.; Yamamoto, T.; Rikukawa, M. and Ogata, N. *Solid State Ionics* **2002**, 147, 189-194.
22. Qing, S.; Huang, W. and Yan, D. *Reactive and Functional Polymers* **2006**, 66, 219-227.
23. Asensio, J. N.; Borros, S.; Gomez-Romero, P. *J. Electrochem. Soc.* **2004**, 151, A304-A310.
24. Chen, C. C.; Wang, L. F.; Wang, J. J.; Hsu, T.C.; Chen, C. F. *J. Mater. Sci.* **2002**, 37, 4109-4115.
25. Xiao, L.; Zhang, H.; Jana, T.; Scanlon, E.; Chen, R.; Choe, E-W.; Ramanathan, L. S.; Yu, S. and Benicewicz, B.C. *Fuel Cells* **2005**, 5, 287-295.
26. Carollo, A.; Quartarone, E.; Tomasi, C.; Mustarelli, P.; Belotti, F.; Magistris, A.; Maestroni, F.; Parachini, M.; Garlaschelli, L. and Righetti, P. P. *J of Power Sources* **2006**, 160, 175-180.
27. Qing, S.; Huang, W.; Yan, D. *Eur. Polym. J.* **2005**, 41, 1589-1595.
28. Asensio, J. N.; Borros, S.; Gomez-Romero, P. *J. Polym. Sci. Part A: Polym Chem* **2002**, 41, 3703-3710.
29. Jouanneau, J.; Mercier, R.; Gonon, L.; Gebel, G. *Macromolecules* **2007**, 40, 983-990.
30. Chuang, S-W.; Hsu, S. L-C. *J. Polym. Sci. Part A: Polym Chem* **2006**, 44, 4508-4513.
31. Li, Z. X.; Liu, J. H.; Yang, S. Y.; Huang, S. H.; Lu, J. D.; Pu, J. L. *J. Polym. Sci. Part A: Polym Chem* **2006**, 44, 5729-5739.
32. Subbaraman, R.; Ghassemi, H. and Zawodzinski Jr., T A. *J. Am. Chem. Soc.* **2007**, 129, 2238-2239.
33. Gunday, S. T.; Bozkurt, A.; Meyer, W. H.; Wegner, G. *J. Polym. Sci.: Part B: Polym Physics* **2006**, 44, 3315-3322.
34. Li, S.; Zhou, Z.; Zhang, Y.; Liu, M. *Chem. Mater.* **2005**, 17, 5884-5886.
35. Kumagai, M.; Takeoka Y. and Rikukawa, M. in proceedings of the 204<sup>th</sup> Electrochemical Society Meeting, Orlando, USA, 2003, P.190.
36. Ponce, M. L.; Gomes, D.; Nunes S. P. *J. Mater. Sci.* **2008**, 319, 14-22.
37. Ponce, M. L.; Boaventura, M.; Gomes, D.; Mendes, A.; Madeira, L. M.; and Nunes S. P. *Fuel Cells* **2008**, 08, 209-216.
38. Li, Q.; Pan, C.; Jensen, O. J.; Noye, P.; Bjerrum, N. J. *Chem. Mater.* **2007**, 19, 350-352.
39. Songa, J. M.; Chab, S. Y.; Lee, W. M. *J of Power Sources* **2001**, 94, 78.
40. Hensema, E. R.; Sena, M. E. R.; Mulder, M. H. V.; Smolders, C. A. *J. Polym. Sci. Part A Polym. Chem.* **1994**, 32, 527-537.
41. Shinn-Horng, C.; Yun, C. *Macromolecules*, **2005**, 38, 53-60.
42. Twieg, R.; Matray, T.; Hedrick, J. L. *Macromolecules* **1996**, 29, 7335-7341.
43. Melendez, A.; De la Campa, Jose, G.; Abajo, J. de *Polymer*, **1998**, 29, 1142-1154.

44. Yuan, M.; Shih, P-I.; Chien, C-H.; Shu, C.-F. *J. Polym. Sci. Part A Polym. Chem.* **2007**, 45, 2925–2937.
45. Yang, C –P; Hsiao, S –H.; Yang, C –C; *J. Polym. Sci., Part A: Polym. Chem.*, 1997, 35, 2147.
46. Liaw, D. –J; Liaw, B. –Y.; Chen, J. –J.; *J. Polym. Sci., Part A: Polym. Chem.* **2000**, 38, 797.
47. Stern, S. A.; *J. Membr. Sci.*, **1994**, 94, 1-65.
48. Li, Q.; He, R.; Berg, R. W.; Hjuler, H. A.; Bjerrum N. J. *Solid State Ionics*, **2004**, 168, 177-185.
49. Li, Q.; He, R.; Jensen J. O. and Bjerrum, N. J. *Fuel Cells* **2004**, 3, 147-159.
50. Kawahara, M.; Morita, J.; Rikukawa, M.; Sanui, K.; Ogata N. *Electrochimica Acta*, **2000**, 45, 1395-1398.
51. Gourdoupi, N.; Andreopoulou, A. K.; Deimede, V.; Kallitsis, K. J. *Chem. Mater.* **2003**, 15, 5044-5050.
52. Musto, P.; Karasz F. E. and MacKnight, W. J. *Polymer*, **1993**, 34, 2934-2945.
53. Samms, S. R.; Wasmus, S. and Savinell, R. F. *J. Electrochem. Soc.* **1996**, 143, 1225-1232.

# Chapter **4**

**Synthesis and characterization  
of polybenzimidazoles and  
copolybenzimidazoles containing  
oxadiazole groups and their application  
as polymer electrolyte membranes for  
fuel cells**

## 4.1 Introduction

Polymer electrolyte membrane fuel cells (PEMFCs) have attracted significant attention due to their high energy efficiency and as environmentally benign source of energy for portable, stationary and automotive applications. Polymer electrolyte membrane (PEM), a key component of fuel cells, normally contains ion containing polymer, bearing sulfonic acid functionality. The currently preferred membrane material is based on perfluorosulfonic acid polymers such as Nafion<sup>®</sup> (DuPont). These polymers have many disadvantages such as, high cost, difficult water management, high fuel crossover, low operational temperature, high sensitivity to impurities (e.g., carbon monoxide) etc., which have prompted researchers to look for alternative less expensive polymer membrane for proton transport capable of operating at higher than 120 °C. Polybenzimidazoles (PBI) are important class of high-performance polymers, which exhibit excellent thermal and hydrolytic stability, high mechanical strength, good chemical resistance, low gas and methanol permeability and good proton conductivity at high temperature on doping with phosphoric acid.<sup>1-4</sup> However, PBI has low proton conductivity (compared to Nafion<sup>®</sup>) at lower than 100 °C, poor oxidative stability at operational conditions and susceptibility to loose unbound phosphoric acid with water or methanol.

Several synthetic methods have been explored to modify the properties of PBI to overcome these limitations as well as to enhance proton conductivity. These include addition of inorganic fillers,<sup>5</sup> composites with heteropolyacids<sup>6,7</sup> and acid-base blends with sulfonated polymers<sup>8</sup> such as, sPEEK<sup>9</sup> sulfonated poly (arylene thioether)s,<sup>10</sup> sulfo-fluorinated poly (arylene sulfo ethers),<sup>11</sup> sulfonated polysulfones<sup>12</sup> PBI-PVDF.<sup>13</sup> PBIs with structural variations have also been reported which include, [poly(2,5-benzimidazole) (i.e., AB-PBI),<sup>14</sup> PBI based on pyridine dicarboxylic acid,<sup>15</sup> naphthalene dicarboxylic acid,<sup>16</sup> and sulfonated isophthalic acid.<sup>17</sup> Parallely, efforts are also being made to develop other thermally stable basic polymers similar to PBI, capable of conducting protons at high temperature.

Polyoxadiazoles and polytriazoles are also heterocyclic polymers having high thermal stability, excellent chemical resistance,<sup>18</sup> good mechanical properties, and good oxidative stability.<sup>19</sup> These polymers, like PBI, are basic in nature capable of conducting protons on doping with strong acids such as phosphoric acid without water and hence, these polymers have drawn attention of many researchers working in this field. Thus,

parallel work is being conducted to investigate suitability of polyoxadiazole, doped with strong acids, for the application as polymer electrolytes for fuel cells.<sup>20</sup>

Recently, proton conductivity and other properties of sulfonated polyoxadiazole, poly (oxadiazole-triazole) copolymers<sup>19,21,22</sup> and phosphonated poly(1,3,4-oxadiazole)s<sup>23</sup> have been investigated. However, these polymers have poor processability and solvent solubility. As copolymerization improves the processability, a few copolymers containing oxadiazole units are documented in literature.<sup>24,25</sup> Considering the resemblance in properties of polybenzimidazole and polyoxadiazole and proton conducting properties on doping with acid at high temperature under similar conditions, polymers containing benzimidazole and oxadiazole groups assume significance to investigate the possibility of applications of these polymers as polymer electrolytes for fuel cells for operation at high-temperature. So we synthesized polybenzimidazoles containing oxadiazole groups.

Thus, this chapter describes synthesis and characterization of high-molecular weight polybenzimidazoles containing oxadiazole groups in main and side chain of PBI by the condensation of two aromatic diacid monomers, namely 3,3'-(1,3,4-oxadiazole-2,5-diyl)dibenzoic acid (ODBA) and 5-(5-phenyl-1,3,4-oxadiazol-2-yl) isophthalic acid (POIA) (described in Chapter-2), with 3,3',4,4'-tetra-amino biphenyl (TAB). Copolybenzimidazoles containing varying extents of oxadiazole groups in main chain and side chain were synthesized by condensing ODBA and POIA with isophthalic acid in different mole ratio (90:10, 70:30, 50:50, 30:70 and 10:90) with TAB to study the effect of oxadiazole groups on properties of polybenzimidazoles. Other commercially available diacids such as terephthalic acid, pyridine 2,6 dicarboxylic acid, adipic acid, and sebacic acid in 50:50 mole ratios, with these two diacids were also employed to synthesize copolybenzimidazoles, with an intension to look for possible structure property relationships. The synthesized polybenzimidazoles were characterized by different instrumental techniques (<sup>1</sup>H NMR, FTIR, XRD, TGA, DSC, etc.) and solvent solubility, inherent viscosity, and mechanical properties. Physico-chemical properties such as water and phosphoric acid-uptake, oxidative stability and proton conductivity of these polymers have also been determined.

## 4.2 Experimental

### 4.2.1 Materials

Isophthalic acid (IPA), terephthalic acid (TPA), pyridine 2,6-dicarboxylic acid (PDCA), adipic acid (AA), sebacic acid (SA), 3,3',4,4'-tetra-amino biphenyl (TAB), calcium hydride (CaH<sub>2</sub>), polyphosphoric acid (115%) (PPA) and trifluoro acetic acid (TFA) were purchased from Aldrich chemicals. IPA, AA, and SA were purified by crystallization from methanol, while TAB and PDCA were recrystallized from water and HCl (1:1) respectively. N-methyl-2-pyrrolidinone (NMP), N, N-dimethylacetamide (DMAc) and N, N-dimethylformamide (DMF) were distilled over CaH<sub>2</sub>. Methanol, ortho phosphoric acid (85%), mohr's salt ((NH<sub>4</sub>)<sub>2</sub>Fe(SO<sub>4</sub>)<sub>2</sub>·6H<sub>2</sub>O), sulfuric acid (96%), methane sulfonic acid (MSA), formic acid (FA), dimethyl sulfoxide (DMSO) and hydrogen peroxide (30%, w/v) were purchased from S.D. fine-Chem. India Ltd. and used without further purification. The diacids 3,3'-(1,3,4-oxadiazole-2,5-diyl)dibenzoic acid (ODBA) and 5-(5-phenyl-1,3,4-oxadiazol-2-yl) isophthalic acid (POIA) were synthesized as per procedure given in Chapter 2.

### 4.2.2 Analytical methods

Elemental analysis was performed on Elementar vario-EL. Inherent viscosity (IV) measurements of all polymers were determined in NMP (0.5 g/dL concentration) at 30 °C using a Ubbelohde viscometer (model F725). The FTIR spectra were recorded on a Perkin Elmer 16 PC FTIR spectrophotometer. Films of 20 µm thickness were used for recording FTIR spectra at room temperature. <sup>1</sup>H NMR spectra were obtained on a Bruker NMR spectrometer operating at a proton frequency of 200 MHz. (DMSO-d<sub>6</sub>) was used as solvents for recording NMR spectra at room temperature. Thermogravimetric analyses (TGA) were recorded using Perkin Elmer TGA-7 instrument from 50 to 900 °C with a scanning rate of 10 °C min<sup>-1</sup> in N<sub>2</sub> atmosphere. Glass transition temperature (T<sub>g</sub>) were measured using DSC Q-10 (TA) instrument. For the DSC measurements, approximately 5-7 mg of samples was taken in an aluminium pan that was tightly crimped with the help of a DSC crimper and then scanned from 50 to 450 °C in N<sub>2</sub> atmosphere at a flow rate 20 mL/min. The wide-angle X-ray diffraction spectra (WAXS) were obtained using Rigaku Dmax 2500 diffractometer with Cu-Kα (1.589 Å) radiation source at room temperature. Tensile properties of polymer films were determined on Instron tensile tester series IX using film strips of size 1.5 x 7 cm and 100 µm thick at a shear rate of 5 mm/min at room temperature.

➤ **Solubility measurement**

The solubility of these polymers in various solvents was determined by dissolving 5 mg of the polymer in 1 mL solvent. A dry sample in powder form was kept in desired solvent for 24 h at ambient temperature with occasional shaking. If necessary, the sample was heated to reflux temperature of low boiling solvents or at 150 °C for high boiling solvents for 10-15 h.

➤ **Membrane casting**

Dense membranes were prepared by solution casting method. A 2% (w/v) polymer solution in NMP was filtered through G-0 sintered funnel on a clean and smooth glass Petri dish. The samples were kept 12 h in an oven at 100 °C to remove the solvent. The films were peeled-off by immersing in water and soaked in water for 2 days in order to remove the residual NMP. Such films were finally dried in vacuum oven at 125 °C for 2 days to remove the last traces of solvent.

➤ **Water uptake**

The water uptake capacity of all membranes was measured at room temperature by immersing accurately weighed dried membranes (40-45 mg) into deionized water for 24 h. The wet membranes were taken out, wiped with tissue paper to remove adhered water and weighed immediately on a microbalance. The water uptake capacity was calculated using following equation (1).

$$WU = \frac{(W_w - W_d)}{W_d} \times 100 \quad (1)$$

where  $W_d$  and  $W_w$  are the weights of dry and wet membrane respectively.

➤ **Oxidative stability**

Oxidative stability was evaluated by the Fenton test.<sup>26</sup> Three pieces of membranes of 2 cm × 2 cm were immersed in 3% H<sub>2</sub>O<sub>2</sub> containing 4 ppm of Fe<sup>2+</sup> (Mohr's salt, (NH<sub>4</sub>)<sub>2</sub>Fe(SO<sub>4</sub>)<sub>2</sub>·6H<sub>2</sub>O) at 70 °C. The samples were taken out from the solution after desired time, washed thoroughly with distilled water, dried at 120 °C for 6 h and weighed. The Fenton solution was replaced with fresh stock solution after every 24 h. Stability was evaluated from the weight losses after each Fenton test.

➤ **Acid doping**

To determine the H<sub>3</sub>PO<sub>4</sub> uptake, accurately weighed dry samples of membranes (size 2 cm × 2 cm and 100 μm thick) were immersed in different molar concentrations of H<sub>3</sub>PO<sub>4</sub> for various time intervals at ambient temperature. The samples were taken out

from the dopant after intended time and the excess of phosphoric acid adhered to samples was removed by blotting with tissue paper and weighed again. The weight gain due to both water and phosphoric acid was obtained by comparing the weight change before and after doping. For determining the acid-uptake by membranes, these membrane samples were further dried at 100 °C under vacuum until an unchanged weight was obtained. The acid-uptake was calculated in wt % by equation:

$$PU = \frac{(W_w - W_d)}{W_d} \times 100 \quad (2)$$

where  $W_d$  and  $W_w$  are the initial weight of dry membrane and after removal of water from doped membrane samples respectively.

#### ➤ Conductivity measurements

The proton conductivity of all the membranes doped with  $H_3PO_4$  was measured using an Auto Lab PGSTST 30 impedance analyzer with FRA software in the frequency range of 0.1-10<sup>5</sup> Hz with amplitude of 10 mV using two-probe conductivity cell. To measure the conductivity at different temperatures, the cell was placed in a sealed glass vessel and the temperature was recorded in close proximity to the membrane sample with a K-type thermocouple. Films of 100 μm thickness were sandwiched between two stainless steel plates and measurements were carried out in a conductivity cell at temperatures ranging from 25 to 175 °C without humidification. The conductivity ( $\sigma$ ) was calculated by the formula:

$$\sigma = \frac{L}{RA} \quad (3)$$

where R, L, and A are the measured resistance, thickness, and cross-sectional area of the membrane, respectively.

#### ➤ Fuel cell performance tests

The electrodes were prepared by brushing the catalyst ink on the gas diffusion layers (GDL), prepared by applying a slurry of Vulcan XC-72, PTFE, water and cyclohexane. The slurry was brushed until a carbon coating of 4 mg cm<sup>-2</sup> was achieved. The GDL was heat treated at 350 °C for 30 minutes before applying the catalyst ink. The catalyst ink was prepared by mixing 20% Pt/C, Nafion, water and isopropyl alcohol using a homogenizer (cole parmer, Model: CV33) for 2 minutes on a 20 second on off basis. The amount of Pt and Nafion loading were 0.5 and 0.6 mg cm<sup>-2</sup> respectively. Finally, a thin layer of PBI was applied on the electrode surface before uni-axially pressing them with the membrane (at 100 °C and 1 ton for 3 minutes) to prepare the



membrane electrode assembly (MEA). Single cell fuel cell experiments of the MEAs were tested on an Arbin fuel cell test station (Model: Arbin-001 MITS Pro-FCTS 5.0-FCTS) at 100, 125 and 150 °C. The single cell was of 5 cm<sup>2</sup> apparent area with serpentine flow fields (Electrochem ink). Prior to the testing, the MEA was conditioned at OCV conditions for 30 min followed by 15 min operation at 0.2 V, after which polarization measurements were carried out with a flow of 0.2 slpm H<sub>2</sub> and O<sub>2</sub>.

### 4.2.3 Synthesis of polybenzimidazoles

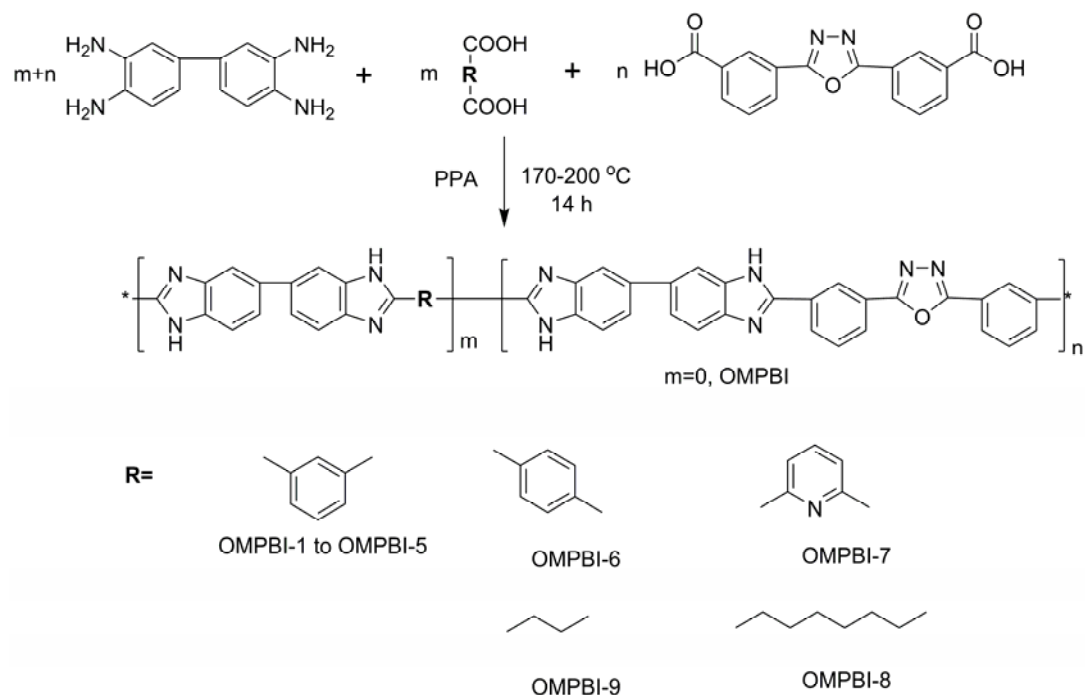
Polybenzimidazoles were synthesized from diacids (1) 3,3'-(1,3,4-oxadiazole-2,5-diyl)dibenzoic acid (ODBA) (Scheme 4.1), and 5-(5-phenyl-1,3,4-oxadiazol-2-yl) isophthalic acid (POIA) (Scheme 4.2) by condensing them with 3,3',4,4'-tetra-amino biphenyl (TAB) by high-temperature solution polycondensation procedure in PPA. The copolymers of these diacids were synthesized by using isophthalic acid, or pyridine dicarboxylic acid, or terephthalic acid, or sebacic acid, or adipic acid as comonomer. A typical procedure for high-temperature solution polycondensation in PPA is described below.

#### 4.2.3.1 Synthesis of PBI having oxadiazole group in main chain and side chain

##### ➤ Synthesis of homo polymer (OMPBI)

A 100 mL three necked round bottom flask equipped with a mechanical stirrer, nitrogen gas inlet and a guard tube was charged with 1.5 g (7.0 mmol) TAB and 45 g of PPA and the mixture was heated to 140 °C with stirring under a stream of nitrogen. After the complete dissolution of TAB, 2.1719 g (7.0 mmol) of ODBA was added slowly with stirring and the temperature was raised to 170 °C. The diacid, ODBA, dissolved in 2 h forming homogeneous solution, which was further heated to 200 °C and maintained at this temperature for 12 h. Then, the solution was poured into 1L water to precipitate the polymer. The polymer was filtered and washed repeatedly with water. To remove residual phosphoric acid, the polymer was stirred overnight in 10% sodium bicarbonate solution. The polymer was filtered and washed with water several times to neutrality. The purified polymer was dried at 150 °C for 48 h in vacuum oven. A brownish yellow polymer was obtained. The inherent viscosity in NMP at 30 °C (0.5g.dL<sup>-1</sup> concentration) was 1.11 dLg<sup>-1</sup>.

Other copolybenzimidazoles and PBI having oxadiazole group in side chain (POIA-based polymers) were also synthesized by a similar procedure and their yields and viscosity values are given in Table 4.1. and Table 4.2, respectively.



**Scheme 4.1** Synthesis of polybenzimidazoles from ODBA

**Table 4.1** Inherent viscosity, yield, film appearance and film nature of PBI containing oxadiazole groups in main chain and its copolymers (ODBA-based polymers)

Polymer Code	Diacid used (% mole ratio)	Inherent Viscosity $\eta_{inh}$ (dL/g) <sup>a</sup>	Yield (%)	Film Appearance (Translucent) film	Film Nature
OMPBI	ODBA 100	1.11	96	Pastel Brown	Flexible
OMPBI-1	ODBA / IPA 90:10	0.98	92	Pastel Brown	Flexible
OMPBI-2	ODBA / IPA 70:30	0.91	97	Brown	Flexible
OMPBI-3	ODBA / IPA 50:50	1.03	95	Brown	Flexible
OMPBI-4	ODBA / IPA 30:70	1.13	98	Brown	Flexible
OMPBI-5	ODBA / IPA 10:90	0.97	96	Brown	Flexible
OMPBI-6	ODBA / TPA 50:50	0.89	99	Brown	Flexible
OMPBI-7	ODBA / PDCA 50:50	0.93	97	Dark brown	Flexible
OMPBI-8	ODBA / SA 50:50	0.71	93	Pastel Brown	Flexible
OMPBI-9	ODBA / AA 50:50	0.5	91	Dark brown	Brittle
PBI	IPA 100	1.2	98	Brown	Flexible

ODBA: 3,3'-(1,3,4-oxadiazole-2,5-diyl)dibenzoic acid; IPA: Isophthalic acid; AA: Adipic acid; SA: Sebacic acid; PDCA: Pyridine dicarboxylic acid; TPA: Terephthalic acid;

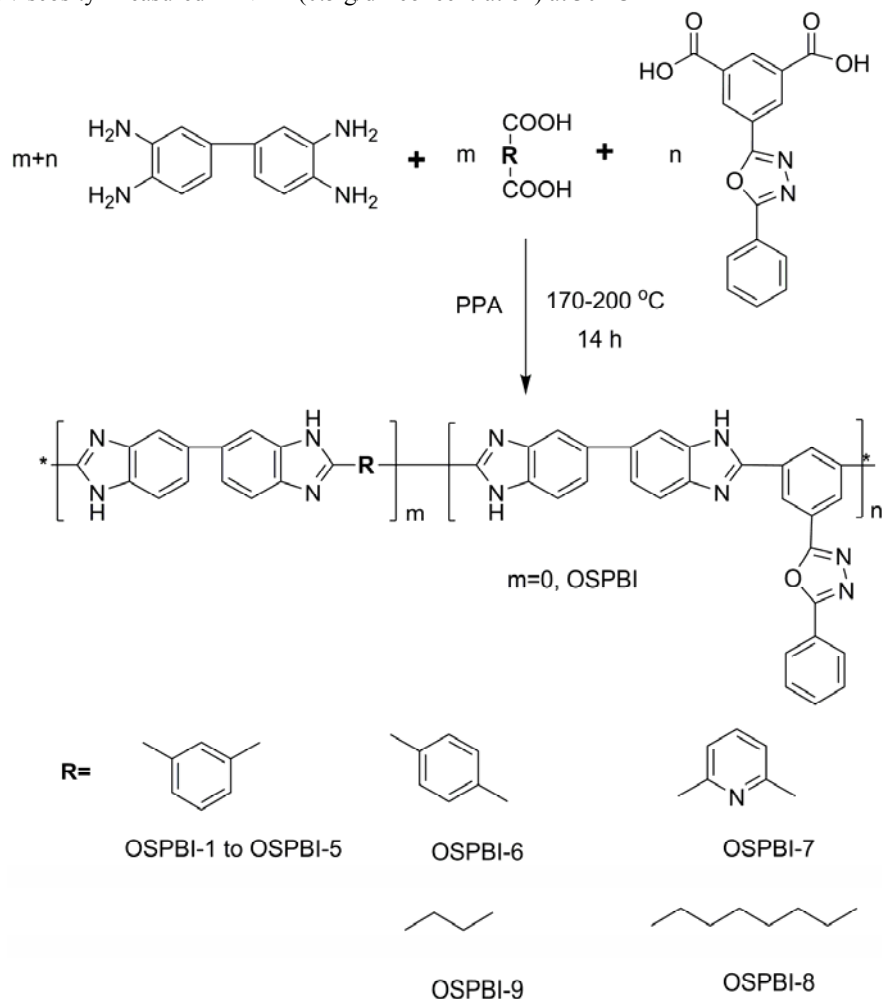
<sup>a</sup>Inherent viscosity measured in NMP (0.5 g/dL concentration) at 30 °C

**Table 4.2** Inherent viscosity, yield, film appearance and film nature of PBI containing oxadiazole groups in side chain and its copolymers (POIA-based polymers)

Polymer Code	Diacids used (% mole ratio)	Inherent Viscosity $\eta_{inh}$ (dL/g) <sup>a</sup>	Yield (%)	Film Appearance (Translucent) film	Film Nature
OSPBI	POIA 100	0.69	94	Brown	Brittle
OSPBI -1	POIA / IPA 90:10	0.76	95	Brown	Flexible
OSPBI -2	POIA /IPA 70:30	0.83	96	Brown	Flexible
OSPBI -3	POIA /IPA 50:50	0.96	98	Brown	Flexible
OSPBI -4	POIA /IPA 30:70	0.98	95	Brown	Flexible
OSPBI -5	POIA /IPA 10:90	1.10	97	Brown	Flexible
OSPBI -6	POIA /TPA 50:50	0.92	99	Brown	Flexible
OSPBI -7	POIA /PDCA 50:50	0.74	96	Light brown	Flexible
OSPBI -8	POIA / SA 50:50	0.67	92	Golden yellow	Brittle
OSPBI -9	POIA / AA 50:50	0.49	94	Brown	Brittle

POIA: 5-(5-phenyl-1,3,4-oxadiazol-2-yl) isophthalic acid;

<sup>a</sup>Inherent viscosity measured in NMP (0.5 g/dL concentration) at 30 °C

**Scheme 4.2** Synthesis of polybenzimidazoles from POIA

### 4.3 Results and Discussion

#### 4.3.1 Synthesis and structural characterization of polybenzimidazoles

Polybenzimidazole containing oxadiazole groups were prepared by condensing TAB with diacid monomers, ODBA, POIA, in PPA and other commercially available diacids such as IPA, TPA, PDCA, SA and AA (Scheme 4.1 and 4.2) by conventional one-step procedure as discussed earlier. Copolymers containing varying extents of oxadiazole group in main chain were synthesized by condensing a mixture of ODBA and IPA in different mole ratios (90:10, 70:30, 50:50, 30:70 and 10:90) with TAB (Schemes 4.1). Similarly copolymers containing varying contents of oxadiazole group in side chain were synthesized by condensing a mixture of POIA and IPA in different mole ratios (90:10, 70:30, 50:50, 30:70 and 10:90) with TAB (Schemes 4.2).

All polymers formed strong thread during precipitation in water. The polymers were obtained in almost quantitative yields and their inherent viscosities ( $\eta_{inh}$ ) measured in NMP were closed to 1 dL/g except for OMPBI-9, OSPBI-8 and OSPBI-9, indicating formation of high molecular weight polymers (Table 4.1 and 4.2). All polymers form tough films on casting 2% solution in NMP.

The polymers were characterized by FTIR and  $^1\text{H}$  NMR spectroscopy. The several characteristic peaks of PBI in FTIR spectrum are reported by Musto et al.<sup>28</sup> Pristine PBI shows characteristic absorption peak at  $3409\text{ cm}^{-1}$  (free non-hydrogen-bonded N-H stretching),  $3140\text{ cm}^{-1}$  (self-associated hydrogen-bonded N-H groups),  $1620\text{ cm}^{-1}$  ( $\text{C}=\text{C}/\text{C}=\text{N}$  stretching of benzimidazole ring),  $1588\text{ cm}^{-1}$  (ring vibration characteristic of conjugation between benzene and imidazole ring),  $1438\text{ cm}^{-1}$  (in plane ring vibration characteristic of 2,6 disubstituted benzimidazole),  $1280\text{ cm}^{-1}$  (imidazole ring breathing). A slight variation in the absorption peaks compared to pristine PBI was observed in case of OMPBI and OSPBI (for e.g., peaks  $3390\text{ cm}^{-1}$ ,  $3152\text{ cm}^{-1}$ ,  $1625\text{ cm}^{-1}$ ,  $1594\text{ cm}^{-1}$ ,  $1443\text{ cm}^{-1}$ ,  $1291\text{ cm}^{-1}$ ) as shown in Figure 4.1. However, characteristic absorption peak due to ( $\text{C}=\text{C}/\text{C}=\text{N}$ ) was found at  $1605\text{ cm}^{-1}$  in OSPBIs as shown in Figure 4.2. The slight difference in absorption peaks compared to PBI is mainly due to the presence of oxadiazole groups.

In OMPBIs and OSPBIs, characteristic absorption peak of oxadiazole groups are observed at  $1548\text{ cm}^{-1}$  and  $1070\text{ cm}^{-1}$  due to  $\text{C}=\text{N}$  (stretching) and  $-\text{C}-\text{O}-\text{C}-$  (stretching) respectively. The peak intensity of  $\text{C}=\text{N}$  (stretching) at  $1548\text{ cm}^{-1}$  and that of  $-\text{C}-\text{O}-\text{C}-$  (stretching) of oxadiazole groups at  $1070\text{ cm}^{-1}$  systematically increases with increase in oxadiazole content in copolymers (Figure 4.3). In pristine PBI, the band due to  $-\text{C}-\text{O}-\text{C}-$

at  $1070\text{ cm}^{-1}$  is completely missing. In PBI, free non-hydrogen bonded N-H stretching and self-associated N-H stretching peaks appear at  $3409\text{ cm}^{-1}$  and  $3140\text{ cm}^{-1}$  respectively, while in OMPBIs and OSPBIs, these peaks are observed at  $3390\text{ cm}^{-1}$  and  $3152\text{ cm}^{-1}$  respectively. Thus, OMPBIs contain both benzimidazole and oxadiazole groups.

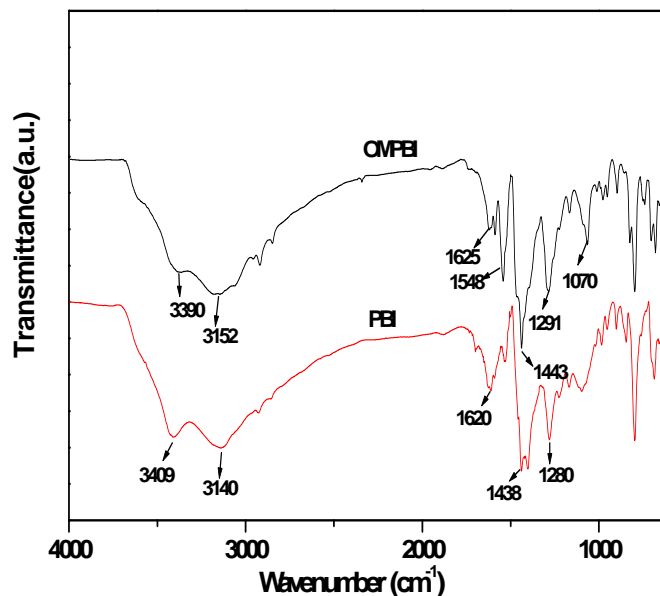


**Figure 4.1** FTIR spectra of oxadiazole groups containing PBI in main chain (OMPBI) and PBI (film)

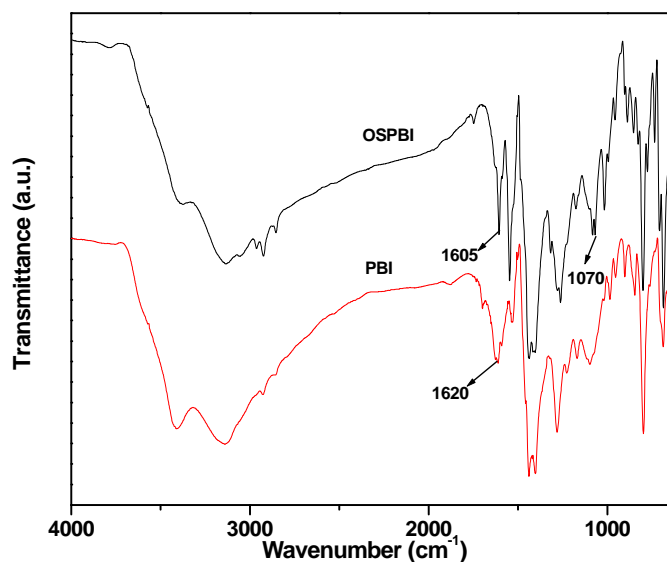


**Figure 4.2** FTIR spectra of oxadiazole groups containing PBI in side chain (OSPBI) and PBI (film)

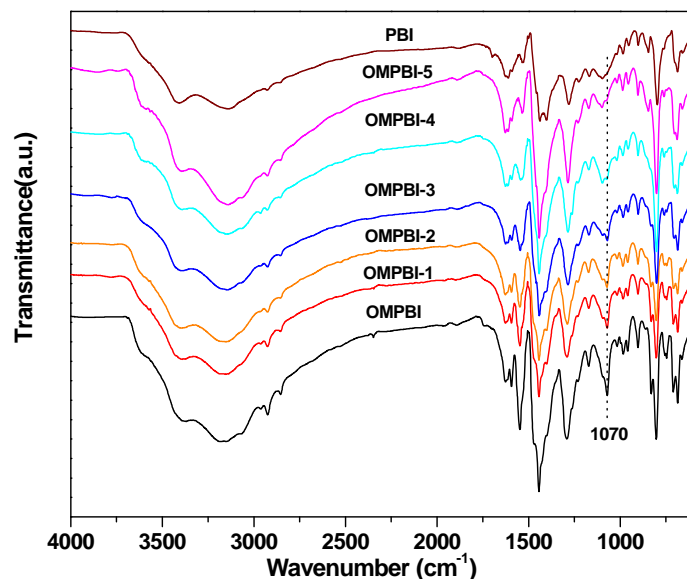


**Figure 4.3** FTIR spectra of polymer films of copolymers of ODBA and IPA. Dotted line shows increase in the peak intensity of  $1070\text{ cm}^{-1}$  (-C-O-C- stretching in oxadiazole ring) with increase in the oxadiazole groups in PBI

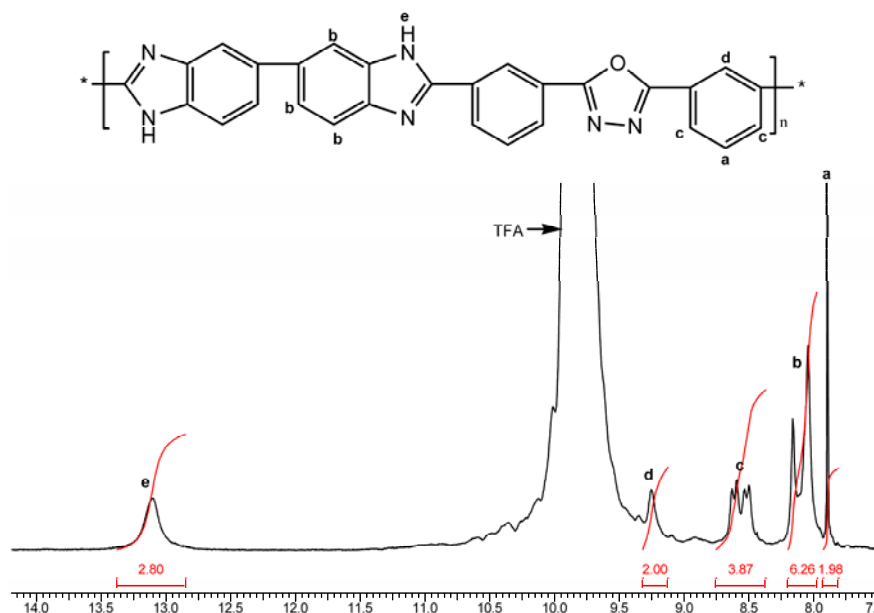


**Figure 4.4**  $^1\text{H}$  NMR spectrum of OMPBI in TFA ( $\text{D}_2\text{O}$  lock)

$^1\text{H}$  NMR measurements of ODBA and POIA-based polymers were carried out in trifluoro acetic acid using  $\text{D}_2\text{O}$  as internal lock as they were insoluble in DMSO. Proper resolution of aromatic protons was very difficult in spite of sample being scanned on a 500 MHz NMR instrument. The integration corresponding to 14 protons is in the required region as shown in Figure 4.4. The imidazole proton peak is observed at 13.22 ppm, and all the aromatic protons are between 7.9 – 8.35 ppm with normal integrations. Similarly, the integration corresponding to 14 protons in OSPBI (Figure 4.5) is in the

expected region. The imidazole proton peak was not seen, may be due to the hydrogen bonding between N-H protons and oxygen of oxadiazole group. All the aromatic protons are found at 7.31 to 9.5 ppm with expected integrations. Thus, FTIR and  $^1\text{H}$  NMR analysis confirmed the formation of desired polybenzimidazoles.

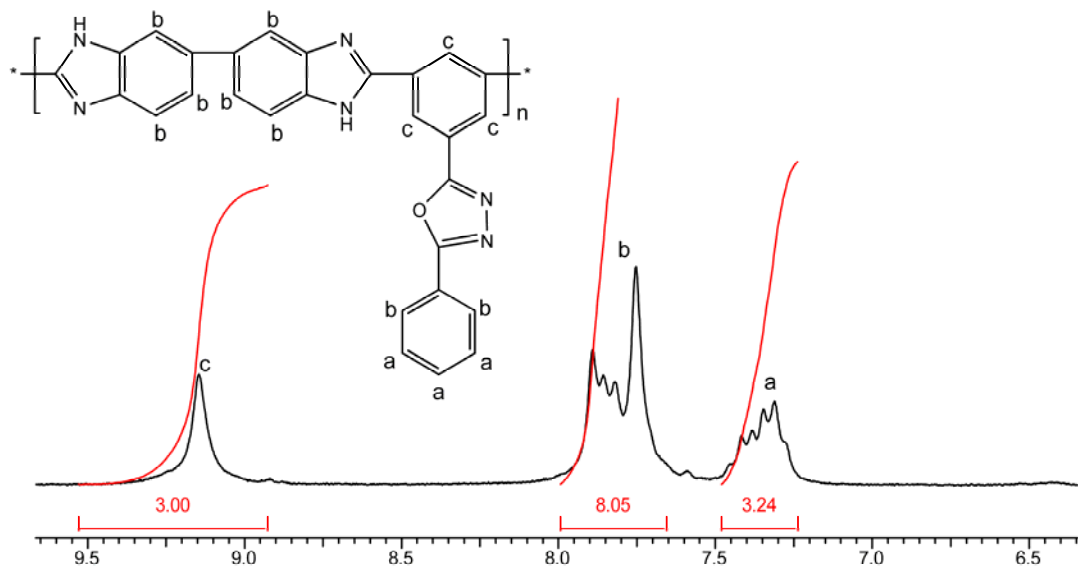


**Figure 4.5**  $^1\text{H}$  NMR spectrum of OSPBI in TFA ( $\text{D}_2\text{O}$  lock)

### 4.3.2 Properties of polybenzimidazoles

The polybenzimidazoles were characterized by solubility measurements, X-ray diffraction, DSC, TGA and mechanical strength. Other studies such as oxidative stability, water uptake, phosphoric acid uptake and proton conductivity of membranes were also carried out.

#### 4.3.2.1 Polymer solubility

Polyoxadiazole synthesized from para or meta phenylene dicarboxylic acid are soluble only in strong acids such as sulfuric acid, chlorosulfonic acid, or methane sulfonic acid,<sup>29</sup> whereas they are poorly soluble in organic solvents. The solubility has been enhanced to some extent by incorporation of substituents such as tert-butyl group on the phenylene ring or bulky moieties such as trimethyl-3-phenylindan, cardo diphenylphthalide, or diphenyl silane into the polymer backbone.<sup>29</sup> The polymer solubility containing benzimidazole and oxadiazole groups was studied qualitatively in various solvents. In case of ODBA-based polymers, these polymers are easily soluble in strong acids such as sulfuric acid, formic acid, methane sulfonic acid etc. These polymers are soluble in NMP and DMAc, and insoluble DMF and DMSO (Table 4.3). Low solubility of OMPBI and OMPBI-1 in DMAc is attributed to high content of

oxadiazole groups compared to other copolymers. Thus, copolymers OMPBI-3 to OMPBI-5 are soluble in aprotic polar solvents and strong acids. Copolymers OMPBI-8 and 9 containing aliphatic groups are not soluble in polar solvents.

**Table 4.3** Solubility behaviour of polybenzimidazoles having oxadiazole groups in main chain

Polymer Code	DMAc	NMP	DMSO	DMF	MSA	FA	H <sub>2</sub> SO <sub>4</sub>	TFA
OMPBI	±	++	--	--	++	++	++	++
OMPBI-1	±	++	±	--	++	++	++	++
OMPBI-2	++	++	±	±	++	++	++	++
OMPBI-3	++	++	+	±	++	++	++	++
OMPBI-4	++	++	+	±	++	++	++	++
OMPBI-5	++	++	+	+	++	++	++	++
OMPBI-6	++	++	±	±	++	++	++	++
OMPBI-7	++	++	±	±	++	++	++	++
OMPBI-8	--	+	--	±	++	++	++	++
OMPBI-9	--	+	--	±	++	++	++	++
PBI	+	+	+	+	++	++	++	++

Concentration: 5mg/mL.

**TFA:** Trifluoro acetic acid; **H<sub>2</sub>SO<sub>4</sub>:** conc. sulfuric acid; **DMF:** N,N-dimethylformamide; **DMAc:** N,N-dimethyl acetamide; **DMSO:** dimethyl sulfoxide; **NMP:** N-methyl-2-pyrrolidone; **MSA:** methane sulfonic acid; **FA:** formic acid; **TPA:** terephthalic acid; **PDCA:** pyridine 2,4-dicarboxylic acid; **SA:** sebacic acid and **AA:** adipic acid.

+ + Soluble at room temperature; + Soluble on heating; ± partially soluble; - - Insoluble

**Table 4.4** Solubility behaviour of polybenzimidazoles having oxadiazole groups in side chain

Polymer Code	DMAc	NMP	DMSO	DMF	MSA	FA	H <sub>2</sub> SO <sub>4</sub>	TFA
OSPBI	--	++	--	--	++	++	++	++
OSPBI-1	--	++	±	--	++	++	++	++
OSPBI-2	+	++	±	±	++	++	++	++
OSPBI-3	++	++	+	±	++	++	++	++
OSPBI-4	++	++	+	±	++	++	++	++
OSPBI-5	++	++	+	+	++	++	++	++
OSPBI-6	++	++	±	±	++	++	++	++
OSPBI-7	++	++	±	±	++	++	++	++
OSPBI-8	+	++	±	±	++	++	++	++
OSPBI-9	±	+	±	±	++	++	++	++
PBI	+	+	+	+	++	++	++	++

Concentration: 5mg/mL; + + Soluble at room temperature; + Soluble on heating; ± partially soluble; - - Insoluble.



The OSPBIs are also soluble in strong acids (Table 4.4). The homo polymer (OSPBI) and OSPBI-1 are soluble in NMP and insoluble in DMAc where as the copolymers OSPBI-2 to OSPBI-7 are soluble in DMAc, and NMP. However these copolymers are partially soluble in DMSO and DMF. It is evident from the solubility study, that the presence of benzimidazole groups enhances solubility of polyoxadiazole. Thus, copolymerization enhances solubility of polymers.

#### 4.3.2.2 Thermal properties

The thermal stability and glass transition temperatures ( $T_g$ ) of the polybenzimidazoles were determined by thermogravimetric analysis (TGA) and differential scanning calorimetry (DSC), respectively.

##### 4.3.2.2.1 Thermogravimetric analyses (TGA)

Thermogravimetric analyses (TGA) were recorded at a heating rate of  $10\text{ }^\circ\text{C min}^{-1}$  in  $\text{N}_2$  atmosphere. To remove absorbed moisture, the samples were preheated to  $150\text{ }^\circ\text{C}$  and after holding for 10 min cooled to  $50\text{ }^\circ\text{C}$ , prior to measurements. The initial decomposition temperature (IDT), the decomposition temperature at 10% weight loss ( $T_{10}$ ) and the maximum decomposition temperature ( $T_{\text{max}}$ ) for polybenzimidazoles, synthesized from ODBA and POIA, are summarized in the Table 4.5 and 4.6 and thermograms of the polymers are shown in Figure 4.6 to 4.9.

TGA results indicate that all the polybenzimidazoles containing oxadiazole groups display good thermal stability, being stable up to  $500\text{ }^\circ\text{C}$ . It was observed that PBI's containing oxadiazole groups in main chain have high thermal stability as compared to PBI containing oxadiazole groups in side chain. The thermal decomposition temperatures of all samples from the two series were very close to each other.

The polybenzimidazoles synthesized from diacid ODBA (OMPBI, OMPBI-1 to OMPBI-9) (Table 4. 5 and Figure 4. ) showed IDT,  $T_5$ , and  $T_{10}$  values in the range  $457\text{--}576\text{ }^\circ\text{C}$ ,  $461\text{--}627\text{ }^\circ\text{C}$  and  $479\text{--}711\text{ }^\circ\text{C}$  respectively. The IDT values of aromatic polyoxadiazole reported in literature<sup>29</sup> vary between  $450\text{--}500\text{ }^\circ\text{C}$ . In the case of copolymers, OMPBI-1 to OMPBI-5, values of IDT increase with increasing benzimidazole content in copolymer. Similar trend is observed in case of  $T_5$  and  $T_{10}$  values. Decomposition of polybenzimidazoles containing oxadiazole groups takes place in two stages the first being  $\sim 500\text{ }^\circ\text{C}$  due to decomposition of oxadiazole groups<sup>29</sup> and the second between  $735\text{--}750\text{ }^\circ\text{C}$  due to decomposition of benzimidazole backbone.<sup>30</sup> In polyoxadiazole, incomplete cyclization or hydrolysis of oxadiazole groups show the

degradation around 300 °C.<sup>31,32</sup> The absence of weight loss at ~300 °C in OMPBI polymers indicate that oxadiazole groups in the polymers are intact. In ODBA and IPA copolymer series, IDT,  $T_5$ ,  $T_{10}$ , increase with increase in IPA, due to increase in rigidity of polymers.

**Table 4.5** Thermal properties of polybenzimidazoles having oxadiazole groups in main chain (ODBA-based polymers)

Polymer Code	IDT (°C) <sup>a</sup>	$T_5$ (°C) <sup>b</sup>	$T_{10}$ (°C) <sup>c</sup>	$T_{Max}$ (°C) <sup>d</sup>	Residue (wt %) <sup>e</sup>	$T_g$ (°C) <sup>f</sup>
OMPBI	480	502	530	510	73	388
OMPBI-1	480	503	545	509	76	392
OMPBI-2	483	512	576	515	78	397
OMPBI-3	485	521	611	517	77	411
OMPBI-4	495	577	709	517	83	406
OMPBI-5	576	627	711	519	81	408
OMPBI-6	493	511	599	513	65	368
OMPBI-7	487	479	575	511	70	409
OMPBI-8	457	461	479	494	53	315
OMPBI-9	479	470	491	499	66	351
PBI	603	683	760	751	85	431

<sup>a</sup> IDT: initial decomposition temperature; <sup>b,c</sup>  $T_5$ ,  $T_{10}$ : temperature at which 5%, 10% wt loss observed; <sup>d</sup>  $T_{max}$ : maximum decomposition temperature; <sup>e</sup> residue at 900 °C; <sup>f</sup>  $T_g$ : glass transition temperature

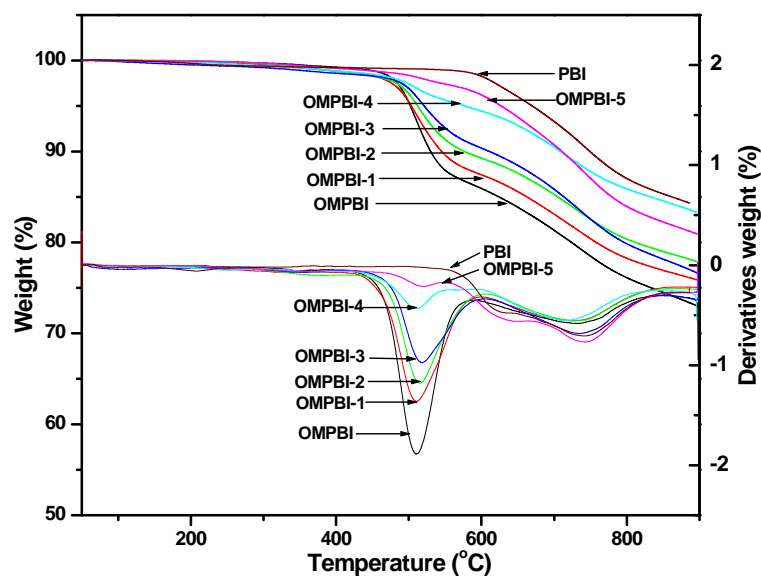


**Figure 4.6** Thermogram and derivatives of thermograms of polybenzimidazoles from ODBA in  $N_2$  atmosphere (purging rate 20 mL/min) recorded at a heating rate 10 °C/min

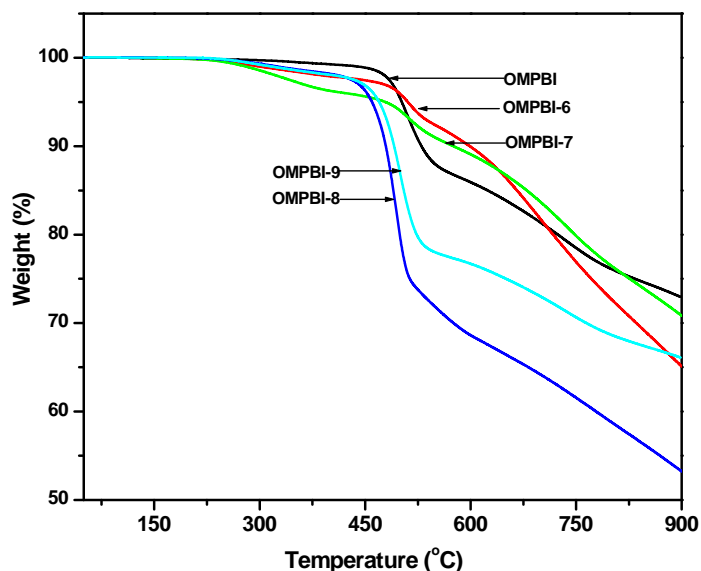


**Figure 4.7** Thermograms of other polybenzimidazoles from ODBA in nitrogen

**Table 4.6** Thermal properties of polybenzimidazole having oxadiazole group in side chain (POIA-based polymers)

Polymer Code	IDT (°C) <sup>a</sup>	T <sub>5</sub> (°C) <sup>b</sup>	T <sub>10</sub> (°C) <sup>c</sup>	T <sub>Max</sub> (°C) <sup>d</sup>	Residue (wt %) <sup>e</sup>	T <sub>g</sub> (°C) <sup>f</sup>
OSPBI	464	478	501	511	65	413
OSPBI-1	456	467	488	491	67	414
OSPBI-2	456	468	492	493	65	413
OSPBI-3	458	476	506	509	64	411
OSPBI-4	457	481	573	511	71	406
OSPBI-5	508	566	662	517	75	412
OSPBI-6	452	480	510	490	64	407
OSPBI-7	449	480	508	492	64	400
OSPBI-8	407	421	447	449	60	325
OSPBI-9	416	440	477	453	62	343
PBI	603	683	760	751	85	431

<sup>a</sup> IDT: initial decomposition temperature; <sup>b,c</sup> T<sub>5</sub>, T<sub>10</sub>: temperature at which 5%, 10% wt loss observed; <sup>d</sup> T<sub>max</sub>: maximum decomposition temperature; <sup>e</sup> residue at 900 °C; <sup>f</sup> T<sub>g</sub>: glass transition temperature

Polybenzimidazoles synthesized from diacid POIA, (Table 4. 6 and Figure 4.8 and 4.9 ) showed IDT, T<sub>5</sub>, and T<sub>10</sub> values in the range 407-508 °C, 421-566 °C and 447-662 °C respectively. The sample OSPBI-5 showed the maximum thermal stability with an IDT, T<sub>5</sub> and T<sub>10</sub> values of 508 °C, 566 °C and 662 °C respectively. It is expected that sebacic acid and adipic based polybenzimidazoles (OSPBI-8 and OSPBI-9) should have relatively low thermal stability compared to fully aromatic polybenzimidazoles (OSPBI, OSPBI-1 to OSPBI-7) due to the aliphatic chain in the polymer backbone. In general, all

polybenzimidazoles showed good thermal properties with no decomposition below 416 °C signifying their potential for many high temperature applications.

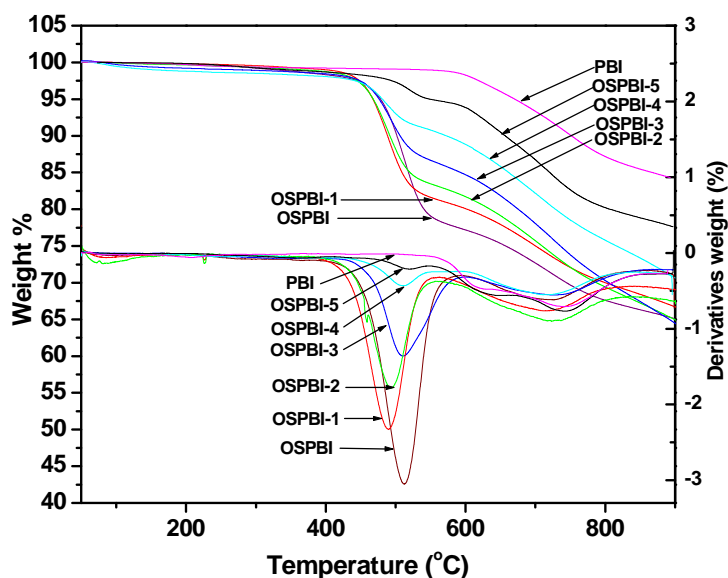


**Figure 4.8** Thermograms and derivatives of thermograms of polybenzimidazoles from POIA in  $N_2$  atmosphere (purging rate 20 mL/min) recorded at a heating rate 10 °C/min

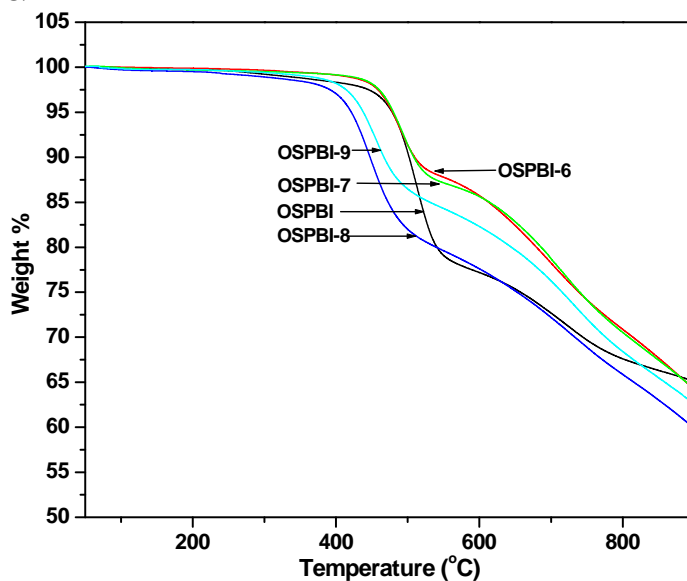


**Figure 4.9** Thermograms of other polybenzimidazoles from POIA in nitrogen

#### 4.3.2.2.2 Glass transition temperature

The glass transition temperature ( $T_g$ ) was measured from 50 °C to 450 °C in nitrogen atmosphere at a heating rate of 20 °C /min. Fully aromatic polyoxadiazoles do not show  $T_g$ , probably due to degradation of polymer before melting.<sup>29</sup> The  $T_g$  values of

polybenzimidazoles synthesized from ODBA, are shown in Table 4.5, while DSC thermograms in Figure 4.10-4.11.

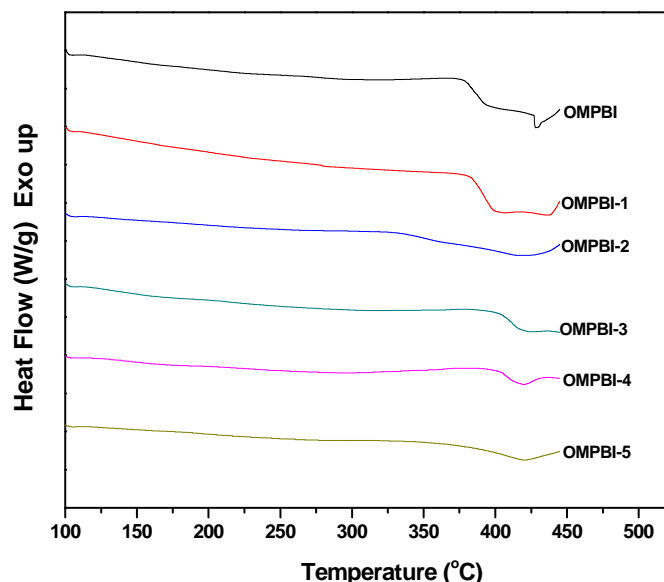


**Figure 4.10** DSC Thermograms of homo polymer and copolymers based on ODBA in  $N_2$ , (heating rate  $20\text{ }^\circ\text{C min}^{-1}$ )

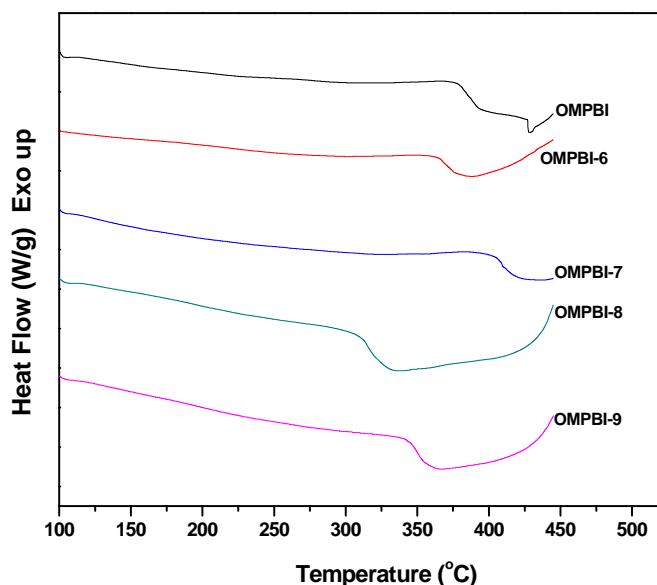


**Figure 4.11** DSC Thermograms of other copolymers based on ODBA in  $N_2$ , (heating rate  $20\text{ }^\circ\text{C min}^{-1}$ )

The homo polymer OMPBI has low  $T_g$  ( $388\text{ }^\circ\text{C}$ ) compared to PBI ( $431\text{ }^\circ\text{C}$ ). Polybenzimidazoles (PBI) normally exhibit high  $T_g$  ( $431\text{ }^\circ\text{C}$ ) due to their rigidity attributable to hydrogen bonding in the polymer chain. Incorporation of 10 mole% of oxadiazole groups in PBI disrupts rigid structure due to random distribution of oxadiazole groups, resulting in lowering of  $T_g$  to  $408\text{ }^\circ\text{C}$  (OMPBI-5). In copolymers OMPBI-1 to OMPBI-5, it is observed that  $T_g$  values decrease with increasing oxadiazole

content. However, copolymer OMPBI-3, synthesized from 50:50 mole% of ODBA:IPA, exhibits slightly higher  $T_g$  (411 °C) than OMPBI-4 and OMPBI-5 ( $T_g$  406 °C and 408 °C respectively), which may be due to symmetrical nature of the para backbone enhance the segmental mobility of the chains and hence OMPBI-5 (para substituted) show a lower  $T_g$  compared to OMPBI-3 (meta substituted).<sup>33</sup> The diacid ODBA, compared to IPA, is more flexible which explains observed low  $T_g$  of oxadiazole group containing PBI.

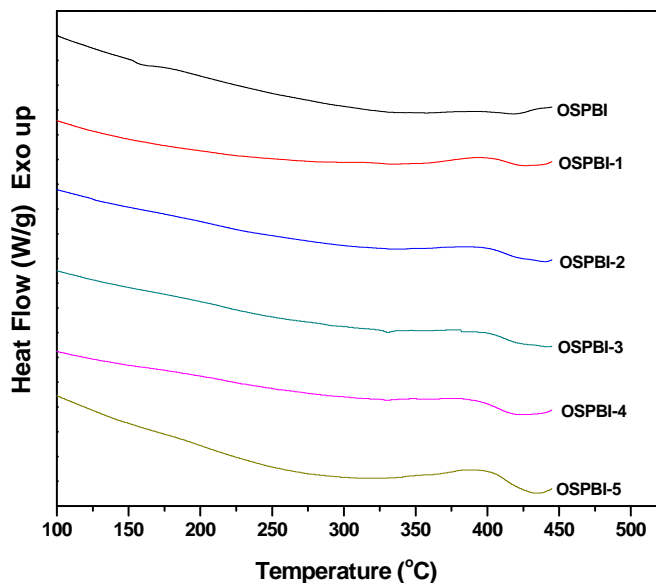


**Figure 4.12** DSC Thermograms of homo polymer and copolymers based on POIA in  $N_2$ , (heating rate  $20\text{ }^\circ\text{C min}^{-1}$ )

In case of polybenzimidazoles synthesized from diacid POIA, (oxadiazole group in side chain) showed high  $T_g$  compared to oxadiazole group in main chain (ODBA-based polymers) (Table 4.6 and Figure 4.12 - 4.13). It is well known that, bulky aromatic group in side chain of a polymer restricts the polymer chain movement and increases  $T_g$ , which explains high  $T_g$  values of PBI containing oxadiazole groups in side chain compared to PBI containing oxadiazole groups in main chain. The homo polymer (OSPBI) has high  $T_g$  413 °C and copolymers based on IPA and PDCA (OSPBI-1 to OSPBI-5, OSPBI-7) also showed high  $T_g$  in the range of 400-414 °C. The examination of  $T_g$  data demonstrates that there is no large variation in  $T_g$  of IPA and PDCA based copolymers. The SA and AA based copolymers (OSPBI-8 and OSPBI-9) showed low  $T_g$  (325 °C and 343 °C) because of aliphatic chain in the polymer backbone. Although, the incorporation of oxadiazole groups in PBI lowers  $T_g$ , these polymers have sufficiently high  $T_g$  for many high temperature applications.

Thus, PBI containing oxadiazole group have low thermal stability and  $T_g$ , compared to pristine PBI, they have sufficiently high thermal stability suitable for many high temperature applications.

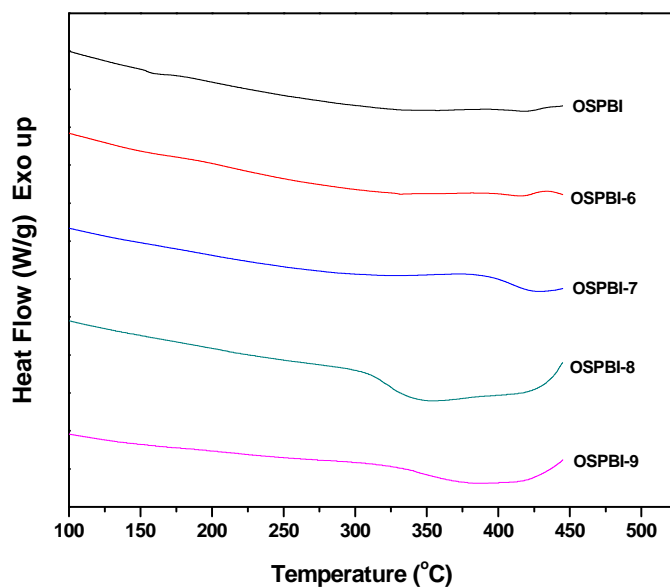


**Figure 4.13** DSC Thermograms of other copolymers based on POIA in  $N_2$ , (heating rate  $20\text{ }^\circ\text{C min}^{-1}$ )

#### 4.3.2.3 Crystallinity

Crystallinity in polymers strongly influences their solubility, thermal and mechanical properties. Highly crystalline polymers have good thermal and mechanical properties but have low solubility. One of the successful methods used to improve their solubility without significantly affecting the thermal and mechanical properties is to incorporate bulky pendant groups into polybenzimidazole backbone. These pendant groups inhibit chain packing and decrease the coplanarity of aromatic rings, thus reducing the inter- and intra-chain interactions to enhance solubility. The wide angle X-ray diffraction studies (WAXS) give information about the inter chain and intra chain packing in polymers, which in turn is an indication of their degree of crystallinity. In the present study the crystallinity of synthesized polybenzimidazoles were evaluated by WAXS measurements.

The WAXS patterns of polybenzimidazoles synthesized from ODBA are shown in Figure 4.14 and 4.15. PBI being amorphous polymer shows a broad peak at 2-theta value of  $24^\circ$  and incorporation of oxadiazole groups shifts this peak to  $26^\circ$ . OMPBIs also do not show sharp peaks, instead a broad peak is observed at  $26^\circ$  indicating amorphous nature of these polymers. However, this peak is relatively sharper compared to PBI,

which indicates close packing in OMPBIs compared to PBI. The sharpness of the peak increases with increasing in oxadiazole content in OMPBIs. Close packing in OMPBIs compared to PBI is observed in d-spacing calculated from WAXS pattern ( $n\lambda=2d \sin\theta$ ). PBI has d-spacing of 3.72, whereas for OMPBIs it varies from 3.43 (for OMPBI) to 3.51 (for OMPBI-7). Generally, polyoxadiazoles shows strong reflection hump indicating a higher packing density<sup>34</sup> which reflects in their poor solvent solubility. In case of OMPBIs, the solvent solubility decreases with increasing in oxadiazole group content, which is consistent with WAXD analysis.

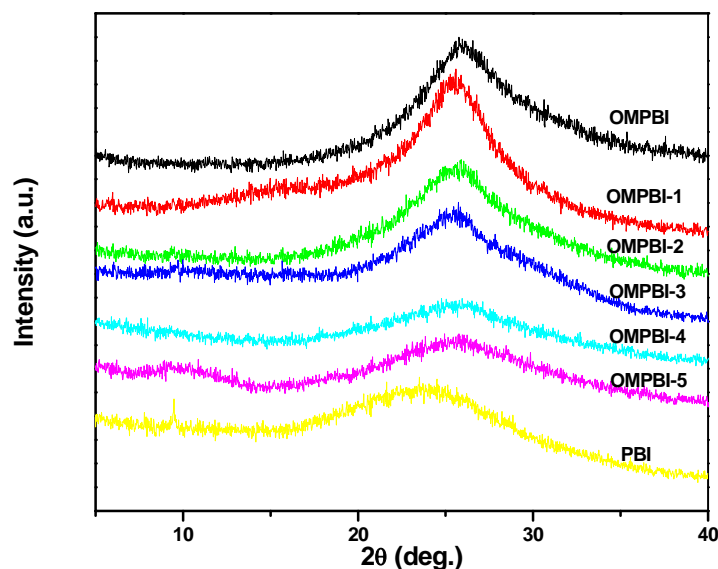


Figure 4.14 WAXS diffractograms of PBIs from ODBA

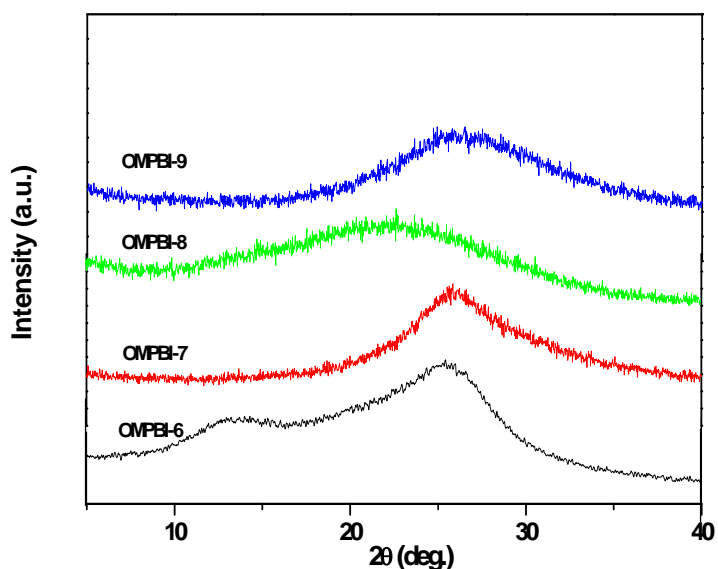
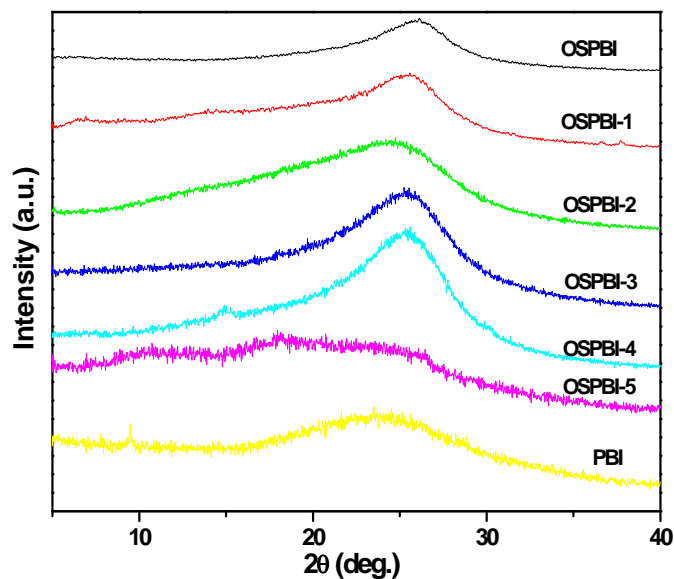
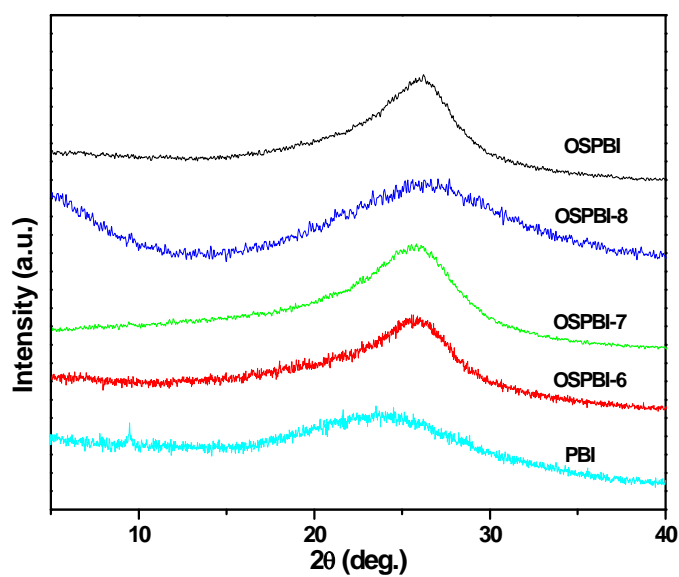


Figure 4.15 WAXS diffractograms of other coPBIs from ODBA





**Figure 4.16** WAXS diffractograms of PBIs from POIA (OSPBI)s



**Figure 4.17** WAXS diffractograms of other coPBIs from POIA (OSPBI)s

The WAXS patterns of polybenzimidazoles synthesized from POIA are shown in Figure 4.16 and 4.17 and are observed to be similar to PBI except that the peaks are slightly sharper. These diffractograms indicate amorphous nature of these polymers.

#### 4.3.2.4 Mechanical properties

In general, mechanical strength of polymer membranes results from attractive forces between polymer molecules, which are dipole–dipole interaction (including hydrogen bonding), induction forces and dispersion or London forces between non-polar molecules. In addition, ionic bonding and ion–dipole interactions also contribute to mechanical strength. For pure PBI membranes, the hydrogen bonding between –N and –NH– groups is the dominant force that determines its mechanical strength. It is known that rigid-rod structured PBIs have very good tensile strength. In the present study, PBI is modified by incorporating oxadiazole group in main and side chain to examine their effect on mechanical properties.

Mechanical properties were evaluated using a tensile tester at room temperature and the polymers display good tensile strength. In case of PBI, synthesized from diacid ODBA, stress vs strain curves are shown in Figure 4.18 and values of tensile strength, modulus, toughness and elongation at break are included the Table 4.7.

**Table 4.7** Mechanical properties ODBA-based PBIs

Polymer Code	Tensile Strength (MPa)	Modulus (MPa)	Toughness (MPa)	Elongation at Break (%)	Water Uptake (wt%)
OMPBI	122	3485	11.09	5.77	17.3
OMPBI-1	73	3299	3.17	2.73	17.5
OMPBI-2	116	2611	35.89	10.39	17.9
OMPBI-3	131	3644	73.16	30.79	18.2
OMPBI-4	80	2383	11.50	12.5	17.3
OMPBI-5	72	2477	24.85	16.24	19.2
OMPBI-6	96	2495	17.35	9.81	17
OMPBI-7	77	3211	6.60	4.9	20
OMPBI-8	70	2872	3.17	3.21	10.8
OMPBI-9	ND	ND	ND	ND	13
PBI	138	3337	4.47	7.1	19

ND: not determined due to brittleness

Homopolymer based on ODBA (OMPBI) has tensile strength of 122 MPa, while, tensile strength of PBI is 138 MPa. The copolymer, OMPBI-1, obtained by the incorporation of 10 mole% IPA into ODBA (90 mole%) and copolymer, OMPBI-5, obtained by the incorporation of 10 mole% ODBA into IPA (90 mole%) have lower values of tensile strength (73 MPa and 72 MPa respectively). This may be due to disruption of regular structure of homopolymers which normally lowers tensile strength. The modulus of homopolymers OMPBI and PBI are 3485 MPa and 3337 MPa

respectively. Whereas modulus of IPA-based copolymers (OMPBI-1 to OMPBI-5) vary in the range of 2377-3644 MPa. The toughness of homopolymers OMPBI and PBI are 11.09 MPa and 4.47 MPa respectively. Highest toughness, modulus and elongation at break of 73.16 Mpa, 3644 Mpa and 30.73% respectively were observed for copolymer OMPBI-3, probably due to regular structure balanced by equimolar (50:50 mole%) monomer ratio in this sample. It also shows high  $T_g$  compared to other copolymers. The lowest tensile strength was observed in case of sample OMPBI-8 may be due to the aliphatic chain in the polymer backbone. Thus, polybenzimidazoles containing oxadiazole groups have sufficiently high tensile properties useful for many applications.

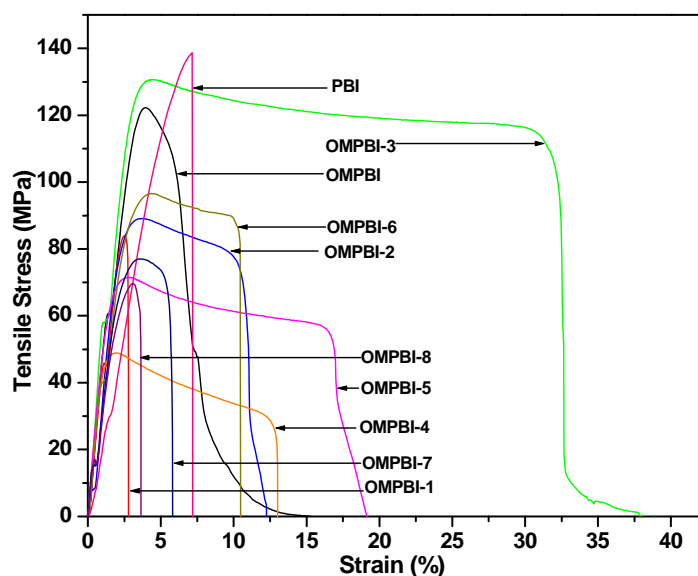


**Figure 4.18** Mechanical properties ODBA-based PBIs

The mechanical properties of POIA-based polymers are shown in the Figure 4.19 and the results are summarised in the Table 4.8. In general, mechanical properties of PBIs are greatly influenced by the molecular weight,<sup>2,35</sup> water uptake<sup>36</sup> and structural modification.<sup>37</sup> In the present study, the incorporation of pendant oxadiazole groups significantly influences the mechanical properties of PBI. The low tensile stress of 34.6 MPa of homopolymer, (OSPBI), compared to 138 MPa of PBI or 122 MPa of OMPBI, indicates that incorporated bulky side groups disrupt rigid regular structure of PBI lowering tensile strength. As the percentage of benzimidazole group increases in the copolymers (OSPBI-1 to OSPBI-5), the tensile strength and modulus increases respectively may be due to increase in the molecular weight and rigidity of polymers. Although, the molecular weight of OSPBI-3 is less than OSPBI-4, tensile strength

(70.75 MPa) and modulus (3151 MPa) are higher than OSPBI-4 (tensile strength 60.47 MPa and modulus 2199 MPa).

**Table 4.8** Mechanical properties POIA-based PBIs

Polymer Code	Tensile Strength (MPa)	Modulus (MPa)	Toughness (MPa)	Elongation to Break (%)	Water uptake (wt%)
OSPBI	34.6	1400	1.03	3.2	16
OSPBI-1	50.33	1386	1.29	1.5	16.5
OSPBI-2	50.72	2787	0.49	1.0	17.2
OSPBI-3	70.75	3151	2.47	6.4	17.7
OSPBI-4	60.47	2199	5.30	5.2	18.8
OSPBI-5	80.39	2633	4.82	9.0	18
OSPBI-6	59.87	2879	4.64	5.22	17.3
OSPBI-7	52.57	1679	3.03	5.73	21
OSPBI-8	ND	ND	ND	ND	13.3
OSPBI-9	ND	ND	ND	ND	14
PBI	138	3337	4.47	7.1	19

ND: not determined due to brittleness

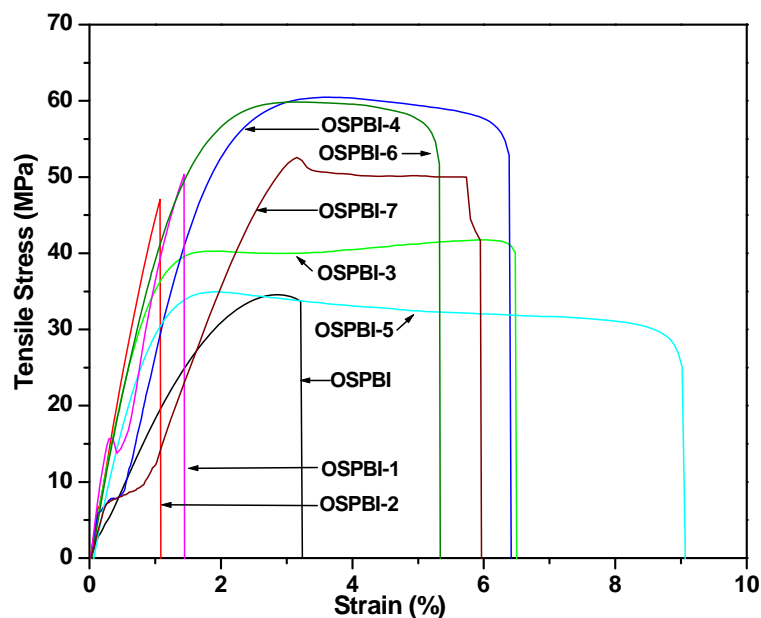


**Figure 4.19** Mechanical properties POIA-based PBIs

The high tensile property of OSPBI-3 is attributed to the regular arrangement of the molecules due to equal mole ratios (50:50) of two monomers. The same phenomenon was observed in the case of ODBA-based polymers (OMPBI-3 and OMPBI-4). The copolymers OSPBI-3 and OSPBI-6 are synthesized from the 50 mole% POIA and 50 mole% of IPA or TPA respectively. OSPBI-3 shows higher tensile strength and modulus

than OSPBI-6 (tensile strength 59.87 MPa and modulus 28.79 MPa). The over all values of tensile strength, modulus, toughness and elongation at break are in the range of 34-80 MPa, 1400-3150 MPa, 0.4-5.3 Mpa and 1.0-9% respectively. The specimen samples of OSPBI-8 and OSPBI-9 copolymers are cracked during measurements indicative of brittle nature.

#### 4.3.2.5 Water uptake

Water plays a very important role in methanol permeability, proton conductivity and mechanical properties of membranes. Absorption of 10% water was led to decrease in 25-30% tensile strength of PBI.<sup>36</sup> PBI is hydrophilic in nature and capable of absorbing 15-19 wt% water from moist atmosphere. The water uptake properties of PBI are due to the intermolecular hydrogen bonding between water and N and N-H groups.<sup>38</sup> The results on water uptake studies of PBI and polybenzimidazoles synthesized from ODBA and POIA films are shown in Table 4.7 and 4.8 respectively. The water uptake capacity of PBI is 19 wt%, which is in good agreement with reported values in the literature.<sup>39</sup> Incorporation of oxadiazole groups in PBI lowers the water uptake properties of the polymers significantly, probably, due to low percentage of benzimidazole (N-H) groups in polymer chain. As a result oxadiazole group containing polymers are less hygroscopic<sup>40</sup> compared to PBI. Homo polymer OMPBI takes 17.3 wt % water, whereas water uptake of other copolymers synthesized, is between 10.8 to 20 wt % (Table 4.7), the highest water uptake being that of PDCA based copolymer.

Similarly, polybenzimidazoles synthesized from POIA (Table 4.8) also exhibited low water uptake values from 14- 21 wt%. However, it is observed that water uptake of PDCA-based copolymers was higher. High water uptake is probably due to the extra nitrogen atom in the polymer backbone. It is also notable that copolymers based on SA and AA revealed low water uptake due to the hydrophobic aliphatic groups in the polymers.

#### 4.3.2.6 Oxidative stability

PBI membranes are known to undergo oxidative degradation by the  $\cdot\text{OH}$  or  $\cdot\text{OOH}$  radicals formed by the decomposition of hydrogen peroxide formed at cathode during the fuel cell operation, which reduces the life of membranes. The membrane stability of the polymers was studied by soaking the film in Fenton's reagent as described in the experimental part.

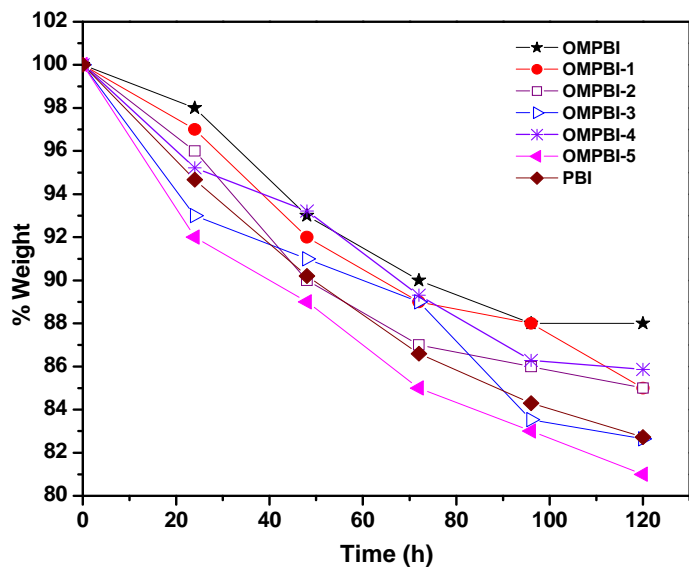


**Figure 4.20** Oxidative stability of PBI and coPBI of IPA containing oxadiazole groups in main chain.

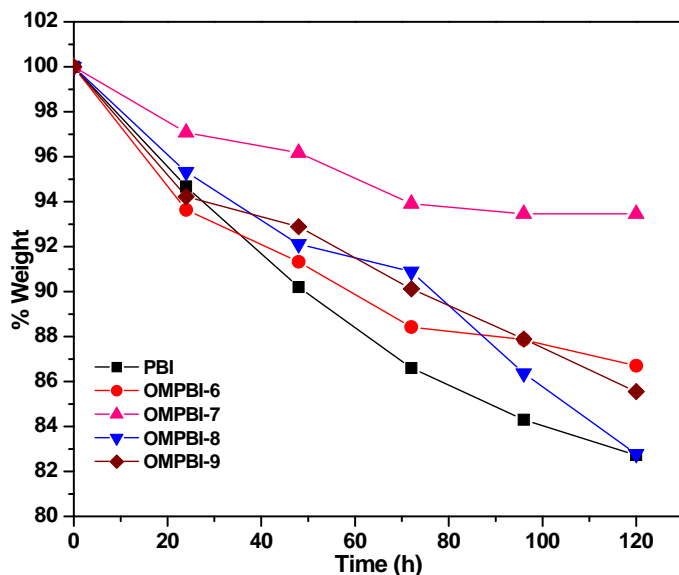


**Figure 4.21** Oxidative stability of PBI and coPBI of other diacids containing oxadiazole groups in main chain.

The OMPBI and OSPBI membranes showed a weight loss of 12 wt% (Figure 4.20) and 10 wt% (Figure 4.22) respectively after 120 h compared to a weight loss of 17 wt% observed for PBI membrane indicating oxadiazole groups enhance oxidative stability of PBI. It is believed that oxadiazole has stable oxidative property because of the nitrogen atoms located on the heterocyclic ring resulting in a stable N-C bond.<sup>19</sup> The oxidative stability of ODBA based copolymers varies from 9-16 wt% except for SA and AA based copolymers (Figure 4.21). SA and AA based copolymers showed lower

oxidative stability with weight loss in the range of 15-18 wt%, due to low molecular weight and aliphatic chains.

Polybenzimidazole synthesized from POIA, OSPBI (homo polymer) showed lower oxidative stability (10 wt% loss) than OSPBI-1 (8 wt% loss) may be due to low molecular weight. Other copolymers showed oxidative stability with weight loss in the range of 9-16 wt% (Figure 4.23). Similar trend of membrane degradation was observed in both the series of OMPBI and OSPBI polymers.

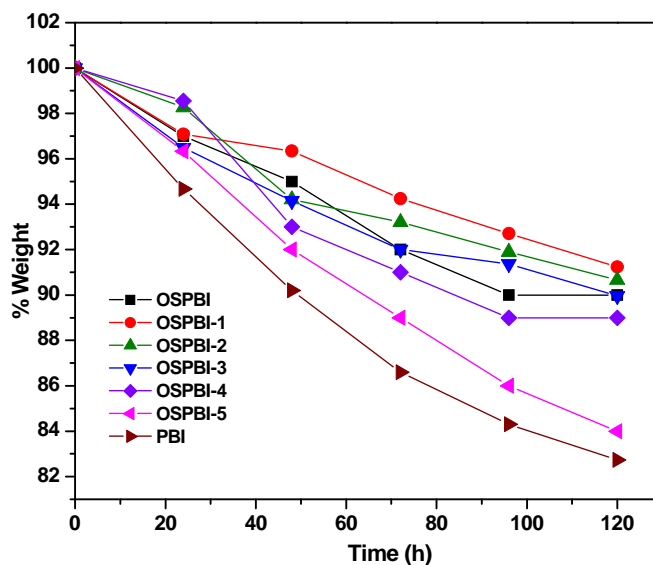


**Figure 4.22** Oxidative stability of PBI and coPBI of IPA containing oxadiazole groups in side chain

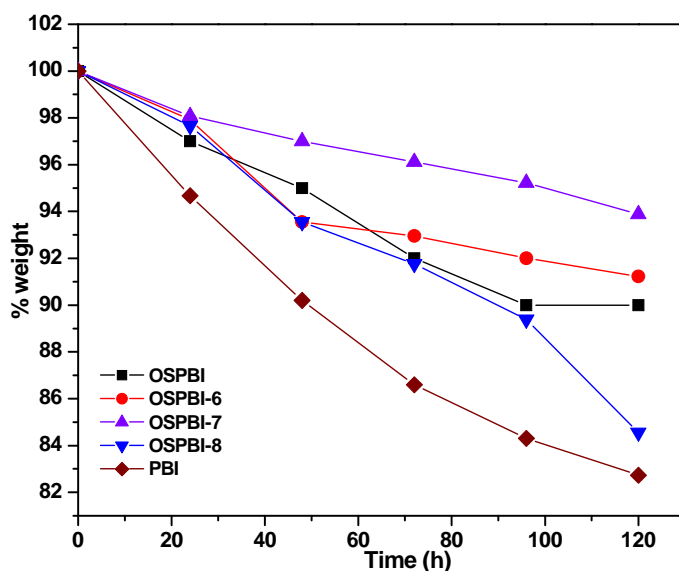


**Figure 4.23** Oxidative stability of PBI and coPBI of other diacids containing oxadiazole groups in side chain

#### 4.3.2.7 Phosphoric acid doping study

PBI membrane as polymer electrolyte for fuel cell is generally doped with phosphoric acid for better performance. The doping level at particular temperature depends on the duration of doping and concentration of phosphoric acid. A desired doping level can be achieved by controlling these two parameters. Hence a detailed study on doping level as a function of duration of doping and concentration of phosphoric acid assumes importance.<sup>39</sup> The acid uptake capacity of homo polymer and copolymer membranes was evaluated by doping in various molar concentrations of  $H_3PO_4$  solutions for 24 h at room temperature as described in experimental part. The doping level is defined in terms of the weight percent of acid per gram of the polymers. The membranes of OMPBI, OMPBI-1, OMPBI-2 and OMPBI-3, OMPBI-7 to OMPBI-9 doped with 85% (~14.0 mole)  $H_3PO_4$  for 24 h at room temperature, found to soften and spread in Petri dish during drying at 100 °C due to dissolution in phosphoric acid present in membrane matrix at elevated temperature. Hence, for these polymers doping study was limited up to 12 molar concentration of phosphoric acid. However, some of the samples OMPBI-7, OMPBI-8 and OMPBI-9 dissolved in 12M phosphoric acid also and hence these polymers were doped in 10 M  $H_3PO_4$  (Figure 4.25).

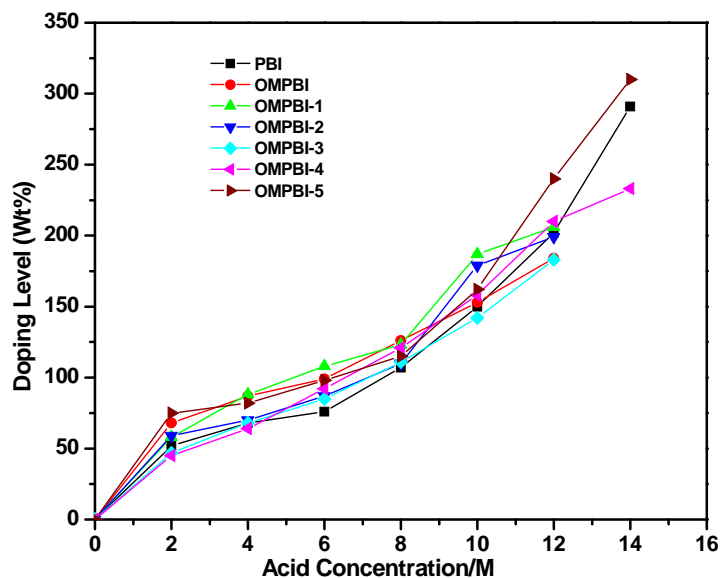


**Figure 4.24** Doping level of phosphoric acid (wt%) in ODBA based polymers as a function of the concentration of  $H_3PO_4$

As expected, the doping level of polymers increases with increasing concentration of phosphoric acid (Figure 4.24 and 4.25). Acid uptake behaviour of homo and co-polymer of ODBA is similar to that of PBI, the acid uptake being slightly higher



for PBI. The equilibrium acid uptake values of OMPBI, OMPBI-1, OMPBI-2 and OMPBI-3 doped in 12M  $H_3PO_4$  are in the range of 190-220 wt%, while acid uptake of other copolymers, OMPBI-4, OMPBI-5, OMPBI-6 and PBI doped in 14M  $H_3PO_4$  is 240, 292, 320 and 297 wt% respectively and OMPBI-7, OMPBI-8 and OMPBI-9 doped in the 10M  $H_3PO_4$  is in the range of 190-205 wt%. Thus, incorporation of oxadiazole groups in polybenzimidazole does not significantly alter acid uptake properties of PBI.

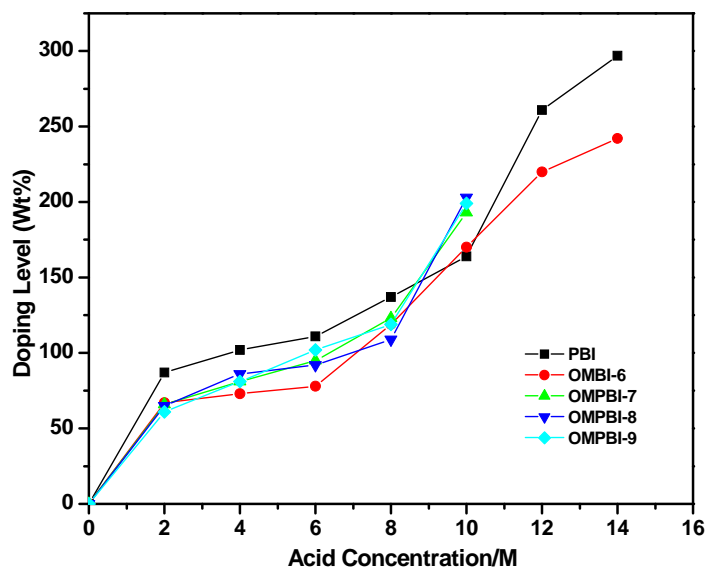


**Figure 4.25** Doping level of phosphoric acid (wt%) in ODPA based polymers as a function of the concentration of  $H_3PO_4$

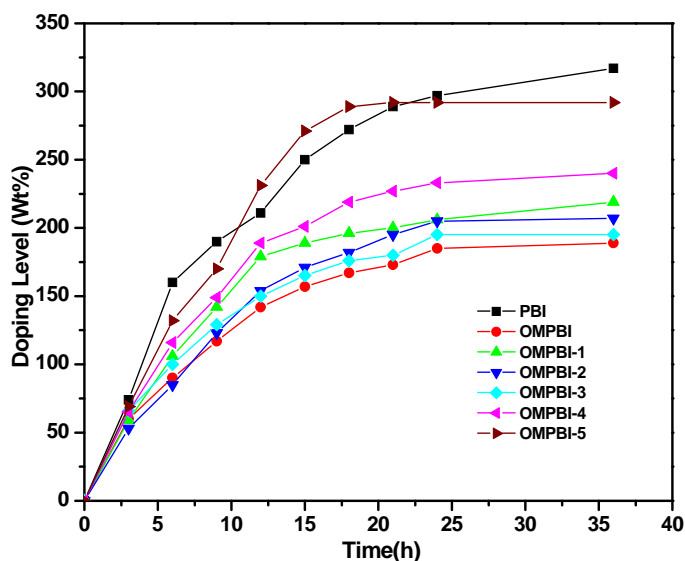


**Figure 4.26** Acid doping levels of ODPA based polymers at different time intervals. Concentration of  $H_3PO_4$  for OMPBI, OMPBI-1, OMPBI-2, OMPBI-3 (12 M), for OMPBI-4 and OMPBI-5 and PBI (14M)

The doping levels as a function of time for a period of 36 h at room temperature for samples PBI, OMPBI-4, OMPBI-5 and OMPBI-6 were determined in 14M  $H_3PO_4$ , and OMPBI, OMPBI-1, OMPBI-2 and OMPBI-3 in 12M  $H_3PO_4$ , (Figure 4.26) and the rest of the copolymers, OMPBI-7, OMPBI-8 and OMPBI-9 in 10M  $H_3PO_4$  (Figure 4.27). The doping behaviour of PBI containing oxadiazole groups (OMPBI) is observed to be similar to that of PBI. The acid uptake increases with time gradually and all samples reach a saturation point in  $\sim 24$  h. Phosphoric acid uptake of OMPBI is 190 wt % compared to 297% for PBI. The acid uptake of other copolymers is in the range between 190-300 wt%.

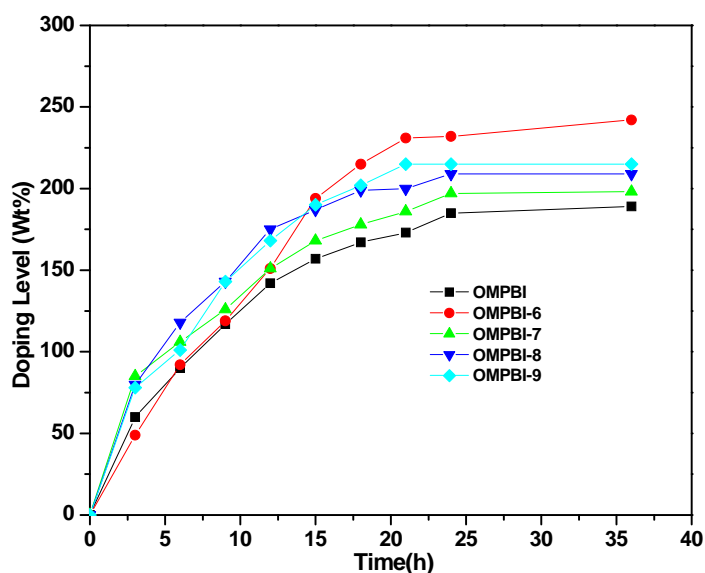


**Figure 4.27** Acid doping levels of ODBA based polymers at different time intervals. Concentration of  $H_3PO_4$  for OMPBI-6(14M) and for OMPBI-7, OMPBI-8 and OMPBI-9 (10M)

Polymers based on POIA, which contain oxadiazole groups in side chain, displayed similar phosphoric acid uptake behaviour as that of ODBA-based polymers. The effect of phosphoric acid concentration on doping level was studied by determining acid uptake after immersing membranes in varying concentration of  $H_3PO_4$  acid solution (2-14 M) for 24 h at room temperature. As anticipated, the doping level of polymers increases with increasing concentration of phosphoric acid. (Figure 4.28 and 4.29) The membranes of OSPBI, OSPBI-1, OSPBI-2, OSPBI-3, OSPBI-4, OSPBI-7 and OSPBI-8 doped with 85% ( $\sim 14.0$  mole)  $H_3PO_4$  for 24 h at room temperature, found to soften and spread in the petri dish during drying at  $100^\circ C$  due to dissolution in phosphoric acid present in membrane matrix. Hence, doping study was restricted up to 12 molar concentration of phosphoric acid for these polymers. However, the samples OSPBI-7 and

OSPBI-8 were found to dissolve even in 12M phosphoric acid and hence these polymers were doped in 10 M H<sub>3</sub>PO<sub>4</sub>.

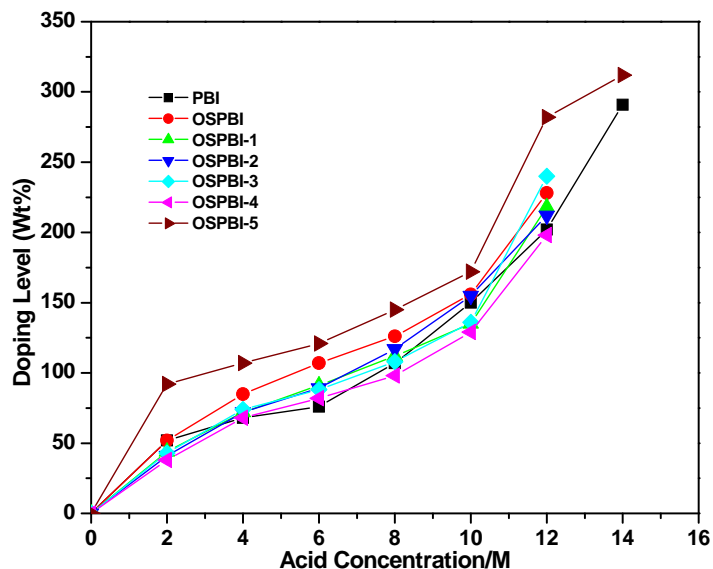


**Figure 4.28** Doping level of phosphoric acid (wt%) in polymers as a function of the concentration of POIA based polymers and PBI

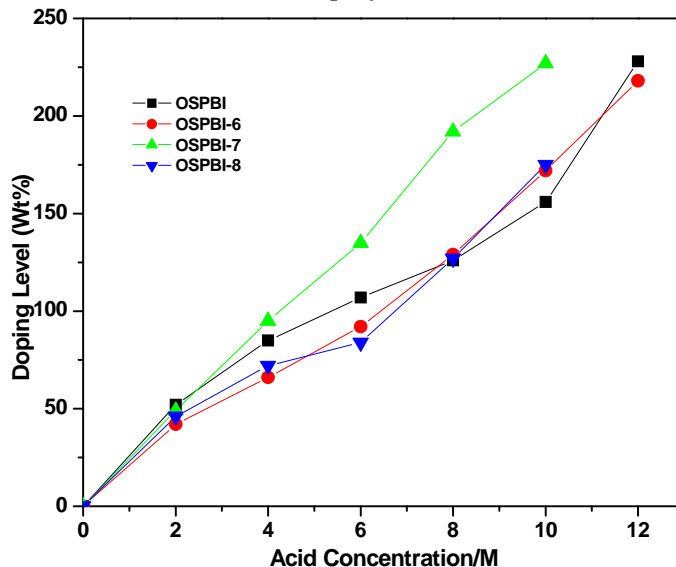


**Figure 4.29** Doping level of phosphoric acid (wt%) in of POIA based other polymers as a function of the acid concentration

The effect of time on doping level of POIA based polybenzimidazoles was studied in different concentration of H<sub>3</sub>PO<sub>4</sub> depending upon the solubility of these polymers (Figure 4.30 and 4.31). Doping level of PBI and OSPBI-5 was determined in 14 M H<sub>3</sub>PO<sub>4</sub>, while OSPBI and OSPBI-1, OSPBI-2, OSPBI-3, OSPBI-4 and OSPBI-6 in 12 M and OSPBI-7 and OSPBI-8 in 10 M H<sub>3</sub>PO<sub>4</sub>. Saturation point (between 12-21 h) for polymers OSPBI and OSPBI-2, OSPBI-7 was in the range of 200-300 wt%, while

for OSPBI-8 it was from 190-200 wt%. The high acid uptake of OSPBI-5 and PBI of was ~300 wt% in 24 h is mainly due to higher concentration of phosphoric acid used. From the data, it appears that the acid uptake increases with time and time dependant acid uptake is controlled by the concentration of dopant.

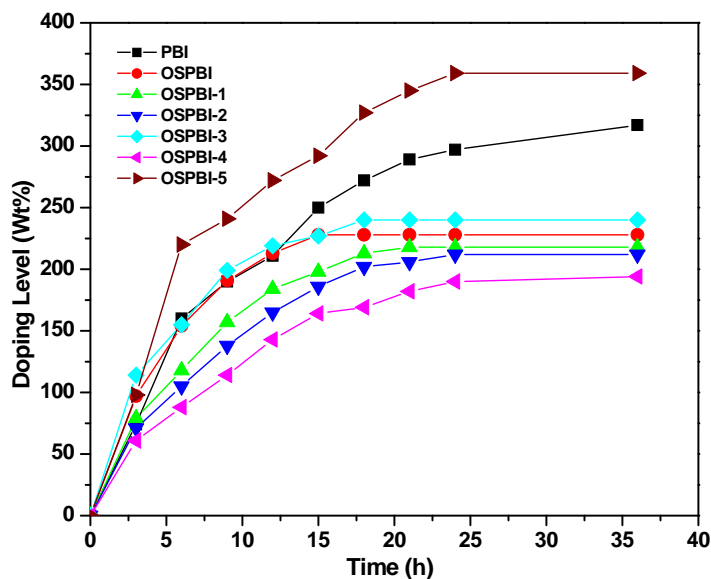


**Figure 4.30** Acid doping levels POIA based polymers and PBI at different time intervals. Concentration of  $H_3PO_4$  for OSPBI, OSPBI-1, OSPBI-2, OSPBI-3 and OSPBI-4 (12 M), for OSPBI-5 and PBI (14M)

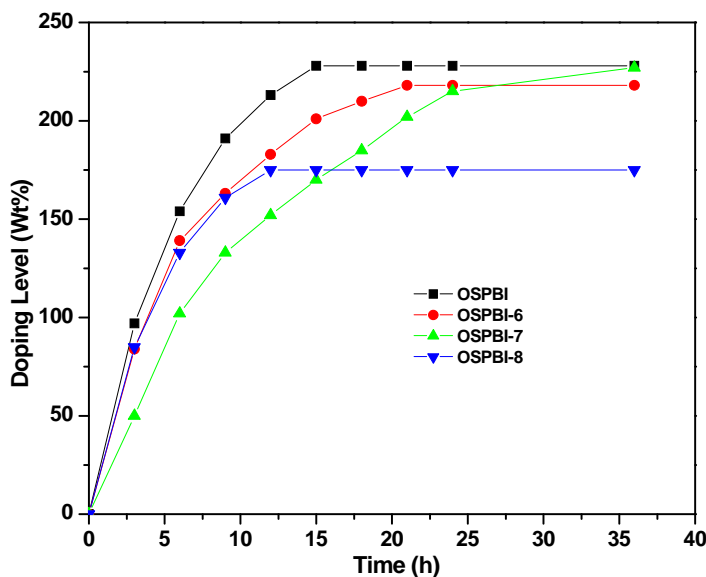


**Figure 4.31** Acid doping levels POIA based polymers and PBI at different time intervals. Concentration of  $H_3PO_4$  for OSPBI-6(12M) and for OSPBI-7, and OSPBI-8 (10M)

### 4.3.2.8 Proton conductivity measurements

The proton conductivity of oxadiazole group containing polybenzimidazoles was measured by AC impedance spectroscopy using a standard two-electrode measurement set up at various temperatures (25 - 175 °C). The proton conductivity of phosphoric acid doped polybenzimidazole membranes depends on phosphoric acid uptake, temperature and relative humidity<sup>41</sup> and normally, increases with increasing acid uptake, temperature and relative humidity. The membrane samples of OMPBI, OMPBI-1, OMPBI-2, and OMPBI-3 doped in 12 M phosphoric acid, OMPBI-4, OMPBI-5 OMPBI-6 and PBI, doped in 14 M phosphoric acid and samples of OMPBI-7, OMPBI-8 and OMPBI-9 in 10 M phosphoric acid for 24 h were used for determining proton conductivity. The temperature dependence of proton conductivity of these polymers is shown in Table 4.9. As anticipated, the proton conductivity increases with increasing temperature.

**Table 4.9** Proton conductivity of ODBA based polymers

Polymer code	Proton conductivity (S/cm) at temperature (°C)						
	25 °C	50 °C	75 °C	100 °C	125 °C	150 °C	175 °C
OMPBI (190)*	$2.89 \times 10^{-4}$	$4.4 \times 10^{-4}$	$9.6 \times 10^{-4}$	$1.75 \times 10^{-3}$	$2.67 \times 10^{-3}$	$4.17 \times 10^{-3}$	$7.95 \times 10^{-3}$
OMPBI-1 (219)*	$1.0 \times 10^{-2}$	$1.31 \times 10^{-2}$	$1.73 \times 10^{-2}$	$2.42 \times 10^{-2}$	$3.17 \times 10^{-2}$	$3.54 \times 10^{-2}$	$3.64 \times 10^{-2}$
OMPBI-2 (207)*	$4.95 \times 10^{-4}$	$1.45 \times 10^{-3}$	$2.67 \times 10^{-3}$	$4.6 \times 10^{-3}$	$5.17 \times 10^{-3}$	$5.73 \times 10^{-3}$	$6.82 \times 10^{-3}$
OMPBI-3 (195)*	$3.61 \times 10^{-3}$	$4.96 \times 10^{-3}$	$8.89 \times 10^{-3}$	$1.19 \times 10^{-2}$	$1.4 \times 10^{-2}$	$1.5 \times 10^{-2}$	$1.52 \times 10^{-2}$
OMPBI-4 (240)*	$4.57 \times 10^{-3}$	$7.96 \times 10^{-3}$	$1.24 \times 10^{-3}$	$1.87 \times 10^{-2}$	$2.3 \times 10^{-2}$	$2.53 \times 10^{-2}$	$2.85 \times 10^{-2}$
OMPBI-5 (292)*	$7.45 \times 10^{-3}$	$9.48 \times 10^{-3}$	$1.46 \times 10^{-2}$	$2.15 \times 10^{-2}$	$2.94 \times 10^{-2}$	$3.38 \times 10^{-2}$	$3.48 \times 10^{-2}$
OMPBI-6 (242)*	$1.01 \times 10^{-2}$	$1.59 \times 10^{-2}$	$2.77 \times 10^{-2}$	$3.03 \times 10^{-2}$	$3.67 \times 10^{-2}$	$4.15 \times 10^{-2}$	$4.50 \times 10^{-2}$
OMPBI-7 (198)*	$1.01 \times 10^{-2}$	$1.26 \times 10^{-2}$	$1.62 \times 10^{-2}$	$1.78 \times 10^{-2}$	$1.91 \times 10^{-2}$	$1.98 \times 10^{-2}$	$2.03 \times 10^{-2}$
OMPBI-8 (209)*	$2.64 \times 10^{-3}$	$3.54 \times 10^{-3}$	$6.35 \times 10^{-3}$	$8.83 \times 10^{-3}$	$1.27 \times 10^{-2}$	$1.37 \times 10^{-2}$	$1.38 \times 10^{-2}$
OMPBI-9 (215)*	$3.79 \times 10^{-3}$	$4.71 \times 10^{-3}$	$6.28 \times 10^{-3}$	$7.75 \times 10^{-3}$	$9.11 \times 10^{-3}$	$1.01 \times 10^{-2}$	$1.16 \times 10^{-2}$
PBI (297)*	$7.42 \times 10^{-3}$	$9.6 \times 10^{-3}$	$1.4 \times 10^{-2}$	$2.05 \times 10^{-2}$	$2.69 \times 10^{-2}$	$3.00 \times 10^{-2}$	$3.17 \times 10^{-2}$

\*Phosphoric acid doping level in weight % of the polymers.

The proton conductivity of homo polymer (OMPBI) with doping level of 190 wt% ranges from  $2.89 \times 10^{-4}$  to  $7.95 \times 10^{-3}$  S/cm in the temperature range of 25 to 175 °C as compared to that of PBI (with 297wt% doping level)  $7.42 \times 10^{-3}$  to  $3.17 \times 10^{-2}$  S/cm. The low value compared to PBI is probably due to low doping level. Copolymers OMPBI-1 (ODBA 90 mol% and IPA 10 mol%) with doping level 219wt% and OMPBI-5 (ODBA 10 mol% and IPA 90 mol%) with doping level 292 wt% exhibited high proton

conductivity in the range of  $1.0 \times 10^{-2}$  to  $3.64 \times 10^{-2}$  S/cm and  $7.45 \times 10^{-3}$  to  $3.48 \times 10^{-2}$  S/cm, respectively in the temperature range of 25 to 175 °C, compared to PBI. It may be noted that proton conductivity of these polymers is higher than that of PBI; even though doping level is lower than PBI. It is known that the regular rigid structure of a polymer is disturbed by the addition of small quantity of another monomer. The addition of 10 mol% of IPA in ODBA (OMPBI-1) and 10 mol% of ODBA in IPA (OMPBI-5) disturb the rigid structure of these polymers which facilitates easy movement of the protons in the matrix due to flexibility of polymer chain enhancing the proton conductivity. The data reveals that polybenzimidazole containing oxadiazole groups, doped with phosphoric acid, exhibit high proton conductivity at high temperature compared to PBI and these polymers have potential for application as polymer electrolyte for fuel cell at high temperature.

The proton conductivity of POIA based polymers is shown in Table 4.10. Due to solubility limitations of some of these polymers in high concentrations of phosphoric acid, the polymer membranes doped in lower concentration of phosphoric acid had to be used for determining proton conductivity. Thus, the membrane samples of OSPBI, OSPBI-1, OSPBI-2, OSPBI-3, OSPBI-4 and OSPBI-6 (doped in 12 M phosphoric acid), OSPBI-7 and OSPBI-8 (doped in 10 M phosphoric acid), OSPBI-5 and PBI (doped in 14 molar phosphoric acid for 24 h) were used for determining proton conductivity. The temperature dependence of proton conductivity of these polymers is shown in Table 4.10.

The doping level of POIA based polymers is higher compared to ODBA based polymers. The high phosphoric acid uptake of these polymers is, probably, due to high free volume generated by bulky side groups. Due to different doping levels of OMPBI's and OSPBI's, having similar mole ratio of these acids and IPA, the comparison of proton conductivity of polymers containing oxadiazole groups in main and those containing oxadiazole groups in side chain is difficult. It appears that, inspite of high acid uptake of OSPBI's compared to OMPBI's, the overall proton conductivity of OSPBI's is lower than that of OMPBI's. This is probably, due to less segmental movement of polymer chain due to bulky side groups.

**Table 4.10** Proton conductivity of POIA based polymers

Polymer code	Proton conductivity (S/cm) at temperature						
	25 °C	50 °C	75 °C	100 °C	125 °C	150 °C	175 °C
OSPBI (228)*	$7.82 \times 10^{-4}$	$9.5 \times 10^{-4}$	$3.58 \times 10^{-3}$	$7.91 \times 10^{-3}$	$8.99 \times 10^{-3}$	$9.83 \times 10^{-3}$	$1.1 \times 10^{-2}$
OSPBI-1 (220)*	$8.1 \times 10^{-4}$	$1.79 \times 10^{-3}$	$4.37 \times 10^{-3}$	$6.9 \times 10^{-3}$	$9.4 \times 10^{-3}$	$1.41 \times 10^{-2}$	$1.4 \times 10^{-2}$
OSPBI-2 (209)*	$3.02 \times 10^{-3}$	$4.13 \times 10^{-3}$	$6.59 \times 10^{-3}$	$1.37 \times 10^{-2}$	$1.90 \times 10^{-2}$	$2.22 \times 10^{-2}$	$2.20 \times 10^{-2}$
OSPBI-3 (240)*	$7.23 \times 10^{-3}$	$8.48 \times 10^{-3}$	$1.12 \times 10^{-2}$	$1.73 \times 10^{-2}$	$2.32 \times 10^{-2}$	$2.67 \times 10^{-2}$	$2.71 \times 10^{-2}$
OSPBI-4 (194)*	$8.13 \times 10^{-4}$	$1.15 \times 10^{-3}$	$3.79 \times 10^{-3}$	$7.72 \times 10^{-3}$	$9.62 \times 10^{-3}$	$1.21 \times 10^{-2}$	$1.42 \times 10^{-2}$
OSPBI-5 (321)*	$7.79 \times 10^{-3}$	$1.0 \times 10^{-2}$	$1.54 \times 10^{-2}$	$2.08 \times 10^{-2}$	$2.66 \times 10^{-2}$	$3.16 \times 10^{-2}$	$3.33 \times 10^{-2}$
OSPBI-6 (222)*	$4.41 \times 10^{-3}$	$5.47 \times 10^{-3}$	$7.68 \times 10^{-3}$	$1.21 \times 10^{-2}$	$1.71 \times 10^{-2}$	$1.92 \times 10^{-2}$	$1.90 \times 10^{-2}$
OSPBI-7 (235)*	$3.95 \times 10^{-3}$	$7.49 \times 10^{-3}$	$1.13 \times 10^{-2}$	$1.66 \times 10^{-2}$	$2.28 \times 10^{-2}$	$2.54 \times 10^{-2}$	$2.50 \times 10^{-2}$
OSPBI-8 (183)*	$9.60 \times 10^{-3}$	$1.10 \times 10^{-2}$	$1.49 \times 10^{-2}$	$1.88 \times 10^{-2}$	$2.11 \times 10^{-2}$	$2.33 \times 10^{-2}$	NM
PBI (297)*	$7.42 \times 10^{-3}$	$9.6 \times 10^{-3}$	$1.4 \times 10^{-2}$	$2.05 \times 10^{-2}$	$2.69 \times 10^{-2}$	$3.00 \times 10^{-2}$	$3.17 \times 10^{-2}$

\* Phosphoric acid doping level in weight % of the polymers.

NM-not measured

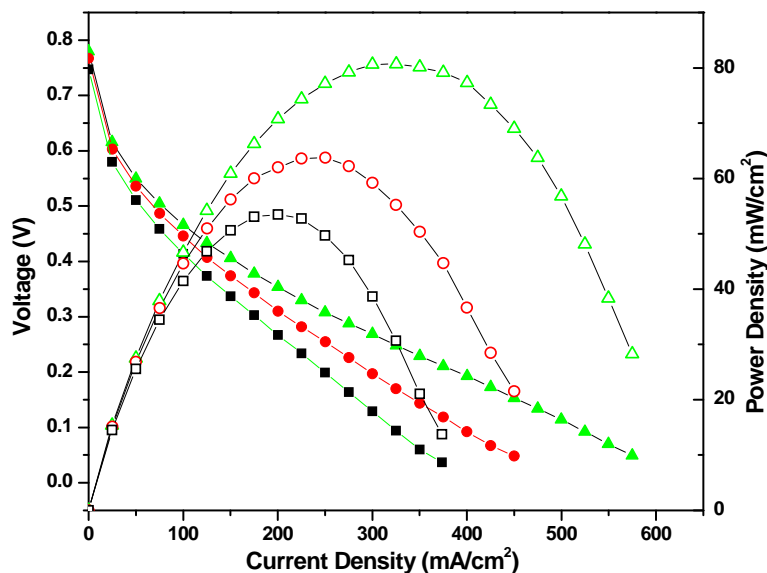
#### 4.3.2.9 Membrane electrode assembly fabrication

The electrodes with a gas diffusion layer (GDL) and a catalyst layer were fabricated by following the same procedure as mentioned in section 3.3.2.9. Membrane samples OMPBI (90  $\mu\text{m}$ ) and OSPBI (75  $\mu\text{m}$ ) were doped in 12M phosphoric acid, where as PBI membrane (90  $\mu\text{m}$ ) was doped in 14 molar phosphoric acid for 24 h. The membranes were wiped out by tissue paper and dried at 100 °C in vacuum oven. The membrane electrode assemblies were made by hot-pressing the pre-treated electrode (5  $\text{cm}^2$ ) membrane under the conditions of 100 °C, 130 atm for 3 min.

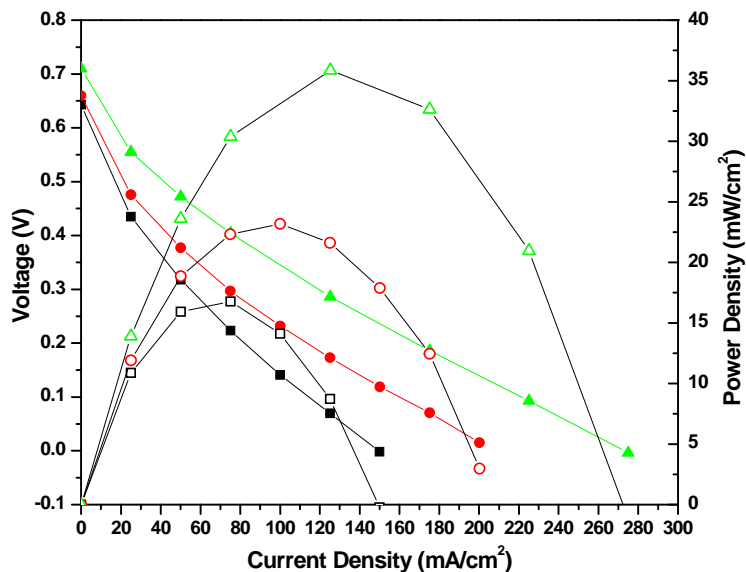
#### 4.3.2.10 Polarization study

Figure 4.32 and 4.33 show the fuel cell performance of OMPBI and OSPBI membranes in terms of polarization plots of MEAs fabricated using 20% Pt/C for both anode and cathode in a single cell experiment, at 100, 125 and 150 °C with a dry  $\text{H}_2/\text{O}_2$  gas flow rate of 0.2 slpm. OMPBI and OSPBI membranes show lower performance than that of the PBI membrane. The OCV obtained with the OMPBI and OSPBI membranes is 0.75 and 0.71V, respectively at 150 °C, whereas for PBI it is 0.92 V. The OMPBI and OSPBI membrane gives a maximum power density 77 and 36  $\text{mW}/\text{cm}^2$ , respectively at 0.3 V, whereas the PBI membrane gives 210  $\text{mW}/\text{cm}^2$  at 0.3 V. The lower fuel cell

performance of OMPBI and OSPBI membrane can be attributed to low  $\text{H}_3\text{PO}_4$  acid content and low proton conductivity of OMPBI and OSPBI membranes.



**Figure 4.32** Polarization curves obtained with OMPBI membrane fuel cell at different temperatures with dry  $\text{H}_2$  and  $\text{O}_2$  (flow rate 0.2 slpm). The cell was conditioned for 30 min at open-circuit potential and at 0.2 V for 15 min before measurements. Key: (■□) 100, (●○) 125 and (▲Δ) 150 °C



**Figure 4.33** Polarization curves obtained with TSPBI membrane fuel cell at different temperatures with dry  $\text{H}_2$  and  $\text{O}_2$  (flow rate 0.2 slpm). The cell was conditioned for 30 min at open-circuit potential and at 0.2 V for 15 min before measurements. Key: (■□) 100, (●○) 125 and (▲Δ) 150 °C



## 4.4 One-pot synthesis of poly (benzimidazole-oxadiazole) copolymers and their use as proton conducting membranes

### 4.4.1 Introduction

The results of comparative study of polybenzimidazoles containing oxadiazole groups in main chain (OMPBI polymers) and oxadiazole groups in side chain (OSPBI polymers) indicate that OMPBI polymers have higher proton conductivity values compared to OSPBI polymers. Synthetic route selected for the preparation of OMPBI polymers was condensation of 3,3',4,4'-tetra-amino biphenyl (TAB) with diacid 3,3'-(1,3,4-oxadiazole-2,5-diyl)dibenzoic acid (ODBA) in polyphosphoric acid (PPA). Synthesis of ODBA consists of three steps, which is described in Chapter-2. Polybenzimidazoles containing oxadiazole groups in main chain can also be synthesized by one-pot synthesis by the condensation of TAB and isophthalic acid dihydrazide with isophthalic acid, thus circumventing the synthesis of diacid ODBA. The polymers obtained by this route are likely to have some uncyclized hydrazide groups.<sup>42</sup> However, this route has some advantages e.g. it eliminates the synthesis of ODBA in the first place and secondly, a part of expensive TAB is replaced by isophthalic acid dihydrazide (IPH). Considering these points, in the present work, polybenzimidazoles containing varying contents of oxadiazole groups were synthesized by condensing a mixture of IPH and TAB in varying ratio, with IPA in PPA at high temperature, with an objective to compare electrochemical and other properties of these polymers with OMPBI polymers, synthesized from a diacid containing preformed oxadiazole groups.

Thus, this work describes synthesis and characterization of polybenzimidazoles containing oxadiazole groups in main chain and examines the potential application as polymer electrolyte for fuel cells.

### 4.4.2 Experimental

#### 4.4.2.1 Reagents and solvents

Isophthalic acid (IPA), 3,3',4,4'-tetra-amino biphenyl (TAB), hydrazine sulphate polyphosphoric acid (115%) (PPA) and trifluoro acetic acid (TFA) were purchased from Aldrich chemicals. Hydrazine hydrate(99%), N-methyl-2-pyrrolidinone (NMP), N, N-dimethylacetamide (DMAc) and N, N-dimethylformamide (DMF) were distilled over CaH<sub>2</sub>. Methanol, ortho phosphoric acid (85%), mohr's salt [(NH<sub>4</sub>)<sub>2</sub>Fe(SO<sub>4</sub>)<sub>2</sub>·6H<sub>2</sub>O], sulfuric acid (96%), methane sulfonic acid (MSA), formic acid (FA), dimethyl sulfoxide

(DMSO) and hydrogen peroxide (30%, w/v) were purchased from S.D. fine-Chem. India Ltd. and used without further purification. Isophthaloyl dimethyl ester and isophthalohydrazide were prepared according the reported procedure.<sup>43</sup>

#### 4.4.2.2 Measurements

Inherent viscosity (IV) measurements of all polymers were carried out in conc. H<sub>2</sub>SO<sub>4</sub> (0.2 g/dL) at 30 °C using a Ubbelohde viscometer (model F725).

##### ➤ Membrane preparation

Membranes were prepared by solution casting method. Fine powder of polymer (3 g) was dissolved in formic acid (100 mL) and the solution was filtered. The membranes were cast in a Petri dish, solvent was evaporated in an oven at 50 °C for 10 h and the membranes were peeled off by immersion in water. Finally, the membranes were dried in vacuum oven at 150 °C for 48 h for removing the residual solvent. The membranes of PBI were cast from DMAc solution by the same procedure mentioned above and solvent was evaporated at 85 °C.

Methods used for determining, thermal properties, mechanical properties, XRD, water uptake, acid uptake, oxidative stability, proton conductivity and Fuel cell performance tests are described in Section 4.2.2.

#### 4.4.2.3 Polymer synthesis

##### ➤ Synthesis of CPBI-90 (IPH:TAB:IPA=10:90:100 mol%)

100 mL three necked round bottom flask, equipped with a mechanical stirrer, nitrogen gas inlet and a guard tube, was charged with 2.0 g (9.334 mmol) 3,3',4,4',-tetra-amino biphenyl (TAB), 0.2012 g (1.0366 mmol) isophthalohydrazide (IPH) and 60 g of polyphosphoric acid (PPA) and the mixture was heated to 140 °C with stirring under a stream of nitrogen till a clear solution is formed. To this solution 1.7236 g (10.3706 mmol) of isophthalic acid (IPA) was added slowly with stirring. Then the temperature was raised to 170 °C and again stirred till a homogeneous solution was obtained. The solution was further heated to 200 °C and maintained at this temperature for 12 h. The resulting gel solution was poured into 1000 mL water to precipitate the polymer. The polymer was then filtered, washed repeatedly with water followed by stirring in 10% sodium bicarbonate solution for 24 h to eliminate residual phosphoric acid. The polymer was washed with water to neutrality to eliminate sodium bicarbonate and the polymer was dried at 150 °C for 48 h in vacuum oven. A brown fibrous polymer was obtained

and the yield was ~ 98%. The inherent viscosity of this polymer, measured in concentrated 96% sulfuric acid at 30 °C at a concentration of 0.2 g.dL<sup>-1</sup> was 0.95 dL./g.

Other polymers with different ratio of 3,3',4,4',-tetra-amino biphenyl and isophthalohydrazide with isophthalic acid were synthesized following same procedure (Table 4.11).

**Table 4.11** Inherent viscosity, yield, film appearance and film nature

Polymer Code	TAB/IPH ratio (% mole ratio)	Inherent Viscosity $\eta_{inh}$ (dL/g)	Yield (%)	Film Appearance (Translucent)	Film Nature
CPBI-90	90/10	0.95	98	Brown	Flexible
CPBI-70	70/30	0.85	98	Light brown	Flexible
CPBI-50	50/50	0.72	97	Light brown	Brittle
CPBI-30	30/70	0.52	96	Golden (opaque)	Brittle
CPBI-10	10/90	0.49	96	NA	NA
POD	--	0.29	95	NA	NA
PBI	--	1.23	99	Brown	Flexible

NA- not applicable; POD- polyoxadiazole; TAB- 3,3',4,4',-tetra-amino biphenyl; IPH- isophthalohydrazide

## 4.4.3 Results and Discussion

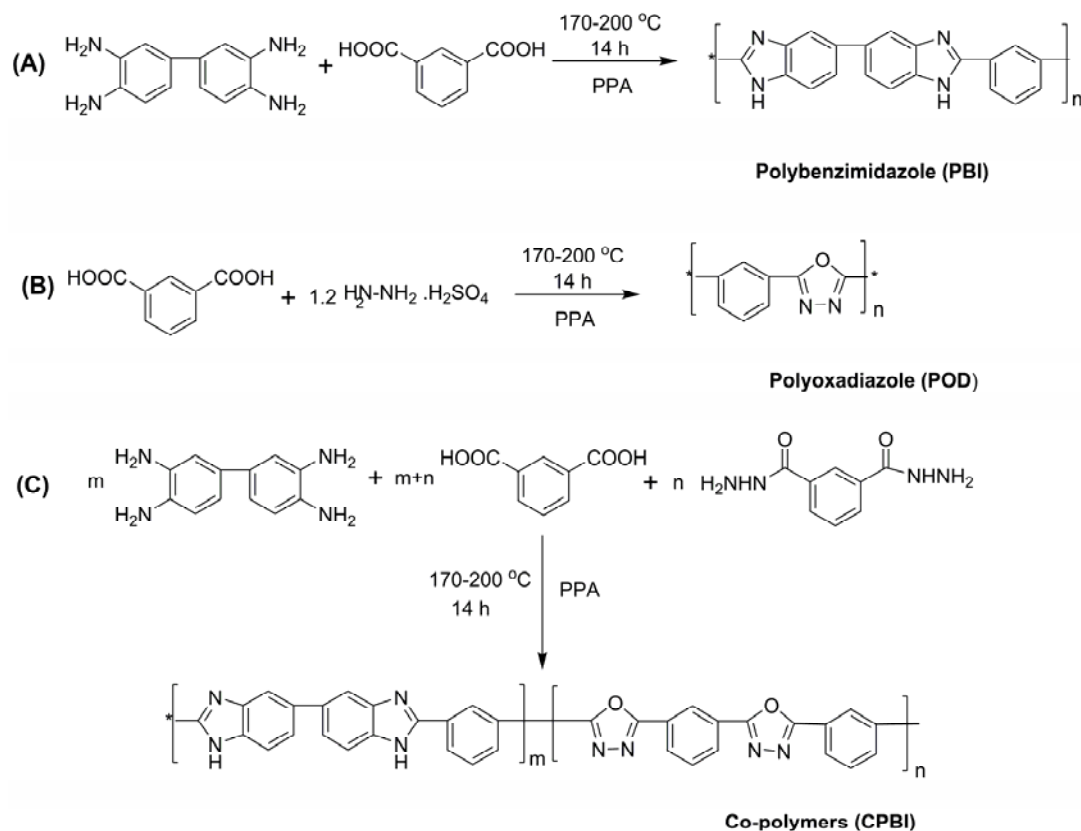
### 4.4.3.1 Polymer synthesis

Both polybenzimidazoles (PBI) and polyoxadiazoles (POD) can be synthesized by solution polymerization in polyphosphoric acid. Thus, polyphosphoric acid is common solvent for both the reactions wherein, polymer formation and cyclization of hydrazide to oxadiazole take place under similar conditions. Following this route, a number of copolymers containing benzimidazole and oxadiazole groups were prepared by the condensation of a tetraamine, viz. TAB, a dihydrazide (isophthalohydrazide) and a diacid (isophthalic acid) in suitable ratio (Table 4.11).

Polyoxadiazole (POD) Scheme 1(B) was synthesized by condensing isophthalic acid and hydrazine sulphate with 1:1.2 molar ratio in PPA according to the reported procedure<sup>44</sup> and polybenzimidazole was synthesized by condensing TAB with IPA (molar ratio 1:1) in PPA as shown in the scheme 1(A)

Thus, polybenzimidazoles containing 10,30,50,70 and 90 mole% of oxadiazole groups were synthesized as described in experimental section. All polymers, except POD and CPBI-90, form strong threads during precipitation in water. Polymers CPBI-90,

CPBI-70, and CPBI-50 form strong, tough films (Table 4.11) on casting from 3% solution in formic acid. Whereas, CPBI-30 polymer forms brittle film and CPBI-10 was not soluble in the common organic solvents.



**Scheme 4.3** Synthesis of (A) polybenzimidazole (PBI), (B) polyoxadiazole (POD) and (C) copolymers (CPBI)

#### 4.4.3.2 FTIR spectroscopy

FTIR spectra of these polymers were recorded by using KBr pellets and the incorporation of oxadiazole moiety was confirmed, Figure 4.34.

Pristine PBI shows characteristic absorption peak at  $3409\text{ cm}^{-1}$  (free non-hydrogen-bonded N-H stretching),  $3140\text{ cm}^{-1}$  (self-associated hydrogen-bonded N-H groups),  $1620\text{ cm}^{-1}$  (C=C/C=N stretching of benzimidazole ring),  $1588\text{ cm}^{-1}$  (ring vibration characteristic of conjugation between benzene and imidazole ring),  $1438\text{ cm}^{-1}$  (in plane ring vibration characteristic of 2,6 disubstituted benzimidazole),  $1280\text{ cm}^{-1}$  (imidazole ring breathing). A slight variation in the absorption peaks compared to pristine PBI was observed in case of CPBI polymers (for e.g., peaks  $1623\text{ cm}^{-1}$ ,  $1594\text{ cm}^{-1}$ ,  $1441\text{ cm}^{-1}$ ) as shown in Figure 4.34. Similarly, formation of oxadiazole group in the polymers was confirmed by the presence of characteristic peak of =C-O-C=

at  $1241\text{ cm}^{-1}$  and  $1067\text{ cm}^{-1}$ . The intensity of the characteristic peak of breathing mode of the imidazole ring systematically increases with increasing percentage of benzimidazole units in the polymers. Similarly, the intensity of the characteristic peak of  $=\text{C}-\text{O}-\text{C}=\text{C}$  at  $1241\text{ cm}^{-1}$  and  $1067\text{ cm}^{-1}$  of oxadiazole group in polymers systematically increase as the percentage oxadiazole groups increase. Whereas, the peaks of  $=\text{C}-\text{O}-\text{C}=\text{C}$  at  $1241\text{ cm}^{-1}$  and  $1067\text{ cm}^{-1}$  were completely absent in the pristine PBI. These observations indicate the formation of desired copolymer containing benzimidazole and oxadiazole groups.

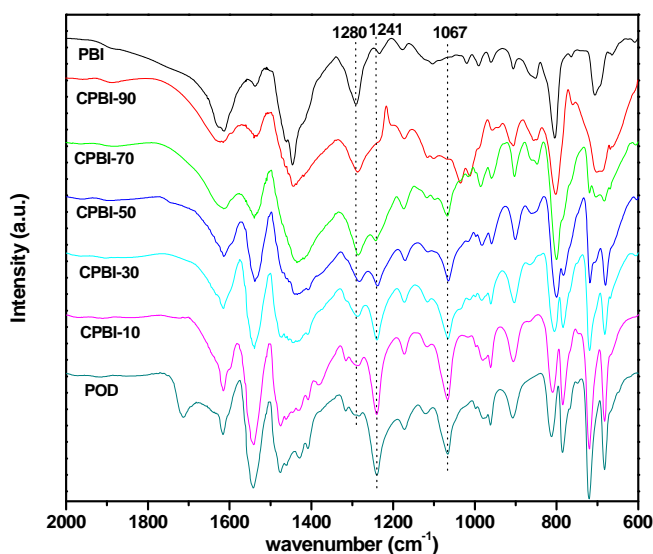


**Figure 4.34** FTIR spectra of (benzimidazole-co-oxadiazole) copolymers (KBr pellets)

#### 4.4.3.3 Polymer solubility and inherent viscosity

Solvent solubility is one of the key parameters in polymers. Both, PBI and POD being rigid polymers have poor solvent solubility. 1,3,4-Polyoxadiazole is soluble only in conc.  $\text{H}_2\text{SO}_4$ . The solubility test (Table 4.12) indicates that the copolymers containing 10 and 30 mole% of oxadiazole groups (CPBI-90 and CPBI-70) are soluble in NMP after heating while copolymer containing 50 mole% (CPBI-50) of oxadiazole groups is partially soluble in NMP and it forms gel like structure. Copolymers containing 70 and 90 mole% of oxadiazole groups (CPBI-30 and CPBI-10) are not soluble in aprotic solvents. These results indicate that the solubility of polyoxadiazole is enhanced by the incorporation of benzimidazole groups.

Since all the polymers were soluble in sulfuric acid, the inherent viscosity of polybenzimidazoles, polyoxadiazole and copolymers were measured in 96%  $\text{H}_2\text{SO}_4$  at  $30\text{ }^\circ\text{C}$ . Polyoxadiazole has the inherent viscosity  $0.29\text{ dL/g}$  and the values of co-polymers vary in the range from  $0.5$  to  $1.0\text{ dL/g}$  (Table 4.11).

**Table 4.12** Solubility behaviour of (benzimidazole-co-oxadiazole) copolymers

Polymer Code	DMAc	NMP	DMSO	H <sub>2</sub> SO <sub>4</sub>	TFA	MSA	Formic Acid
PBI	+	+	+	++	++	++	++
CPBI-90	+	+	±	++	++	++	++
CPBI-70	±	+	±	++	++	++	++
CPBI-50	±	±	--	++	++	++	++
CPBI-30	--	--	--	++	+	++	++
CPBI-10	--	--	--	++	±	++	±
POD	--	--	--	++	--	++	--

++ soluble at room temperature; + soluble on heating; ± partially soluble; -- insoluble

#### 4.4.3.4 Thermal properties

The thermal stability of these polymers was studied by thermo-gravimetric analysis (TGA) in nitrogen atmosphere at a heating rate of 10 °C min<sup>-1</sup> and the results are shown in (Table 4.13) whereas the thermograms of these polymers are shown in Figure 4.35.

Oxadiazole groups containing polybenzimidazole copolymers have high thermal stability. The initial decomposition temperature (IDT) of copolymers ranging from 472 – 499 °C while IDT of polyoxadiazole (POD) and polybenzimidazole (PBI) are 486 °C and 603 °C, respectively. Slightly low IDT of CPBI-10 (472 °C), compared to IDT of POD (486 °C) is may be due to disruption of rigid structure of POD by small quantity of benzimidazole groups. But, the overall behaviour shows that the IDT of copolymers is low compared to PBI, mainly due to decomposition of oxadiazole units. The values of T<sub>10</sub>, temperature at which 10% weight loss takes place are 760 °C and 499 °C for PBI and POD respectively. In case of copolymers, T<sub>10</sub> varies in the range from 488–536 °C and it increases with increase in benzimidazole groups in copolymer. Similar trend was observed in case of maximum decomposition temperature (T<sub>max</sub>). Thus, polybenzimidazoles containing oxadiazole groups have good thermal stability for applications at high temperature.

The glass transition temperature (T<sub>g</sub>) of the polymers was determined using DSC Q-10 (TA) from 50 °C to 450 °C in nitrogen atmosphere at a heating rate of 20 °C/min. (Table 4.13). T<sub>g</sub> of these polymers vary between 349 - 428 °C depending on percentages of oxadiazole and benzimidazole groups in the polymer chain. The T<sub>g</sub> of polybenzimidazole is 431 °C and T<sub>g</sub> of copolymers decrease with increasing oxadiazole units.

Thermo gravimetric and DSC analysis indicate that the thermal stability and  $T_g$  of copolymers, though low compared to PBI, are sufficiently high to be used as polymer electrolyte for fuel cell at high temperature.

**Table 4.13** Thermal properties of (benzimidazole-co-oxadiazole) copolymers

Polymer Code	IDT ( $^{\circ}\text{C}$ ) <sup>a</sup>	$T_{10}$ ( $^{\circ}\text{C}$ ) <sup>b</sup>	$T_{\text{max}}$ ( $^{\circ}\text{C}$ ) <sup>c</sup>	Residue (wt %) <sup>d</sup>	$T_g$ ( $^{\circ}\text{C}$ ) <sup>e</sup>
CPBI-90	499	656	531	77	428
CPBI-70	496	536	523	73	388
CPBI-50	486	512	510	69	385
CPBI-30	488	508	511	61	373
CPBI-10	472	488	499	56	349
POD	486	499	510	52	NF
PBI	603	760	751	84	431

<sup>a</sup> IDT: initial decomposition temperature; <sup>b</sup>  $T_{10}$ : temperature at which 5%, 10% wt loss observed; <sup>c</sup>  $T_{\text{max}}$ : maximum decomposition temperature; <sup>d</sup> residue at 900  $^{\circ}\text{C}$ ; <sup>e</sup>  $T_g$ : glass transition temperature  
NF: not found

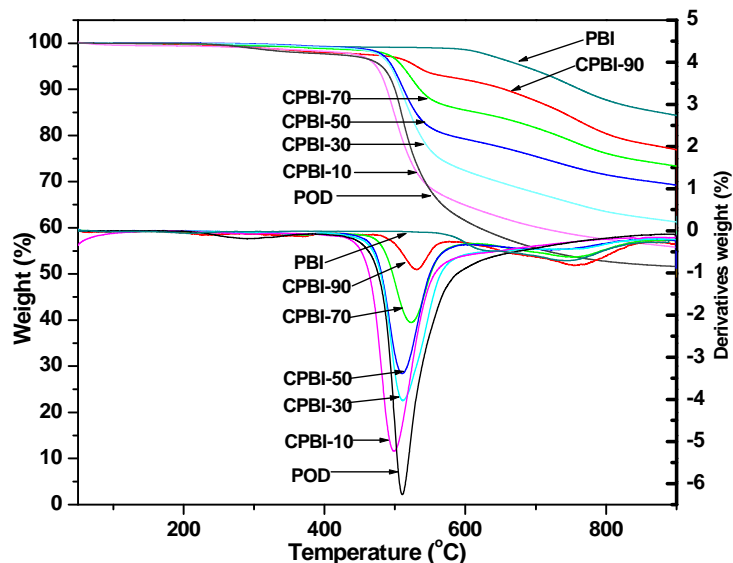


**Figure 4.35** Thermograms and derivatives of thermograms of (benzimidazole-co-oxadiazole) copolymers in  $\text{N}_2$  atmosphere (purging rate 20 mL/min) recorded at a heating rate 10  $^{\circ}\text{C}/\text{min}$

#### 4.4.3.5 Crystallinity

To study the morphology of the oxadiazole group containing polybenzimidazole, the films prepared from the polymers were examined by WAXS and the patterns are shown in Figure 4.36. The appearance of broad peak in all film specimens indicates the absence of crystallinity, which could be due to the oxadiazole moiety in the backbone of polymer. In case of CPBI-50 and CPBI-70 the new peaks appear at  $7.5^{\circ}$  and  $13.5^{\circ}$ .

Intensity of these peaks increases with increase in oxadiazole content indicating semicrystalline morphology.<sup>45</sup>

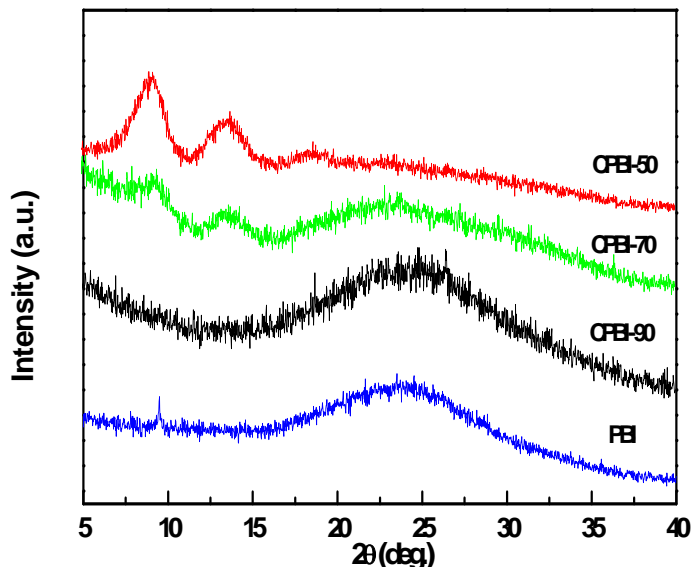


**Figure 4.36** WAXS diffractograms of PBI and its copolymers with varying oxadiazole contents

#### 4.4.3.6 Mechanical properties

Mechanical properties of all polymers were determined using tensile tester at room temperature. Figure 4.37 shows stress vs strain curves of PBI and its copolymers with varying oxadiazole contents and the results are summarized in Table 4.14.

**Table 4.14** Mechanical properties of PBI and its copolymers with varying oxadiazole contents

Polymer Code	Tensile Stress (MPa)	Modulus (MPa)	Toughness (MPa)	Elongation at Break (%)
CPBI-90	100	2609	10.8	6.9
CPBI-70	68	2531	1.8	2.5
CPBI-50	27	1749	0.28	0.9
PBI	138	3337	4.4	7.2

The overall mechanical properties of poly (benzimidazole-co-oxadiazole) copolymers are lower compared to the values of PBI probably due to disruption of regular structure of PBI and low molecular weight of copolymers. The incorporation of 10% oxadiazole groups (CPBI-90) in PBI lowers the tensile strength and modulus from 138 to 100 MPa and 3337 to 2609 MPa respectively, where as toughness increases from 4.4 MPa to 10.8 MPa. However, the tensile strength of CPBI-70 and CPBI-50 is 68 MPa and 27 MPa respectively. The least mechanical properties was observed in the CPBI-50



may be due to low molecular weight of copolymers. As the oxadiazole contents increases in the copolymers, tensile strength, modulus, toughness and elongation at break decreases.

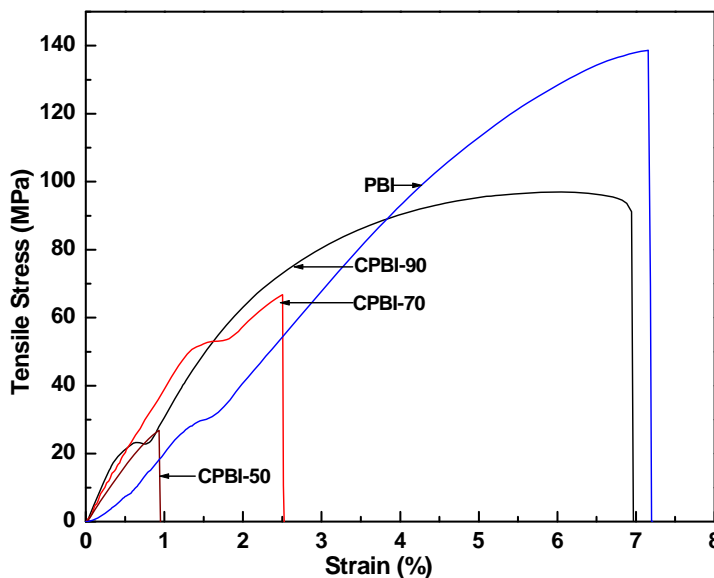


**Figure 4.37** Tensile stress versus strain measurements of PBI and its copolymers with varying oxadiazole contents

#### 4.4.3.7 Water uptake

One of the important properties of membrane is its water uptake. It is well known that water plays important role in increasing the overall permeability and proton conductivity of membrane at the cost of mechanical properties. It is observed that the water uptake in copolymer CPBI-10, was similar to PBI, where as in CPBI-70 and CPBI-50, the values were 21% and 25% respectively (Table 4.15). The results indicate that water uptake increases with the increasing oxadiazole content. This behaviour may be due to the loose packing of polymer chains resulting in random arrangement of benzimidazole and oxadiazole functionality.

#### 4.4.3.8 Oxidative stability

Oxidative stability was determined by Fenton test as described in the experimental part and the data are shown in Table 4.15. The samples CPBI-90, CPBI-70 and CPBI-50 showed a weight loss of 19%, 22% and 28% respectively after 120 h compared to a weight loss of 17% observed for PBI membrane. The above results point out that oxidative stability decreases with the increasing oxadiazole content. It is observed earlier that oxadiazole groups enhance oxidative stability for PBI containing oxadiazole groups in main chain. The observed low values of oxidative stability of these

copolymers with increasing in oxadiazole content are probably due to low molecular weight. The inherent viscosity of copolymers decreases with increasing oxadiazole content, which is consistent with observed results.

**Table 4.15** Oxidative stability and water uptake of PBI and its copolymers with varying oxadiazole contents

Polymer Code	% Weight loss <sup>a</sup>	Water uptake (wt%) <sup>b</sup>
CPBI-90	19	19
CPBI-70	22	21
CPBI-50	28	25
PBI	17	19

<sup>a</sup> Membrane degradation in terms of %wt. loss of a membrane measured after 120 h.

<sup>b</sup> The water uptake capacity of all membranes were measured at room temperature by immersing accurately weighed dried membranes (40-45 mg) into deionized water for 24 h.

#### 4.4.3.9 Phosphoric acid doping study

The acid uptake capacity of copolymers was evaluated by doping in various molar concentrations of H<sub>3</sub>PO<sub>4</sub> solutions for 24 h at room temperature as described in experimental part and the results are depicted in (Figure 4.38). The doping level is defined in terms of the weight percent of acid per gram of the polymer. Acid uptake of copolymers is observed to be quicker than that of PBI in all concentrations and acid uptake increases with increasing in acid concentration. In case of CPBI-50 and CPBI-70, the acid uptake is faster above 10 molar acid concentrations, whereas, acid uptake of PBI and CPBI-90 gradually increases till 14 molar concentration and reaches ~300%, where as acid uptake of CPBI-50 is ~460% in 14 molar solutions. High acid uptake of these copolymers is probably due to PBI rigidity being disturbed by bulky oxadiazole groups. The membranes of CPBI-90, CPBI-70 and CPBI-50 doped with 85% (~14.0 mole) H<sub>3</sub>PO<sub>4</sub>, found to soften and loose their mechanical strengths during drying at 100 °C due to dissolution in phosphoric acid present in membrane matrix. Hence, time dependent doping study of these polymers was carried out in 12 molar phosphoric acid. (Figure 4.39).

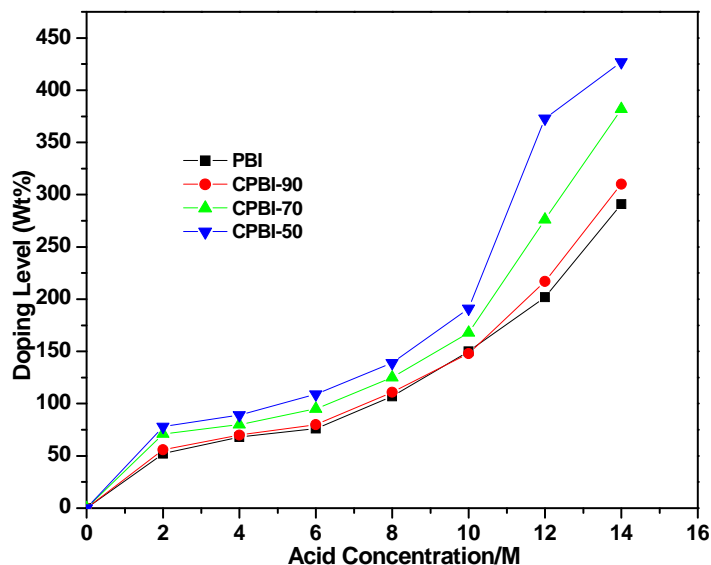


**Figure 4.38** Doping level of phosphoric acid (wt%) in (benzimidazole-co-oxadiazole) copolymers, as a function of the concentration of  $H_3PO_4$

Doping level as a function of time was determined for a period of 36 h at room temperature. Doping level of PBI was determined in 14 M  $H_3PO_4$ , while that of other copolymers CPBI-90, CPBI-70 and CPBI-50 in 12 M  $H_3PO_4$ . The acid uptake increases with time and all copolymers reach a saturation point in ~20 h. Phosphoric acid uptake of CPBI-50 is 377 wt % compared to 297% for PBI, while acid uptake of CPBI-90 and CPBI-70 was 218 wt % and 280 wt % respectively.

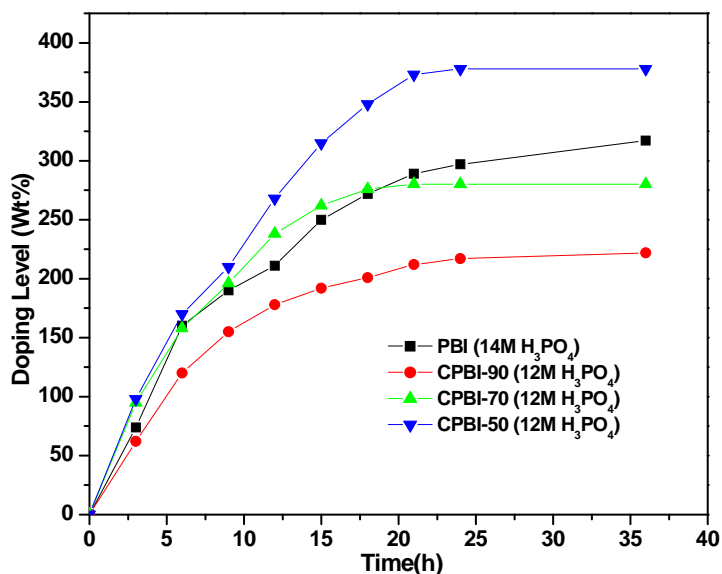


**Figure 4.39** Acid doping levels of (benzimidazole-co-oxadiazole) copolymers at different time intervals

#### 4.4.3.10 Proton conductivity measurements

A key feature of a polymer electrolyte membrane is its proton conductivity and is mainly influenced by phosphoric acid uptake, temperature and relative humidity. Proton conductivity normally increases with increasing acid uptake, temperature and relative humidity. The proton conductivity of (benzimidazole-co-oxadiazole) copolymers was measured by AC impedance spectroscopy using a standard two-electrode measurement set up at various temperatures (25 - 175 °C).

For the proton conductivity measurements, PBI membranes were doped in 12 M and 14 M H<sub>3</sub>PO<sub>4</sub>, where as all copolymer membranes (CPBI-90, CPBI-70 and CPBI-50) were doped in 12 M phosphoric acid for 24 h. The doping level of PBI, doped in 12 M and 14 M H<sub>3</sub>PO<sub>4</sub> is 185 wt% and 297 wt%, respectively. The doping level of CPBI-50, CPBI-70 and CPBI-90 in 12 M phosphoric acid is 377 wt%, 280 wt% and 218 wt%, respectively. The proton conductivity of CPBI-50 (doping level 377 wt%) is  $3.91 \times 10^{-2}$  to  $6.35 \times 10^{-2}$  S/cm (Table 4.16) in the temperature range of 25 to 175 °C. The proton conductivities of CPBI-70, CPBI-90 and PBI (297 wt% doping level) are in the range of  $4.4 \times 10^{-3}$  to  $2.14 \times 10^{-2}$ ,  $2.61 \times 10^{-3}$  to  $1.66 \times 10^{-2}$ , and  $7.42 \times 10^{-3}$  to  $3.17 \times 10^{-2}$  (Figure 4.40) respectively. The above results reveal that doping level and proton conductivity of copolymers increase with increasing oxadiazole content. It appears that, high proton conductivity of copolymers compared to PBI (185 wt% doping level) is mainly due to high phosphoric acid doping level. CPBI-50 with high doping level showed highest proton conductivity of  $6.35 \times 10^{-2}$  S/cm at 175 °C. All copolymer membranes retain good strength in spite of high doping levels.

**Table 4.16** Proton conductivity of benzimidazole-co-oxadiazole copolymers

Polymer code	Proton conductivity (S/cm) at temperature (°C)						
	25 °C	50 °C	75 °C	100 °C	125 °C	150 °C	175 °C
CPBI-50 (377)*	$3.91 \times 10^{-3}$	$6.26 \times 10^{-3}$	$1.08 \times 10^{-2}$	$2.12 \times 10^{-2}$	$4.52 \times 10^{-2}$	$5.91 \times 10^{-2}$	$6.35 \times 10^{-2}$
CPBI-70 (280)*	$4.4 \times 10^{-3}$	$7.3 \times 10^{-3}$	$9.11 \times 10^{-3}$	$1.2 \times 10^{-2}$	$1.56 \times 10^{-2}$	$1.9 \times 10^{-2}$	$2.14 \times 10^{-2}$
CPBI-90 (218)*	$2.61 \times 10^{-3}$	$4.1 \times 10^{-3}$	$6.23 \times 10^{-3}$	$8.83 \times 10^{-3}$	$1.09 \times 10^{-2}$	$1.38 \times 10^{-2}$	$1.66 \times 10^{-2}$
PBI (297)*	$7.42 \times 10^{-3}$	$9.6 \times 10^{-3}$	$1.4 \times 10^{-2}$	$2.05 \times 10^{-2}$	$2.69 \times 10^{-2}$	$3.00 \times 10^{-2}$	$3.17 \times 10^{-2}$
PBI (185)*	$3.29 \times 10^{-3}$	$5.38 \times 10^{-3}$	$6.92 \times 10^{-3}$	$7.01 \times 10^{-3}$	$7.34 \times 10^{-3}$	$1.01 \times 10^{-2}$	$1.25 \times 10^{-2}$

\* Phosphoric acid doping level in weight % of the polymers.

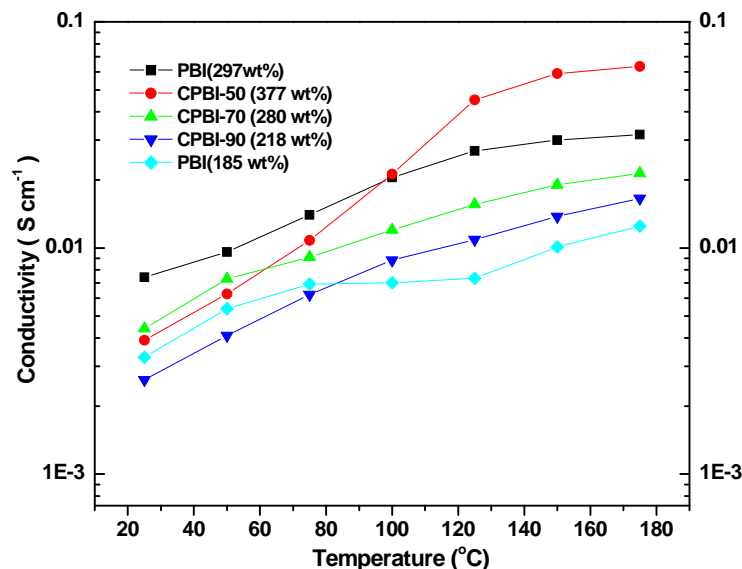


**Figure 4.40** Conductivity of phosphoric acid doped PBI and benzimidazole-co-oxadiazole) copolymers

Both OMPBI polymers, described earlier in this chapter and present CPBI polymers, have oxadiazole groups in main chain of polybenzimidazole. Both series of polymers were synthesized by solution condensation polymerization in PPA at high temperature. However, monomers used for the synthesis of these polymers are different. Thus, OMPBI polymers are synthesized from a diacid containing preformed oxadiazole group, where as in CPBI polymers, oxadiazole groups are generated from dihydrazide groups during polymerization. The structure and ratio of benzimidazole:oxadiazole groups in both series of polymers are different. As such it is difficult to compare the properties of these two series of polymers. However, attempt has been made to compare general trend in change of properties with increasing benzimidazole group content in both the series. As per feed ratio of monomers, benzimidazole group content in OMPBI series, increases in sequence as OMPBI-5 > OMPBI-4 > OMPBI-3, where as in CPBI polymers increasing benzimidazole content is in sequence as CPBI-90 > CPBI-70 > CPBI-50. In OMPBI series tensile stress decreases with increase in benzimidazole content, observed in limited range of three polymers OMPBI-3, 4 and 5 where as in CPBI series, tensile stress increases with increase in benzimidazole group content in polymers (Table 4.17). In case of OMPBI polymers, benzimidazole group content has significant effect on thermal stability and IDT increases with increase in benzimidazole content, where as in case of CPBI series, IDT is does not change much with increase benzimidazole content (Table 4.17). Opposite results are obtained in case of  $T_g$ . Thus, in

OMPBI series,  $T_g$  values do not change much with increase in benzimidazole content, where as in CPBI series,  $T_g$  increases with increase in benzimidazole content.

This difference in change in trend of properties in both the series is, probably due to microstructure of these polymers. WAXS diffractogram of OMPBI shows amorphous nature of polymers with single broad peak around  $26^\circ$  value irrespective of benzimidazole content, where as in CPBI series, crystallinity increases with increases in oxadiazole content.

Thus, distribution of oxadiazole and benzimidazole groups in polymers has significant effect on properties of polymers. Since, our objective in this work was to assess the possibility of using polybenzimidazoles containing oxadiazole groups as membrane material for development of polymer electrolyte for PEMFC, attempts were not made to correlate properties with microstructure by extending this work in this direction.

**Table 4.17** Comparative data of OMPBI and CPBI polymers

Polymer code	benzimidazole content (Mole%)	H <sub>3</sub> PO <sub>4</sub> doping concentration (Molar)	H <sub>3</sub> PO <sub>4</sub> doping level (wt%)	Proton conductivity (S/cm) 175(°C)	IDT (°C)	T <sub>g</sub> (°C)	Tensile stress (MPa)
OMPBI-3	50	12	195	$1.52 \times 10^{-2}$	485	411	131
OMPBI-4	70	14	240	$2.85 \times 10^{-2}$	495	406	80
OMPBI-5	90	14	292	$3.48 \times 10^{-2}$	576	408	72
CPBI-50	50	12	377	$6.35 \times 10^{-2}$	486	385	27
CPBI-70	70	12	280	$2.14 \times 10^{-2}$	496	388	68
CPBI-90	90	12	218	$1.66 \times 10^{-2}$	499	428	100

#### 4.4.3.11 Membrane electrode assembly fabrication

The electrodes with a gas diffusion layer (GDL) and a catalyst layer were fabricated by following the same procedure as mentioned in Section 3.3.2.9. A Polymer electrolyte membrane, CPBI-70 (85  $\mu\text{m}$ ) was doped in 12 molar phosphoric acid where as PBI membrane (90  $\mu\text{m}$ ) was doped in 14 molar phosphoric acid for 24 h. Then membranes were wiped out by tissue paper and dried at 100 °C in vacuum oven. The membrane electrode assemblies were prepared by hot-pressing the pre-treated (5 cm<sup>2</sup>) membrane under the conditions of 100 °C, 130 atm for 3 min.

#### 4.4.3.12 Polarization study

Figure 4.41 shows the fuel cell performance of CPBI-70 membrane in terms of polarization plots of MEA fabricated using 20% Pt/C for both anode and cathode in a single cell experiment, at 100, 125 and 150 °C with a dry H<sub>2</sub>/O<sub>2</sub> gas flow rate of 0.2 slpm. CPBI-70 membrane shows lower performance than that of the PBI membrane. The open-circuit voltage (OCV) obtained with the CPBI-70 membrane is 0.56 V at 150 °C, whereas for PBI it is 0.92 V. The CPBI-70 membrane gives a maximum power density 163 mW/cm<sup>2</sup> at 0.3 V, whereas the PBI membrane gives 210 mW/cm<sup>2</sup> at 0.3 V. The lower fuel cell performance of CPBI-70 membrane can be attributed to low H<sub>3</sub>PO<sub>4</sub> acid content and low proton conductivity. Even though CPBI membranes show lower power density than that of PBI, the activation and ohmic drop is comparatively less than that of PBI. Hence, CPBI membrane could be great alternative for PBI, if OCV of this membrane could be improved.

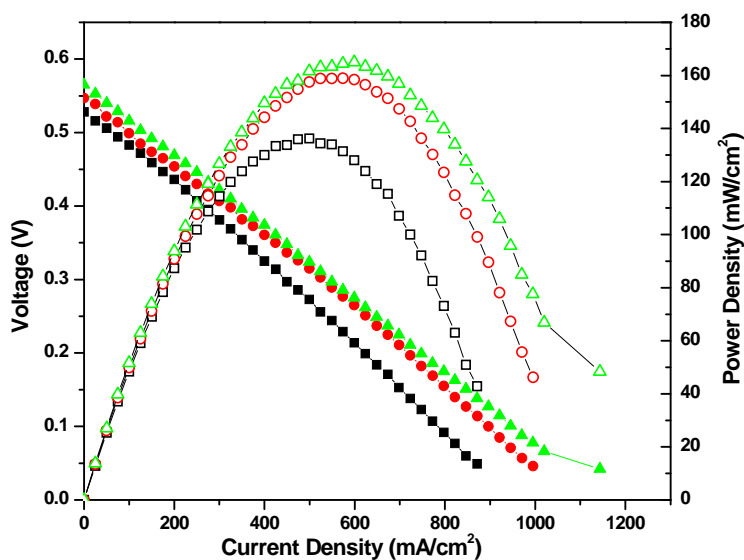


**Figure 4.41** Polarization curves obtained with CPBI membrane fuel cell at different temperatures with dry H<sub>2</sub> and O<sub>2</sub> (flow rate 0.2 slpm). The cell was conditioned for 30 min at open-circuit potential and at 0.2 V for 15 min before measurements. Key: (■□)100, (●○) 125 and (▲Δ) 150 °C

## 4.5 Conclusions

- New series of polybenzimidazoles having oxadiazole groups in main chain and side chain were synthesized from substituted diacids 3,3'-(1,3,4-oxadiazole- 2,5-diyl)dibenzoic acid. 3,3'-(1,3,4-oxadiazole- 2,5-diyl)dibenzoic acid (ODBA) and 5-(5-phenyl-1,3,4-oxadiazol-2-yl) isophthalic acid (POIA) with 3,3',4,4',-tetra-amino biphenyl (TAB) using high temperature solution polycondensation in PPA.
- These polymers have high inherent viscosity and good solubility in aprotic solvents at room temperature and they form tough and flexible films.
- These polymers exhibit high thermal stability and good mechanical strength.
- Oxadiazole groups containing polybenzimidazoles exhibit good oxidative stability.
- The homo polymers (OMPBI and OSPBI) or copolymer containing higher content of oxadiazole groups enhances the phosphoric acid uptake. At high concentration of phosphoric acid (14M), however, at higher doping level these membranes are soluble or lose their mechanical integrity.
- These polymers showed adequate proton conductivity, at less phosphoric acid doping levels. These polymers are useful contenders for the applications as membrane material for high temperature polymer electrolyte for proton exchange membrane fuel cells (PEMFCs).
- Polybenzimidazoles containing oxadiazole groups were also synthesized by alternative route by reacting a mixture of TAB and dihydrazide of IPA (in different ratio) with IPA in PPA at high temperature. It appears that the microstructure of these polymers is different from that of OMPBI polymers as evidenced by comparative data of properties. These polymers also exhibit good proton conductivity.
- OSPBI polymers offer sites for sulfonation at pendent phenyl rings, which may improve proton conductivity further.
- These polymers may be useful as membranes for separation technology at high temperature.



## References

1. Jones, D. J. and Roziere, J. *J. Membr. Sci.* **2001**, 185, 41-58.
2. He, R.; Li, Q.; Bach, A.; Jensen, J. O.; Bjerrum, N. J. *J. Membr. Sci.* **2006**, 277, 38-45.
3. Pu, H.; Liu, Q.; Liu, G. *J. Membr. Sci.* **2004**, 241, 169-175.
4. Rikukawa, M.; Sanui, K. *Prog. Polym. Sci.* **2000**, 25, 1463-1502.
5. Jang, M.Y.; Yamazaki, Y. *J. Power Sources* **2005**, 139, 2-8.
6. Staiti, P.; Minutoli, M. and Hocevar, S. *J. Power Sources* **2000**, 90, 231-235.
7. Staiti, P.; Minutoli, M. *J. Power Sources* **2001**, 94, 9-13.
8. Kerres, J. A.; Ullrich, A.; Haring, T.; Baldauf, M.; Gebhard, U. and Preidel, W. *J. New Mater. Electrochem. Syst.* **2000**, 3, 229-239.
9. Kerres, J. A.; Ullrich, A.; Meier, F.; and Haring T. *Solid State Ionics* **1999**, 125, 243-249.
10. Lee, J. K. and Kerres, J. *J. Membr. Sci.* **2007**, 294, 75-83.
11. Schönberger, F. and Kerres, J. *Solid State Ionics* **2007**, 178, 547-554.
12. Hasiotis, C.; Deimede, V.; and Kontoyannis, C. G. *Electrochim Acta* **2001**, 46, 2401-2406.
13. Arunbabu, D.; Sannigrahi, A. and Jana, T. *J. Phys. Chem. B* **2008**, 112, 5305-5310.
14. Asensio, J. N.; Borros, S.; Gomez-Romero, P. *J. Electrochem. Soc.* **2004**, 151, A304-A310.
15. Xiao, L.; Zhang, H.; Jana, T.; Scanlon, E.; Chen, R.; Choe, E-W.; Ramanathan, L. S.; Yu, S. and Benicewicz, B.C. *Fuel Cells* **2005**, 5, 287-295.
16. Carollo, A.; Quartarone, E.; Tomasi, C.; Mustarelli, P.; Belotti, F.; Magistris, A.; Maestroni, F.; Parachini, M.; Garlaschelli, L. and Righetti, P. *J. of Power Sources* **2006**, 160, 175-180.
17. Asensio, J. N.; Borros, S.; Gomez-Romero, P.; *J. Polym. Sci. Part A: Polym Chem.* **2002**, 40, 3703-3710.
18. Cassidy, P. E. *Thermally stable polymers*, Marcel Dekker, New York, 1989.
19. Gomes, D.; Roeder, J.; Ponce, M. L.; Nunes, S. P. *J. Membr. Sci.* **2007**, 295, 121-129.
20. Zaidi, S. M. J.; Chen, S. F.; Mikhailenko, S. D. and Kaliaguine, S. *J. New Materials Electrochem. Syst.* **2000**, 3, 27-32.
21. Ponce, M. L.; Gomes, D.; Nunes, S. P. *J. Membr. Sci.* **2008**, 319, 14-22.
22. Ponce, M. L.; Boaventura, M.; Gomes, D.; Mendes, A.; Madeira, L. M. and Nunes, S. P. *Fuel Cells* **2008**, 8, 209-216.
23. Shaplov, A. S.; Lozinskaya, E. I.; Odinet, I. L.; Lyssenko, K. A.; Kurtova, S. A.; Timofeeva, G. I.; Iojoiu, C.; Sanchez, J-Y.; Abadie, M. J. M.; Voytekunas, V. Y.; Vygodskii, Y. S. *Reactive & Functional Polymers* **2008**, 68, 208-224.
24. Hsiao, S.-H.; Chang, L.-M. *J. Polym. Sci. Part A: Polym Chem.* **2000**, 38, 1599-1608.
25. Thaemlitz, C. J.; Weikel, W. J. and Cassidy, P. E. *Polymer* **1992**, 33, 3278-3285.
26. Li, Q.; Pan, C.; Jensen, O. J.; Noye, P.; Bjerrum, N. *J. Chem. Mater.* **2007**, 19, 350-352.
27. Songa, J. M.; Chab, S. Y.; Lee, W. M. *J. of Power Sources* **2001**, 94, 78.
28. Musto, P.; Karasz, F. E. and Macknight, W.J. *Polymer* **1993**, 34, 2934-2945.
29. Schulz, B.; Bruma, M. and Brehmer, L. *Adv. Mater.* **1997**, 9, 601-613.
30. Samms, S. R.; Wasmus S. and Savinell, R. F. *J. Electrochem Soc.* **1996**, 143, 1225-1232.
31. Gomes, D.; Pinto, J. C.; Borges, C. P. *Polymer* **2003**, 44, 6223-6233.

32. Gomes, D.; Borges, C. P.; Pinto, J. C. *Polymer* **2001**, 42, 851-865.
33. Sannigrahi, A. ; Arunbabu, D.; Sankar, M. and Jana, T. *J. Phys. Chem. B* **2007**, 111, 12124-12132.
34. Hsiao, S.-H.; Dai, L.-R.; He, M.-H. *J. Polym. Sci. Part A: Polym Chem.* **1999**, 37, 1169–1181.
35. Lobato, J.; Canizares, P.; Rodrigo, M. A.; Linares, J. J.; Aguilar, J. A. *J. Membr. Sci* **2007**, 306, 47–55.
36. Chung, T-S. *Polymer Reviews* **1997**, C37, 277-301.
37. Qing, S.; Huang, W.; Yan, D. *Reactive & Functional Polymers* **2006**, 66, 219–227.
38. Li, Q.; He, R.; Berg, R. W.; Hjuler, H. A.; Bjerrum, N. J. *Solid State Ionics* **2004**, 168, 177-185.
39. Li, Q.; He, R.; Jensen J.O. and Bjerrum, N. J. *Fuel Cells* **2004**, 3,147-159.
40. Thaemlitz, C. J.; Weikel, W. J. and Cassidy, P. E. *Polymer* **1992**, 33, 3278-3285.
41. Kawahara, M.; Morita, J.; Rikukawa, M.; Sanui, K.; Ogata, N. *Electrochimica Acta* **2000**, 45,1395-1398.
42. Hensema, E. R.; Sena, M. E. R.; Mulder, M. H. V.; Smolders, C. A. *J. Polym. Sci. Part A Polym. Chem.* **1994**, 32, 527-537.
43. Campbell, T. W.; Foldi, V. S. and Farago, J. *Journal of Applied Polymer Science* **1959**, 5, 155-162.
44. Iwakura, Y.; Uno, K. and Hara, S. *J. Polym. Sci. Part A* **1965**, 3, 45-54.
45. Chen, C.-F.; Qin, W.-M.; Huang, X.-A. *Polymer Engineering and Science* **2008**, 1151-1156 (DOI 10.1002/pen.21066)

# Chapter **5**

**Summary and conclusions**

## 5.1 Summary of the work

The objective of the present work was to synthesize novel polybenzimidazoles containing N-phenyl 1,2,4-triazole (NPT) and 1,2,4-oxadiazole moiety in the main as well as side chain to study effect of these groups on the properties of polybenzimidazole and to explore possible application of these polymers as polymer electrolytes for fuel cells. Accordingly, four aromatic diacids monomers namely, (i) 3,3'-(4-phenyl-4H-1,2,4-triazole-3,5-diyl) dibenzoic acid (PTDBA), (ii) 5-(4,5-diphenyl-4H-1,2,4-triazol-3-yl)isophthalic acid (DTIA) (iii) 5-(5-phenyl-1,3,4-oxadiazol-2-yl) isophthalic acid (POIA) and (iv) 3,3'-(1,3,4-oxadiazole- 2,5-diyl)dibenzoic acid (ODBA) were synthesized . Based on these diacid monomers a series of polybenzimidazoles having NPT and 1,2,4-oxadiazole moiety in the main and side chain were synthesized by condensing these diacids with 3,3',4,4,'-tetra amino biphenyl (TAB). To study the structure-property relationship, various copolymers were also synthesized with other diacids, namely, pyridine dicarboxylic acid, terephthalic acid, sebacic acid, adipic acid and isophthalic acid (IPA). Copolymers containing varying content of NPT and 1,2,4-oxadiazole moieties were synthesized by condensing a mixture of IPA and these aromatic diacids in different mole ratio (90:10, 70:30, 50:50, 30:70 and 10:90) with TAB to study the effect of NPT and 1,2,4-oxadiazole functionality on properties of polybenzimidazoles.

The effect of NPT groups in the main and side chain, on the solubility, thermal stability, crystallinity and mechanical properties of these polybenzimidazoles was investigated. Physico-chemical properties such as water and oxidative stability, phosphoric acid-uptake and proton conductivity of these polymers have also been examined.

The NPT group containing polybenzimidazole derived from PTDBA and DTIA, respectively provided improved solubility, high oxidative stability and high acid uptake compared to the commercial PBI. These polymers could maintain the thermal stability up to 500 °C. The mechanical properties of these polymers decreased compared to PBI may be due to rigid polymer backbone being perturbed by the bulky NPT group. These polymers exhibit excessive acid uptake capacity and loose the mechanical integrity at high temperature; hence it is necessary to dope them in H<sub>3</sub>PO<sub>4</sub> of low concentration to control the acid uptake, which results in low doping level and low proton conductivity as compared to PBI.

The series of polybenzimidazole and copolybenzimidazoles having oxadiazole group in main and side chain were prepared from ODBA and POIA, respectively. These polymers have high inherent viscosity, good solubility in aprotic solvents and they form tough and flexible films. Incorporation of oxadiazole groups in polybenzimidazole improves the acid uptake and oxidative stability of the polymers. These polymers exhibit high thermal stability and good mechanical strength but slightly lower than commercial PBI. These polymers exhibit good oxidative stability compared to PBI. These polymers also show excessive acid uptake capacity and lose the mechanical integrity, and hence it was required to dope them in low acid concentration to control the acid uptake, which results in low doping level and in turn low proton conductivity as compared to PBI. From the results of chapter 4 it is clear that the synthesized oxadiazole group containing polybenzimidazoles can be used as polymer electrolyte membranes for operation at high temperature and also as polymeric material for other high temperature applications.

To compare difference in properties of copolybenzimidazoles, synthesized by condensation of ODBA, IPA and TAB, with those prepared without diacid monomer (ODBA) containing preformed oxadiazole groups by condensing IPA, dihydrazide of IPA with TAB were synthesized, characterized and properties of these two type of polymers were compared.

The investigation of high temperature polymers for fuel cell applications, as discussed in the preceding chapters, has allowed us to gain valuable insight into the properties necessary for a successful PEM.

## 5.2 Conclusions

- Three new diacid monomers namely, 3,3'-(4-phenyl-4H-1,2,4-triazole-3,5-diyl) dibenzoic acid (PTDBA), 5-(4,5-diphenyl-4H-1,2,4-triazol-3-yl)isophthalic acid (DTIA) containing preformed NPT group and 5-(5-phenyl-1,3,4-oxadiazol-2-yl) isophthalic acid (POIA) containing preformed oxadiazole group were successfully synthesized by simple condensation reactions with high purity and good yields, by using the inexpensive commercially available starting materials.
- A oxadiazole group containing diacid monomer, 3,3'-(1,3,4-oxadiazole- 2,5-diyl)dibenzoic acid containing oxadiazole group was also synthesized with high purity and good yields.
- Several novel homo and copolybenzimidazoles were synthesized and the structure-property relationship was studied.

- The solubility is dependent on the nature of diacid monomers. It was observed that incorporation of NPT groups in polybenzimidazoles improved the solubility without affecting the thermal properties significantly.
- The thermal stability and glass transition temperatures were dependent on the diacid monomers. The introduction of alkyl groups decreased the glass transition temperatures to large extent.
- Polybenzimidazoles containing oxadiazole and NPT groups enhance the oxidative stability of PBI.
- Incorporation of NPT and oxadiazole moiety in the polybenzimidazoles increases the phosphoric acid uptake. At higher doping level, these membranes are soluble in phosphoric acid in polymer matrix at high temperature.
- Polybenzimidazoles containing oxadiazole groups were also synthesized by alternative route by reacting a mixture of TAB and dihydrazide of IPA, in different ratio with IPA in PPA at high temperature. These polymers also exhibit good proton conductivity.
- These polymers showed reasonably good proton conductivity for the applications as membrane material for high temperature polymer electrolyte for proton exchange membrane fuel cells (PEMFCs).

### 5.3 Future work

The study carried out ascertains a new cost effective and efficient route for the synthesis of novel polybenzimidazoles, which have potential applications like polymer electrolyte membranes for PEMFCs, gas separation technology and high temperature military applications.

Following are the suggestions for the future work.

Polybenzimidazoles containing N-phenyl 1,2,4-triazole (NPT) and 1,2,4-oxadiazole functionality exhibit excessive acid uptake capacity and lose their mechanical integrity, necessitating to dope them in low acid concentration to control the acid uptake, which results in low doping level and low proton conductivity as compared to PBI. One way to alleviate this problem is to prepare covalently cross-linked polybenzimidazoles using *p*-xylene dibromide or *p*-xylene dichloride as crosslinker.

Incorporation of NPT groups enhances solvent solubility and oxidative stability of PBI. The pendant N-phenyl group offers sites for aromatic electrophilic substitution

e.g sulphonic acid ( $\text{SO}_3\text{H}$ ) groups. Thus, PBI-containing NPT groups can be easily sulfonated leading to enhanced proton conductivity. Similarly, PBI containing oxadiazole groups in side chain can also subjected to electrophilic substitution reactions such as sulfonation for enhanced proton conductivity. Moreover, these monomers are ideal for the synthesis of other polymers such as polyesters and polyamides-containing NPT and oxadiazole group.

For better and consistent fuel cell performance, it is necessary to standardize the membrane electrode assembly.

It is well known that polyoxadiazole, polytriazoles and polybenzimidazoles are used for high temperature separation technology applications. A systematic study on gas separation and other separation technologies of these polymers is worth investigating. These polymers have potential as membrane materials for separation technology at high temperature also.

## LIST OF PUBLICATIONS

1. Polybenzimidazoles tethered with phenyl triazole units as polymer electrolytes for fuel cell. Ravindra Potrekar, Mahesh Kulkarni, R. A. Kulkarni S. P. Vernekar *Journal of Polymer Science Part A: Polymer Chemistry*. 2009, 47, 2289-2303
2. Variation in acid moiety of polybenzimidazoles: Investigation of physico-chemical properties towards their applicability as proton exchange and gas separation membrane materials. S.C. Kumbharkar, Md. Nazrul Islam, R. A. Potrekar, U. K. Kharul *Polymer* 2009, 50, 1403-1413
3. Nitrophenoxy groups containing Polybenzimidazoles as polymer electrolytes for fuel cells: Synthesis and Characterization. Mahesh Kulkarni, Ravindra Potrekar, R. A. Kulkarni, S. P. Vernekar *Journal of Applied Polymer Science*. (Accepted Manuscript)
4. Synthesis and characterization of novel polybenzimidazoles bearing pendant phenoxyamine groups. Mahesh Kulkarni, Ravindra Potrekar, R. A. Kulkarni, S. P. Vernekar *Journal of Polymer Science Part A: Polymer Chemistry* 46, 2008, 5776-5793
5. Designing superior analogues of polybenzimidazole for fuel cell applications. Ravindra A. Potrekar, Mahesh P. Kulkarni, Rajendra A. Kulkarni, Subhash P. Vernekar ( to be communicated)
6. Synthesis and characterization of polybenzimidazoles having pendant oxadiazole groups for fuel cell applications. Ravindra A. Potrekar, Mahesh P. Kulkarni, Rajendra A. Kulkarni, Subhash P. Vernekar (to be communicated)
7. One-pot synthesis of poly (benzimidazole-oxadiazole) copolymers for fuel cell applications. Ravindra A. Potrekar, Mahesh P. Kulkarni, Rajendra A. Kulkarni, Subhash P. Vernekar ( to be communicated)
8. Polybenzimidazoles tethered with oxadiazole groups as polymer electrolytes for fuel cell. Ravindra A. Potrekar, Mahesh P. Kulkarni, Rajendra A. Kulkarni, Subhash P. Vernekar *Journal of Polymer Science Part A: Polymer Chemistry*. ( to be communicated)
9. An exceedingly efficient and chemoselective esterification with activated alcohols using  $\text{AlCl}_3/\text{NaI}/\text{CH}_3\text{CN}$  system. N.N. Karde, S.G. Shirodkar, R.A. Potrekar *Synthetic Communication*. 2004, 34, 391
10. A Convenient and improved montmorillonite K-10 catalysed friedel-craft benzylation with activated esters. N.N. Karde, S.G. Shirodkar, R.A. Potrekar *Journal of Chemical Research* 2003, 10, 652



11. Diacetoxyiodobenzene-mediated oxidative addition of 1,3-dicarbonyl compounds to olefins: an efficient one-pot synthesis of 2,3-dihydrofuran derivatives. N.N. Karde, S.G. Shirodkar, R.A. Potrekar, N.H. Karde *Tetrahedron Letters* 44, 2003, 6729

# **Synopsis**

## Introduction

Polymer Electrolyte Membrane Fuel Cells (PEMFC) have attracted considerable attention of research workers through out the world, as pollution free alternative energy source, particularly, for the vehicular and portable applications. PEMFC is a device which generates electrical power directly via the employment of fuel sources such as hydrogen and oxygen (or air) and the by-product is water.

Polymer electrolyte membrane is one of the important components of PEMFC. Presently, perfluorosulfonic acid (Nafion<sup>®</sup>) polymer is the most studied polymer as a polymer electrolyte membrane at low temperature (<80 °C). Nafion<sup>®</sup> has serious drawbacks such as high cost, difficult water management, high fuel crossover, low operational temperature and catalyst poisoning leading to loss of efficiency with time. Various types of polymers have been studied as polymer electrolytes, which include polymers containing sulfonic acid groups such as polyimides, poly ether ketone, poly ether sulfone, poly (styrene sulfonic acid) etc. Though they have good proton conductivity, they suffer from low operational temperature due to requirement of water for proton conduction. Thus, the developments of alternative membranes overcoming these problems are strongly desired for PEMFC. A good polymer electrolyte membrane should have high operating temperature >120 °C, good thermoxidative stability and chemical resistance, good H<sub>2</sub>, O<sub>2</sub> and methanol barrier properties, high proton conductivity, high current density and long service life. High operational temperature has advantages of zero electro-osmotic drag, simple water management, and enhanced kinetics for both electrode reactions at high temperature, reduced catalyst poisoning effect of carbon monoxide in fuel etc.

Polybenzimidazole (PBI) is one of the most promising candidates as high temperature (>120 °C) proton-exchange membranes. It exhibits good proton conductivity after doping with H<sub>2</sub>SO<sub>4</sub> or H<sub>3</sub>PO<sub>4</sub>. But it has poor solubility, poor oxidative stability, low proton conductivity at low temperature compared to Nafion<sup>®</sup> and propensity for the loss of efficiency due to leaching out of dopant by water/methanol. Several approaches have been explored to modify the properties of PBI to overcome these limitations. These include addition of inorganic fillers, composites with heteropolyacids and acid-base blends with sulfonated polymers such as, SPEEK, polysulfone, poly (arylene thioether)s etc. PBIs with structural variations have also been reported which include, poly(2,5-benzimidazole) i.e., AB-PBI, PBI based on, 1,2,4,5-tetraaminobenzene such as pyridine dicarboxylic acid, naphthalene dicarboxylic acid,

sulfonated isophthalic acid, 2,2-Bis(4-carboxyphenyl)hexafluoropropane and hyperbranched PBI (HPBI).

Polytriazoles and polyoxadiazoles are another class of thermally stable high performance heterocyclic polymers known for their high thermal stability and good chemical resistance. 1,2,4 triazoles and polyoxadiazoles transport protons similar to imidazoles and have adequate electrochemical stability to be used in fuel cell conditions as polymer electrolyte. But the main hurdle for application of these polymers is its processability due to their high softening point and poor solubility in organic solvents. So, little attention has been paid towards the application of polymers containing triazole and oxadiazole groups as polymer electrolyte for fuel cells. The present work is intended to synthesize polymers containing triazole and oxadiazole groups and study their properties as polymer electrolytes for fuel cells. This work presents synthesis and characterization of novel polybenzimidazoles containing 1,2,4 triazole and 1,2,4-oxadiazole moiety in the main as well as side chain and their application as polymer electrolytes for fuel cells in five chapters:

- Synthesis of aromatic diacid monomers having phenyl 1,2,4-triazole functionality in main chain and side chain.
- Synthesis of aromatic diacids containing oxadiazole moiety in main chain and side chain
- Synthesis and characterization of polybenzimidazole and a series of copolybenzimidazoles from these diacids.
- One pot synthesis of copolymers containing benzimidazole and oxadiazole groups.
- General characterization of these polymers and as polymer electrolyte membranes.
- Application of these polymers as polymer electrolyte membrane for fuel cells.

### **Chapter 1: Introduction and literature review**

Chapter 1, includes a detailed review of literature on the polymer electrolyte membrane fuel cells in general, with a special focus on polybenzimidazoles from different diacids and tetraamines and their use for fuel cell applications. This chapter also includes the scope and objective of the thesis.

### **Chapter 2: Synthesis and characterization of monomers**

Chapter 2, presents synthesis and characterization of four aromatic diacids having triazole and oxadiazole groups, viz. (i) 3,3'-(4-phenyl-4H-1,2,4-triazole-3,5-diyl)

dibenzoic acid (PTDBA), (ii) 5-(4,5-diphenyl-4H-1,2,4-triazol-3-yl)isophthalic acid (iii) 5-(5-phenyl-1,3,4-oxadiazol-2-yl) isophthalic acid and (iv) 3,3'-(1,3,4-oxadiazole- 2,5-diyl)dibenzoic acid.

### **Chapter 3: Synthesis and characterization of polybenzimidazoles and copolybenzimidazoles containing triazole groups and their application as polymer electrolyte membranes for fuel cells.**

This chapter presents a detailed study on the synthesis of polybenzimidazoles and co-polybenzimidazoles from two aromatic diacids, viz. 3,3'-(4-phenyl-4H-1,2,4-triazole-3,5-diyl) dibenzoic acid (PTDBA) and 5-(4,5-diphenyl-4H-1,2,4-triazol-3-yl) isophthalic acid and characterization of these polymers by solubility tests, inherent viscosity measurement, IR spectroscopy, X-ray diffraction, differential scanning calorimetry, thermogravimetry and tensile properties. Apart from these, physicochemical properties such as water and phosphoric acid uptake, oxidative stability, and proton conductivity of membranes of these polymers were studied to explore the probable application for polymer electrolyte membrane fuel cells.

### **Chapter 4: Synthesis and characterization of polybenzimidazoles and copolybenzimidazoles containing oxadiazole groups and their application as polymer electrolyte membranes for fuel cells.**

This chapter presents a detailed study on the synthesis and characterization of polybenzimidazole and co-polybenzimidazoles based on two aromatic diacids, viz, 5-(5-phenyl-1,3,4-oxadiazol-2-yl) isophthalic acid and 3,3'-(1,3,4-oxadiazole- 2,5-diyl)dibenzoic acid. This chapter also describes the synthesis and characterization of poly (benzimidazole-co-oxadiazole) copolymers containing varying extents of benzimidazole and oxadiazole content by the polycondensation of a tetraamine, a dicarboxylic acid and a dihydrazide of a dicarboxylic acid. This chapter also includes a detailed study on physico-chemical properties such as water and phosphoric acid uptake, oxidative stability, and proton conductivity of membranes with a view to explore the possible applications as electrolyte membrane for fuel cells.

### **Chapter 5: Summary and conclusions**

This chapter presents the summary, conclusions drawn and summary of the possible future work.